DESIGN AND SYNTHESIS OF NEW CYANOPYRIDINE BASED CONJUGATED POLYMERS FOR OPTOELECTRONIC APPLICATIONS
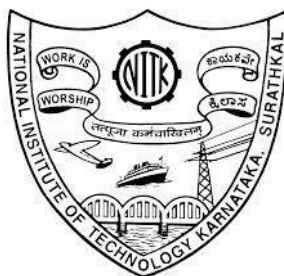
Thesis

Submitted in partial fulfilment of the requirements for the degree of

DOCTOR OF PHILOSOPHY

By

NAVEENCHANDRA P.

DEPARTMENT OF CHEMISTRY

NATIONAL INSTITUTE OF TECHNOLOGY KARNATAKA

SURATHKAL, MANGALORE - 575 025

September, 2020

DECLARATION

By the Ph.D. Research Scholar

I hereby declare that the Research Thesis entitled "**Design and synthesis of new cyanopyridine based conjugated polymers for optoelectronic applications**" which is being submitted to the **National Institute of Technology Karnataka, Surathkal** in partial fulfilment of the requirements for the award of the Degree of **Doctor of Philosophy** in **Chemistry** is a *bonafide report of the research work carried out by me*. The material contained in this Research Thesis has not been submitted to any University or Institution for the award of any degree.

Naveenchandra P.
Reg. No. 135005CY13P01
Department of Chemistry

Place: NITK - Surathkal
Date:

CERTIFICATE

This is to certify that the Research Thesis entitled "**Design and synthesis of new cyanopyridine based conjugated polymers for optoelectronic applications**" submitted by **Mr. Naveenchandra P.** (Register Number: **135005CY13P01**) as the record of the research work carried out by him *is accepted as the Research Thesis submission* in partial fulfillment of the requirements for the award of degree of Doctor of Philosophy.

Prof. A. Vasudeva Adhikari

Research Guide

Date:

Chairman - DRPC

Date:

DEDICATED TO MY BELOVED FAMILY

ACKNOWLEDGEMENTS

ABSTRACT

Conducting polymers (CPs) have been widely investigated due to their several advantages over the traditional materials, such as wide and tunable electrical conductivity, facile production approach, high thermal stability, light-weight, low-cost and ease in material processing. Consequently, they are potential candidates for several applications in the field optoelectronics. In recent years, a great deal of interest has been focused on the synthesis of novel D-A configured conjugated polymers with desired properties through proper structural modifications, particularly for PLED application. In this context, the proposed research work has been aimed at design and synthesis of new D-A type conjugated polymers with improved photonic properties as good emissive materials.

Based on the literature review, six new series of D-A type conjugated polymers (**Series 1-6**) carrying various electron donor and acceptor moieties have been designed with possible applications in PLEDs. Required bi-functional monomers have been prepared using appropriate synthetic procedures. Structures of new intermediates/monomers have been evidenced using spectral and elemental analyses. From these monomers, six new series of target polymers, *viz.* (i) phenylene-cyanopyridine based polymers having vinylene linkage as π-conjugated spacers, **VPPy$_{1-3}$** (**Series-1**), (ii) thiophene-cyanopyridine based polymers carrying vinylene linkage as π-conjugated spacers, **VTPy$_{1-3}$** (**Series-2**), (iii) phenylene-cyanopyridine based polymers containing phenylene as auxiliary donors, **PPy$_{1-3}$** (**Series-3**), (iv) thiophene-cyanopyridine based polymers containing phenylene as auxiliary donors, **TPy$_{1-3}$** (**Series-4**), (v) cyanopyridine based polymers carrying thiadiazole units, **TDPy$_{1-4}$** (**Series-5**), and (vi) heteroaromatic-cyanopyridine based polymers carrying imine linkage as π-conjugated spacers, **Py$_{1-4}$** (**Series-6**) have been successfully synthesized and their synthetic protocols have been established. Their structures have been confirmed by different spectroscopy and elemental analyses. Their molecular weights have been determined by GPC technique and thermal properties have been evaluated by TGA studies. Electrochemical properties have been studied using CV and photophysical properties have been evaluated by UV-visible absorption and PL spectroscopy. Their fluorescent quantum yields have been determined. Finally, their electroluminescence behaviour has been investigated. Most of the polymers have exhibited promising results in the device. Also, their structure-property correlation studies have been carried out.

Keywords: D-A type Conjugated polymers, Fluorescence, DFT studies, Poly(thiophene), PLED.

CONTENTS

CHAPTER 1

AN OVERVIEW OF CONJUGATED POLYMERS AND PLED'S

CHAPTER 2

LITERATURE REVIEW, SCOPE, OBJECTIVES AND DESIGN OF NEW CONJUGATED POLYMERS

CHAPTER 3

SYNTHESIS AND STRUCTURAL CHARACTERIZATION

CHAPTER 4

PHOTO PHYSICAL, ELECTROCHEMICAL, THEORETICAL AND THERMAL STUDIES

CHAPTER 5

ELECTROLUMINESCENCE STUDIES

CHAPTER 6

SUMMARY AND CONCLUSIONS

LIST OF FIGURES, DESIGNS, SCHEMES AND TABLES

FIGURES

DESIGNS

SCHEMES

TABLES

ABBREVIATIONS

CB	Conduction band
CDCl$_3$	Deuterated chloroform
CHCl$_3$	Chloroform
CNPPV	Poly(cyanoterphthalylidene)
CV	Cyclic voltammetry
D-A	Donor-acceptor
DC	Direct current
DFT	Density functional theory
DMF	*N,N*-Dimethylformamide
DMSO D^6	Deuterated dimethyl sulfoxide
DMSO	Dimethyl sulfoxide
EA	Electronic affinity
EDOT	Ethylene dioxythiophene
E$_g$	Band gap
EL	Electro luminescence
ESA	Excited state absorption
ETL	Electron-transporting layer
FET	Field effect transistor
FMO	Frontier molecular orbital
FTIR	Fourier transform infra red
GPC	Gel permeation chromatography
HOMO	Highest occupied molecular orbital
HTL	Hole-transporting layer
ICT	Intra molecular charge transfer
IP	Ionization potential
ITO	Indium tin oxide
LUMO	Lowest unoccupied molecular orbital
M$_n$	Number average molecular weight
M$_w$	Weight average molecular weight
NMR	Nuclear magnetic resonance

PA	Poly(acetylene)
PCE	Power conversion efficiency
PDI	Polydispersity index
PDI	Poly dispersity index
PEDOT	Propylene dioxythiophene
PEDOT	Poly(3,4-ethylenedioxythiophene
PL	Photo luminescence
PLEDs	Polymer light emitting diodes
PPP	Poly(p-phenylene)
PPV	Poly(p-phenylenevinylene)
PPy	Poly(pyrrole)
PS	Poly(styrene)
PSS	Poly(styrenesulphonate)
PTh	Poly(thiophene)
PV	Photovoltaic
RT	Room temperature
SCE	Standard calomel electrode
TBAP	Tetrabutylammoniumperchlorate
TFT	Thin film transistor
T_g	Glass transitions temperature
TGA	Thermo gravimetric analysis
THF	Tetrahydrofuran
UV	Ultra violet
VB	Valence band
ε	Molar absorption coefficient
Φ_f	Fluorescence quantum yield

AN OVERVIEW OF CONJUGATED POLYMERS AND PLED'S

Abstract

This chapter covers an introduction to conjugated polymers including their brief history, synthetic methods, and different properties such as optical, electrochemical and electronic behavior. It also comprises the description on different types of aromatic and hetero aromatic based conjugated polymers. Finally, it involves a brief introduction to applications of conjugated polymers in PLED devices, followed by broad objectives as well as thesis structure.

1.1 INTRODUCTION ON CONJUGATED POLYMERS

Thirty years ago, all the carbon based polymers were known to be insulators. Consequently, these polymers were largely utilized as inactive and packaging materials. This narrow perspective changed when a new class of polymers referred as conjugated polymers or electro-active polymers has been discovered. In principle, the conjugated polymers are polymers with alternate single and double bonds. Here, the π-electrons are highly delocalized and easily polarizable. In such materials, presence of wide delocalization of π-electrons is highly responsible for the array of notable optical and electronic properties, exhibited by them.

1.2 BRIEF HISTORY

In 1958, the well-known conjugated polymer poly(acetylene) (**S-1.1**) was synthesized by Natta and his coworkers for the first time as a blackish solid and was found to be semiconducting in nature with conductivity in the order of 10^{-11} to 10^{-3} S/cm. Later, Shirakawa H., MacDiarmid A.G. and Heeger A. J. showed that, the conductivity of the *cis*-poly(acetylene) films increased to an extent of several thousand times by doping it with iodine. The prepared films looked like shining golden yellow metallic sheets with very high conductivity. For this discovery they received Nobel Prize in the year 2000. Later, it was shown that, conductivity could be imparted to many organic conjugated polymers through appropriate doping. At present, conjugated polymers with conductivity equivalent to that of copper can be easily obtained. Literature reports (Heeger et al. 1988; Heeger et al. 1986; Skotheim et al. 1986) on earlier work in the area of conjugated polymers clearly indicate that doping is an important factor which influences the properties of them.

During the past two decades, many conjugated polymers like poly(thiophene)s [PTs] **(S-1.2)** (Pei et al. 2000), poly(*p*-phenylene)s [PPPs] **(S-1.3)** (Grem et al. 1992), poly(*p*-phenylene vinylene)s [PPVs] **(S-1.4)** (Burroughes et al. 1990) and poly(fluorene)s [PFs] **(S-1.5)** (Leclerc et al. 2001), with potential applications were developed. These polymers can be viewed as a sp^2p_z carbon chain, structurally analogous to that of *cis/trans*-poly(acetylene). Also, these polymers are known to be thermally more stable than poly(acetylene) and even some polymers can be prepared in doped state itself.
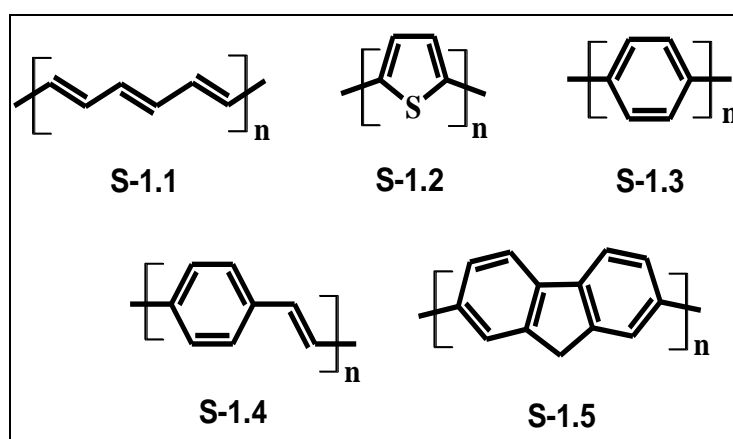
Figure 1.1: Structures of organic moieties which can act as conjugated polymers

1.3 SYNTHETIC ROUTES

Synthetic methods for conjugated polymers are extremely versatile and may include classical polymer chemistry approach like coordination polymerization, conventional organic chemistry techniques or electrochemical routes. In general, conjugated polymers are synthesized by two different methods, *viz*.

a) Chemical polymerization
b) Electrochemical polymerization

1.3.1 Chemical polymerization

Chemical polymerization technique involves different methods of polymerization such as condensation polymerization, addition polymerization, oxidative polymerization *etc*. Generally, the chemical polymerization methods make use of different types of well-known organic reactions like Suzuki-polymerization,

Gilch polymerization, Knoevenagel polymerization, Wittig polymerization, Sonogoshira coupling, Yamamoto polymerization, Zigler-Nutta polymerization, Grignard polymerization *etc*. for which details are given in *Chapter 2*.

The first known conjugated polymer 'poly(acetylene)' was synthesized by Natta et al. in the year 1958 (Natta et al. 1958). Since then, different routes have been proposed for its synthesis. These include Ziegler-Natta polymerization (Natta et al. 1958), high pressure polymerization (Aoki et al. 1988), and Durham method (Edwards et al. 1984) from acetylene. Many other conjugated polymers like poly(*p*-phenylene)s, poly(*p*-phenylenevinylene)s, poly(thiophene)s, poly(fluorene)s *etc*. have been synthesized using different synthetic methods. Few important routes for the synthesis of conjugated polymers have been discussed in the following section.

1.3.1.1 Yamamoto condensation

Yamamoto reported a unique method to synthesize PPPs through condensation reaction. The method involves the reaction between dihaloaromatic compounds and magnesium metal in the presence of various low valency Ni catalysts (Schlüter et al. 1993; Tour et al. 1994). When a mixture of equimolar quantities of 1, 4-dibromobenzene (**S-1.8**), Mg metal, and dichloro-Ni (bipyridyl) in THF was refluxed, a low molecular weight PPP (**S-1.9**) was obtained (**scheme 1.1**). This is a convenient method to incorporate benzene nucleus in the polymer backbone.

S-1.8   **S-1.9**
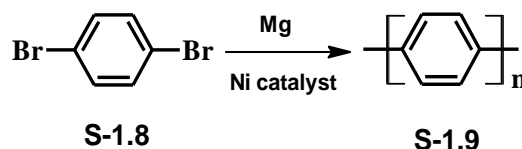
Scheme 1.1

1.3.1.2 Suzuki coupling

The Suzuki polymerization is one of the good methods to obtain conjugated polymers carrying aromatic species. In this condensation method, 1,4-dibromobenzenes (**S-1.10**) were first converted into boronic acid derivatives (**S-1.11**), which were then polymerized using Pd catalysts to get corresponding PPPs (**S-1.12**) (Rehahn et al. 1989) in good yield. A general example of Suzuki coupling reaction leading to formation of a polymer has been depicted in **Scheme 1.2a**. Further,

Scheme 1.2b summarizes the actual mechanism involved in the formation of the product, showing all the steps clearly.

where R is substituted alkyl groups
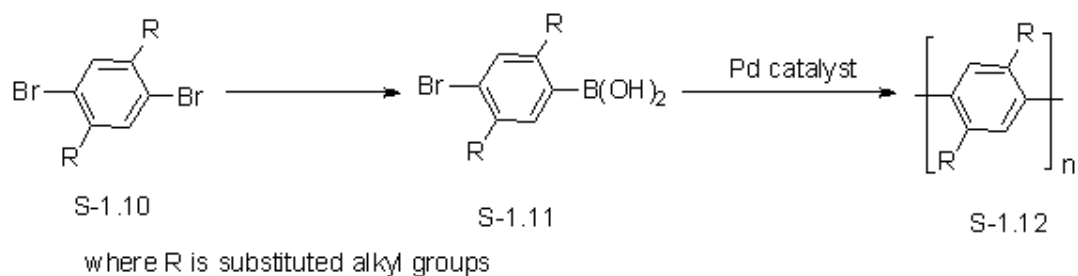
Scheme 1.2a

Scheme 1.2b
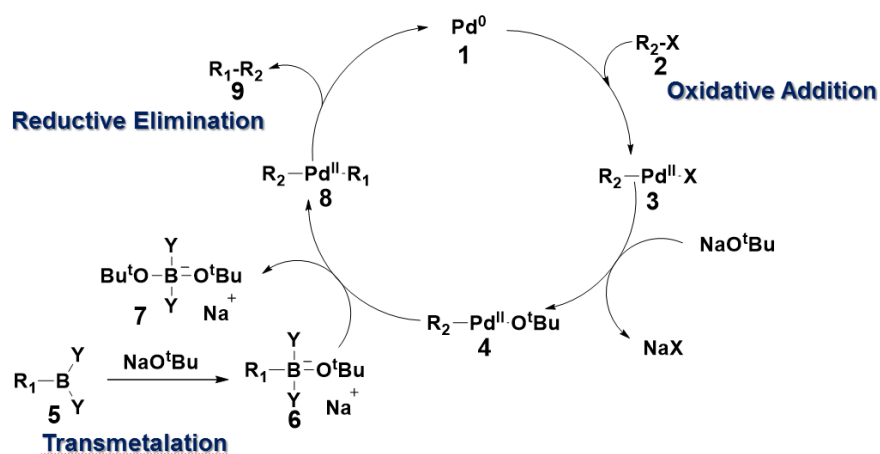
1.3.1.3 Polycondensation

Polycondensation is an important method for the preparation of conjugated donor-acceptor (D-A) type polymers. In this method, two molecules containing active bifunctional groups undergo polycondensation reaction with the elimination of small molecules such as H_2O, HCl *etc*. For example, substituted dialdehydes (**S-1.23**) and bisacetonitriles (**S-1.24**) undergo Knoevenagel polycondensation reaction with the help of potassium tertiary butoxide (*tert*-BuOK) as catalyst to give poly(cyanovinylene)s (**S-1.25**, **Scheme 1.3**).

S-1.23   **S-1.24**   **S-1.25**
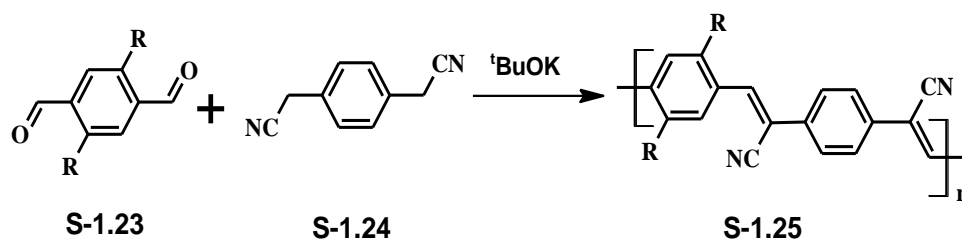
where R is substituted alkyl groups

Scheme 1.3

In another example, biscarbohydrazides (**S-1.26**) react with diacid chlorides to give polyhydrazides (**S-1.27**, **Scheme 1.4**). These polyhydrazides undergo cyclization reaction in presence of dehydrating agents like phosphorous oxychloride (POCl$_3$) to give conjugated polyoxadiazoles (**S-1.28**) (Meng et al. 1999).

S-1.26

where R$_1$ is substituted alkyl group

where R$_2$ is substituted phenyl group
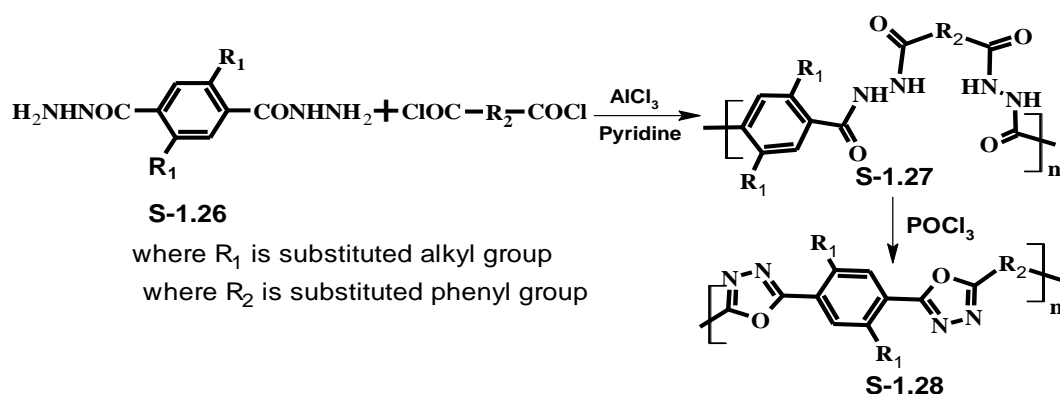
Scheme 1.4

1.3.2 Electrochemical polymerization

Electrochemical polymerization method has gained much importance because of its simplicity as well as additional advantage of obtaining a conducting polymer being simultaneously doped. Normally, this polymerization is conducted in a single or dual compartment electrochemical cell by using a standard three-electrode system with the help of a supporting electrolyte, dissolved in a suitable solvent. It can be performed potentiometrically by using an appropriate power supply. Following this technique, conjugative conducting polymers like poly(pyrrole)s, poly(thiophene)s, poly(furan)s can be synthesized from their monomers in a single step. Simultaneously, the obtained polymer would be in its doped state and hence the

polymer thus obtained is pure and uniform. The mechanism of polymerization includes the following steps:

i) Oxidation of organic monomer molecules to generate corresponding radical cation

ii) Dimerization of generated radical cations, accompanied by a proton loss to give a neutral dimer

iii) Oxidation of neutral dimer to yield its radical cation

iv) Combination of dimer radical cation with an additional radical cation

Finally, the growing chain terminates *via* exhaustion of reactive radical species accompanying oxidative or other chain termination process in the vicinity of the electrode. Mechanism of electrochemical polymerization is illustrated in **Figure 1.2.**
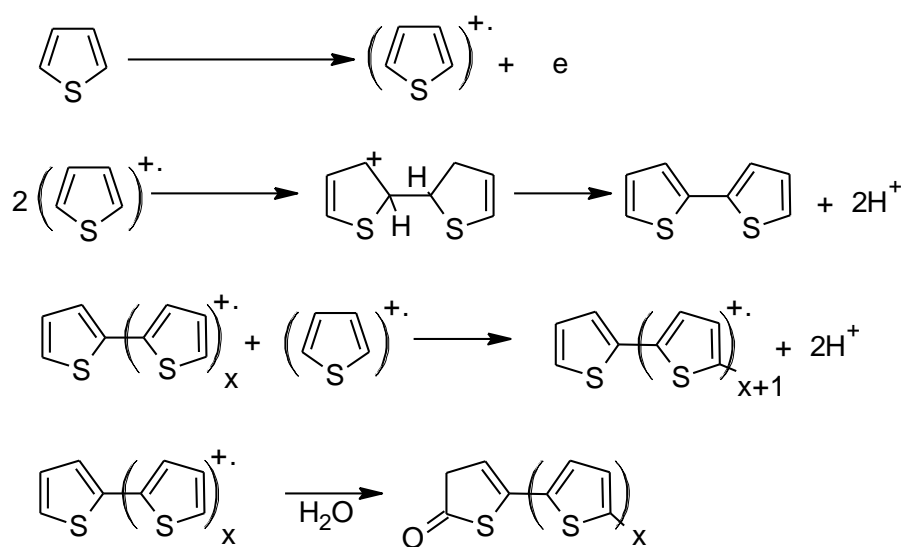
Figure 1.2: Mechanism of electrochemical polymerization

1.4 PROPERTIES OF CONJUGATED POLYMERS

Conjugated polymers exhibit many characteristic properties. Some of them have been described below.

1.4.1 Conductivity and charge storage

The earliest known conjugated polymer, *i.e.* poly(acetylene) was found to be shiny, insoluble and inflexible, with conductivity comparable to that of

semiconductors. Further investigations had shown that exposure of this to iodine increased its conductivity by several millions fold. When it was partially oxidized by substances such as iodine, its conductivity enhanced to nearly 10^{-1} S/cm. Later, in the 1990's, polyheteroaromatics were developed as a new class of conducting polymers. They were shown to be more stable than poly(acetylene), though their conductivity values were not as much as poly(acetylene). By incorporating different substituents to the polymer main chain, derivatives with enhanced solubility with organic solvents were synthesized. Introduction of certain side groups also changed their inherent properties like color, reactivity towards oxidizing and reducing agents. **Figure 1.3** shows the comparative account of conductivities of some well-known conjugated polymers and metals.

Conductivity

(S cm^{-1})

10^7	
10^6	copper metal
10^5	poly(acetylene) doped with AsF$_5$
	poly(acetylene) doped with I$_2$
10^4	liquid mercury
10^3	poly(phenylene) doped with AsF$_5$
10^2	poly(pyrrole) doped with I$_2$
10	
	poly(aniline)
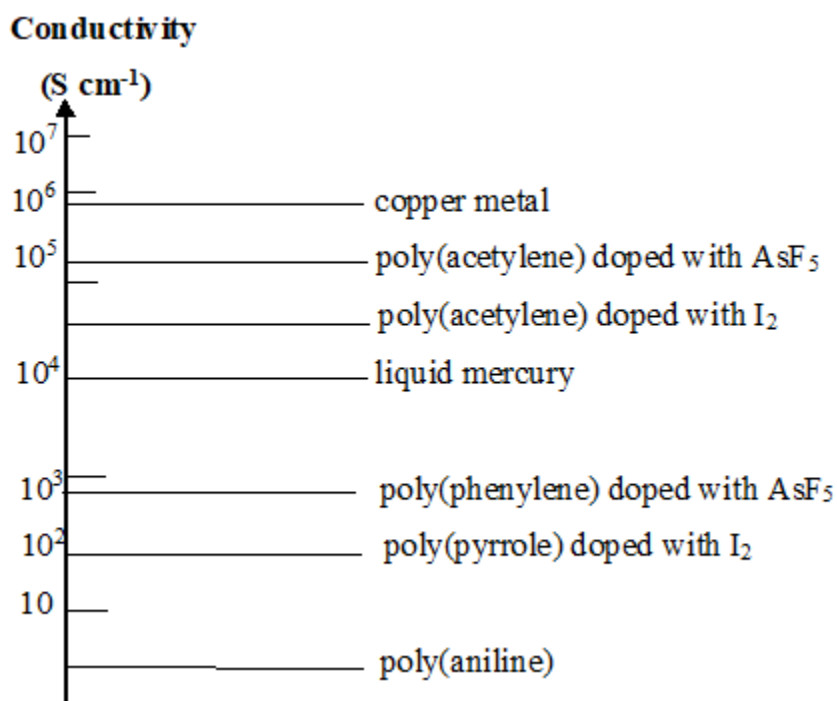
Figure 1.3: Conductivities of some metallic and polymeric materials

Conducting polymeric materials differ from inorganic semiconductors in many ways. The most notable distinction between them is about/on the extent of mobility of charges. With the invention of new conducting polymers and the development of novel processing techniques, this difference is diminishing. Generally, low charge carrying mobility is related to structural disorder in the conducting polymer. Indeed, conduction in such relatively disordered polymers is a function of 'mobility gaps',

(McGinness et al. 1972) with phenomenona such as phonon-assisted hopping, polaron-assisted tunnelling *etc*., between localized states, as observed in inorganic amorphous semiconducting materials.

Typically 'doping' the conducting polymers involves oxidizing or reducing the material. Enhancement of the conductivity by doping has led to an understanding of the mechanism of charge storage as well as charge transfer in the polymer chain. Normally, doped polymers suffer from disadvantages like poor processibility and air stability. As a result, the latest research in this area has focused on development of new charge-carrying polymers with good stability and processibility.

According to the band theory, semi-conductivity in any conjugated polymer is due to the presence of partly filled valence band (VB) that could be formed from continuous delocalized π-electrons. This causes a band width of about 2.5 eV in the molecule making it a large band gap semiconductor. Such a polymer can be converted into a conducting one by properly doping it with either an electron donating or an electron accepting species. This is analogous to doping of silicon-based extrinsic semiconductors wherein pure silicon is doped with either pentavalent arsenic or trivalent boron. Normally, doping of silicon brings about a donor energy level near to the conduction band (CB) or an acceptor level close to the VB. However, in case of conducting polymer, the situation is different. Generally, the doped polymers do not have a large enough concentration of free spins. This was evidenced by electron spin resonance spectroscopy. In the polymers, at first the free spin concentrations increases with increase in concentration of dopant and reaches maximum value of free spin levels at larger concentrations. The storage of charge along the polymer backbone and its effect can be better understood from its structural features.

The conducting polymer may store charge largely in two ways. The polymer, in an oxidative process could either lose an electron from one of the bands or it could localize the charge over a small section of the polymer chain. Here, localizing the charge may bring about a local distortion due to a change in geometry, which expenses the polymer certain energy. However, the acquisition of this local geometry decreases the ionization energy of the polymer molecule and enhances its electron affinity making it more capable to accommodate the newly generated charges. This

enhances the energy of the polymer less than it would have if the charge has been delocalized. This has been confirmed by Raman spectroscopy. Also, in a reductive process, a similar scenario occurs.

Some of the the typical oxidizing dopants used are iodine, arsenic pentachloride, iron (III) chloride and nitrosyl hexafluorophosphate (NOPF$_6$). A classic reducing dopant is sodium naphthalide. **Figure 1.4** explains the oxidative doping of poly(pyrrole) with a general dopant. An electron is detached from the π-system of the polymer backbone yielding a free radical and a spinless positive charge. The obtained radical and cation are coupled to each other *via* local resonance of the charge and the radical. In this case, a series of quinoid-like ring structure is used. The distortion produced by this is of greater energy than the remaining part of the chain. The formation and separation of these defects expense a substantial amount of energy. This controls the number of quinoid-like ring structures that can link these two species bonded each other. In the case of poly(pyrrole), it is assumed that, the lattice distortion extends over four pyrrole rings. This combination of a radical and a charged site is termed as a polaron which consequences in the formation of either a radical cation or a radical anion. The newly formed charge sites create restricted electronic states in the gap, with the lower energy states being occupied by single unpaired electrons. The polaron states of poly(pyrrole) are symmetrically located about 0.5 eV from the band edges, as shown in **Figure 1.4a**.
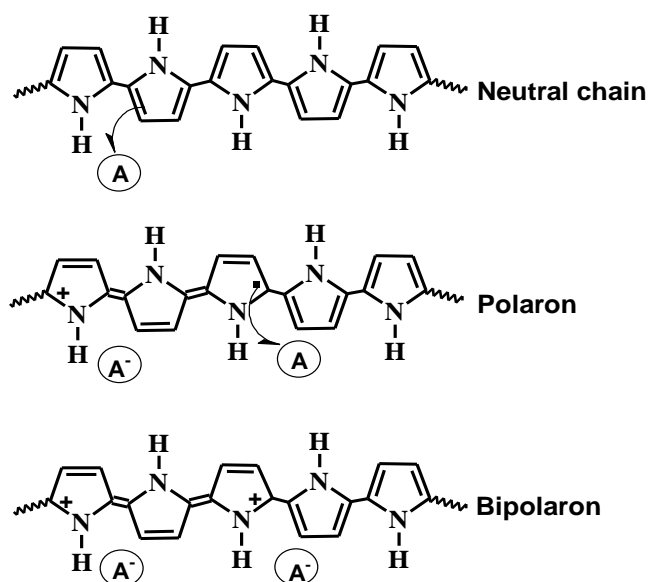
Figure 1.4: Polaron and bipolaron states in poly(pyrrole)

Conduction band

Valence band

Neutral polymer   **Polaron**   **Bipolaron**   **Bipolaron bands**

(a)   **(b)**   **(c)**
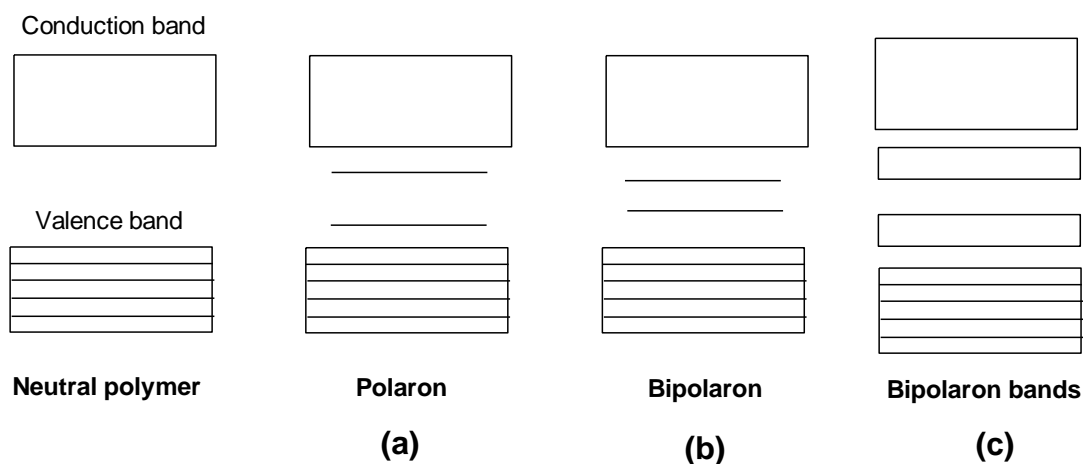
Figure 1.4a: Polaron and bipolaron bands in poly(pyrrole)

On further oxidation, the free radical of the polaron creates a new spinless defect called a bipolaron. This process is of lower energy than the creation of two distinct polarons. At higher doping levels, it may be possible that, two polarons unite to form a bipolaron. Therefore, at higher doping levels, the polarons are replaced with bipolarons. In case of poly(pyrrole), the bipolarons are situated symmetrically with a band gap of 0.75 eV as seen from **Figure 1.4b**. This eventually creates a continuous bipolaron bands with continued doping. Further, their band gap also enhances as newly formed bipolarons are obtained at the expense of the band edges. For a heavily doped conjugated polymer it is believed that, the upper and the lower bipolaron bands (**Figure 1.4c**) would amalgamate with the conduction and the valence bands, respectively to obtain partially filled bands, which brings about metallic like conductivity in the polymer.

1.4.2 Factors affecting band gap

Band gap is termed as the energy separation between filled valence band and empty conduction band of the solid state material. The band gap of any conducting polymer can be tuned by various techniques. Among them, structural modification is one of the methods. The major factors that affecting the bandgap in conductive polymers are mainly bond length alteration ($E^{\Delta r}$), the mean deviation from planarity (E^{Θ}), the aromatic resonance energy (E^{res}), the electronic effects, *viz.* inductive and mesomeric effects of substituents (E^{sub}), and the inter-chain interactions (E^{Int}) as shown in equation (1.1) and **Figure 1.5**.

$$E_g = E^{\Delta r} + E^{\Theta} + E^{res} + E^{sub} + E^{Int} \qquad\qquad (1.1)$$
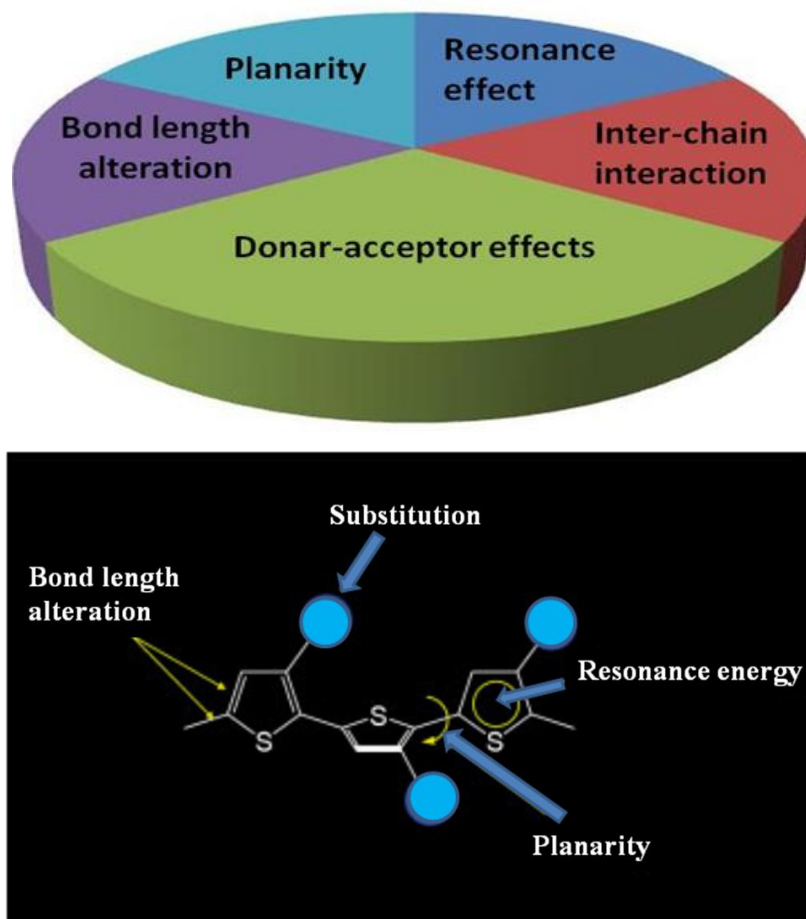
Figure 1.5: Factors affecting bandgap

In the above equation, bond length alternation is defined as the difference between single and double bond lengths in poly(acetylene) chain. However this definition cannot be used for poly(aromatic)s such as poly(thiophene) that differs from poly(acetylene) by their non-degenerate ground state. In poly(aniline), there are two resonance forms; *viz.* aromatic and quinonoid structures which are not energetically equal (Lowe et al. 1984). So, a new theory was proposed by (Bredas et al. 1985); accordingly, the bond length change is defined as maximum difference between the lengths of C-C bond inclined relative to the chain axis and C-C bond parallel to the chain axis (Bredas et al. 1985). The authors have observed that, the bandgap of the polymer reduces as the contribution of the aromatic geometry decreases or quinoid geometry increases.

According to (Liu et al. 2001), the existence of single bond between the aromatic heterocycles brings about inter-annular rotations in conjugative polymeric backbone **Figure 1.6**. This induces a rotational distortion about the single bonds, which leads to reduction in the effective conjugation along the polymer chain with the weakening of the extent of overlap. Thus, any deviation in the co-planarity would cause an enhancement of the bandgap.
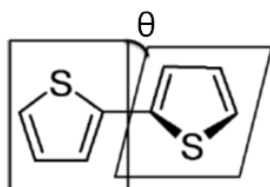
Figure 1.6: Conjugated Polymers exhibiting intra annular rotations

The band gap of conjugative polymer normally decreases with decline in the resonance energy per electron. This results in a competition between π-electron confinement within the aromatic rings and delocalization along the polymer chain. In general, incorporation of various substituents along the polymeric back bone has a pronounced effect on the extent of bandgap. Also, the character and position of substituent plays important role. Normally, electron donating substituents enhance the HOMO energy, while electron withdrawing groups decrease the LUMO energy.

1.4.3 Stability of conjugated polymers

Stability is an important property of conjugated polymers, particularly from the point of view of their device fabrication. When their stability is concerned, there are two discrete kinds, *viz.* extrinsic stability and intrinsic stability. Extrinsic stability is linked to susceptibility of polymers to external environmental agents like oxygen, water, peroxides. It is a measure of the susceptibility of charged polymer sites to attack by nucleophiles, electrophiles and free radicals of the environment. If a conductive polymer is extrinsically less stable, then it must be protected by a stable coating. However, several conducting polymers degrade intrinsically over time even in dry as well as oxygen free environment. This intrinsic stability is thermodynamic in origin. It may be caused by irreversible chemical combination between charged sites of conjugative polymer and either the dopant counter ion or the π-system of an adjacent neutral chain, which generates a *sp³* hybridized carbon that leads to breakage

in the conjugation. Intrinsic instability in polymers can also be attributed to a thermally driven mechanism which causes the polymer to lose its dopant. This occurs when the charge sites become unstable mainly due to conformational changes in the polymer chain.

1.4.4 Optical properties of conjugated polymers

The overlap of π and π^* molecular orbitals of a conjugative polymer molecule produces a continuous system of electron density along its backbone. The magnitude of this overlap in conjunction with the bond alternation determines the Highest Occupied Molecular Orbital (HOMO), Lowest Unoccupied Molecular Orbital (LUMO) and bandgap of the polymer. Generally, conjugative polymers possess the bandgaps in the order of 1-4 eV, permitting stable optical excitations and mobile charge carriers. Excitations can be created by charge injection, light or chemical doping. Generally, excitation results in a local deformation of the molecule around the site of electronic excitation (Hedger et al. 1988). The change of polymer backbone geometry (from aromatic to quinoa) has the effect of pulling energy levels away from the band edges into the gap. The extent of delocalization is largely depending on the nature of the conjugative structure. Usually, aromatic rings tend to localize the excitation. This is because of the fact that, among the alternative electronic configuration, the quinoa form is possessing higher energy than aromatic one. These materials are often highly fluorescent, and they emit light in the range from near infrared to the ultraviolet region. Particularly, PPVs and PTs are of great interest, mainly due to the combination of their emission behavior in the visible wavelength region and possession of high luminescence quantum yields. A schematic representation of radiative decay of a conjugated polymer chain after photoexcitation is summarized in **Figure 1.7**.
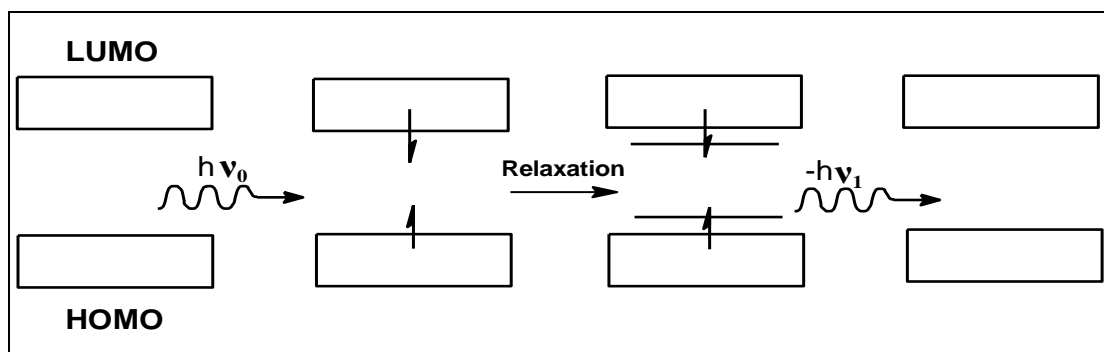
Figure 1.7: Radiative decay of a conjugated polymer chain after photoexcitation

The wavelength of emission depends upon the degree of conjugation or delocalization and can be monitored by alteration of the chemical structure of the conjugative polymer. This can be possibly done by attaching the functional groups, which alter the electronic structure of the conjugative polymer main chain or by making polymers with non π-conjugated groupings, which intrude the π-orbital overlap. Accordingly, light emission is possible over the whole visible range of the spectrum by chemical tuning the HOMO-LUMO band gap of the polymer. The tunable emissive properties are especially attractive for lighting and display applications, particularly in combination with generally low material expense and the possibility of large area device fabrication. The observed transitions in UV-Vis absorption spectroscopy of conjugated polymers is generally ascribed to excitation of electrons from π to π^* states and it is from π^* to π states for emission spectroscopy.

Various photo physical processes like fluorescence or phosphorescence including radiation-less decay may happen upon electronic excitation of the polymer (Guillet et al. 1985). Fluorescence is perceived after singlet relaxation from the first excited state. If intersystem crossing happens, a triplet excited state is obtained, whose relaxation will bring about phosphorescence. In case, the emission does not happen, a non-radiative path is dominant, and the electronic excitation is transformed into rotational or vibrational motion within the structure of polymer. Indeed, the difference between the absorption and emission maxima of the of UV-Vis spectra is called Stokes shift and it happens when emission from the lowest vibrational excited energy level to different vibrational states of the electronic ground state. Generally, quantitative measure of the emission efficiency of the polymer is denoted by its

quantum yield of luminescence (Φ_{PL}). The quantum yield is defined as the ratio of actual number of photons emitted to the number of photons absorbed, as given in **equation 1.2**.

$$\Phi_{PL} = \frac{\text{Photons}_{EM}}{\text{Photons}_{ABS}} \qquad (1.2)$$

As per the law of conservation of energy, the maximum value of quantum yield should be 1. Its value is related to the rates of radiative (τ_r) and non-radiative (τ_{nr}) decays, as shown in **equation 1.3** (Lakowitz et al. 1999; Klessinger et al. 1995).

$$\Phi_{PL} = \frac{\tau_r}{\tau_r + \tau_{nr}} \qquad (1.3)$$

As τ_{nr} approaches zero, luminescence's quantum yield approaches unity. Usually, Φ_{PL} is the highest in dilute solutions, where the emitting molecules are isolated from each other. In most instances, increase in polymer concentration reduces the luminescence quantum yield mainly due to concentration quenching of the polymer.

The luminescence quantum yield can be estimated either by secondary or primary techniques (Eaton et al. 1988). In the secondary technique, the Φ_{PL} of a sample solution is determined relative to a standard reference sample of known quantum yield with the help of **equation 1.4** (Davey et al. 1995).

$$\Phi_s = \Phi_r \left(\frac{A_r}{A_s} \frac{I_s}{I_r} \right) \qquad (1.4)$$

The above-mentioned equation, Φ represents luminescence quantum yield, A indicates the absorbance observed at the excitation wavelength and I denotes the corresponding relative integrated fluorescence intensity. Here, subscript 's' indicates an unknown sample and 'r' represents a standard reference. Typical standard substance used are 9,10-diphenylanthracene in the solvent cyclohexane ($\Phi_{PL} = 0.90$) (Hamai et al. 1983; Meech et al. 1983), quinine sulfate in 1 N sulphuric acid ($\Phi_{PL} = 0.546$) (Meech et al. 1983) and rhodamine 101 in ethanol ($\Phi_{PL} = 1$) (Karstens et al. 1980). This technique assumes that, the emission from the sample is isotropic (that means equal in all directions), as is the case in very dilute sample solutions.

1.5   COMPUTATIONAL STUDIES OF CONJUGATED POLYMERS

One of the primary objectives in the field of conductive polymers is to develop a comprehensive knowledge of the relationship between the chemical structure of the polymer and its electronic as well as conduction properties. The required electronic properties in such polymers could be achieved by specific synthesis following appropriate structural design. According to the band theory of solids, the conduction properties of an undoped conjugated polymer are known to be related to its electronic properties, like ionization potential (IP), electronic affinity (EA), and band gap. The main factor that determines the intrinsic characteristics of the conjugated polymers is their band structures, especially the position of the conduction band and valence band as well as the band gap between them. Thus, π-electrons play an important role in determining their electrical conductivity and band structure in conducting polymers. The energy gap between the valence band and conduction band is related to the lowest energy level of its monomer units and the bandwidth resulting from the overlap between orbitals of the monomer molecules. A band gap is considered as the difference between the highest occupied molecular orbital (HOMO) energy level and the lowest unoccupied molecular orbital (LUMO) energy of the polymer as given in **equation 1.5**. According to the equation, electrical conductivity is directly related to HOMO and LUMO energy energy levels of the polymer molecule.

$$E_{gap} \ = \ E_{LUMO} - E_{HOMO} \ \ eV \qquad\qquad (1.5))$$

Further, computational modeling studies can provide factors that affect opto-electronic properties like light absorption, chain conformations, electronic structures, HOMO-LUMO levels *etc*. In literatures, many quantum-mechanical simulations on different types of conjugative polymer systems have focused on the donor–acceptor (D-A) concept in order to study the required structural fine-tuning in relation to energy level modulation. Thus, in future judicious rational design of conjugative polymers with specific properties, computational studies are quite useful for material chemists. Time dependent density functional theory (TD-DFT) can be used effectively to investigate the excited-state properties such as excitation energies, oscillator strengths, and absorption as well as emission spectra. The results from calculations need to be compared to experimental data as much as possible in order to

correlate structural related properties and to overcome the limitations affecting opto-electronic applications.

1.6 DIFFERENT TYPES OF CONJUGATED POLYMERS

Conjugated polymers are of different types depending on their properties, structures and processibility. Based on structures, they are considered to be simple conjugated polymers and redox or donor-acceptor (D-A) architectured conjugated polymers.

1.6.1 Simple conjugated polymers

Simple conjugated polymers consist of same type of repeating units in their chain and they are either hole or electron carriers. Usually hole-carrying property is dominating in this type of polymers. They show lower conductivity in undoped state and hence it is necessary to add dopants to increase the charge-carrying property. In such polymers, the redox sites are highly delocalized over a conjugated π-system. Examples of this type of polymers include poly(acetylene) (**S-1.1**), poly(thiophene) (**S-1.2**) and poly(*p*-phenylene) (**S-1.3**).

The simple conjugated polymers have several drawbacks. Some of them are as follows. They are not stable in ambient temperature for long time. The polymers undergo reduction in presence of moisture. Removal of dopant is difficult and that dopant may damage the fabricated devices. Fabrication of electronic and opto-electronic devices from these polymers requires either *p*-type or *n*-type materials to conduct electricity.

1.6.2 Donor-acceptor type conjugated polymers

In redox or donor-acceptor (D-A) configured conjugated polymers, there exists localized redox sites. These polymers are known to transport electrons by hopping or self-exchange between donor site and acceptor site. They consist of both 'electron-donors' and 'electron-acceptors' along the polymer backbone. Their conductivity value is relatively lower than that of simple conjugative polymers, probably due to slow electron transport to/from the redox sites. But, they exhibit low band gap and show good charge-carrying property. It has been reported that, presence

of alternating donor-acceptor units leads to broadening of the energy bands and hence causes a narrow band gap (Sonmez et al. 2003).

The interaction between the electron donor (D) and acceptor (A) units in alternating donor-acceptor type conjugative polymer can result in the hybridization of the high-lying HOMO energy level of the donor and low-lying LUMO energy level of the acceptor. This leads to a relatively small band gap polymer semiconductor with favorable electronic structure and ambipolar charge transport properties (Pai et al. 2006) as explained in **Figure 1.8**. Such D-A configured conjugative polymers can extend to bipolar charge transfer materials for LED applications (Tarkka et al.1996).
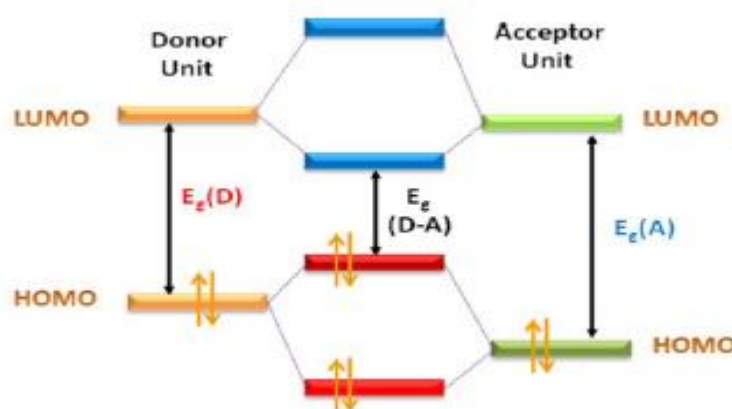
Figure 1.8: Schematic representation of band gap in case of D-A type conjugated polymer.

Also, it has been proven that, such D-A configured polymers possess novel physical properties related to the alteration of donor and acceptor units on the polymer chain, which could lead to applications in devices requiring high charge storage ability like batteries and super capacitor applications (Akoudad et al.1998). For donor-acceptor type conjugated polymers, doping is not necessary to enhance their charge-carrying property. This advantage is exploited while considering them for different opto-electronic applications. **Figure 1.9a** and **1.9b** display structures of important aromatic/heteroaromatic donor and acceptor systems, respectively.
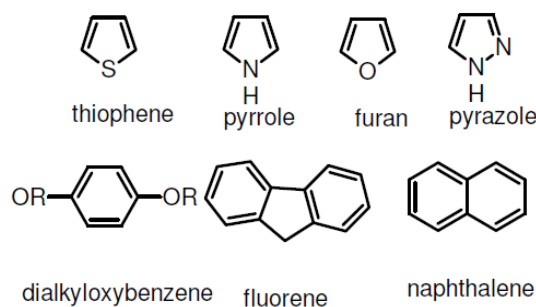
Figure: 1.9a Structures of aromatic/heteroaromatic donor systems
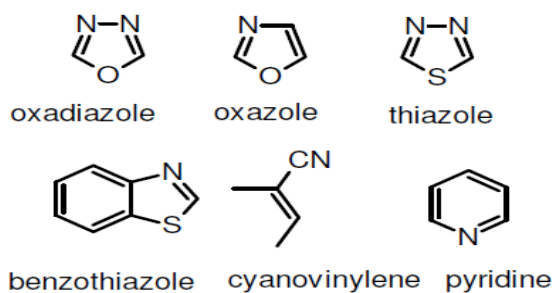
Figure: 1.9b Structures aromatic/heteroaromatic acceptor systems

1.6.3 Chemistry of heteroaromatics

Heteroaromatics include various aromatic heterocyclic compounds. Among them, thiophene, carbazole and oxadiazole play an important role in the field of conjugated polymers.

Thiophene:

Thiophene is a five membered heterocyclic compound with the molecular formula C_4H_4S. It undergoes extensive substitution reactions. Thiophene is less aromatic than that of benzene but known for rigorous substitution reactions. The "electron pairs" on sulfur atom are significantly delocalized in the π electron system. Thiophene acts as electron donor and hole transporter showing higher thermal stability and solubility in the polymer main chain. Thiophene structure can be tuned by substituting different functional groups to adjust band gap between HOMO and LUMO levels of resulting polymers. Structural features of thiophene ring have been summarized in **Figure 1.10**.
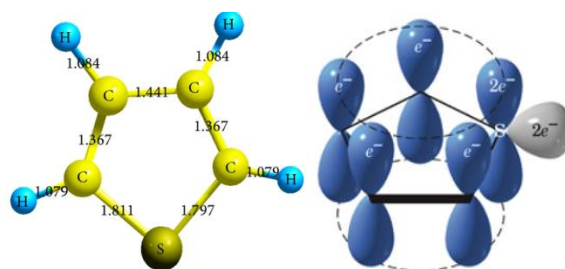
Figure 1.10: Structural features of thiophene ring

There are several methods available to synthesize thiophene derivatives. Two methods have been highlighted in the following section.

Paal-Knorr synthesis

The Paal-Knorr synthesis for thiophene is depicted in **scheme 1.5**. Condensation of a 1,4-dicarbonyl compound in the presence of phosphorous pentasulfide or Lawesson's reagent forms thiophene derivatives with good yield.
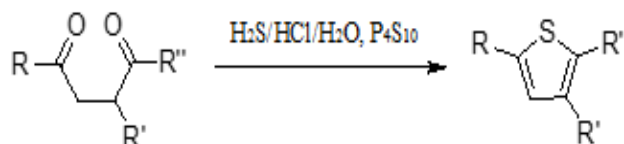
Scheme 1.5: Paal-Knorr synthesis

Gewald reaction

The Gewald reaction involves formation of substituted 2-aminothiophenes through a multi-component condensation reaction between sulfur dust, a α-methylene carbonyl derivative and a α-cyanoester, as shown in **scheme 1.6**.
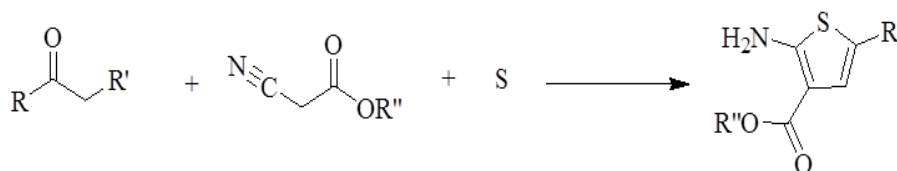
Scheme 1.6: Gewald reaction

1.7 INTRODUCTION ON PLED'S

Electroluminescence (EL) is an electro-optical phenomenon where a material emits light energy in response to an electric field applied through it, or to a strong electric current. This phenomenon requires injection of electrons from one electrode

and holes from the other electrode, the capture of oppositely charged carriers (so-called recombination), and the radiative decay of the excited electron-hole state (Exciton) generated by this recombination process. From the time after discovery of metallic conductivities in 'doped' polyacetylene, the field of conductive polymers has advanced rapidly. In recent times, much of interest has been shown in developing LED devices made from conducting polymers, mainly due to their potent applications in the field of optoelectronics.

It is evident that conjugative polymers originate their semiconducting properties by having delocalized π-electron system along the polymer backbone. Here the π (bonding) and π* (anti-bonding) molecular orbitals produce highly delocalized valence as well as conduction wave functions, which facilitate mobile charge carriers. This electroluminescence phenomenon was first reported in 1990; the light emitting device using the conducting polymer PPV, as a single semiconductor layer between metallic electrodes, is illustrated in **Figure 1.11**. In this device, the ITO layer acts as a transparent electrode system, and permits the light rays generated within the diode to leave the structure. The uppermost electrode layer has been conveniently made by thermal evaporation of a metal. LED operation is achieved when the device is biased effectively to accomplish injection of positive and negative charge carriers from opposite electrodes. Thus, capture of oppositely charged carriers within the region of the polymer layer can then lead to photon emission.
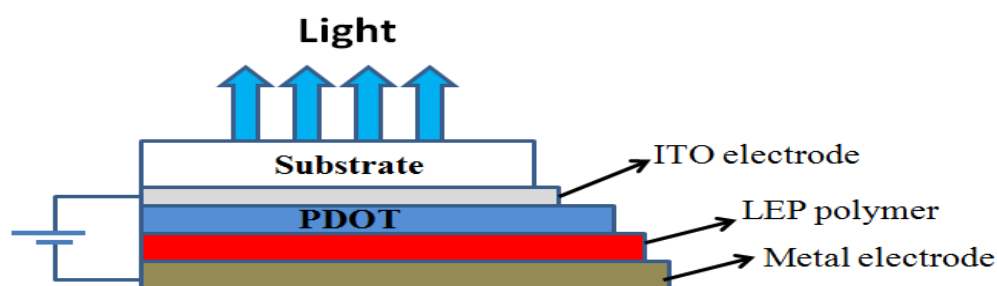
Figure 1.11: Schematic representation of polymer light emitting diode

Polymer LEDs operate on the principle involving the injection of electrons from negative electrode and holes from positive electrodes in the device. The injected electrons and holes combine with each other within the polymer film, forming neutral bound excited states (termed as excitons). These excitons in conjugative polymers are

considered to be more strongly localized than excitons in three-dimensional semiconducting materials. The spin wave function of the exciton, generated from the two spin electronic charges, can be either singlet (S = 0) or triplet (S = 1). A consequence of the confinement of the excitation is that the energy difference between singlet and triplet (the exchange energy) levels may also be large. Then, spin-allowed radiative emission (fluorescence) is from the singlet only. When the exchange energy is large, it is unlikely to cross-over from triplet to singlet, so that triplet excitons do not produce light emission, other than by indirect processes like triplet-triplet annihilation or by phosphorescence process.

Thus, PLED is operational when the device is biased adequately to have injection of positive and negative charge carriers from oppositely charged electrodes and capture these charged carriers resulting in photon emission through transparent electrode. The wavelength and intensity of emitted light photon is measured by the detection system, thereby the device efficiency of PLED can be calculated. **Figure 1.12** depicts the device structure showing different layers of substances used and their mode of formation during fabrication of the device.

Polymer based diodes presently are showing eye-catching device characteristics, including efficient light generation in all interesting colors, and there are several development programs being set up to establish procedures for manufacturing of these LED's. The major interest in the use of conducting polymers lies in the fact that, there is a scope for low-cost manufacturing to form a thin film by utilizing solution-processing technique. Further, these polymer light emitting diodes can be used in several devices such as digital display, lighting, TV and computer screens *etc*.
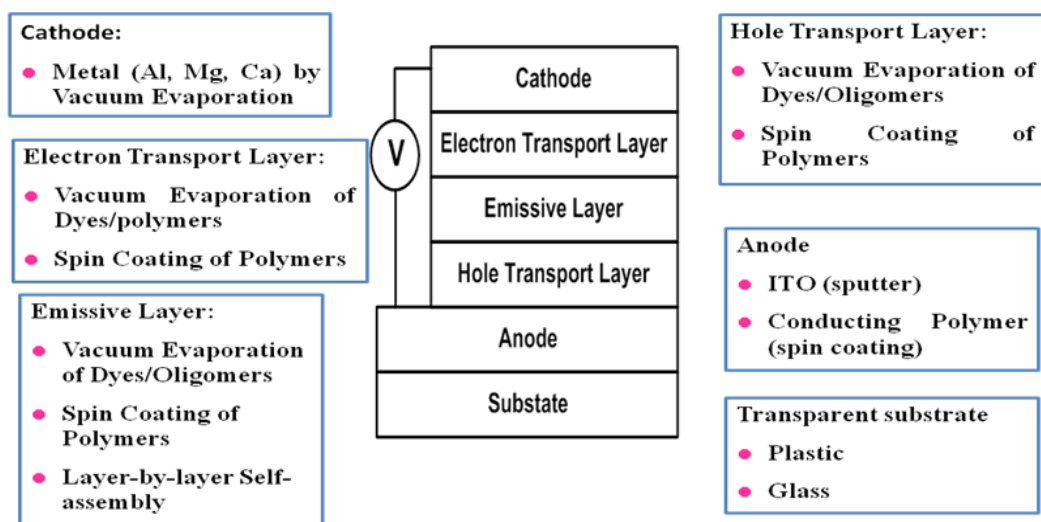
Figure 1.12: Different layers in PLEDs and their mode of formation

1.8 BROAD OBJECTIVES OF CURRENT RESEARCH WORK

Conjugated polymers, being an interesting class of organic semiconductors are important class of materials which find extensive applications in many fields, such as PLEDs, PVs, TFTs, NLOs and various types of sensors, etc. In principle, conjugated polymers should be able to show almost all the properties of inorganic semiconductors which may further lead to development of "molecular electronics".

The main advantage of these conjugated polymers over their inorganic counterparts is their easy processability during the fabrication of electronic devices. Also, their beneficial merits such as solubility, thermal stability, film forming behavior, electron transport nature, light emitting characteristics, electronic and photovoltaic properties made them potential candidates for applications in the fields of electronics and optoelectronics. Thus, it is important to note that the goal with organic polymer-based devices is not only to attain or exceed the level of performance of inorganic semiconductor technologies (silicon is still the best at the many things that it does) but also to benefit from a unique set of characteristics achieved by combining the properties of both metals and plastics.

During the past several years various types of conjugated polymers were synthesized and their optoelectronic properties were evaluated in detail. But, at the earlier stages the electronic devices fabricated using conjugated polymers showed very low efficiency due to the imbalanced charge carrying property, lack of

environmental stability, and poor film forming ability *etc*. Recently, polymer researchers focused their efforts to overcome these drawbacks by developing a new approach, called donor-acceptor strategy. In this approach, donor and acceptor moieties are alternatively arranged in the polymer chain and consequently, its HOMO-LUMO energy levels would be altered, resulting in polymer with improved charge carrying property. Thus, by the introduction of suitable donor-acceptor moieties along the polymer chain, its electronic and electrical properties can be tailored. In the literature, several donor-acceptor architectured polymers were reported with the possible applications in optoelectronic and photonic devices. However, these polymers did not achieve all the above said requirements. Still, there is a scope to investigate new donor-acceptor type polymers with novel properties such as good thermal stability, processability, favorable optical and electrochemical properties.

The present research investigation has been aimed at design, synthesis, and characterization of new donor-acceptor type conjugated polymers containing interesting scaffolds like thiophene, biphenylene, phenylenevinylene, cyanovinylene, with possible application in PLED devices. These polymers were expected to possess required electrical, electrochemical and optical properties. Further, there was a scope for modification of polymeric structure through functionalization of their monomers, which may lead to achieve desired properties in the resulting polymers. Keeping these facts in view, a detailed literature survey has been carried out and pertaining literature reviews have been highlighted in **Chapter 2**.

1.9 THESIS STRUCTURE

The whole thesis is systematically divided into **six** chapters. **Chapter 1** covers an introduction to conjugated polymers including their brief history, synthetic methods, and different properties such as optical, electrochemical and electronic behavior. It also comprises the description on different types of aromatic and hetero-aromatic based conjugated polymers. Finally, it involves a brief introduction to applications of conjugated polymers in PLED devices, followed by broad objectives. **Chapter 2** includes a detailed literature review on heterocyclic based π-conjugated polymers. Further, it comprises the scope and objectives of the present research work

derived from the literature survey carried out. At the end, design of six new series of D-A type cyanopyridine based conjugated polymers with various electron releasing and electron withdrawing substituents, *viz*. **VPPy$_{1-3}$**, **VTPy$_{1-3}$**, **PPy$_{1\sim3}$**, **TPy$_{1\sim3}$**, **TDPy$_{1-4}$**, and **Py$_{1\sim4}$**, has been described. **Chapter 3** deals with optimized synthetic protocols used for all the newly designed π-conjugated polymers belonging six series and their structural characterization using FTIR, NMR spectroscopy and elemental analyses. Also, it involves GPC analysis of the new polymers. **Chapter 4** covers a detailed investigation of photophysical, electrochemical, thermal properties of newly synthesized π-conjugative polymers. It also includes their computational studies involving HOMO-LUMO calculations. Further, the correlations between their structure and properties have been discussed. **Chapter 5** comprises a brief introduction to electroluminescence devices and fabrication studies of PLEDs using newly synthesized conjugative polymers as emissive materials. It also includes a concise discussion on the results of device studies. Finally, **Chapter 6** contains summary of the entire work carried out and important conclusions drawn from it. It also includes a brief account on the scope for future work.

LITERATURE REVIEW, SCOPE, OBJECTIVES AND DESIGN OF NEW CONJUGATED POLYMERS

Abstract

This chapter includes a detailed literature review on heterocycle based π-conjugated polymers. Further, it comprises the scope and objectives of the present research work derived from the literature survey carried out. At the end, design of six new series of D-A type cyanopyridine based conjugated polymers with various electron releasing and electron withdrawing substituents has been described.

2.1 INTRODUCTION

Conjugated polymers have attracted widespread interest during the last three decades, because of their useful electronic, optoelectronic, electrochemical and non-linear optical properties. Since these polymers show unique physical properties, significant research efforts directed to better understanding of their chemistry, physics and engineering have been undertaken. Their interesting properties, particularly electrical conductivity along with luminescence and electroluminescence behavior, are responsible for their applications as organic semiconductors in the field of organic electronics. (Ong et al. 2004, Akcelrud et al. 2003, Xue et al. 2004 and Epstein et al. 1996). Literature reports clearly reveal that, the molecular structure of conjugated polymers plays an important role in the tuning of their physical and electrochemical properties. Among various conjugated polymers, those carrying D-A type architecture are gaining much more attention in recent times. The most striking fact is that, the type and arrangement of donor and acceptor moieties in the polymer chain can lead to remarkable enhancement in the electronic and photonic properties of them.

2.2 LITERATURE REVIEW

In recent years several donor-acceptor type conjugated polymers were designed and synthesized for varied applications. The systematic approach for designing such polymers includes selection of appropriate donor and acceptor scaffolds and incorporating them into the main/side chain in order to achieve the expected properties in the resulting macroscopic assembly.

In the following section, a brief description on literature reports available on the important donor-acceptor type conjugated polymers carrying different types of moieties have been highlighted. These reported polymers mainly consist of interesting heteroaromatic/aromatic systems such as thiophene, naphthalene, pyrazole, phenylene, pyridine, fluorene, oxdiazole as electron donor groups and 1,3,4-oxadiazole, cyanovinylene, cyanopyridine and cyclicdiimide as strong electron acceptor units in their chains. Further, their synthetic methodologies and their structure-property relationships, particularly with respect to physical, optical, and electrochemical properties have been outlined.

2.2.1 Pyridine based conjugated polymers

Different types of nitrogen heterocycles are incorporated into various conjugated polymer backbones in order to tune their optoelectronic and photonic properties. Amongst a variety of heterocyclic systems, pyridine plays an important role as it is a strong electron accepting ring. Some of the most extensively studied conjugated structures carrying the pyridine moiety include poly(2,5-pyridine), poly(3,5pyridine), poly(*p*-pyridylene vinylene)s and poly(phenylene vinylene pyridylene vinylene)s (Akcelrud et al. 2001). Also pyridine containing polymers showed enhanced donor-acceptor nature with good optical limiting threshold (Wang et al. 2006). A brief account on some of the selected literatures available on pyridine based conjugated polymers are presented below.

In an interesting study, Wang et al. (2006) synthesized three new donor acceptor conjugated polymers (**S-1** to **S-3**) derived from 3,5-dicyano-2,4,6-tristyrylpyridine through the Knoevenagel reaction. The polymers showed good solubility in common organic solvents and high molecular weight. Their UV-vis. absorption maxima were found to be 417, 443 and 448 nm, respectively and photoluminescence was observed at 596, 564 and 570 nm, respectively. From the results of their optical power limiting study, the authors concluded that fluorene containing conjugated polymer emerged as good optical power limiter with the power limiting value 728 m J/cm^2.
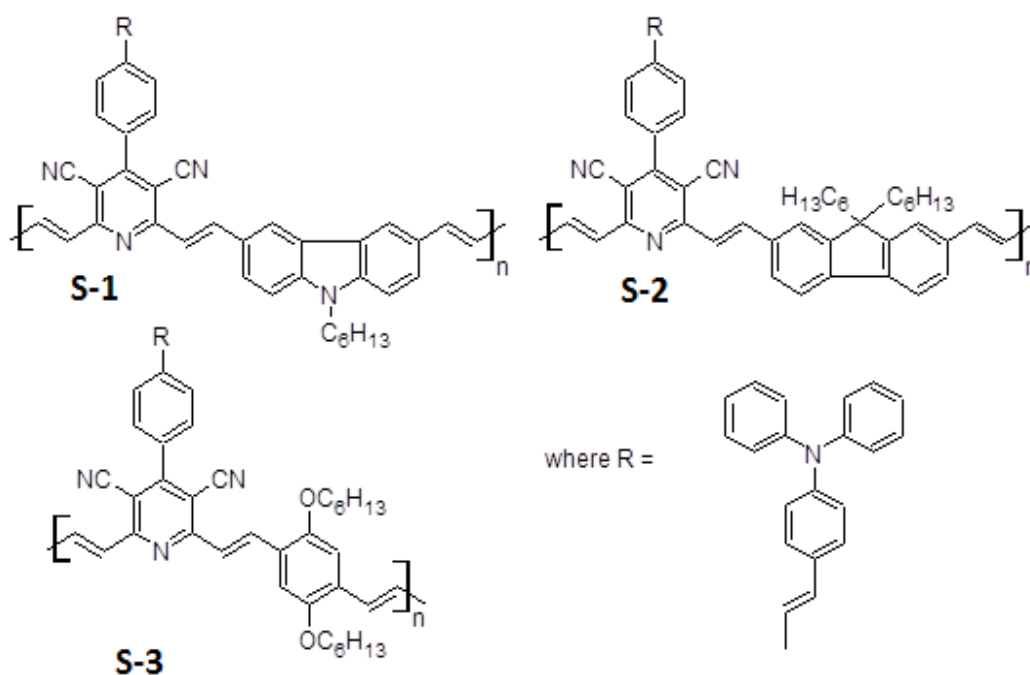
An interesting class of new 2,4,6-triphenylpyridine based conjugated polymers (**S-4** and **S-5**) containing fluorene or carbazole moiety were synthesized by Mikroyannidis et al. in the year 2009 *via* Heck coupling. According to authors, the polymers showed good thermal stability with the degradation temperature around 300 $^\circ$C. Presence of 2,4,6-triphenylpyridine units along the polymer backbone caused a partial interruption of the π-conjugation. The polymers emitted blue-green light with emission maxima at 446-464 nm and showed quantum yields of 0.52 and 0.28 in THF solution, respectively. Their electroluminescence spectra showed a strong red shift to its emission maxima, which might be attributed to the direct cross recombination transition between electrons and holes trapped on carbazole or triphenylpyridine subunits. They showed good efficiency in electroluminescence devices with luminescence of 647 and 615 cd/m^2.
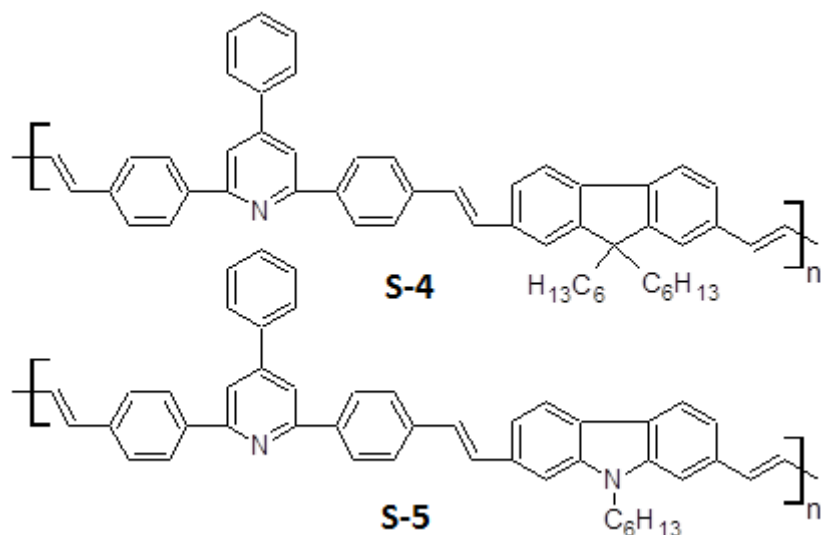
In another research publication, three new donor acceptor type conjugated polymers (**S-6**) bearing 3,4-dialkoxythiophene and (1,3,4-oxadiazolyl)pyridine moieties were designed and synthesized by Hegde et al., through poly-condensation method (Hegde et al. 2009). The authors reported good thermal stability with the onset decomposition temperature up to 300 ºC for them. The absorption maxima of the polymers were found in the range of 342-360 nm. Further, they were shown to display bluish-green fluorescence in solution state and their band gaps were determined to be about 2.55 eV. They were found to be good NLO materials with x^3 values 0.881×10^{-12}, 0.901×10^{-12}, 1.03×10^{-12}esu, respectively.
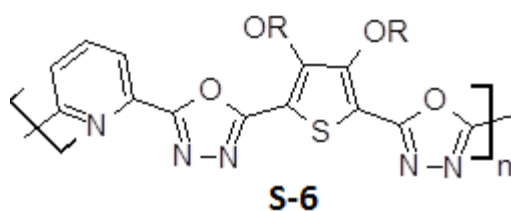
where R = C$_3$H$_7$, C$_5$H$_{11}$, C$_7$H$_{15}$

Sonar et al. (2004) reported two new pyridine based conducting polymers with fluorene and indofluorene units in the main chain (**S-7** and **S-8**). The polymers displayed reduction potentials about 0.5 V lower than that of the corresponding fluorene and indenofluorene homo polymers, indicating much improved electron-accepting properties. Light emitting diodes, fabricated using these polymers as the emitting layers produced blue-green emission with low turn-on voltages with aluminum electrodes confirming their improved electron affinity. While, the

indenofluorene polymer showed an irreversible red shift in emission at high voltages, which is attributed to oxidation of the indenofluorene units.

S-7

S-8
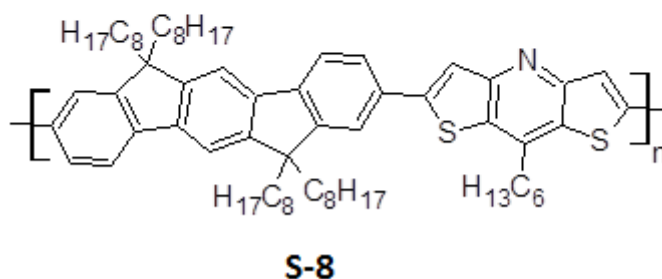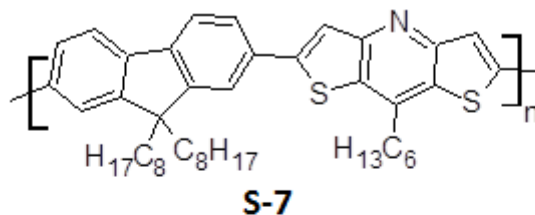
Choon et al. (2001) evaluated the optical and electrochemical properties of a novel polymer (**S-9**) containing poly(2,5-dialkoxy-1,4-phenylene-*alt*-2,5-pyridine) functionalized with alternating donor/acceptor repeat units. The polymer was synthesized using Suzuki-coupling reaction. Study of optical properties of the polymer revealed that, the absorption maxima and band gap of it are 383 nm and 3 eV, respectively. Further, it was found that the polymer is facile *n*-doping and good electron transporting material due to the presence of electron-withdrawing pyridine unit. The polymer displayed bathochromic shift when protonated with trifluoro acetic acid in chloroform solution.

S-9
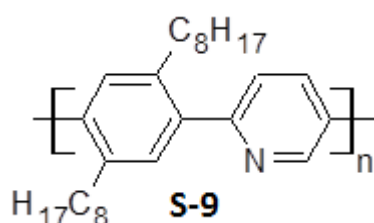
Recently, Hemavathi B et al. (2015, 2016) synthesized two new D-A configured conjugated polymers (**S-10**) containing highly electron withdrawing cyanopyridine scaffold. In these polymers cyanopyridine is linked with two phenylene systems as donors at positions 4 and 6 and electron withdrawing cyano group at position 3. Here, *p*-phenyl vinylene acts as a spacer in between two cyanopyridine heterocyclic systems. These polymers were prepared in good yield

following Heck polymerization method. They were considered to be potential candidates for electroluminescence and photovoltaic (PV) devices.
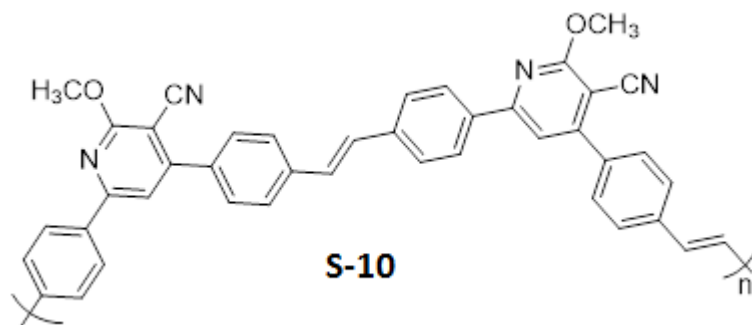
On the basis of literature reports, it can be concluded that introduction of electron withdrawing pyridine nucleus in the polymer backbone enhances the thermal stability and solubility of the resulting polymer. Also, presence of electron withdrawing pyridine hetero-cycle in the polymer chain influences the optical and electrochemical property. Further, cyanopyridine being a fluorescent chromophore with electron withdrawing property enhances the fluorescence emission maxima of the polymer if it is connected adjacent to the highly electron releasing systems. However, very few reports are available in the literature on synthesis of cyanopyridine based conjugative polymers.

Keeping the above facts in view, it has been planned to introduce the cyanopyridine moiety as one of the main electron withdrawing units next to electron releasing aromatic/heteroaromatic system/s, in the design of new polymers, with the hope that the resulting D-A type polymers would possess good fluorescent emission and thermal stability.

2.2.2 Thiophene based conjugated polymers

Literature survey reveals that thiophene based conjugated polymers are currently under intense investigations. Such polymers are promising materials for optoelectronic properties, due to their easy processability, chemical stability, readiness to functionalization, good film forming ability, optical transparency, adequate mechanical strength and solubility in common organic solvents (Elsenbaumer et al. 1986 and Miller et al. 1986). According to the latest reports, optical and electrochemical properties can be synthetically tuned in D-A type poly(thiophene)s by

incorporating proper electron releasing and electron accepting segments in the polymer chain. This would result in improved delocalization in the molecule and hence cause the enhancement of the required properties.

In an important study, (Zhang et al. 2009) synthesized a conjugated polymer (**S-11**) with thiophene as repeating unit *via* palladium (0)-catalyzed Stille coupling reaction. Molecular weight of the polymer was found to be 62000 Da. The synthesized polymer exhibits good thermal stability with decomposition temperature of 340 °C and glass-transition temperature of 136 °C. Also, it shows strong absorption peak at 505 nm in dilute solution and 518 nm in thin film with an optical band gap of 2.0 eV. Also, it exhibits intense emission peak at 550 nm in solution and 603 nm in film state. Cyclic voltammetric study revealed that the HOMO and LUMO energies of the polymer were −5.4 and −3.4 eV, respectively. Polymer solar cells were fabricated based on the blend of the polymer. The authors observed the power conversion efficiency of 0.7 % with polymer: PCBM (1:4, w/w) as active layer.

S-11
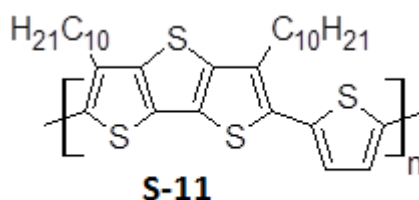
In another study, (Yu et al. 2009) synthesized two-dimensional polythiophene (**S-12**) carrying alkyl-thiophene side chains by Stille coupling reactions. Optical measurements indicated that the band gap of these polymers were in the range of 1.98-1.77 eV. In the study, the power conversion efficiency (η) of the polymers were found to be about 2.5 % under simulated solar illumination (AM 1.5 G, 100 mW) from a polymer solar cell comprising an active layer containing 25 wt % polymer and 75 wt % (6,6)-phenyl-C71 butyric acid methyl ester (PC71BM).

S-12
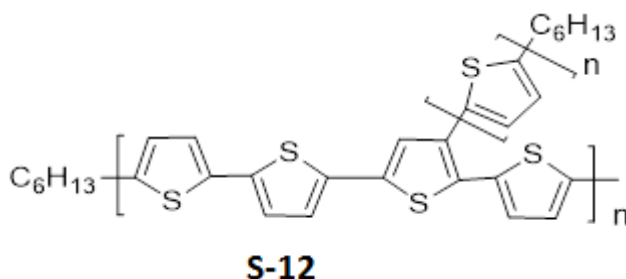
A research group led by Baek, in an attempt to obtain low bandgap material, synthesized a new thiophene/phenylene vinylene-based conjugated polymer (**S-13**) from simple alkoxythiophene derivative (Baek et al. 2009). In solution state, the polymer showed an absorbance in the range of 400-600 nm and, exhibited bandgap energy of 1.8 eV. Its UV-vis absorption and PL emission maxima in solid state were red shifted when compared to that of its solution. This bathochromic shift is resulted from the closer intermolecular electronic interactions in the solid state. However, the polymer displayed slightly higher power conversion efficiency (PCE, 0.30 %) of photovoltaic device, fabricated using this polymer with (6,6)-phenyl-C61-butyric acid methyl ester (PCBM) than that of reported PCE (0.15 %) devices fabricated in the same configuration.
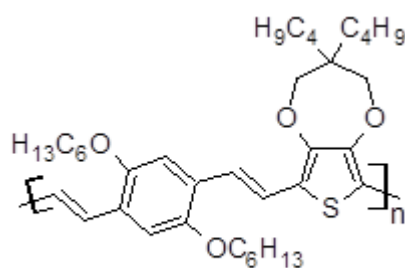
S-13

Yu and coworkers synthesized thiophene based third-order nonlinear optical polymers *via* Stille poly-condensation reaction. These poly(1,4-phenylene-2,5-thiophene)s **S-14**, were soluble in common organic solvents and they exhibited high thermal stability. Also, polymers showed good third order nonlinear optical properties with succeptebility ($\chi 3$) values of value of 1.77×10^{-13} esu. This was determined in chloroform solution with a concentration of 0.527 g/L using degenerate four-wave mixing.

where n = 4, 8, 12, 16
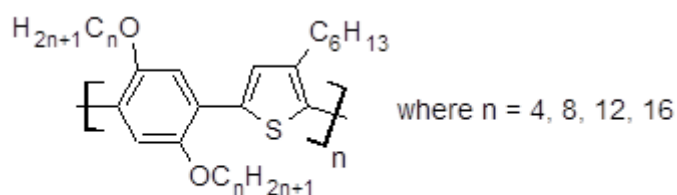
S-14

A research team, Chen et al. (2010) designed and synthesized three novel conjugated polymers (**S-15**), *via* the alternative copolymerization of the electron-

donating monomer benzodithiophene (BDT) and three different electron accepting monomers. Amongst them, naphthalenediimide (NDI) based conjugated polymer exhibited very low bandgap of 1.63 eV with HOMO and LUMO energy levels –5.62 and –3.99 eV respectively. The results suggested that, the absorption range and the electrochemical properties of the conjugated polymers can be tuned by appropriate structure-tailoring, which would help in exploring ideal conducting polymers for potential applications in polymer optoelectronics, especially in polymer solar cells.

where R = ethylhexyl

S-15
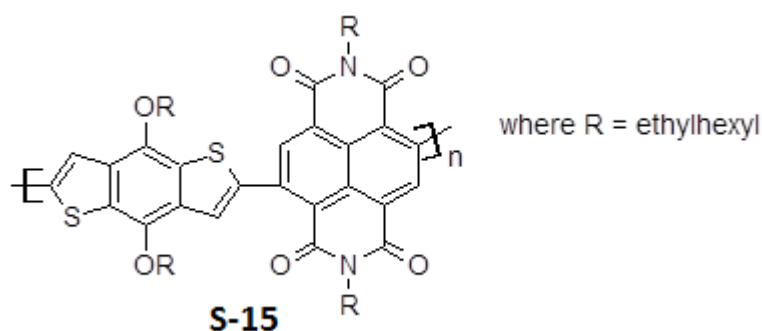
Interesting new poly(3-alkoxythiophene) (P3AOT) derivatives were synthesized with octoxyl, dodecaoxyl (**S-16**) and 4-nitro-benzyloxyl (**S-17**) as side-chains (Yanamo et al. 2010) as potential optical limiting materials. The absorption spectra of polymers indicate that, length of the side groups affect the electrochemical and optical band gap of poly(thiophenes). The nonlinear optical (NLO) properties of these polymers were investigated using Z-scan method. The third-order NLO susceptibility (χ^3) of these polymers showed that the optical nonlinearity has a strong dependence on the length of the alkoxyl side chains and polarity of polymers, which affect the intra- and intermolecular charge transfer process. So this type of poly(thiophene) derivatives can be used in optical limiting devices.

where R = octyl, dodecyl

S-16   **S-17**
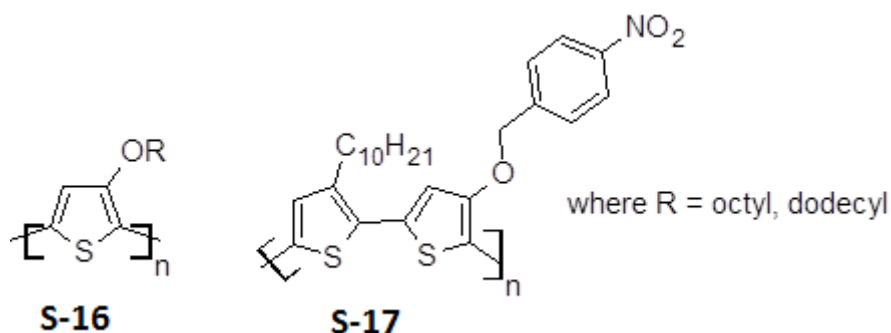
Three novel conjugated polymers (**S-18** to **S-20**) comprised of 2,5-dioctyloxy-1,4-phenylenevinylene and terthiophene derivatives with / without di(*p*-tolyl)phenylamine (TPAV) and oxadiazole (OXD) side groups (Chen et al. 2010) were synthesized *via* the Witting-Horner reaction. The introduction of TPAV and OXD side chain has enhanced the optical properties. The polymer with triphenyl amine substitution showed low bandgap compared to the remaining. The photovoltaic cells were fabricated using these polymers containing the donors and (6, 6)-phenyl-C61-butyric acid methyl ester (PCBM) as the acceptor in a 1:4 weight ratio. The device based on polymer with triphenylamine substitution displayed maximum power conversion efficiency of 1.75 % under simulated AM 1.5 G solar irradiation (100 mW/cm^2).
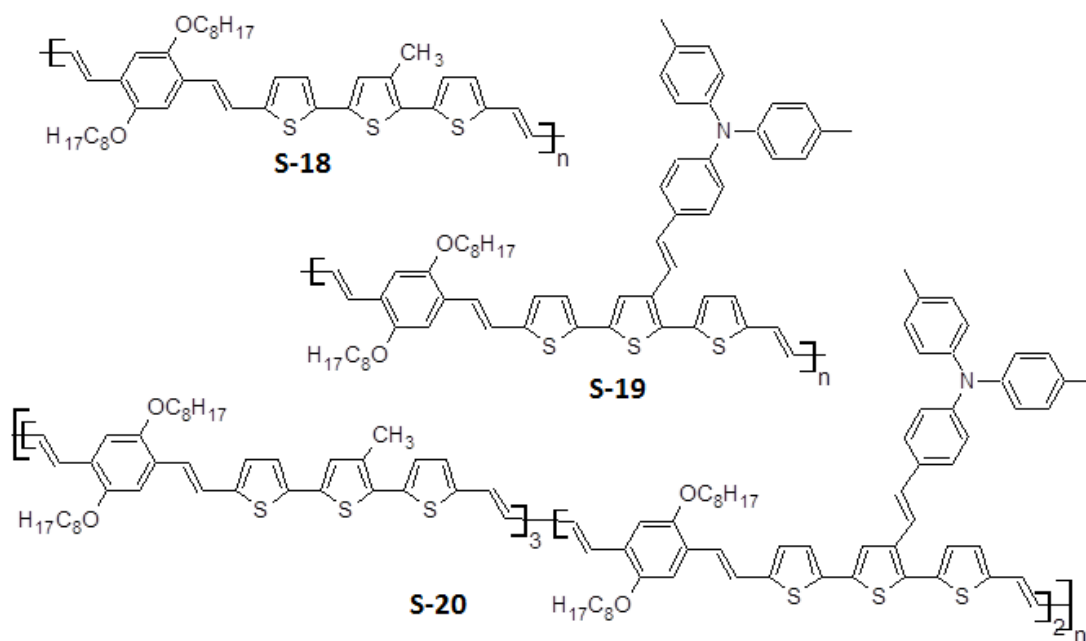
In a quest for new OFET materials, Schroeder et al. 2011 synthesized two novel thiophene based conjugated polymers (**S-21** and **S-22**) with benzotrithiophene (BTT) moiety in their backbone. These two polymers showed promising organic field-effect transistor (OFET) performance. The authors found that, the choice of co-monomer is very important in determining the inter-chain interaction and polymer solubility. According to them, regio-random nature of the alkyl-bearing BTT unit is quite remarkable and these polymeric materials are very good semiconductors. Despite molecular disorder introduced by a branched solubilizing alkyl chain and a

region-random polymerization of the asymmetric benzotrithiophene unit, these co-polymers exhibit hole mobility as high as 0.24 cm^2/(V s).
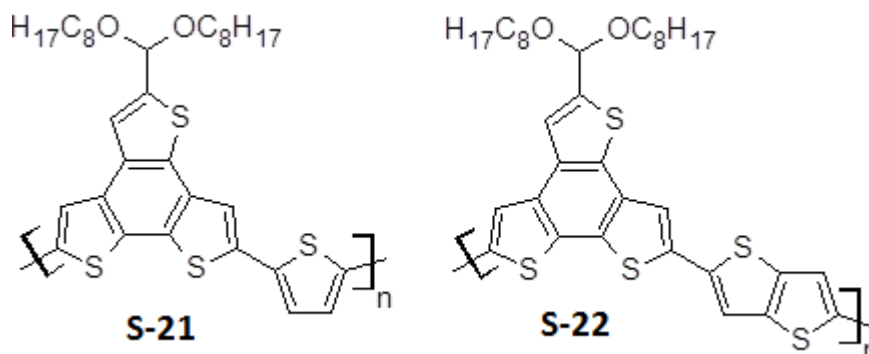
A series of low band gap conjugated polymers (**S-23** and **S-24**), consisting of alternating 3,4-dodecylthienothiophene-2-carboxylate with one/two thiophene rings were synthesized by Myung-Jin et al. (2010) *via* Gilch polymerization technique. The bandgap and HOMO energy levels of these polymers were found to be 1.58/1.61 and –5.15/–5.20 eV, respectively. Here, introduction of thiophene units along the polymer back bone reduced the band gap. Photovoltaic devices were fabricated using DTT-T2 and a fullerene derivative (PCBM), and whose power conversion efficiency was 0.21 % under the illumination of AM 1.5 (100 mW/cm^2). They found that the introduction of thiophene ring increased the conjugation path length, solubility as well as the power conversion efficiency.
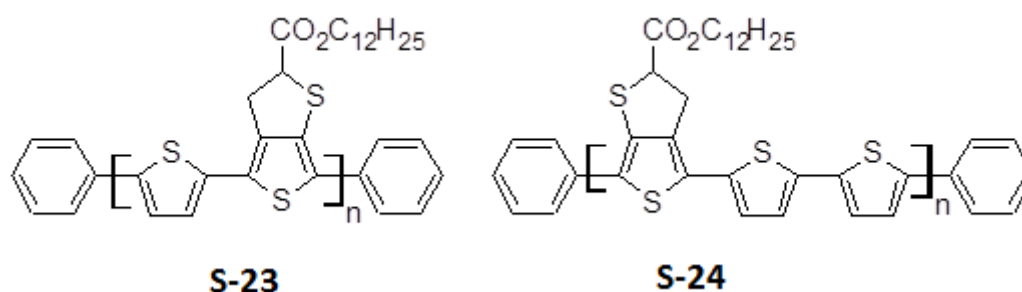
Yu et al. (1998) synthesized a new light-emitting polymer (**S-25**) carrying alternating segments of 3,3c-didecyl-2,2c-bithiophene and 2,6-bis(1,3,4-oxadiazolyl)-toluene, which are *p*-dopable and *n*-dopable, respectively. Synthesized polymer was found to be electro-active, both in the cathodic region and in the anodic region. Further, it showed green emission in its film state and displayed strong solvatochromism both in absorption and emission processes.

S-25
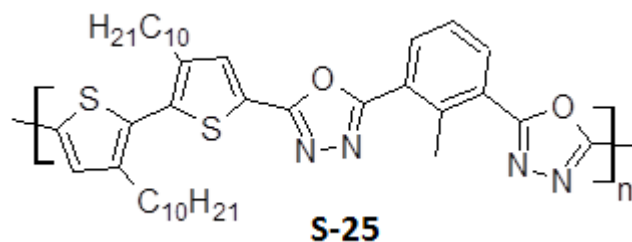
In an interesting study, Liang et al. (2009) synthesized a new regio-regular polymer (**S-26**) containing a thieno(3,4-b)thiophene segment. The presence of thieno(3,4-b)thiophene extends the absorption of the polymer molecule to longer wavelength region. The polymer showed higher solar energy conversion efficiency in bulk heterojunction (BHJ) solar cell. The polymer displayed a strong absorption peak at 575 nm in thin film with an optical bandgap 1.62 eV and exhibited intense fluorescence emission at 800 nm. The HOMO energy level of the polymer was found to be –4.92 eV.

S-26
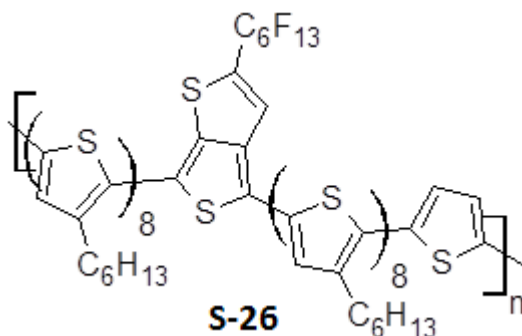
A series of novel conjugated polymers (**S-27**) comprised of 9,9-dihexylfluorene and thiophene or substituted thiophene moieties (Pal et al. 2007), was synthesized *via* the palladium-catalyzed Suzuki coupling reaction. In their design, both electron-donating and electron withdrawing substituents were incorporated. The steric effects of the bulkier substituents influenced the absorption and photoluminescence properties of the polymers. These polymers showed good solubility and thermal stability. Polymer having ester substitution on thiophene ring displayed low band gap compared to other polymers.
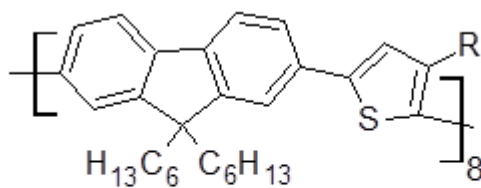
S-27

where R = C_6H_{13}, $-CH_2OC_6H_{13}$, $-COOC_6H_{13}$, $-CN$

Zoombelt et al. (2008) synthesized three new low band gap conducting polymers (**S-28**) carrying alternating dithiophene and thienopyrazine units *via* Yamamoto coupling polymerization. The polymers showed an optical band gap of about 1.3 eV in the solid state. The solubility of the polymer was achieved by varying the chemical nature of the side chains. These polymers showed good solar cell performance with short-circuit currents of 5.2 mA/cm^2. An efficiency of 0.8 % was achieved under estimated standard solar light conditions, (AM 1.5 G, 100 mW/cm^2) with spectral response up to 950 nm.
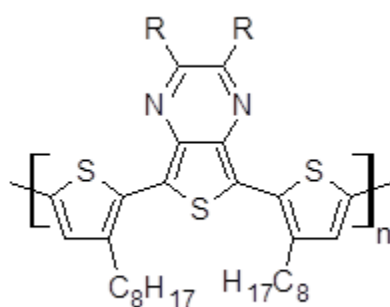
where R = ethylhexyl, octyl

S-28

In 2007, Bundgard's research group synthesized interesting thiophene based conjugated polymers (**S-29** and **S-30**) with benzothiazole and benzothiadiazole as acceptor units. According to authors, incorporation of 3,7,11-trimethyldodecyl side chains brings about solubility and better film forming properties than the use of 2-ethylhexyl, hexyl, or dodecyl as side chains. The HOMO and LUMO levels were determined to be –5.2 and –3.6 eV, respectively with a band gap of 1.65 eV for benzothiadiazole containing polymer (**S-29**) and at –5.1 and –4.4 eV for benzo-bisthiadiazole containing polymer (**S-30**). The electrochemical results indicate that,

these acceptor units effectively lower the LUMO level of the polymer keeping the HOMO level more or less constant. These polymers showed good photovoltaic performance in devices.

S-29   **S-30**
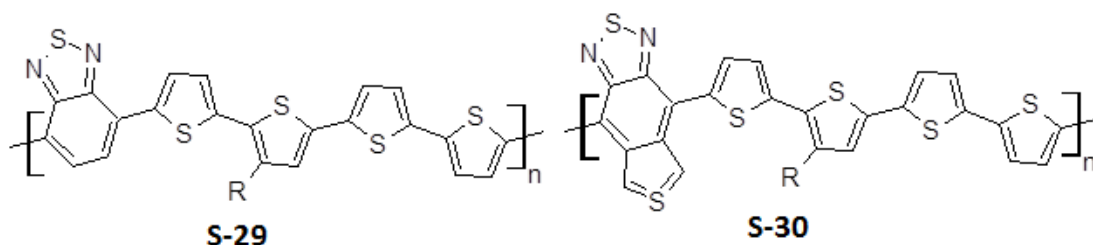
where R = 2-ethylhexyl, hexyl, or dodecyl

Three new conjugated polymers (**S-31** to **S-33**) carrying electron accepting benzothiadiazole and electron donating alkoxythiophene were synthesized by Wienk et al. (2006). Here, presence of alkyloxy side-chains resulted in enhancement of electron donating nature of the thiophene ring with increased solubility of the polymers. The optical band gap of polymer **S-21** was found to be 1.55 eV in the solid state. This polymer was further modified, using a different type of acceptor unit, *i.e.* a diphenylthienopyrazine unit. Then, the bandgap of the polymer **S-22** decreased to 1.28 eV. Also, they observed the shift in the HOMO and LUMO levels of the polymers when the alkyl chains were replaced by phenyl groups. Its band gap was found to be 1.20 eV in thin film.

S-31   **S-32**   **S-33**
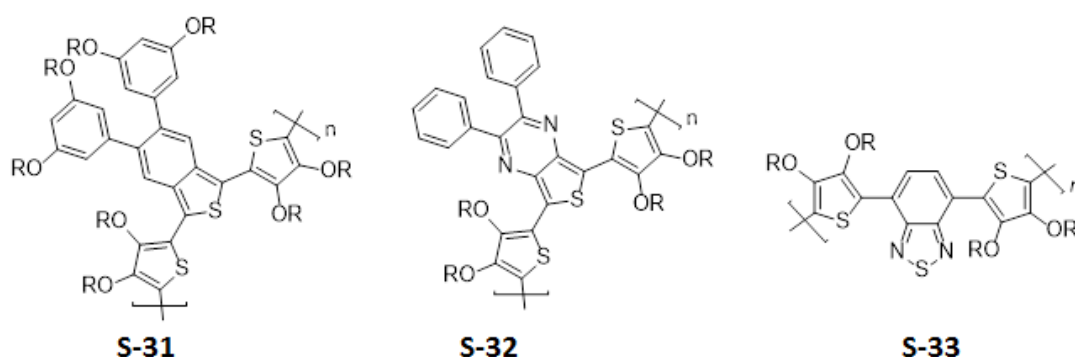
In an interesting study, two new conjugated poly(thiophene)s, *i.e.* 3,4-diphenyl substituted poly(thienylene vinylene)s (DP-PTV) (**S-34** and **S-35**) were synthesized (Chan et al. 1998) *via* dithiocarbomate route. The authors reported that, these polymers possess band gap in the range of 1.7 to 1.8 eV and good stability up to 400

°C. As per the report, the solubility of the polymer can be improved by attaching the alkyl side chains into the phenyl group on 3,4-diphenylthiophene ring of the polymer backbone.
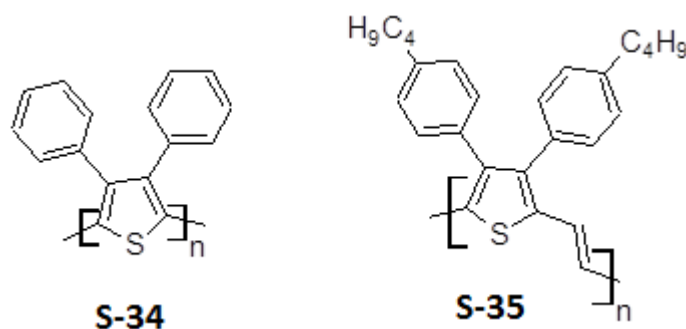
In a pioneering work, Shin et al. (2007) developed the synthetic method for a new low bandgap D-A type conjugated polymer (**S-36**) based on 3,4-disubstituted thiophene. In this molecule, alkoxy thiophene functions as a donor and benzothiazole acts as an acceptor. Due to the high electron releasing capacity of thiophene and withdrawing nature of benzothiazole, the HOMO and LUMO energy levels of these polymers were found to be –4.82, –3.7 eV, respectively. The optical bandgap of the polymer was determined to be 1.5 eV and it was used in bulk hetero junction solar cell.
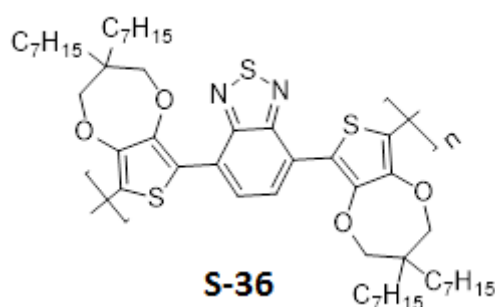
Thus, literature survey on the thiophene based conjugated polymers reveals that, introduction of thiophene ring in the polymer main chain or side chain enhances the stability, charge carrying nature, linear/nonlinear optical behavior, and optoelectronic properties, thereby reducing the band gap. Keeping this in view, in the present work it has been planned to design new thiophene based donor-acceptor type conjugated polymers carrying thiophene units as electron rich segments along with the other electron deficient moieties with the hope that the resulting polymers would

show improved solubility, charge carrying potential, optical, electrochemical and EL properties.

2.2.3 Cyanovinylene based conjugated polymers

It has been well-established that, cyanovinylene based conjugated polymers possess very good electroluminescence properties and hence they are suitable as hole-injecting and electron transporting materials (Bradley et al. 1993). These polymers are generally synthesized *via* Knoevenagel condensation between aromatic diacetonitrile and corresponding aromatic dialdehydes.

Conjugated polymers based on cyanovinylene groups are known for their low bandgap. Since cyano group is a good electron-accepting unit, its presence along with electron donor system in a polymer chain makes it strongly *p*-type. Such polymers offer various attractive features for use in a variety of device architectures like thin-film transistor (TFT), Light Emitting Diodes (LED), Non Linear Optical devices (NLO), Photovoltaic cells *etc*. Some of the selected literature reports on D-A type polymer containing cyanovinylene units as a strong electron acceptor are given below.

Colladet et al. (2007) synthesized a series of new D-A type conjugated polymers (**S-37** and **S-38**) carrying bis(1-cyano-2-thienylvinylene)phenylene in the main chain, *via* oxidative polymerization using $FeCl_3$ as oxidizing agent. They reported that, the polymers are readily soluble in common organic solvents because of the presence of alkyl and alkyloxy side chains. Absorption maxima of these polymers were found to be 720 and 780 nm respectively. Optical and electrical properties showed that their band gaps are 1.72 and 1.59 eV, respectively. These low bandgap polymers blended with PCBM showed efficient charge transfer, which was confirmed by photo luminescence studies.
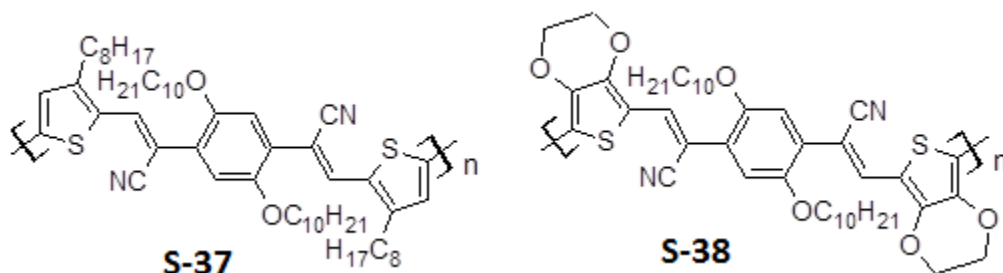
A new electroluminescent conjugated polymer (CN-P3PV) (**S-39**) containing cyano groups as electron withdrawing units was synthesized (Wu et al. 2001) and studied for its optoelectronic properties. It showed high thermal stability ($T_d \sim 360$ °C, $T_g \sim 151$ °C), high electron affinity, and good film forming ability. Electrical characterization of a double-layer organic LED on the structure of ITO/CuPc/CN-P3PV/Ca/Ag displayed high electron transporting ability and good electroluminescence performance with the emission of bright orange light.

S-39
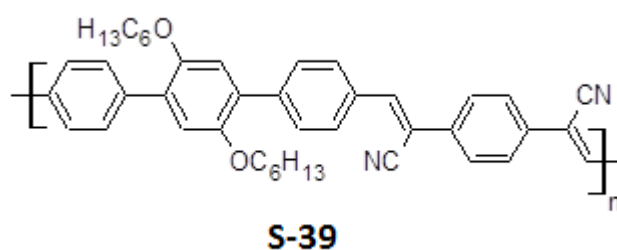
An interesting class of low band gap cyanovinylene based polymers (**S-40** and **S-41**) were designed and synthesized by Galand and his co-workers using Knoevenagel condensation method (Galand et al. 2006). The authors introduced linear and branched alkoxy chains in the backbone to increase the solubility and film forming ability of the polymer. A blue shift in absorption spectra was observed when linear alkoxy chain was replaced by a branched chain in the polymer side chain. Their optical band gap is in the range of 1.70-1.75 eV. They showed significant photovoltaic performance of 0.4-0.5 %, when used as electron donors and combined with an electron acceptor such as (6,6)-phenyl C61-butyric acid methyl ester (PCBM) in bulk heterojunction photovoltaic devices.

S-40   **S-41**
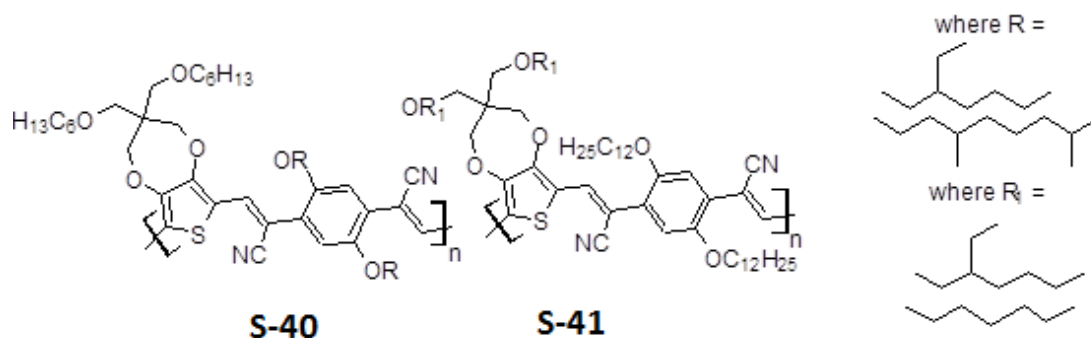
Kim et al. (2003) reported the synthesis and optoelectronic properties of a new poly(*p*-phenylenevinylene) derivative (**S-42**) carrying pendent 1,2-diphenyl-2-cyanoethene unit following Heck coupling reaction. In this polymer, electron withdrawing pendant (1,2-diphenyl-2-cyanoethene) unit is linked to main chain through linear 1,6-hexamethylenedioxy chain. Its band gap figured out from the UV-vis spectrum was 2.10 eV and photoluminescence (PL) maximum appeared at 582 nm. Their HOMO and LUMO energy levels were found to be –4.99 and –2.89 eV from the cyclic voltammetry and the UV-vis spectral studies, respectively. A single layer EL device based on this polymer has an efficiency of 0.114 cd/A. These results indicate that the pendent 1, 2-diphenyl-2-cyanoethene (CNST) unit is a good electron transporting material.

S-42
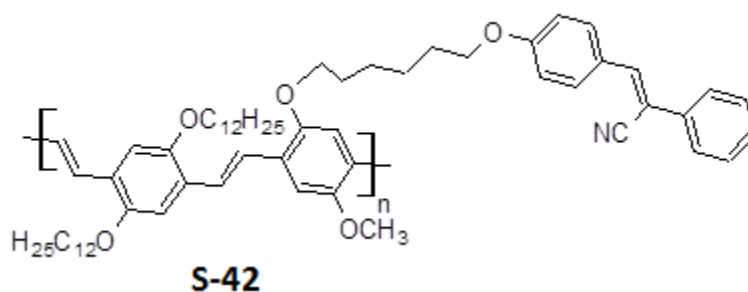
Zou et al. (2009) designed three new D-A type conjugated polymers (**S-43 to S-45**) containing cyanovinylene group and a triple bond in the main chain for their applications in photovoltaics. The new design resulted in increase in their reduction potentials. Their absorption maxima were found to be 453, 431 and 512 nm, and the observed bandgaps are 2.03, 2.02, and 1.7 eV, respectively. Because of their high absorption range and good electron acceptor nature, they are most suited for solar cell applications.

S-43

S-44

S-45
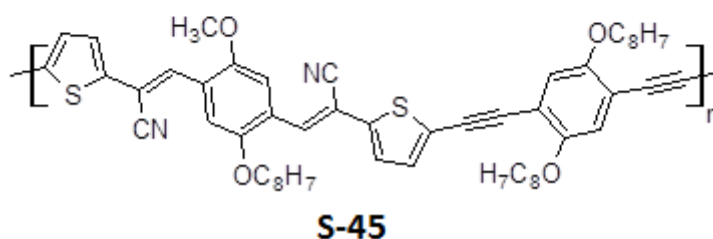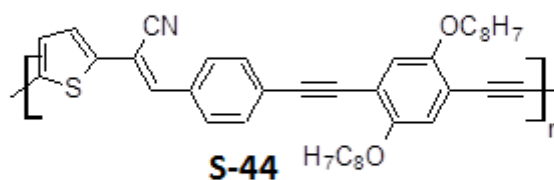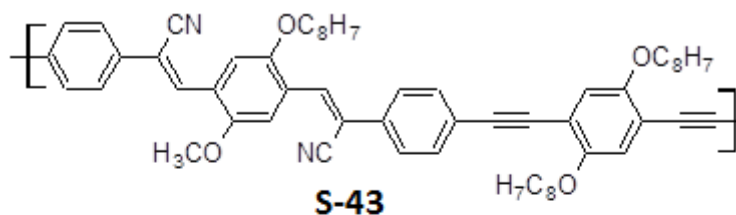
Colladet and his group (2007) synthesized interesting two cyanovinylene based conjugated polymers [**S-46** and **S-47**] carrying bis(1-cyano-2-thienylvinylene)phenylene in the polymer chain. The polymers have been synthesized through oxidative polymerization using an oxidizing agent, $FeCl_3$. The newly synthesized polymers possess good solubility in common organic solvents because of the presence of long chain alkyl and alkoxy side chains. In their UV-Vis spectra, absorption maxima of these polymers were found to be 720 nm and 780 nm, respectively. Their optical and electrical properties indicated that the band gaps of these polymers are 1.72 eV and 1.59 eV, respectively. These low band gap cyanovinylene based polymers, when blended with PCBM exhibited an efficient charge transfer phenomena, which was confirmed by electroluminescence device studies.

S-46

S-47
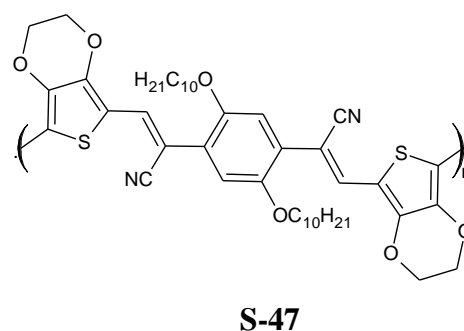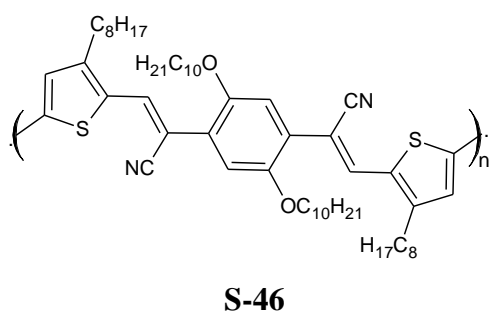
In 2010, Pramod Kumar Hegde et al. reported a new poly(thiophene) **S-48** linked with cyanophenylne vinylene units using Knovenagel condensation technique. The red colored conjugative polymer has a well-defined structure, high thermal stability and a narrow band gap of 1.78 eV. It shows green fluorescence emission in solution state as well as in film form.
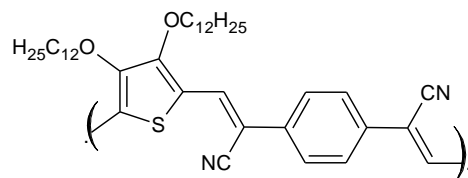
S-48

A new cyanovinylene polymer derived from 3,4-dialkoxy thiophene **S-50** was synthesized by Manjunatha et al. (2009) following multistep reaction schemes. The polymer **S-50** was shown to be thermally stable up to 300℃ under nitrogen atmosphere. Its optical and charge-transporting properties were investigated by UV-visible, PL spectroscopic and CV studies. The monomer **S-49** emits intense green-light in solution state and the corresponding polymer **S-50** exhibits bright red-fluorescence in solution as well as solid state. The fluorescence quantum yield of the newly synthesized polymer was found to be 43%. CV studies reveal that the polymer possesses good charge carrying ability. The electrochemical band gap was estimated to be 1.8 eV. The studies indicate that the new cyanovinylene polymer **S-50** is a promising candidate for the development of efficient optoelectronic devices. The electrochemical properties showed that the polymer possesses high-lying HOMO energy level (-5.53 eV) and low lying LUMO energy level (-3.73 eV). The energy barrier between the emitting polymer and electrode was determined be -0.16 eV.
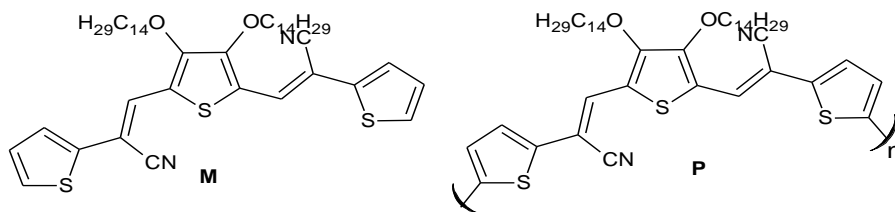
S-49

S-50

From the preceding account, it is clear that the polymers containing cyanovinylene units in the backbone possess very low band gap and hence they can be

employed in the polymer solar cells as emissive materials. Further, incorporation of cyanovinylene units would improve the optoelectronic property of the conjugated polymers. In view of this, it has been contemplated to design the new conjugative polymers with cyanovinylene as potent electron accepting unit in the polymer main chain.

2.2.4 (*p*-Phenylenevinylene) (PPV) based conjugated polymers

Poly-(*p*-phenylenevinylene) (PPV) is an interesting material for electro-optical applications. This was the first electro luminescent polymer that showed green yellow emission. It possesses good thermal stability with high photoluminescence efficiency. However, it is insoluble and infusible making it difficult to fabricate into thin films. Interestingly, incorporation of alkyloxy or alkyl as side chains into these PPV derivatives makes them soluble in common organic solvents and it enhances the optical and electrochemical properties of the polymers (Akcelrud et al. 2001). Also, these polymers showed excellent nonlinear optical response in their film state (Samoc et al. 1998).

Junjian et al. (2008), in an approach to develop new materials for LEDs, synthesized two new conjugated polymers (**S-51** and **S-52**) containing triphenyl amine-substituted poly(*p*-phenylenevinylene) derivatives through Wittig-Hornor reaction. UV-vis absorption spectra of these polymers showed absorption maxima at 348 and 478 nm, respectively in their film state. The optical band gaps of these copolymers were found to be 2.8 and 2.25 eV, respectively. Polymer light-emitting diodes fabricated by these polymers showed the maximum luminance of 3003 cd/m^2 at 10 V.

whre R = triphenyl amine
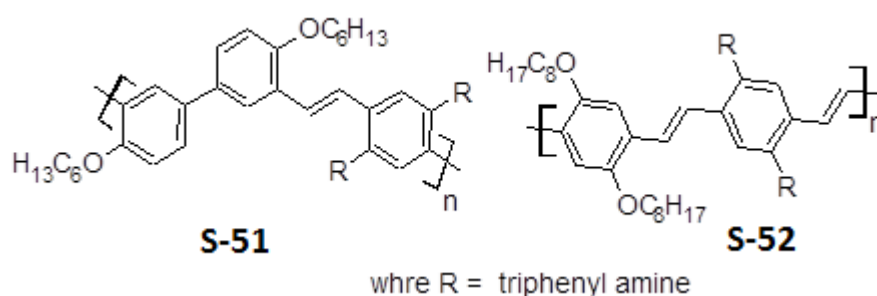
Novel poly(*p*-phenylenevinylene) derivatives (**S-53**) with an electron-withdrawing cyano-phenyl group on the polymer backbone, synthesized by Seung et al. *via* the Gilch polymerization (Seung et al. 2002) were shown to be good electroluminescent materials. The polymers displayed thermal resistance up to 400 °C and showed high glass transition temperature (T_g above 180 °C), rendering that electroluminescence (EL) devices constructed from these polymers thermally stable. Here, presence of electron-withdrawing cyano-phenyl group lowered the HOMO and LUMO energy levels to that of common PPV derivatives. PLED device constructed from these polymers exhibited good electroluminescence at 546 and 516 nm, respectively.

S-53
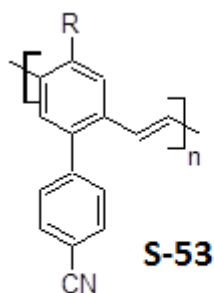
where R = ethylhexyloxy, dimethyl octylsilyl

Kim et al. (2001) demonstrated that, the newly synthesized poly(*p*-phenylenevinylene) derivatives (**S-54** and **S-55**) carrying hole transport carbazole as pendent through Gilch polymerization technique, are very good donor materials in PLED. Electroluminescence spectra of these polymers revealed that, the polymer containing alkoxy side chain is yellow-green light emitter (**S-54**) (530 nm) and that of other polymer (**S-55**) is green light emitter (490 nm), maximum luminance of alkoxy substituted polymer was found to be 30390 cd m^2 at an electric field 1.50 MV cm^{-1}.

S-54   **S-55**
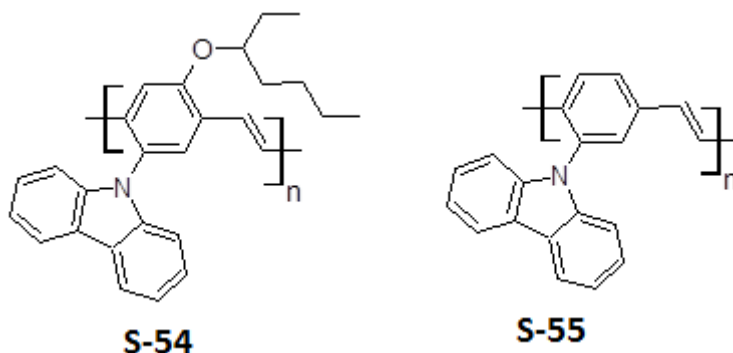
Babudri and co-workers (Babudri et al. 2003) synthesized a polymer carrying tetrafluoro and dialkoxy-substituted poly(*p*-phenylenevinylene) (PPV) with a high percentage of fluorinated units, *via* Stille cross-coupling reaction. The polymer showed good third order nonlinear optical activity with enhanced susceptibility values. The introduction of electron-deficient aromatic rings gave a high $\chi^{(3)}$ coefficient of 6.2×10^{-10} esu. This susceptibility value is more than one order of magnitude larger than that of its homo-polymeric counterpart in the absence of fluorinated units.

S-56
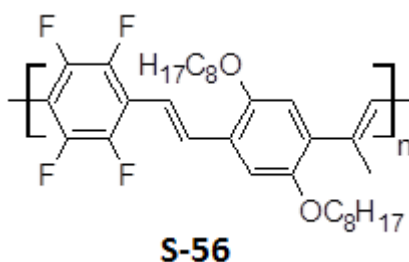
A series of D-A type conjugated polymers (**S-57**) carrying oxadiazole and phenylenevinylene units in the backbone, synthesized by Udayakumar et al. (2006) was shown to possess high NLO response. The authors explored the third order nonlinear property of the polymers using Z-scan and four-wave mixing techniques (DFWM). Z-scan measurement results showed a negative nonlinear refractive index (n_2) whose magnitude is of the order of 10^{-10} esu with enhanced optical limiting property. These results suggested that such donor acceptor polymers are useful in photonic switching and optical limiting devices.

S-57
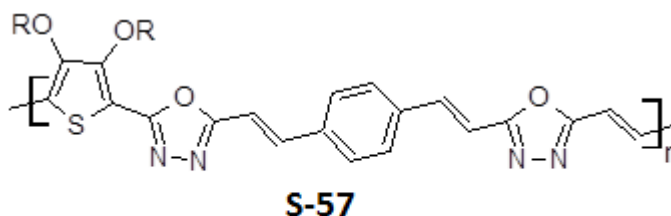
where R = C_6H_{13}, C_8H_{17}, $C_{10}H_{31}$

In search of novel NLO materials, Manjunatha et al. (2009) synthesized a series of new conjugated polymers (**S58**) carrying 3,4-dialkoxythiophene as electron donor and 1,3,4-oxadiazole ring as electron acceptor by Wittig condensation method.

The optical bandgaps of these polymers were observed in the range of 2.47 to 2.55 eV. Electrochemical study revealed that, these polymers possess good charge carrying property and a strong NLO absorption behavior.
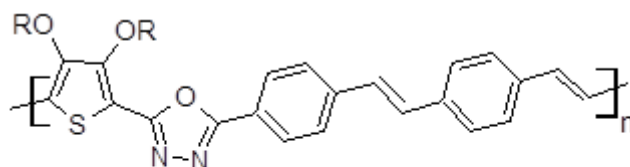
S-58

where R = C_3H_7, C_5H_{11}, C_7H_{15}

In 1999, Bao et al. synthesized a new soluble PPV derivative (**S-59**) carrying an electron transporting pendant, an alkoxy group on the phenylene ring with an oxymethylene spacer placed in between the pendant and the backbone. This material shows λ_{max} at 580 nm, and the PLED device with configuration, ITO/ polymer/Al exhibited an external quantum efficiency of 0.02% at a current density of about 8 mA/cm^2.
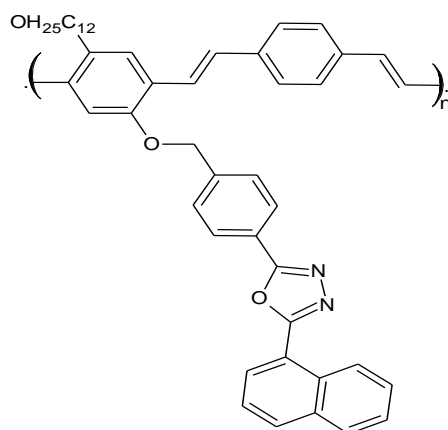
S-59

Peng and Zhang in 1999, reported a new conjugative polymer **S-60** containing the oxadiazole units in the main chain and as main chain substituent. They found the efficiency of 0.15% for the fabricated device with the configuration ITO/polymer/Ca cathode and 0.07% for the device in which the Al was used as cathode. The molecule showed external quantum efficiency of 0.045% in the above said device.
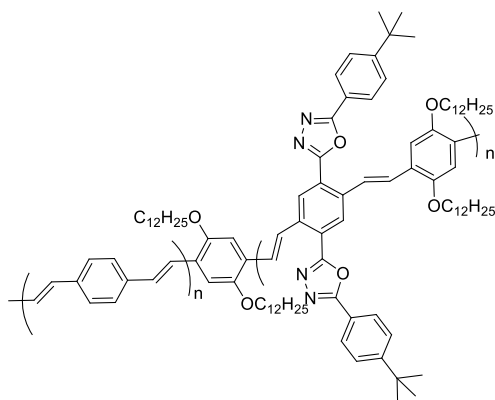
S-60

In 2000, Lee et al. described the luminescence properties of the polymers **S-61** and **S-62** containing 2-(4-*tert*-butylphenyl)-5-phenyl-1,3,4-oxadiazole (BPD) pendants directly linked to the PPV backbone. A simple structural modification of the conjugative polymer resulted in a much higher EL efficiency, *i.e.* 16 times higher than that of simple PPV. The polymer was found to be soluble at room temperature in common organic solvents such as 1,1,2,2-tetrachloroethane, toluene *etc*. It is evident that, attachment of long alkoxy substituents on the phenylene rings increases the interchain distance, leading to enhanced LED device efficiency on account of diminished formation of interchain polar on pairs.
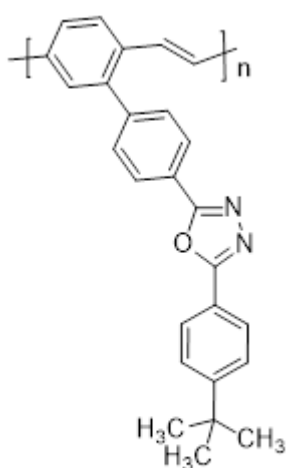
S-61
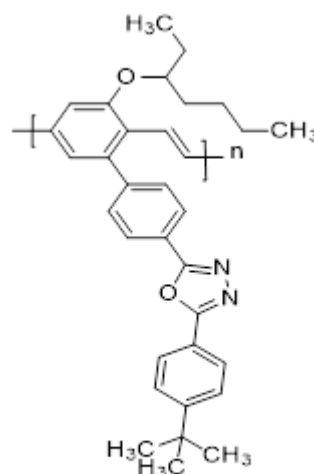
S-62

Mikroyannidis and his co-workers in 2003 synthesized PPV based conductive polymers **S-63** and **S-64** carrying oxadiazole pendants in the polymer main chain. These polymers were shown to be hole-conducting materials with high-lying LUMO

levels. However, they possess disadvantages such as unbalanced charge carrier transport properties and the relative high barrier for electron injection from electrode metals such as aluminum. So, in the device, introduction of additional layers of aryl-substituted 1,3,4-oxadiazole with high electron affinity between the luminescent material and the metal has reduced the barrier for electron injection. Polymer **S-63** was shown to be more soluble in common organic solvents, less thermally stable with a lower T_g and higher fluorescence with lower optical band gap than **S-64** polymer.

S-63

S-64
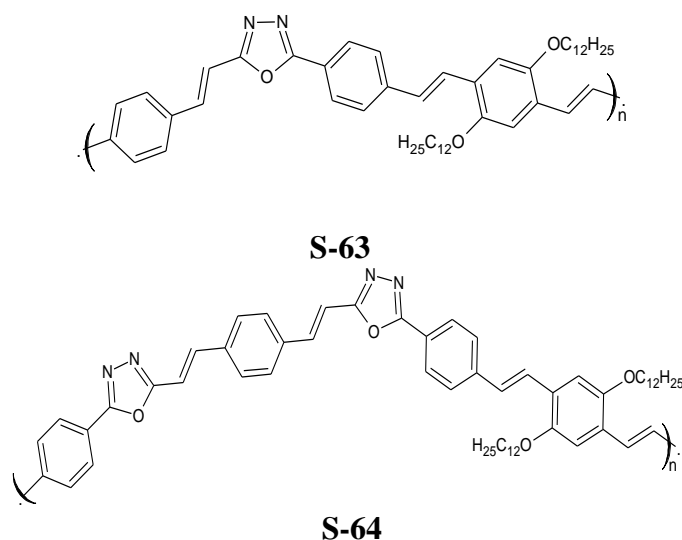
Further, the same group in 2003, synthesized poly(*p*-phenylene vinylene) with 1,3,4 oxadiazole on a vinylene unit as shown in **S-65**. These polymers with linear or branched alkoxy substituents displayed low efficiency because of the fact that the injection of holes is much more favorable than the injection of electrons. As reported by authors, derivatives of **S-65** containing electron-withdrawing functionalities such as cyano (CN), 1,3,4-oxadiazole (OXD), fluoroaryl, quinolone in the main chain or side chains can be used as efficient electron transporting materials in PLEDs. Also, it was observed that, oxidation of the vinyl groups of the PPV derivatives is one of the major causes for their low efficiency and stability. According to authors, introduction of electronegative OXD units in the polymer main chain lowers the electron density in the vinyl group, leading to enhancement of stability and efficiency of the fabricated EL device.

The number average molecular weight of the polymer was found to be 14585 with a polydispersity index of 4.70 as determined by GPC. The point corresponding to

5% weight loss in the TGA thermogram of OXD-PPV appeared at 397 °C. The polymer was shown to be readily soluble in common organic solvents such as chloroform, THF, or toluene and capable of forming a good transparent film on the surface of ITO coated glass. The maximum quantum efficiency of the device with Al cathode was found to be 0.34% at 11.0 V and 0.077 A/cm^2 and the maximum luminance was shown to be 1457 cd/m^2 at 13.0 V and 0.22 A/cm^2. The device with an Al cathode showed a high EL efficiency. When a Ca cathode was used in place of an Al cathode, the maximum external quantum efficiency was 0.43% at 11.0 V (0.25 A/cm^2) and the maximum luminance was 5140 cd/m^2 at 12.5 V (0.61 A/cm^2) with the turn-on voltage of 5.5 V. Despite a lower work function (2.9 eV) of Ca than that of Al (4.2 eV), it was observed no significant improvement in EL efficiency by replacing the Al cathode with a Ca cathode. This clearly indicates that, the electron-transporting property has been improved significantly by the presence of OXD units in the polymer. The device based on a Ca cathode has lower turn-on voltage and higher brightness than that of the device based on an Al cathode. The lower turn-on voltage and higher brightness achieved in the Ca-cathode-based device is due to the more improved injection ability of electrons.
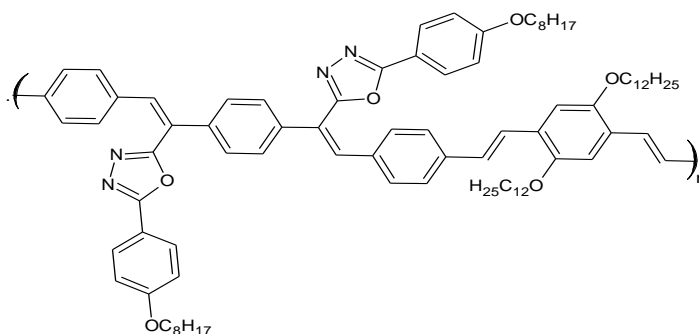
S-65

Two new PPVs with 1,3,4 oxadiazole pendant on vinylene unit, reported by Mikroyannidis et al. (2004) are shown in **S-66** and **S-67**. Among the two, **S-67** displayed excellent solubility in common organic solvents such as THF, chloroform, 1,2-dichloroethane and toluene. While, **S-66** that lacked alkoxy groups, was found to be less soluble than **S-67**. It dissolved partially in THF and chloroform and completely in 1,1,2,2-tetrachloroethane and chlorobenzene. The number-average molecular weights ($\overline{M}_n$) were determined by GPC analysis technique against a

polystyrene standard, and they were shown to be 7,800 and 12,300 with a polydispersity index of 1.8 and 2.5 for **S-66** and **S-67**, respectively. The polymers were stable up to 310-320 °C in N_2 and afforded anaerobic char yield of about 65% at 800 °C. **S2.9** was less thermostable than **S-66** due to the presence of the thermally sensitive alkoxy groups. On the other hand, **S-67** showed lower molecular weight, higher solubility in common organic solvents, lower T_g as well as thermal stability than **S-66**. Further, **S-67** emitted blue-green light both in solution and thin film with PL maxima at 456-517 nm, while **S-66** emitted violet-blue light with PL maximum at 362-470 nm. The PL efficiency of polymers in THF solution was estimated to be 0.17 and 0.14 for **S-67** and **S-66**, respectively.

S-66   **S-67**
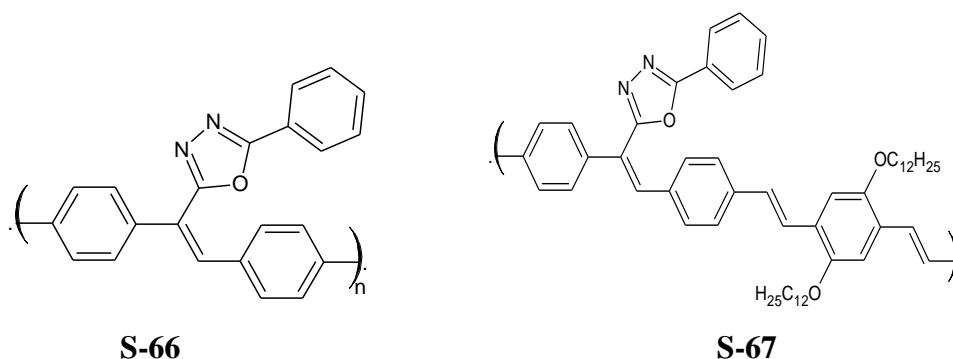
Udaya Kumar D. et al. (2007) investigated a new class of copolymers **S-68** containing oxadiazole, thiophene and phenylene vinylene units. These polymers were prepared using precursor poly hydrazide route. They possess well defined structures and exhibit good thermal stability with the onset decomposition temperature in nitrogen atmosphere at around 330 °C. The UV-vis absorption spectra of polymers in solution showed a maxima at around 380 nm. The polymers displayed bluish-green fluorescence in solutions and green fluorescence in thin films. Cyclic voltammetry studies revealed that, these copolymers have low lying LUMO energy levels ranging from 3.25 to 3.31 eV and HOMO energy levels in the order of 5.48 to 5.56 eV, which indicated that, these polymers are expected to provide enhanced charge transporting (electron transport/hole blocking) properties, making them potential candidates for the development of efficient polymer light-emitting diodes (PLEDs).

S-68
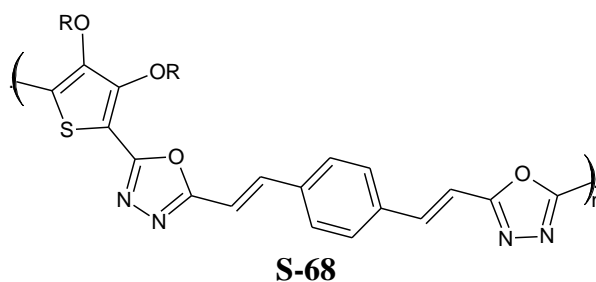
In 2009, Manjunatha et al. reported a new series of donor acceptor type conjugated polymers **S-69** and **S-70** synthesized *via* Wittig condensation method. The optical band gaps of these polymers were found to be in the range of 2.47 to 2.55 eV. Their electrochemical study revealed that, these polymers exhibit good charge carrying property and hence they are the most suitable candidates for polymer light emitting diodes as emitters.

S-69

S-70
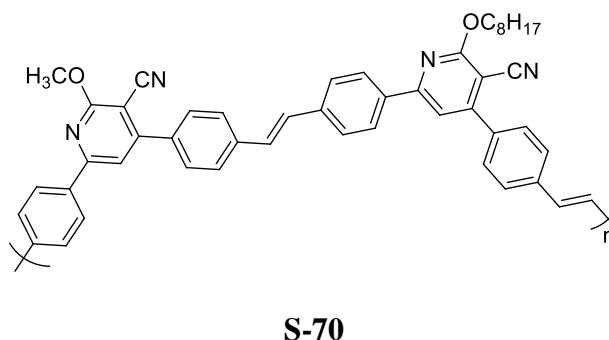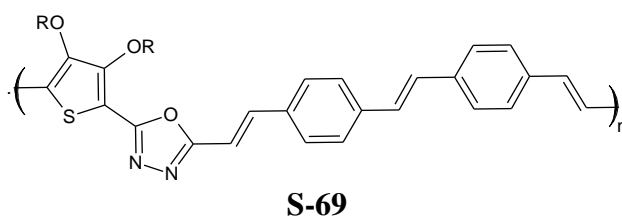
From the foregoing account, it is clear that, the introductions of phenylenevinylene linkage along the polymer main chain increases the conjugation path length leading to enhancement in the absorption maxima and hence decreases in band gap. Keeping this in view, it has been planned to design new D-A type conjugated polymers containing phenylenevinylene moiety in the backbone, with the hope that new design would show improved optical response.

2.3 SCOPE AND OBJECTIVES OF PRESENT WORK

Conjugated polymers are important class of current materials with potential applications in the fields of PLEDs, PVs, TFTs, NLO, various types of sensors *etc*. Since, these polymers exhibit characteristic properties of inorganic semiconductors, they are promising materials in molecular electronics.   They possess several advantages such as good processability, solubility, thermal stability, film-forming ability and favorable properties like electron-transport, light-emitting, and electronic, over their inorganic counterparts.   However, the benefit from a unique set of characteristics by combining the electrical/semi-conducting properties with the typical plastic properties such as low cost, versatility of chemical synthesis, ease of processing, and flexibility, may be encashed.

Based on the above facts and a detailed literature survey, the following objectives have been intended in the present research work.

1. To design and synthesize new conjugated polymers containing aromatic moieties like cyanopyridine and thiadiazole as acceptors and phenylene, thiophene, biphenyl and fluorene as donors, by using various types of condensation and coupling reactions starting from appropriate monomers with the following sub-objectives:

    (i)   To characterize new monomers as well as polymers by FTIR, ^{1}H NMR spectroscopy techniques followed by elemental analysis and to determine the molecular weight of polymers by GPC technique

    (ii)   To study the optical properties of polymers using UV-Visible and photoluminescence spectroscopy

    (iii)   To evaluate the electrochemical properties of polymers using cyclic voltammetry technique

    (iv)   To study thermal properties polymers using thermo gravimetric analysis

2. To carry out theoretical studies of polymers using Turbo mole V7.2 software

3. To fabricate PLED devices employing the new polymers as emitters and to determine the performance parameters

4. To study polymer structure-property relationship with regard to photophysical, electrochemical, thermal as well as device characteristics

Conclusively, the present research investigation has aimed at design, synthesis, and characterization of new donor-acceptor type conjugated polymers carrying interesting units, *viz.* thiophene, thiadiazole, phenylenevinylene, cyanovinylene, biphenylene and bithiophene, with possible application in PLEDs. These polymers were expected to show favorable optical, electrochemical and thermal properties for their use as emitters in devices. A detailed account on design of six new series of conjugative polymers has been highlighted in the following section.

2.4 MOLECULAR DESIGN OF NEW POLYMERS

As per literature survey, cyanopyridine-based conjugated polymers are promising candidates for PLEDs due to their favorable optical, electrochemical and thermal properties. Cyanopyridine is a strong electron withdrawing heterocyclic system possessing good electron transporting ability. Presence of it in the backbone enhances the charge carrying property of polymer. Further, such polymers show an excellent florescence behavior as cyanopyridine itself is a good light emitting scaffold. Further, their photophysical properties can be tuned easily by incorporating various electron donor/π-spacer functionalities in the polymer backbone. Additionally, the inclusion of long chain alkoxy group to cyanopyridine ring would increase the solubility and processability of the resulting polymer. Moreover, the high electron affinity of cyanopyridine based polymers enables the use of relatively stable conductors like Al, LiF as electron injecting contacts in the PLED devices. As described in the literature, in order to achieve optimum device performance, conjugative polymer must carry both hole transporting segment and electron affinitive moiety. Against this background, six new series of cyanopyrdine based conjugative polymers have been designed.

2.4.1 Design of phenylene-cyanopyridine based polymers carrying vinlylene linkage, VPPy₁₋₃ (Series-1)

In the present research work, on the basis of literature review, three new donor-acceptor type conjugated polymers of **Series-1**, *viz.* **VPPy₁₋₃** carrying cyanopyridine ring as a strong electron acceptor, thiophene and phenylenevinylene

units as electron donors, have been designed. In the new design, presence of electron withdrawing nitrile group (-CN) on vinylene unit of **VPPy₁**, as well as electron accepting bromo (-Br) functionality on phenyl ring of **VPPy₃** is expected to improve charge carrying ability of polymer chains. Further, hexadecyl side chain (-C_7H_{15}) on cyanopyridine ring would bring about good solubility and film forming ability for the polymers. Thus, the resulting polymers have been predicted to possess promising structural requirements for exhibiting favorable optical properties with wide band gap and good thermal stability, which arise from both the backbone and functional groups. **Design-1** illustrates the design strategy used for polymers, **VPPy₁₋₃**(**Series-1**).
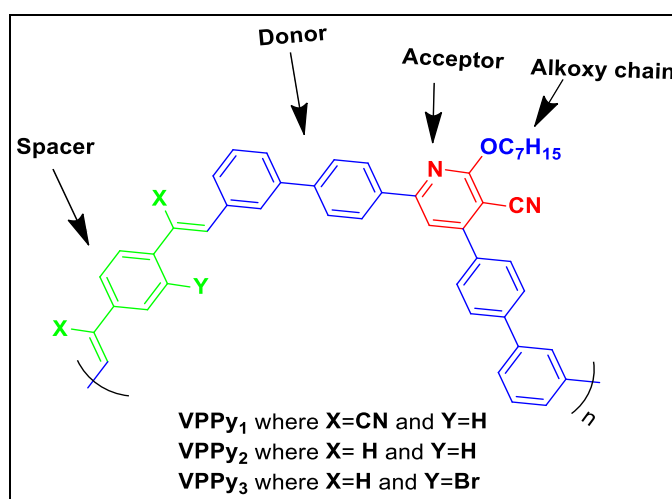
Design-1: Phenylene-cyanopyridine based polymers carrying vinlylene linkage, **VPPy₁₋₃ (Series-1)**

2.4.2 Design of thiophene-cyanopyridine based polymers carrying vinlylene linkage, VTPy₁₋₃ (Series-2)

Based on the literature reports, **Series-2** comprising three new donor-acceptor type conjugated polymers, *viz.* **VTPy₁₋₃** carrying cyanopyridine ring as a strong electron acceptor, thiophene and phenylenevinylene units as electron donors, has been designed. In the new architecture, presence of electron accepting nitrile unit (-CN) on vinylene unit of **VTPy₁**, as well as electron withdrawing bromo (-Br) group on phenyl ring of **VTPy₃** is anticipated to improve charge carrying ability of polymer chains. In addition, incorporation of hexadecyl side chain (-$C_{16}H_{33}$) on cyanopyridine ring would result in good solubility and film forming ability. Thus, the resulting polymers

have been expected to possess promising structural features for showing required optical properties with wide band gap and thermal stability. The schematic design strategy employed for polymers, **VTPy₁₋₃ (Series-2)** has been outlined in **Design-2**.
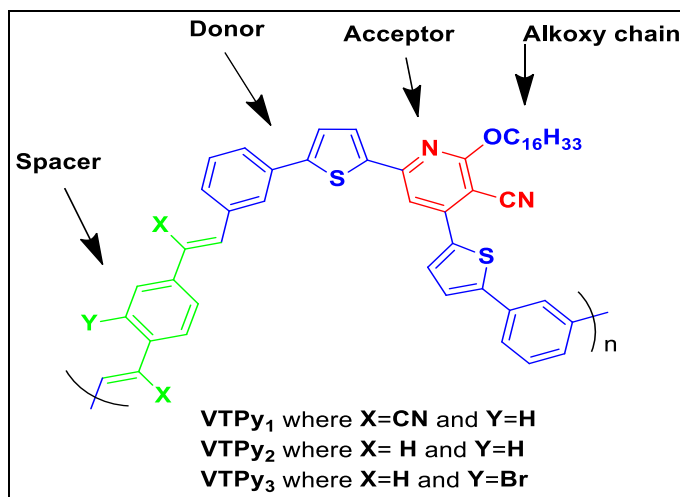
Design-2: Thiophene-cyanopyridine based polymers carrying vinylene linkage, **VTPy₁₋₃ (Series-2)**

2.4.3 Design of phenylene-cyanopyridine based polymers, PPy₁₋₃ (Series-3)

As described in the literature survey, a third series of donor-acceptor (D-A) type conjugated polymers **PPy₁₋₃** has been designed. These newly designed polymers consist of 2-heptoxylcyanopyridine as an electron acceptor along with phenylene (**PPy₁**), biphenyl (**PPy₂**) and fluorene (**PPy₃**) moieties as auxiliary donors in the main chain primarily for enhancing the electrochemical and optical properties as well as the overall stability and rigidity of resulting polymers. Here, being a strong electron acceptor, cyanopyridine facilitates good charge transporting behavior, while thiophene rings on either side of cyanopyridine core function as strong electron donors. Further, presence of bulky alkoxy chain would bring good solubility as well as film forming property of the polymers. The newly designed polymers were expected to possess desired properties such as high molecular weight with great degree of solubility in common organic solvents, attractive charge carrying ability, good thermal stability, wide band gap, excellent quantum yield and blue fluorescence. The design concept adopted for the new polymers, **PPy₁₋₃ (Series-3)** is illustrated in **Design-3**.

PPy$_1$ where **A=Phenylene**
PPy$_2$ where **A=Biphenyl**
PPy$_3$ where **A=fluorene derivative**
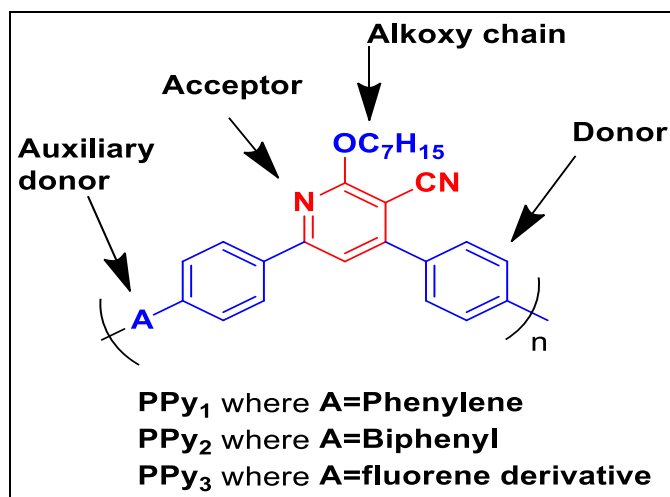
Design-3: Phenylene-cyanopyridine based polymers, **PPy$_{1-3}$** (**Series-3**)

2.4.4 Design of thiophene-cyanopyridine based polymers, TPy$_{1-3}$ (Series-4)

On the basis of reported literatures, a new series of push-pull type 2-hexadecoxylcyanopyridine based polymers, **TPy$_{1-3}$ (Series-4)** carrying thiophene rings in the main chain was designed. The new configuration includes phenylene (**TPy$_1$**), biphenyl (**TPy$_2$**) and fluorene (**TPy$_3$**) moieties as π-conjugation bridges in the main chain primarily for improving the electrochemical as well as optical behavior. It was also expected to enhance the overall stability and rigidity of final polymers. Here, presence of cyanopyridine system facilitates good charge transporting property, while thiophene rings on either side of cyanopyridine ring function as strong electron donating units. Further, bulky alkoxy chain imparts good solubility as well as film forming ability to the polymers. The new polymers were expected to own desired properties such as high molecular weight with great degree of solubility in common organic solvents, attractive charge carrying ability, good thermal stability, wide band gap, high quantum yield and blue fluorescence. The design strategy used for the polymers, **TPy$_{1-3}$** (**Series-4**) is presented in **Design-4**.
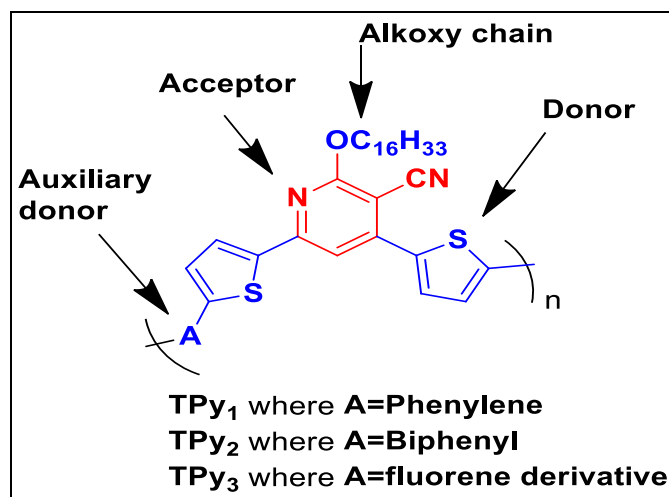
Design-4: Thiophene-cyanopyridine based polymers, **TPy₁₋₃** (**Series-4**)

2.4.5 Design of thiadiazole-cyanopyridine based polymers, TDPy₁₋₄ (Series-5)

Based on literature review, four new thiadiazole-cyanopyridine based donor-acceptor configured polymers, *viz.* **TDPy₁₋₄** (**Series-5**), carrying cyanopyridine and thiadiazole moieties as strong electron acceptors, thiophene and phenylene units as electron donors, have been designed. Here, introduction of long alkoxy side chain onto cyanopyridine ring would bring about good solubility and film forming ability for the new polymers. Thus, the newly designed polymers have been predicted to show favorable optical properties with wide band gap and thermal stability, which arise from both the backbone and functional groups. **Design-5** depicts the design approach followed for polymers, **TDPy₁₋₄** (**Series-5**).
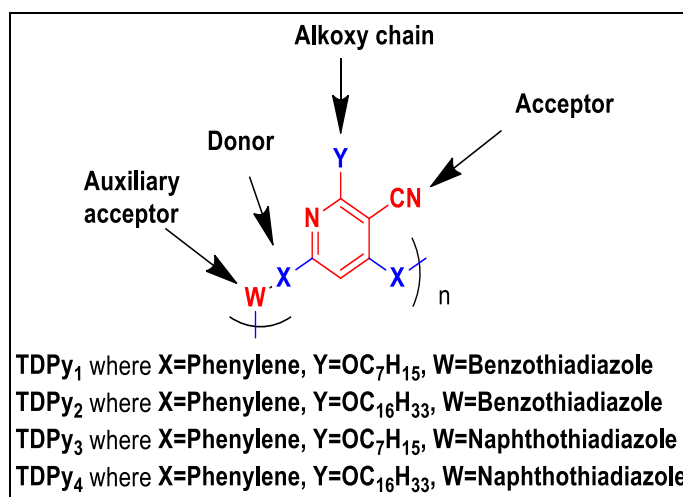
Design-5: Thiadiazole-cyanopyridine based polymers, **TDPy₁₋₄** (**Series-5**)

2.4.6 Design of cyanopyridine based polymers carrying imine linkage, Py₁₋₄ (Series-6)

While designing four new conjugative polymers, *viz.* **Py₁₋₄** belonging to **Series-6**, strong electron accepting cyanopyridine scaffold has been introduced in the main chain along with highly electron donating thiophene and phenylene units. In the newly designed polymers, imine functional groups (-C=N-) incorporated into the conjugated system provides improved charge carrying ability of polymer molecules. Further, long alkoxy side introduced onto cyanopyridine ring causes good solubility and film forming ability in the polymers. Thus, the new polymers have been anticipated to possess required structural features for exhibiting favorable optical and electrochemical properties, as well as good thermal stability. The schematic design strategy used for **Py₁₋₄ (Series-6)** has been summarized in **Design-6**.
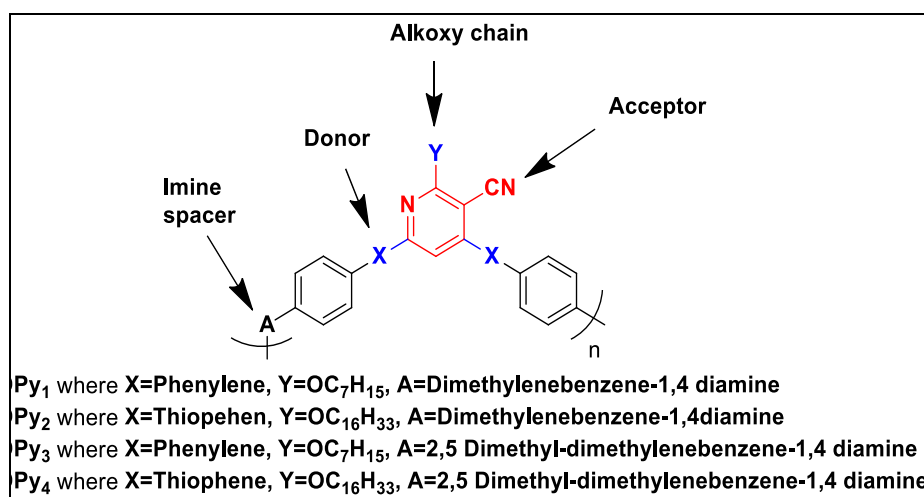
Design-6: Cyanopyridine based polymers carrying imine linkage, **Py₁₋₄ (Series-6)**

From the aforesaid design strategies, it is clear that, incorporation of certain structural units in the polymer chain would bring about drastic changes in their basic characteristics. For instance, the luminescent color can be controlled through a synthetic design over the electron donating or withdrawing character of the substituents on monomers or the comonomers in polymers. Therefore, it has been contemplated to synthesize following newly designed six series of D-A type conjugative polymers, consisting of twenty polymers and to investigate the effect of the incorporated groups on the photophysical, electrochemical and electroluminescence properties of the new polymers.

    (i) Phenylene-cyanopyridine based polymers carrying vinlylene linkage, **VPPy₁₋₃ (Series-1)**

    (ii) Thiophene-cyanopyridine based polymers carrying vinlylene linkage, **VTPy₁₋₃ (Series-2)**

    (iii) Phenylene-cyanopyridine based polymers, **PPy₁₋₃ (Series-3)**

    (iv) Thiophene-cyanopyridine based polymers, **TPy₁₋₃ (Series-4)**

    (v) Thiadiazole-cyanopyridine based polymers, **TDPy₁₋₄ (Series-5)**

    (vi) Cyanopyridine based polymers carrying imine linkage, **Py₁₋₄ (Series-6)**

The polymers have been synthesized from their respective monomers using various synthetic methods, as shown in **Schemes 3.4**, **3.5**, **3.6, 3.7, 3.8** and **3.9**, given in **Chapter 3**. The reaction parameters for monomer synthesis were optimized and their smooth polymerization to target polymers was established. The new polymers and their intermediates were well-characterized using NMR, FTIR spectroscopy techniques and elemental analysis. Their number and weight average molecular weights ($\overline{M}_n$ and $\overline{M}_w$) along with polydispersity index (PDI) were determined from Gel Permeation Chromatography (GPC) technique. Their thermal stability was investigated by the Thermo Gravimetric Analysis (TGA). Further, their photophysical properties in both solution as well as solid film were studied by employing UV-Vis. absorption as well PL emission spectroscopy. In addition, their HOMO-LUMO energy levels were determined using both spectral as well as cyclic voltammetric (CV) method. Further, DFT (Density Functional Theory) studies were performed on the newly synthesized polymers, by considering the repeating units (monomers) at B3LYP/TZVP level using Tmolex. Finally, electroluminescence behavior of newly synthesized polymers was determined by fabricating PLED devices. The devices were fabricated with the configuration, ITO/PEDOT: PSS/Polymer/Al, where the polymer functions as a light emissive layer in their respective device. In addition, the polymer structure and its effect on the various optical, thermal, electrochemical and EL properties have been discussed in depth.

A detailed synthetic protocol used for all intermediates, monomers and polymers along with their structural characterization data has been included in **Chapters 3.** Further, the details of photophysical, electrochemical, thermal and theoretical studies of polymers are given in **Chapters 4**. Finally, **Chapter 5** covers electroluminescence device characterization of new polymers.

SYNTHESIS AND STRUCTURAL CHARACTERIZATION

Abstract

This chapter deals with optimized synthetic protocols used for all the newly designed π-conjugated polymers belonging six series and their structural characterization using FTIR, NMR spectroscopy and elemental analyses. Also, it involves GPC analysis of the new polymers.

3.1 INTRODUCTION

In the previous chapter, the design of six new series of conjugative polymers has been described. These newly designed polymers have been synthesized starting from respective monomers with various conjugative functionalities. The cyanopyridine based monomer **4** and **7**, required for the synthesis of polymers of **Series-1**, **-3**, **-5** -and -**6** have been synthesized starting from substituted benzaldehyde and acetophenone, through multi-step reactions as summarized in **Scheme 3.1**. The co-monomers, *viz.* Wittig salts **10** and **13**, employed for the synthesis of polymers belonging to **Series-1** and **-2** were prepared as shown in **Scheme 3.2**. Further, **Scheme 3.3** depicts the synthesis of the monomers **17** and **18**, starting from simple thiophene based cyanopyridine, required for the synthesis of polymers pertaining to **Series-4** and **Series-2** respectively. The newly synthesized monomers were further polymerized to respective polymers possessing vinylene linkage as π-conjugated spacers, **VPPy$_{1-3}$** (**Series-1**), thiophene-cyanopyridine based polymers carrying vinylene linkage as π-conjugated spacers, **VTPy$_{1-3}$** (**Series-2**), phenylene-cyanopyridine based polymers containing phenylene as auxiliary donors, **PPy$_{1\sim3}$** (**Series-3**), thiophene-cyanopyridine based polymers containing phenylene as auxiliary donors, **TPy$_{1\sim3}$** (**Series-4**), cyanopyridine based polymers carrying thiadiazole units, **TDPy$_{1-4}$** (**Series-5**) and heteroaromatic-cyanopyridine based polymers carrying imine linkage as π-conjugated spacers, **Py$_{1\sim4}$** (**Series-6**) as described in **Schemes 3.4**, **3.5**, **3.6**, **3.7**, **3.8** and **3.9**, respectively.

3.2 MATERIALS AND INSTRUMENTATION

The required starting materials, *viz*. 4-bromobenzaldehyde (**1**), 4-bromoacetophenone (**2**), 5-bromo-2-thiophenecarboxaldehyde (**14**), 2-acetyl-5-bromothiophene (**15**), 3-bromobenzaldehyde, 2-bromo-1,4-dimethylbenzene (**11**), *p*-xylene (**8**) and 1,4-phenylenediacetonitrile were procured from Sigma Aldrich and were used without purifying further. All the solvents were dried prior to use. The reactions were performed under inert atmosphere and completion of reaction was confirmed by Thin Layer Chromatography (TLC) technique. All the compounds were purified using column chromatography and recrystallization techniques. The melting points of the final products were determined using SMP-10 melting point apparatus (Stuart Make) and were uncorrected. FTIR spectra were run using Bruker Alpha Spectrophotometer. ^{1}H NMR spectra were recorded using Bruker Advance 300 MHz using deuterated chloroform (CDCl$_3$) as solvent and TMS as an internal standard whereas the elemental analysis was carried out on Flash EA1112 CHNSO analyzer (Thermo Electron Corporation). Molecular weights of polymers were determined with WATER's make Gel Permeation Chromatograph (GPC) against polystyrene standards using THF as an eluent.

3.3 SYNTHESIS OF CYANOPYRIDINE CARRYING PHENYLENE ON BOTH SIDES (MONOMER 7)

The monomer, cyanopyridine derivative, **7** required for the synthesis of polymers belonging to **Series-1, Series-3**, **Series-5** and **Series-6** were prepared as per **Scheme 3.1**.
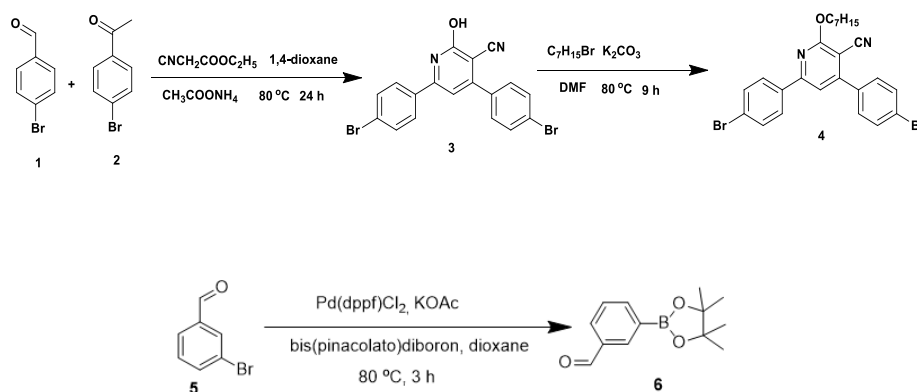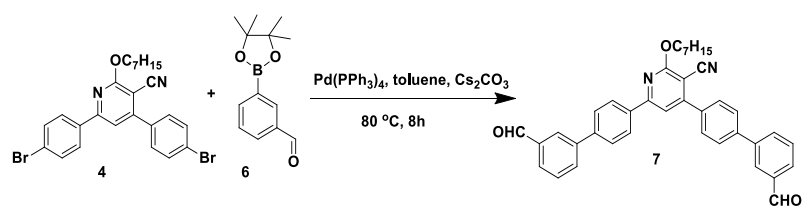
Scheme 3.1: Synthesis of cyanopyridine carrying phenylene, **7**

3.3.1 Chemistry

As shown in **Scheme 3.1**, 4-bromobenzaldehyde was condensed with 4-bromoacetophenone in presence of ethyl cyanoacetate to form cyanopyridine derivative **3**, which was further converted into monomer **4**, *i.e.* dibromo derivative of O-alkylated cyanopyridine, by O-alkylation, in good yield. Separately, boronic ester derivative, **6** of 3-bromobenzaldehyde was prepared using Pd(dppf)Cl$_2$ as a catalyst. The required monomer, **7** was synthesized by coupling dibromo derivative of O-alkylated cyanopyridine, monomer **4** with freshly prepared boronic ester, **6** using Pd(PPh$_3$)$_4$ as a catalyst, under anhydrous condition, in presence of cesium carbonate, following renowned Suzuki method.

3.3.2 Synthesis and characterization

Synthesis of 4,6-bis(4-bromophenyl)-2-hydroxypyridine-3-carbonitrile (3)

Compound 4-bromobenzaldehyde (2 g, 10.8 mmol) and compound 4-bromoacetophenone (2.15 g, 10.8 mmol) were dissolved in 35 mL of 1,4-dioxane. Ammonium acetate (6.6 g, 85.7 mmol) was added to it followed by 1.5 mL of ethyl cyanoacetate (12.9 mmol) with constant stirring and the reaction mixture was kept at 80 °C, with stirring for 24 hrs. Then, the product was cooled and poured into 100 mL of ice-cold water and stirred for 10 min. The obtained precipitate was filtered and the filtrate was thoroughly washed with 1,4-dioxane and dried to afford a white product **3**. The crude product was dissolved in a minimum amount of CHCl$_3$, followed by re-precipitation using methanol to get the pure intermediate **3**. Finally, it was recrystallized from chloroform-methanol. Yield: 1.66 g, 36%. FTIR (cm^{-1}): 1635 (C=O), 2219 (C≡N). ^{1}H NMR (300 MHz, CDCl$_3$, δ ppm): 3.56 (s, 1H), 7.68 (d, J = 2 Hz, 2H), 7.70 (d, J = 2 Hz, 2H), 7.73 (d, J = 2 Hz, 1H), 7.75 (d, J = 2 Hz, 2H), 7.77 (t, J = 2 Hz, 2H), 7.79 (d, J = 2 Hz, 1H). ESI-MS, exact mass calculated for

$C_{18}H_{10}Br_2N_2O$, $[M+H]^+$: 430.09, Found: 431.2; Elemental Anal. Calcd (%) for $C_{18}H_{10}Br_2N_2O$: C 50.27, H 2.34, Br 37.16, N 6.51, O 3.72.

Synthesis of 4, 6-bis (4-bromophenyl)-2-(heptoxy)pyridine-3-carbonitrile (4)

Compound **3** (0.33 g, 0.767 mmol) was dissolved in 8 mL of DMF. 1-Bromoheptane (0.15 mL, 0.777 mmol) was then added, followed by 148 mg of potassium carbonate (1.072 mmol) and the reaction mixture was stirred at 90 ºC for overnight. The reaction mixture was cooled and poured into ice cold water with constant stirring. The obtained precipitate was filtered, washed with water and dried to obtain creamy yellow dibromo derivative of O-alkylated cyanopyridine (monomer) **4**. The obtained crude product was dissolved in a minimum amount of CHCl$_3$, followed by re-precipitation using methanol to get the pure intermediate **3**. Finally it was recrystallized from CHCl$_3$ and methanol mixture. Yield: 280 mg, 75%. FTIR (cm^{-1}): 1540 (C=O), 2219 (C≡N), 2918 (Aromatic CH stretching). ^{1}H NMR (300 MHz, CDCl$_3$, δ ppm) : 0.88 (t, J = 4.8 Hz, 3H), 1.33 (t, J = 6.4 Hz, 3H), 1.39 (t, J = 4Hz, 3H), 1.51 (d, J = 7.2 Hz, 2H), 1.89 (m, J = 6.8 Hz, 2H), 4.576 (t, J = 6.4 Hz, 2H), 7.26 (s, 1H) 7.52 (d, J = 6.8 Hz, 2H), 7.61 (d, J = 2 Hz, 1H), 7.63 (d, J = 2 Hz, 1H), 7.66 (d, J = 2 Hz, 1H), 7.68 (d, J = 2 Hz, 1H), 7.92 (d, J = 2 Hz, 1H), 7.94 (d, J = 2 Hz, 1H). ESI-MS, exact mass calculated for ($C_{25}H_{24}Br_2N_2O$), $[M+H]^+$: 528.28; Found : 529.4. Elemental Anal. Calcd (%) for $C_{25}H_{24}Br_2N_2O$: C, 56.84; H, 4.58; N, 5.30; Found: C, 56.82; H, 5.54; N, 5.33.

Synthesis of 3-(4,4,5,5-tetramethyl-1,3,2-dioxaborolan-2-yl)benzaldehyde (6)

A solution of **5** (2.72 g, 10 mmol), *bis*(pinacolato)diboron (5.08 g, 20 mmol), PdCl$_2$(dppf) (860 mg, 1 mmol), and KOAc (3.94 g, 30 mmol) in degassed 1,4-dioxane (80 mL) was stirred at 80 ºC for 6 h under N$_2$. The reaction was quenched by adding water, and extracted by dichloromethane (100 mL x 3). The organic phase was dried over Na$_2$SO$_4$, and concentrated to get a residue under reduced pressure. The crude product was purified by silica gel column chromatography (petroleum ether/dichloromethane, 1:3) to give compound **6;** Yield: 2.78 g, 86.3% as white solid. ^{1}HNMR (300 MHz, CDCl$_3$) δ: 1.36 (s, 12 H), 7.51-8.31 (m, 4H), 10.1 (s, 1H) . ESI-MS, exact mass calculated for ($C_{13}H_{17}BO_3$), $[M+H]^+$: 232.08; Found : 232.10.

Elemental Anal. Calcd (%) for $C_{13}H_{17}BO_3$: C, 67.28: H, 7.38; Found: C, 67.28; H, 7.31.

*Synthesis of 4,6-bis-(3'-formyl-biphenyl-4-yl)-2-heptyloxy-nicotinonitrile (**7**)*

A clear solution of dibromo derivative of O-alkylated cyanopyridine, **4** (2 g, 3.8 mmol), 3-formylphenylboronic acid (**6**, 1.76 g, 7.6 mmol), Pd(PPh₃)₄ (0.44 g, 0.38 mmol) in 20 mL of toluene, and Cs_2CO_3 (8.67 g, 26.6 mmol) was refluxed under argon atmosphere for 8 h. Reaction was monitored by TLC and the produce was allowed to cool to room temperature. Toluene was removed under reduced pressure. Crude product was dissolved in dichloromethane and passed through Celite bed to remove Pd traces. Obtained filtrate was washed with excess of distilled water to remove traces of base and toluene. The product was extracted with dichloromethane (100 mL x 3) and organic layer was dried over anhydrous sodium sulphate. Solvent was removed under reduced pressure using rotary evaporator. The crude product was purified by column chromatography on silica with hexane / ethyl acetate mixture (100:25). Product **7** was obtained as off-white solid. Yield 59%. mp = 89 °C. ATR-IR (cm⁻¹): 1230 (C-O), 1635 (C=O), 2219 (C≡N). ¹H NMR (300 MHz, CDCl₃, δ ppm): 0.81-1.86 (m, 13 H), 4.56-4.58 (t, 2H), 7.18-8.16 (m, 17H), 10.05 (s, 2H). ESI-MS, exact mass calculated for ($C_{39}H_{34}N_2O_3$), [M+H]⁺: 578.70; Found : 579.02. Elemental Anal. Calcd (%) for ($C_{39}H_{34}N_2O_3$): C, 80.94: H, 5.92: N, 4.84; Found: C, 80.92: H, 5.91: N, 4.85.

3.3.3 Results and discussion

The structure of newly synthesized dibromo derivative of O-alkylated cyanopyridine derivative, **4** was confirmed by FTIR and ¹H NMR spectral data. FTIR spectrum of it showed sharp peak at 2221 cm⁻¹ (**Figure 3.1**) indicating the presence of C≡N group. Further, its ¹H NMR spectrum (**Figure 3.2)** showed peaks at δ 4.5 ppm for -O-CH₂ protons and a triplet at δ 0.88 ppm for methyl group protons of alkyl chain. The multiplet around δ 7.22-7.94 ppm confirms the presence of aromatic protons. Further, ¹H NMR spectrum displayed a sharp peak at around δ 10 ppm confirming the formation of the monomer **7. Figures 3.1** and **3.2** show FTIR and ¹H NMR spectra of monomer **4,** while **Figures 3.3** and **3.4** indicate FTIR and ¹H NMR spectra of monomer **7**.
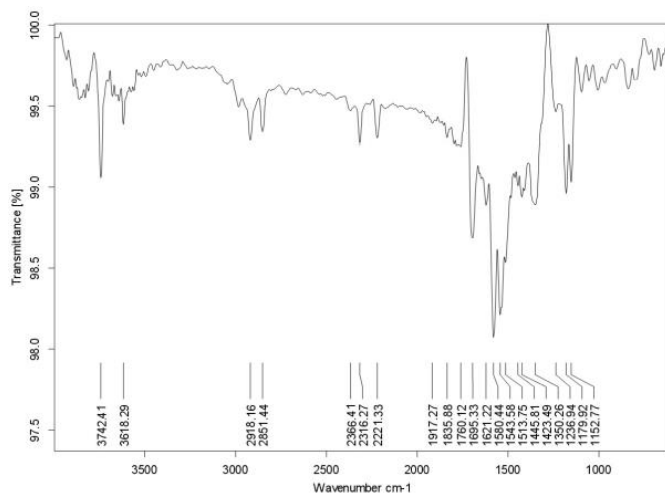
Figure 3.1: FTIR spectrum of monomer **4**
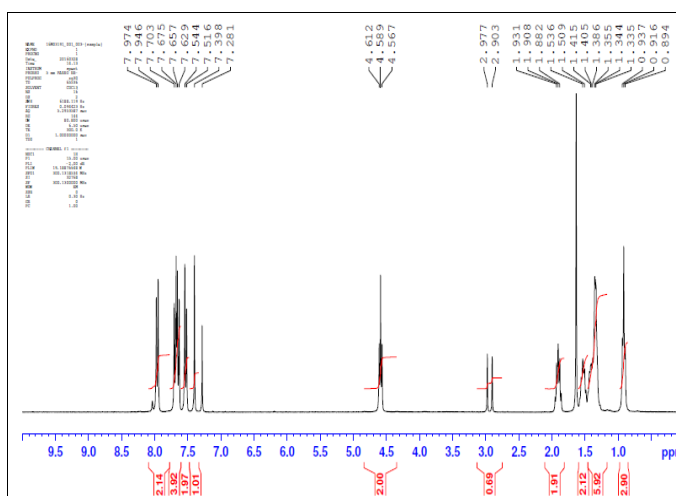
Figure 3.2: ^{1}H NMR spectrum of monomer **4**
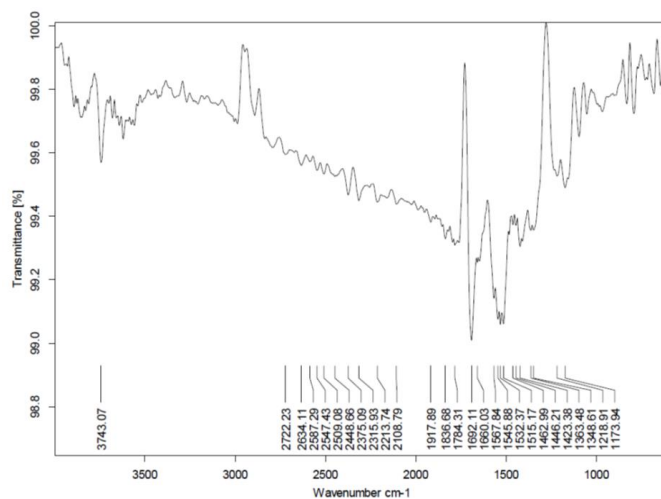
Figure 3.3: FTIR spectrum of monomer **7**

Figure 3.4: ^{1}H NMR spectrum of monomer **7**

3.4 SYNTHESIS OF WITTIG SALTS, 10 AND 13

The multistep synthesis of Wittig salts, **10** and **13** starting from *p*-xylene (**8**) and 2-bromo-1,4-dimethylbenzene (**11**) respectively, is summarized in **Scheme 3.2**.

Scheme 3.2: Synthesis of Wittig salts, **10** and **13**

3.4.1 Chemistry

As depicted in **Scheme 3.2**, the *p*-xylene (**8**) as well as 2-bromo-1,4-dimethylbenzene (**11**) was brominated by Wohl-Ziegler method using N-bromo succinimide (NBS) in carbontetrachloride (CCl₄) and the resulting 1,4-bis(bromomethyl)benzene (**9**) and 2-bromo-1,4-bis(bromomethyl)benzene (**12**) and was further converted into their corresponding Wittig salts and on treatment with triphenylphosphine in presence of DMF yield 1,4-

bis((bromotriphenylphosphoranyl)methyl)benzene (**10**) and ((2-bromo-1,4-phenylene)bis(methylene))bis(bromotriphenylphosphorane) (**13**), respectively. Details of their synthetic procedures and structural characterization data are as follows.

3.4.2 Synthesis and characterization

The required Wittig salts **10**, **13** were synthesized starting from *p*-xylene (**8**) and 2-bromo-1,4-dimethylbenzene (**11**) by following previously reported procedures. Details of synthesis are given in the following section.

*Procedure for synthesis of Wittig salt, **10***

A mixture of 1,4-bis(bromomethyl)benzene (**9**) (1.15 g, 1.07 mmol) and triphenylphosphine (0.565 g, 2.157 mmol) in 5 mL of DMF was refluxed with stirring for 10 h. The reaction mixture was cooled to room temperature and poured into 50 mL of ethyl acetate. The resulting precipitate was filtered off, washed with excess of ethyl acetate and dried at 40 $^{\circ}$C for 18 h. The product was used directly for the next step without purification. White solid, Yield: 62 %. ^{1}H NMR (400 MHz, DMSO, δ ppm): 6.80-7.90 (m, 34H, Ar-H), 5.25 (s, 4H, Ar-CH$_2$--). Elemental Anal. Calcd (%) for C$_{44}$H$_{38}$Br$_3$P$_2$: C, 67.02; H, 4.86.

*Procedure for synthesis of Wittig salt, **13***

A mixture of 2-bromo-1,4-bis(bromomethyl)benzene (**12**) (1 g, 1.07 mmol) and triphenylphosphine (0.565 g, 2.157 mmol) in 5 mL of DMF was refluxed with stirring for 8 h. The reaction mixture was cooled to room temperature and poured into 50 mL of ethyl acetate. The resulting precipitate was filtered off, washed with excess of ethyl acetate and dried at 40 $^{\circ}$C for 10 h. It was used directly for the next step without further purification. White solid Yield: 59 %. ^{1}H NMR (400 MHz, DMSO, δ ppm): 6.81-7.91 (m, 33H, Ar-H), 5.25 (s, 4H, Ar-CH$_2$-P-). Elemental Anal. Calcd (%) for C$_{44}$H$_{37}$Br$_3$P$_2$: C, 60.92; H, 4.30.

3.4.3 Results and discussion

Formation of Wittig salts **10** and **13** was confirmed by ^{1}H NMR studies **Figures 3.5** and **3.6** depict ^{1}H NMR of compounds **10** and **13**. It showed a peak at δ 5.25 ppm indicating the presence of phenylene -CH$_2$- groups. The protons attached to

aromatic ring with phosphonium groups on either side displayed a peak ranging from δ 6.80-7.92 ppm confirming the formation of Wittig salts **10** and **13**. ^{1}H NMR spectra of Witting salts **10** and **13** were represented in **Figures 3.5** and **3.6**.
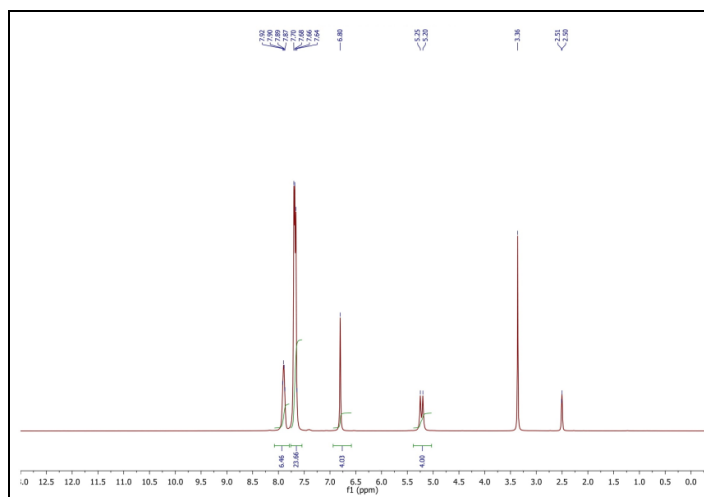
Figure 3.5: ^{1}H NMR spectrum of 10
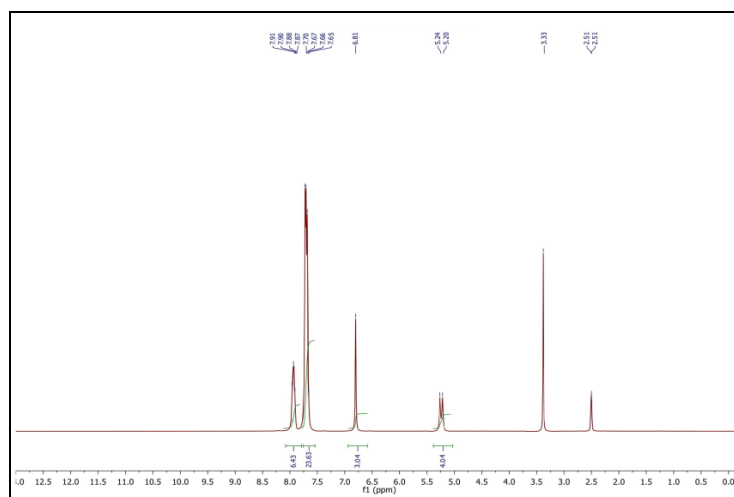
Figure 3.6: ^{1}H NMR spectrum of 13

3.5 SYNTHESIS OF CYANOPYRIDINE CARRYING THIOPHENE ON BOTH SIDES (MONOMER 18)

The synthetic strategy used for the preparation of cyanopyridine carrying thiophene on both sides (monomer **18**), starting from **14** is summarized in **Scheme 3.3**.
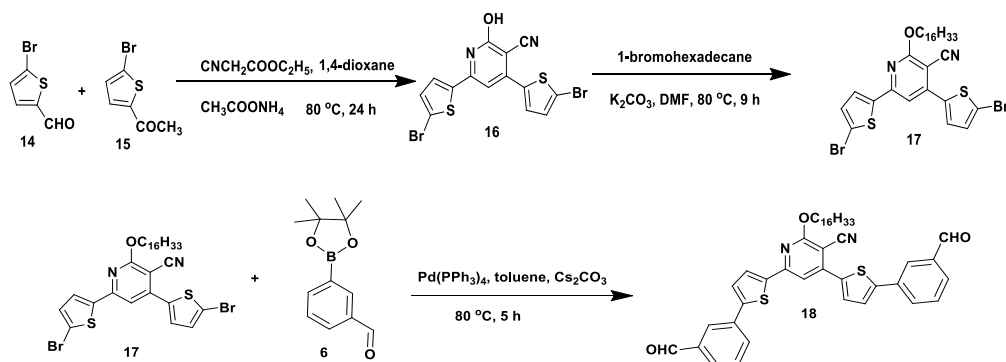
Scheme 3.3: Synthesis of cyanopyridine carrying thiophene, **18**

3.5.1 Chemistry

As shown in **Scheme 3.3**, 5-bromo-thiophene-2-carboxaldehyde was condensed with 2-acetyl-5-bromothiophene in presence of ethyl cyanoacetate to form cyanopyridine derivative **16**, which was further transformed into alkylated cyanopyridine derivative, **17** by O-alkylation, in good yield. The required dialdehyde derivative of cyanopyridine carrying thiophene on both sides, **18** was synthesized by coupling cyanopyridine carrying thiophene, **17** with freshly prepared boronic ester, **6** using Pd(PPh₃)₄ as a catalyst, under anhydrous condition, in presence of cesium carbonate following well-known Suzuki technique.

3.5.2 Synthesis and characterization

*Synthesis of 2,5-bis(4-bromothiophene)-2-hydroxypyridine-3-carbonitrile (**16**)*

A mixture of 5-bromo-2-thiophenecarboxaldehyde (**14**, 1.86 g, 9.74 mmol) and 2-acetyl-5-bromothiophene (**15**, 2 g, 9.75 mmol) was dissolved in 35 mL of 1,4-dioxane. To this ammonium acetate (6.77 g, 87.7 mmol) was added slowly with shaking followed by 1.25 mL of ethyl cyanoacetate (11.7 mmol) drop-wise and the temperature was raised to 80 °C. The reaction mixture was kept at 80 °C under stirring for 24 h. Progress of the reaction was monitored using TLC. The content was then cooled and poured onto 100 mL of ice-cold water and stirred for about 10 min. The obtained precipitate was filtered, and thoroughly washed with 1,4-dioxane and finally dried to afford a white solid product **16**. It was purified by re-crystallization from chloroform-methanol. Yield 36%; mp 310.7 °C; ATR-IR (cm⁻¹):1635 (C=N), 2220 (C≡N). ¹H NMR (300 MHz, CDCl₃, δ ppm): 6.97 (s, 1H), 7.62-7.67 (d, 4H).

Elemental Anal. Calcd (%) for $C_{14}H_6Br_2N_2OS_2$: C, 38.03; H, 1.37; N, 6.34; S, 14.50; Found: C, 38.01; H, 1.36; N, 6.33.

*Synthesis of 2, 5-bis (4-bromothiophene)-2-(hexadecoxyl)pyridine-3-carbonitrile (**17**)*

Compound, 2,5-*bis*(4-bromothiophene)-2-hydroxypyridine-3-carbonitrile (**16,** 0.5 g, 1.131 mmol) was dissolved in 8 mL of DMF. To this 1-bromohexadecane (0.35 mL, 1.146 mmol) was then added, followed by 148 mg of potassium carbonate (1.072 mmol) and the reaction mixture was stirred at 80 °C for overnight. Progress of the reaction was monitored using TLC. It was then cooled and poured onto 150 mL of ice-cold water with constant stirring. The obtained precipitate was filtered, washed with water and dried to obtain creamy yellow product. It was recrystallized using chloroform-methanol to give product, **17**. Yield 75%; mp 71.1 °C; ATR-IR (cm^{-1}): 2220 (C≡N), 2919 (C-H). ^{1}H NMR (300 MHz, CDCl$_3$, δ ppm): 0.81-1.86 (m, 31H), 4.56-4.58 (t, 2H), 7.73-7.86 (m, 5H). Elemental Anal. Calcd (%) for $C_{30}H_{38}Br_2N_2OS_2$: C, 54.06; H, 5.75; N, 4.20; Found: C, 54.05; H, 5.76; N, 4.21.

*Synthesis of 1,4-bis-(2'-formyl-phenylene-thiophene-5-yl)-2-hexadecoxyl-nicotinonitrile (**18**)*

A clear solution of cyanopyridine derivative (**17,** 1 g, 1.5 mmol), 3-formylphenylboronic ester (**6**, 0.77 g, 3.3 mmol), Pd(PPh$_3$)$_4$ (0.17 g, 0.15 mmol), and Cs$_2$CO$_3$ (3.4 g, 10.4 mmol) in 20 mL toluene was refluxed under argon atmosphere for 5 h. Progress of the reaction was monitored by TLC. After completion of the reaction, toluene was removed under reduced pressure to get the crude product. It was then dissolved in dichloromethane and passed through Celite bed to remove Pd traces. Obtained filtrate was washed with excess of distilled water to remove traces of base and toluene. The crude product was extracted using dichloromethane (100 mL x 3) and the combined organic layer was dried over anhydrous sodium sulphate. The solvent was removed under reduced pressure. The crude product was purified by column chromatography on silica (60-120 mesh) with hexane/ethyl acetate mixture (100:25). The product was obtained as off-white solid. Yield 59%. mp 79.2 °C. ATR-IR (cm^{-1}): 1692 (C=O), 2213 (C≡N). ^{1}H NMR (300 MHz, CDCl$_3$, δ ppm): 0.81-1.86

(m, 31H), 4.54-4.58 (t, 2H), 7.69-8.16 (m, 13H), 10.1(d, 2H). Elemental Anal. Calcd (%) for $C_{44}H_{48}N_2O_3S_2$: C, 73.71; H, 6.75; N, 3.91; Found: C, 73.72; H, 6.74; N, 3.92.

3.5.3 Results and discussion

The structures of newly synthesized dibromo derivative of O-alkylated cyanopyridine, **17** and cyanopyridine carrying thiophene derivative, **18** were confirmed by FTIR, ^{1}H NMR spectral and elemental analysis data. FTIR spectrum of compound **17** showed sharp peaks at 2220 cm^{-1} (C≡N) and 2919 cm^{-1} (C-H). Further, in its ^{1}H NMR spectrum it displayed peaks at δ 0.81-1.86 ppm (long chain alkyl protons), δ 4.56 ppm (OCH$_2$), and δ 7.73-7.86 ppm (aromatic protons). The monomer **18** showed NMR signals at δ 10.1 ppm (-CHO) which confirms the coupling of the monomer **17** and 3-formylphenylboronic ester (**6**). In FTIR spectrum of monomer **18**, sharp peak at 1695 cm^{-1} indicates the presence of >C=O functionality. **Figures 3.7** and **3.9** show FTIR spectra of intermediates **17** and **18**, respectively, while **Figures 3.8** and **3.10** indicate ^{1}H NMR spectra of intermediates **17** and **18**, respectively.
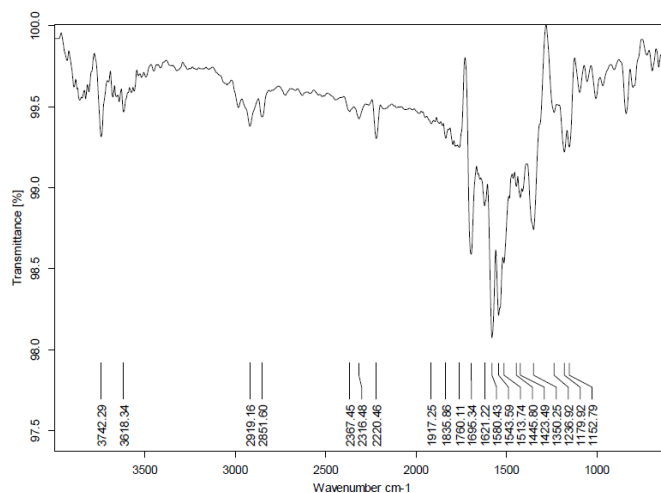
Figure 3.7: FTIR spectrum of intermediate **17**
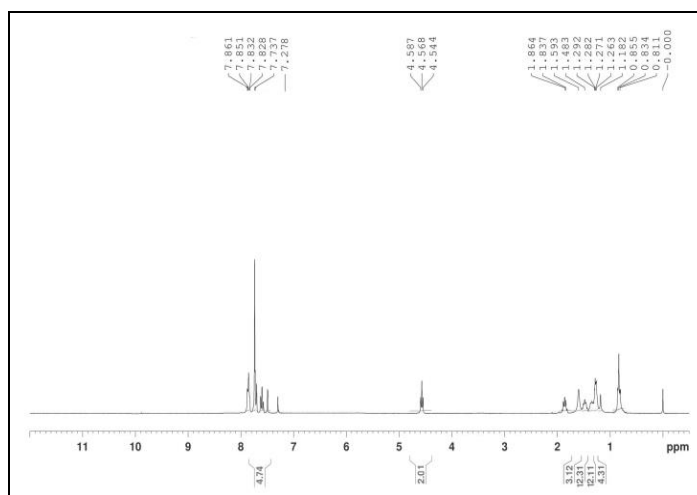
Figure 3.8: ^{1}H NMR spectrum of intermediate **17**
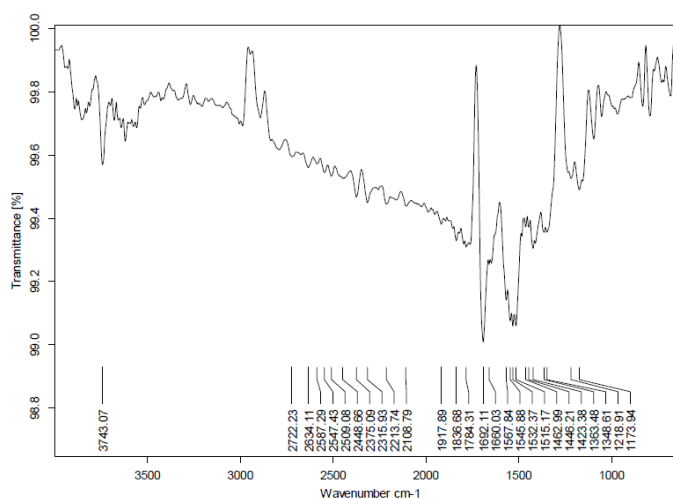
Figure 3.9: FTIR spectrum of intermediate **18**
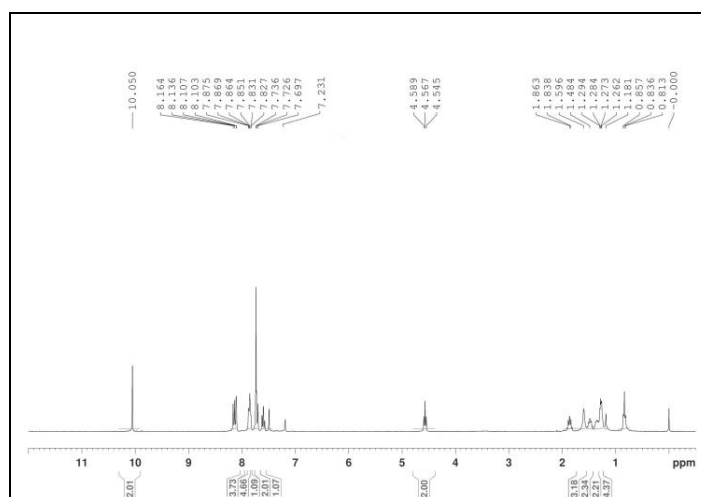
Figure 3.10: ^{1}H NMR spectrum of intermediate **18**

3.6 SYNTHESIS OF PHENYLENE-CYANOPYRIDINE BASED POLYMERS CARRYING VINLYLENE LINKAGE, VPPy$_{1-3}$ (SERIES-1)

Synthetic scheme for the polymerization of monomers to obtain target phenylene-cyanopyridine based polymers carrying vinylene linkage, **VPPy$_{1-3}$** (**Series-1**) has been illustrated in **Scheme 3.4**.
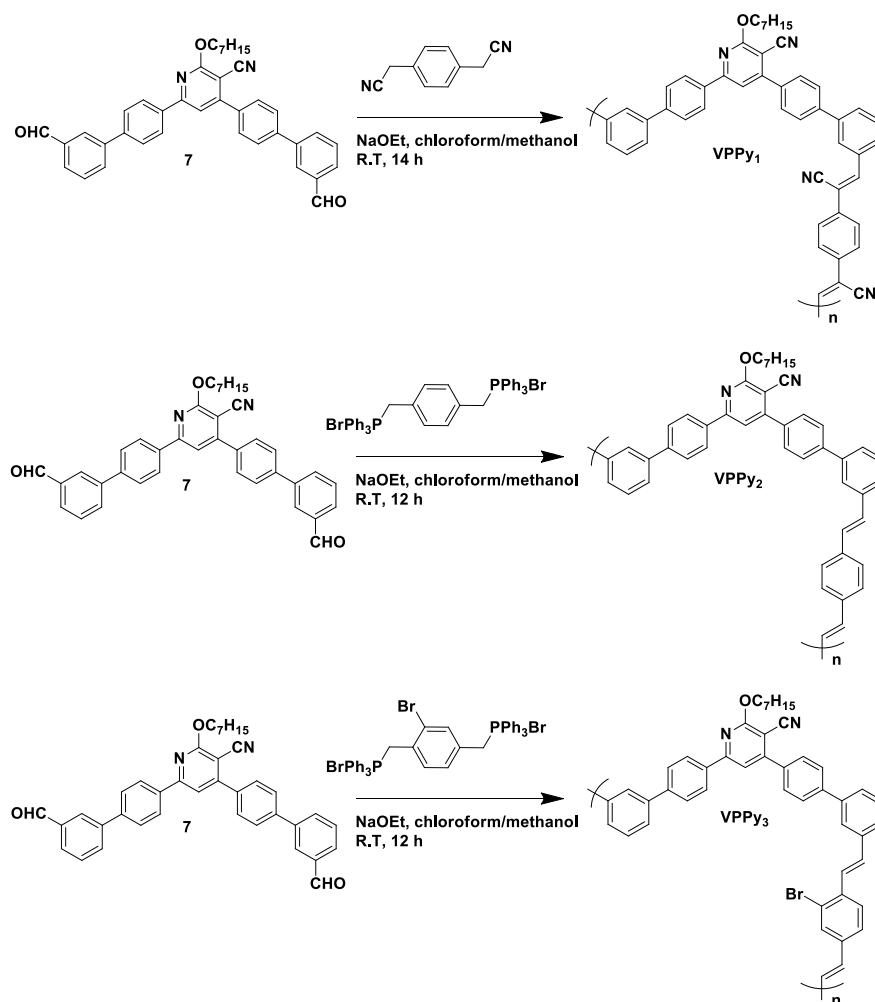
Scheme 3.4: Synthesis of target polymers **VPPy$_{1-3}$**

3.6.1 Chemistry

As outlined in **Scheme 3.4,** polycondensation of monomer, **7** with 1,4-phenylenediacetonitrile to form polymer, **VPPy$_1$** was achieved by Knoevenagel condensation technique. Whereas copolymerization of monomer, **7** with Wittig salts **10** and **13** to yield **VPPy$_2$** and V**PPy$_3$** respectively, was carried out by Witting method.

3.6.2 Synthesis and characterization

The detailed procedures used for the synthesis of polymers; **VPPy₁₋₃** were given below.

3.6.2.1 Synthesis of new polymer VPPy₁

Monomer, **7** (0.1 g, 0.13 mmol) and phenylene diacetonitrile (0.03 g, 0.19 mmol) were dissolved in a mixture of 5 mL of chloroform and 15 mL of ethanol. Freshly prepared sodium ethoxide (0.020 g, 1 mmol in 10 mL of ethanol) was added to the reaction mixture at room temperature under nitrogen atmosphere. Yellow colored reaction mixture was stirred for 9 h at room temperature. After completion of the reaction, solvent was removed under reduced pressure. The crude reaction mass was poured into excess of methanol and stirred for 20 mins. The obtained polymer **VPPy₁** was filtered and washed thoroughly with acetone. Crude product was re-dissolved in chloroform and poured into excess of methanol to remove oligomers. Thus, obtained precipitate was filtered off and dried at 40 ℃ under vacuum for 20 h to give fluorescent pale color powder. Yield 62%. FTIR (cm⁻¹): 2219 (C≡N), 2919 (C-H). 1H NMR (300 MHz, CDCl3, ppm): 1.19-1.86 (m, 13H), 4.56-4.59 (t, 2H), 7.24-8.21 (m, 23H). $\overline{M}_w$: 11,120 g/ mol, PDI: 1.94. Elemental Anal. Calc. (%) for **VPPy₁**: C, 83.80; H, 6.34; N, 7.67; Found: C, 83.85; H, 6.37; N, 7.65.

3.6.2.2 Synthesis of new polymer, VPPy₂

Monomer, **7** (0.1 g, 0.13 mmol) and 1,4 *bis*((bromotriphenylphosphoranyl)-methyl)benzene (**10**, 0.14 g, 0.18 mmol) were dissolved in a mixture of 5 mL of chloroform and 15 mL of ethanol. Freshly prepared sodium ethoxide (0.020 g, 1 mmol in 10 mL of ethanol) was added to the reaction mixture at room temperature under nitrogen atmosphere. Reaction mixture turned into yellow color. It was then stirred for 9 h at room temperature. After completion of the reaction, solvent was removed under reduced pressure. The crude reaction product was poured into excess of methanol and stirred for 20 mins. The obtained polymer, **VPPy₂** was filtered and washed thoroughly with acetone. Crude product was re-dissolved in chloroform and poured into excess of methanol to remove oligomers. Thus, obtained pure precipitate was filtered off and dried at 40 ℃ under vacuum for 20 h to give fluorescent yellow

coloured powder. Yield 53%. FTIR (cm^{-1}): 2219 (C≡N), 2919(C-H). ^{1}H NMR (300 MHz, CDCl$_3$, δ ppm): 1.19-1.87 (m, 13H), 4.55-4.59 (t, 2H), 6.93-8.10 (m, 24H). $\overline{M}_w$: 7.50 kDa, PDI : 1.97. Elemental Anal. Calc. (%) for **VPPy$_2$**: C, 86.43; H, 7.11; N, 4.11; Found: C, 86.49; H, 7.06; N, 4.15.

3.6.2.3 Synthesis of new polymer, *VPPy$_3$*

A mixture of monomer, **7** (0.1 g, 0.13 mmol) and ((2-bromo-1,4-phenylene)*bis*(methylene)) bis(bromotriphenylphosphorane) (**13**, 0.15 g, 0.17 mmol) were dissolved in a mixture of 5 mL of chloroform and 15 mL of ethanol. Freshly prepared sodium ethoxide (0.020 g, 1 mmol in 10 mL of ethanol) was added to the reaction mixture at room temperature under nitrogen atmosphere. Reaction mixture turned into yellow color and it was stirred for 9 h at room temperature. After the completion of the reaction, solvent was removed under reduced pressure. The crude reaction mass was poured into excess of methanol and stirred for 20 mins. The obtained polymer **VPPy$_3$** was filtered and washed thoroughly with acetone. Crude product was re-dissolved in chloroform and poured into excess of methanol to remove oligomers. Thus, obtained precipitate was filtered off and dried at 40^{0}C under vacuum for 20 h to give fluorescent yellow coloured powder. Yield 56%. FTIR (cm^{-1}): 2222 (C≡N), 2918 (C-H). ^{1}H NMR (300 MHz, CDCl$_3$, δ ppm): 1.17-1.86 (m, 13H), 4.56-4.59 (t, 2H), 7.74-8.11 (m, 23H). $\overline{M}_w$: 7.81 kDa, PDI: 1.95. Elemental Anal. Calc. (%) for **VPPy$_3$**: C, 77.46; H, 6.23; N, 3.69; Found: C, 77.59; H, 6.13; N, 3.62.

3.6.2.4 Results and discussion

Polycondensation of monomer, **7** with 1,4-phenylenediacetonitrile to form polymer **VPPy$_1$** was achieved by Knoevenagel condensation technique. On the other hand, polymers, **VPPy$_2$** and **VPPy$_3$** were synthesized from their monomers by Witting method. The structures of the new intermediates and the target polymers were established by FTIR, ^{1}H NMR spectral and elemental analyses and their molecular weights were determined by gel permeation chromatographic technique. The monomer, **7** in its FTIR spectrum showed a strong peak in the region of 1635 cm^{-1} due to the presence of –CHO, which disappeared on polymerization. The disappearance of a peak at around δ 10.0 ppm in the ^{1}H NMR spectra of polymers

indicates the participation of aldehydic group in polymerization. The weight-average molecular weights of the polymers **VPPy₁**, **VPPy₂** and **VPPy₃** were found to be 11,120, 7,502 and 7,810 g mol^{-1}, respectively. The polydispersity indexes of these polymers are 1.94, 1.97 and 1.95, respectively. **Figures 3.11** and **3.13** display FTIR spectra of polymers **VPPy₁** and **VPPy₃**, respectively, while **Figures 3.12** and **3.14** show ^{1}H NMR spectra of polymers **VPPy₁** and **VPPy₃**, respectively.
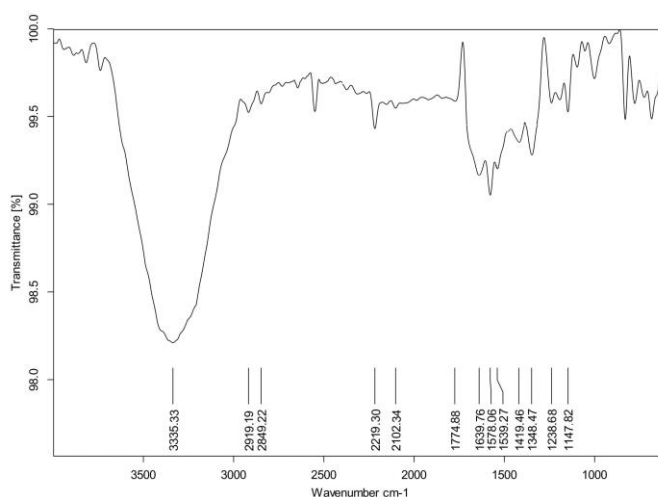
Figure 3.11: FTIR spectrum of polymer, **VPPy₁**
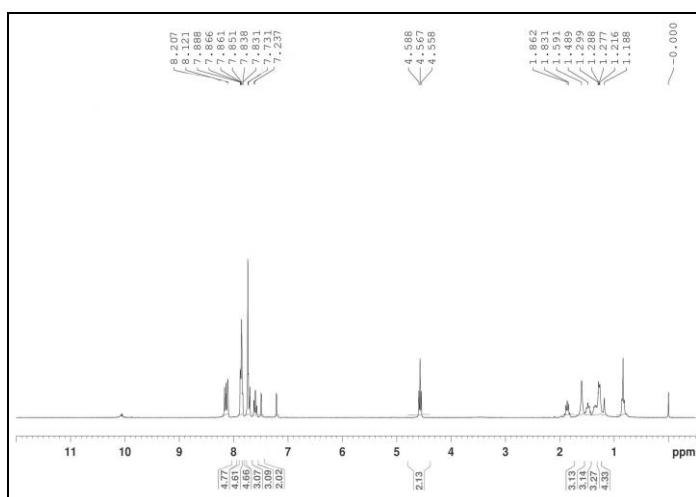
Figure 3.12: ^{1}H NMR spectrum of polymer, **VPPy₁**
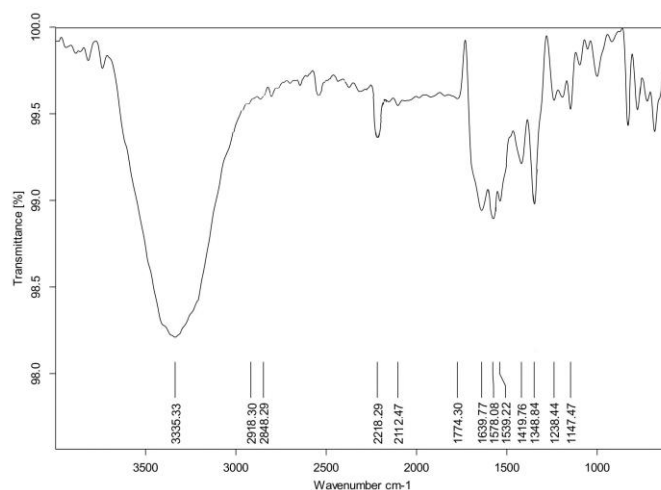
Figure 3.13: FTIR spectrum of polymer **VPPy₃**
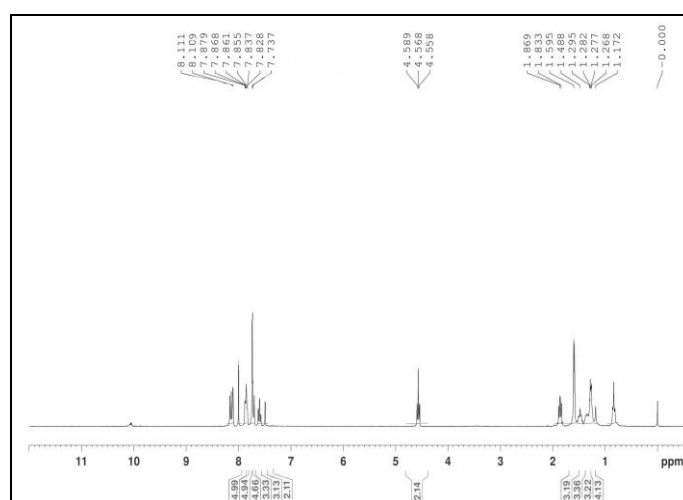
Figure 3.14: ¹H NMR spectrum of polymer **VPPy₃**

3.7 SYNTHESIS OF THIOPHENE-CYANOPYRIDINE BASED POLYMERS CONTAINING VINLYLENE LINKAGE, VTPy₁₋₃ (SERIES-2)

Synthetic route for the polymerization of monomers to obtain required thiophene-cyanopyridine based polymers carrying vinylene linkage, **VTPPy₁₋₃** (**Series-2**) has been described in **Scheme 3.5**.
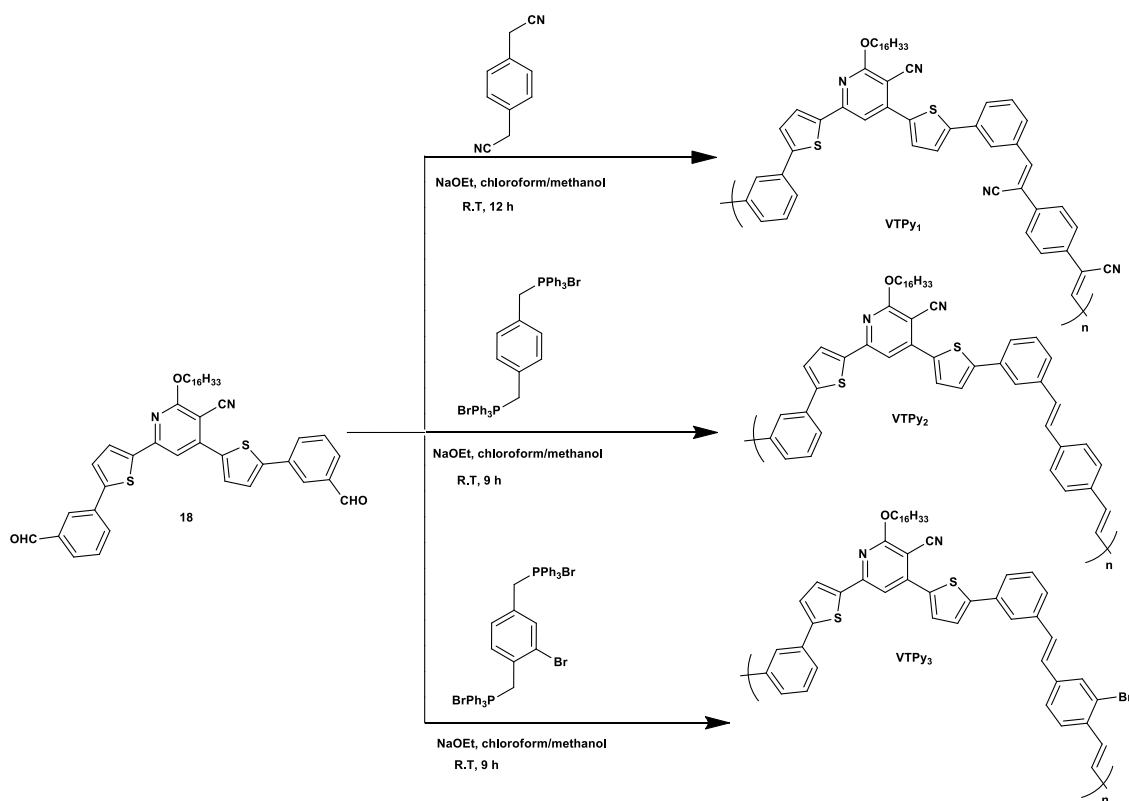
Scheme 3.5: Synthesis of polymers **VTPy1-3**

3.7.1 Synthesis of new polymer VTPy1

Cyanopyridine carrying thiophene derivative **18**, (0.5 g, 0.68 mmol) and phenylene diacetonitrile (0.13 g, 0.83 mmol) were dissolved in a mixture of 5 mL of chloroform and 15 mL of ethanol. Freshly prepared sodium ethoxide (0.06 g, 2.6 mmol in 10 mL of ethanol) was added to the reaction mixture at room temperature under nitrogen atmosphere. The content turned to yellow color and it was further stirred for 12 h at room temperature. Reaction was monitored by TLC. After completion of the reaction, solvent was removed under reduced pressure. The crude reaction mass was poured onto excess of methanol and stirred for 20 min. The obtained polymer **VTPy1** was filtered and washed thoroughly with acetone to remove traces of monomers. The crude product was re-dissolved in chloroform and poured onto excess of methanol to remove oligomers. Obtained precipitate was filtered off and dried at 40 ^{0}C under vacuum for 20 h to give fluorescent yellow color powder. Yield 65%. FTIR (cm^{-1}): 2217 (C≡N), 2917 (C-H). ^{1}H NMR (300 MHz, CDCl$_3$, δ ppm): 1.18-1.86 (m, 31H), 4.54-4.58 (b, 2H), 7.23-8.1 (m, 20H). $\overline{M}_w$: 18.93 kDa,

PDI: 1.62. Elemental Anal. Calcd (%) for **VTPy$_1$**: C, 77.56; H, 6.74; N, 6.46; Found: C, 77.52; H, 6.72; N, 6.43.

3.7.2 Synthesis of new polymer VTPy$_2$

A mixture of cyanopyridine carrying thiophene derivative **18**, (0.5 g, 0.68 mmol) and 1,4 bis{(bromotriphenylphosphoranyl)methyl}benzene (0.95 g, 1.05 mmol) was dissolved in a blend of 5 mL of chloroform and 15 mL of ethanol. Freshly prepared sodium ethoxide (0.1 g, 4.3 mmol in 10 mL of ethanol) was added drop-wise to the reaction mixture under nitrogen atmosphere. Reaction mixture turned to pale yellow color after 30 min rigorous stirring. It was further stirred for 9 h at room temperature to complete polycondensation reaction. Then, solvent was removed under reduced pressure. The crude reaction mass was thoroughly washed with excess of methanol followed by acetone to remove traces of monomers. Crude product was purified by re-precipitation technique using chloroform and methanol solvent system. The obtained precipitate **VTPy$_2$** was filtered off and dried at 40 ^{0}C under vacuum for 20 h to give pale yellow powder. Yield 59%. ATR-IR (cm^{-1}): 2219 (C≡N), 2919 (C-H). ^{1}H NMR (300 MHz, CDCl$_3$, δ ppm): 1.18-1.87 (m, 31H), 4.54-4.58 (b, 2H), 6.93-8.1 (m, 21H). $\overline{\text{M}}_w$: 15.37 kDa, PDI: 1.73. Elemental Analysis calcd. for **VTPy$_2$**: C, 79.37; H, 7.40; N, 3.43; Found: C, 79.33; H, 7.39; N, 3.42.

3.7.3 Synthesis of new polymer VTPy$_3$

The monomers, *i.e.* cyanopyridine carrying thiophene derivative **18**, (0.5g, 0.68 mmol) and 1,4 bis((bromotriphenylphosphoranyl)methyl)bromobenzene (0.91 g, 1.04 mmol) were dissolved in a mixture of 5 mL of chloroform and 15 mL of ethanol. Freshly prepared sodium ethoxide (0.1 g, 4.3 mmol in 10 mL of ethanol) was added drop-wise to the reaction mixture at room temperature under nitrogen atmosphere. Reaction mixture turned to light pale-yellow color after continuous stirring for 30 min. Further condensation reaction was continued for 12 h at room temperature. Progress of reaction was monitored by TLC. After completion of the reaction, solvent was removed, and crude reaction mass was poured onto excess of methanol under stirring for 20 min. The obtained polymer **VTPy$_3$** was filtered and washed thoroughly with acetone to remove traces of monomers. Crude product was re-dissolved in

chloroform and poured onto excess of methanol to precipitate the pure polymer. The precipitate was filtered off and dried at 40 ^{0}C under vacuum for 20 h to give whitish yellow coloured powder. Yield 55%. ATR-IR (cm^{-1}): 2222 (C≡N), 2918 (C-H). ^{1}H NMR (300 MHz, CDCl$_3$, δ ppm): 1.18-1.86 (m, 31H), 4.54-4.58 (b, 2H), 7.25-8.1 (m, 20H). $\overline{M}_w$: 15.28 kDa, PDI: 1.81. Elemental Anal. Calcd (%) for **VTPy$_3$**: C, 72.38; H, 6.64; N, 3.13. Found: C, 72.36; H, 6.62; N, 3.12.

3.7.4 Results and discussion

Polycondensation of monomer, **18** with 1,4-phenylenediacetonitrile to form polymer, **VTPy$_1$** was achieved by Knoevenagel condensation technique. While, synthesis of polymer, **VTPy$_2$** from monomer, **18** and Wittig salt, **10** was carried out by Wittig method. The same method was followed for the preparation of polymer, **VTPy$_3$** from monomer, **18** and Wittig salt, **13**. The structures of the new intermediates and the target polymers were established by FTIR, ^{1}H NMR and elemental analyses. The monomer, **18** in its FTIR spectrum showed a strong peak in the region of 1700 cm^{-1} due to –CHO functionality, which disappeared on polymerization. The disappearance of a peak at about δ 10.0 ppm in the ^{1}H NMR spectra of polymers confirmed the involvement of aldehydic group in polymerization. The the weight-average molecular weights of the polymers were determined by GPC technique. Accordingly, $\overline{M}_w$ of **VTPy$_1$**, **VTPy$_2$** and **VTPy$_3$** were found to be 18,932, 15,367 and 15,275 g mol^{-1}, respectively. The polydispersity indices of these polymers are 1.62, 1.73 and 1.81, respectively. **Figures 3.15** and **3.17** display FTIR spectra of polymers **VTPy$_1$** and **VTPy$_3$**, respectively, while **Figures 3.16** and **3.18** show ^{1}H NMR spectra of polymers **VTPy$_1$** and **VTPy$_3$**, respectively.
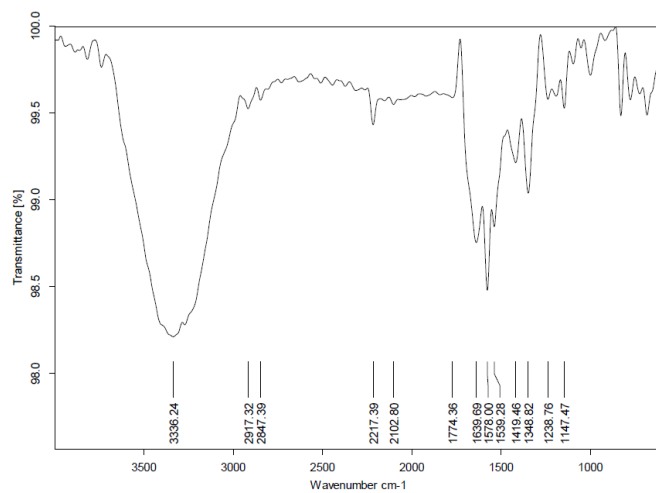
Figure 3.15: FTIR spectrum of polymer **VTPy₁**
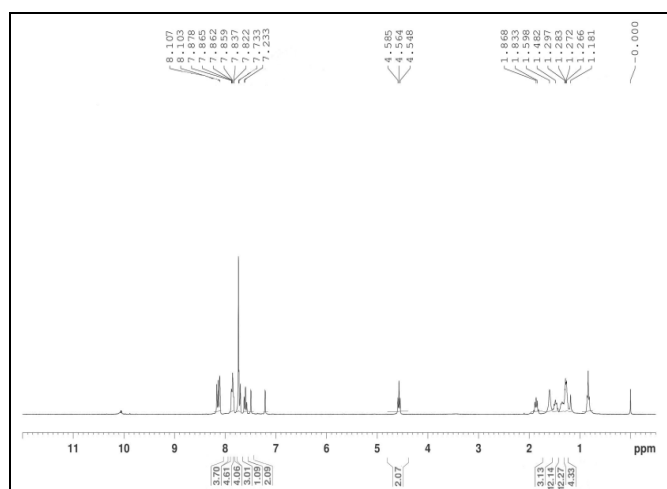
Figure 3.16: ^{1}H NMR spectrum of polymer **VTPy₁**
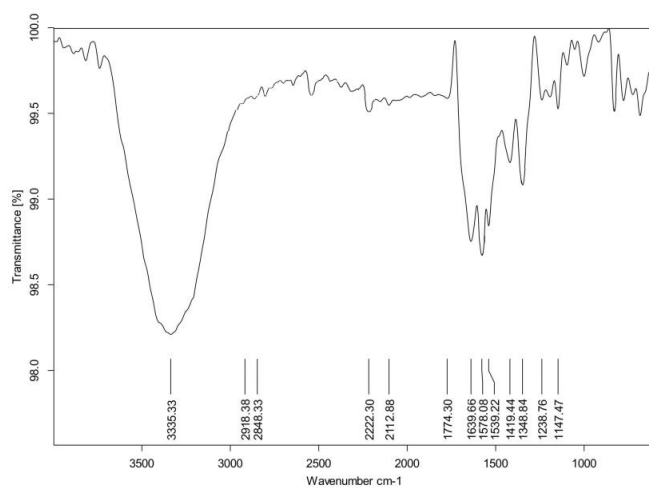
Figure 3.17: FTIR spectrum of polymer **VTPy₃**
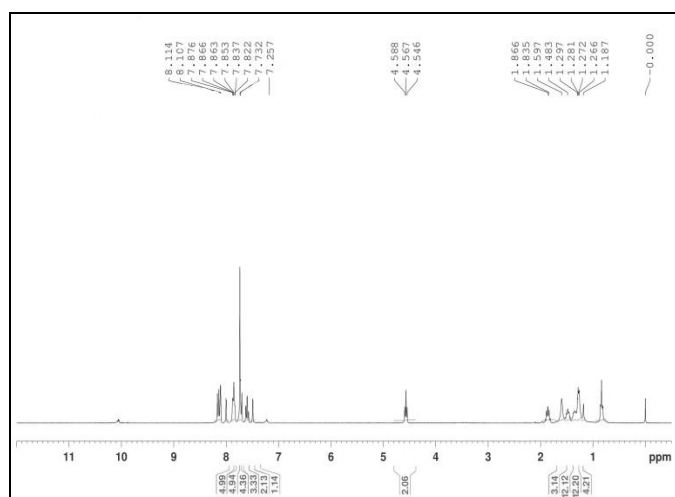
Figure 3.18: ^{1}H NMR spectrum of polymer **VTPy₃**

3.8 SYNTHESIS OF PHENYLENE-CYANOPYRIDINE BASED POLYMERS, PPy$_{1-3}$ (SERIES-3)

Synthetic pathway for the polymerization of monomer, **4** with boronic acids *viz.* 1,4-phenylenebisboronic acid **4a**, 4,4′-biphenyldiboronic acid **4b**, and 9,9-dihexylfluorene-2,7-diboronic acid **4c** to obtain target phenylene-cyanopyridine based polymers **PPy$_{1-3}$** (**Series-3**) has been described in **Scheme 3.6**.
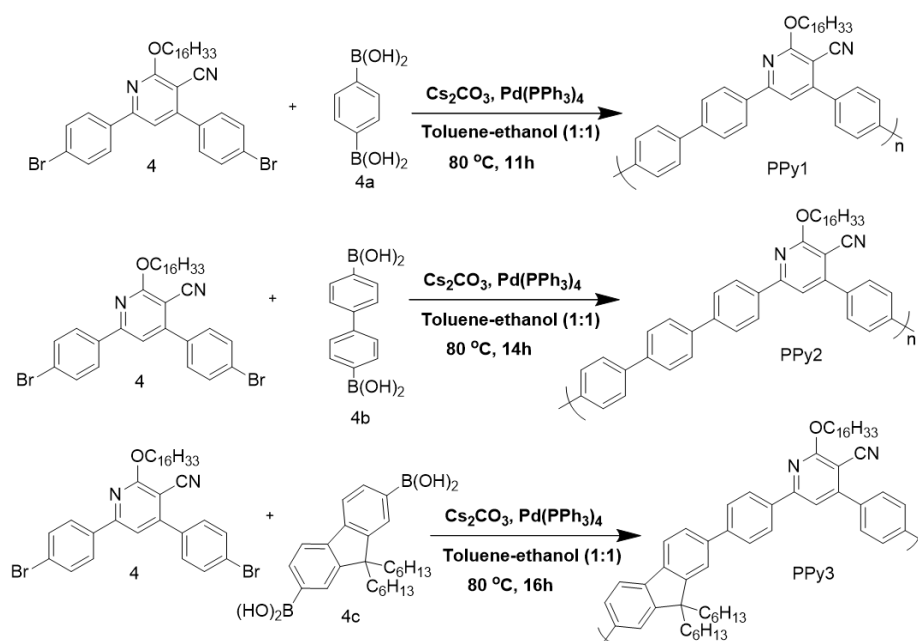
Scheme 3.6: Synthesis of polymers **PPy$_{1-3}$**

3.8.1 General method for the synthesis of polymers PPy₁₋₃

A solution of cyanopyridine based monomer **4,** (1 g, 1.5 mmol), Cs_2CO_3 (3.4 g, 10.5 mmol), and $Pd(PPh_3)_4$ (0.84 g, 0.75 mmol) in 20 mL of dried 1:1 mixture of toluene and ethanol was taken in a 100 mL two neck round bottom flask. To above mixture, 1.5 mmol of respective boronic acid, *viz.* 1,4-phenylenebisboronic acid, **4a** (for **PPy₁**), 4,4′-biphenyldiboronic acid **4b** (for **PPy₂**) or 9,9-dihexylfluorene-2,7-diboronic acid **4c** (for **PPy₃**) was added and refluxed under inert atmosphere. The reaction mixture was cooled to room temperature and excess solvent was removed under reduced pressure. The obtained reaction mass was dissolved in CH_2Cl_2 and filtered using the Celite bed to remove catalytic traces. The filtrate was thoroughly washed with distilled water to remove traces of solvent and base. Then, the solvent in the organic layer was removed under the vacuum. Further, to remove the lower weight oligomer fractions, the resultant crude product was subjected to Soxhlet extraction using the solvents methanol, acetone and hexane sequentially. Finally, the crude product was dissolved in a minimum amount of $CHCl_3$, followed by re-precipitation using methanol to get the pure polymer.

PPy₁: Yellow solid, Yield 61%. FTIR (cm^{-1}): 2224 (C≡N), 2912 (C-H), NMR (300 MHz, $CDCl_3$, δ ppm): 0.89-1.93 (m, 13H), 4.56-4.61 (b, 2H), 7.28-7.97 (m, 13H). $\overline{M}_w$: 38.8 kDa, PDI: 1.34. Elemental Anal. Calcd (%) for **PPy₁** : C, 83.37; H, 6.77; N, 6.27; Found: C, 83.35; H, 6.74; N, 6.26.

PPy₂: Pale yellow powder, Yield 69%. FTIR (cm^{-1}): 2217 (C≡N), 2918 (C-H).¹H NMR (300 MHz, $CDCl_3$, δ ppm): 0.89-1.93 (m, 13H), 4.56-4.61 (b, 2H), 7.31-7.79 (m, 17H). $\overline{M}_w$: 38.97 kDa, PDI: 1.35. Elemental Anal. Calcd (%) for **PPy₂**: C, 85.04; H, 6.76; N, 5.22; Found: C, 85.02; H, 6.73; N, 5.21.

PPy₃: Whitish yellow solid, Yield 72%. FTIR (cm^{-1}): 2222 (C≡N), 2918 (C-H). ¹H NMR (300 MHz, $CDCl_3$, δ ppm): 0.89-2.25 (m, 39H), 4.56-4.61 (b, 2H), 7.51-8.07 (m, 15H). $\overline{M}_w$: 57.73 kDa, PDI: 1.13. Elemental Anal. Calcd (%) for **PPy₃**: C, 85.42; H, 8.32; N, 3.98; Found: C, 85.41; H, 8.31; N, 3.96.

3.8.2 Results and discussion

Scheme 3.6 depicts the synthetic pathways for the preparation of the new polymers **PPy$_{1-3}$**. The prerequisite monomer 2-heptoxyl cyanopyridine (**4**) was synthesized according to Suzuki coupling. Further, the final polymers **PPy$_{1-3}$,** were obtained in good yield by reacting monomer, **4** with three different boronic acids, *viz.* 1,4-phenylenebisboronic acid **4a**, 4,4′-biphenyldiboronic acid **4b** and 9,9-dihexylfluorene-2,7-diboronic acid **4c** following renowned Suzuki coupling method. The chemical structures of the polymers **PPy$_{1-3}$** were established by ^{1}H NMR, FTIR spectral and elemental analyses. Further, ^{1}H NMR spectrum of all the polymers showed peaks at δ 0.8-1.9, 4.5 and 7.2-7.9, ppm indicating the presence of alkyl chain, -OCH$_2$ and the aromatic protons, respectively. The gel permeation chromatographic technique was used to determine the weight-average molecular masses and polydispersity indices of the polymers **PPy$_{1-3}$**. Their $\overline{M}_w$ were found to be 38,816, 38,966 and 57,730 g/mol, respectively and the polydispersity indices are in the order of 1.34, 1.35 and 1.13, respectively. **Figures 3.19** and **3.21** display FTIR spectra of polymers **PPy$_1$** and **PPy$_3$**, respectively, while **Figures 3.20** and **3.22** show ^{1}H NMR spectra of polymers **PPy$_1$** and **PPy$_3$**, respectively.
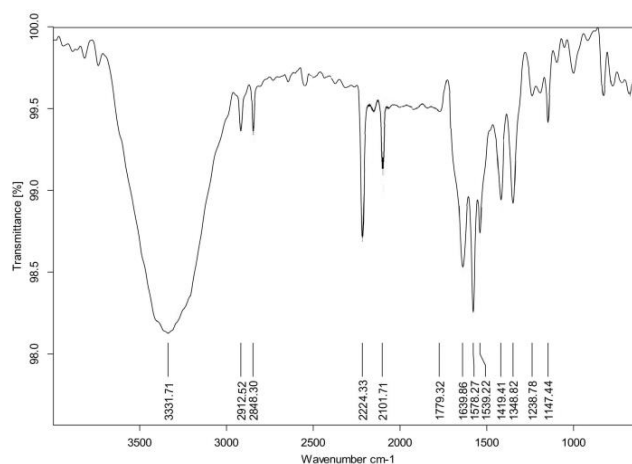
Figure 3.19: FTIR spectrum of polymer **PPy$_1$**

Figure 3.20: ^{1}H NMR spectrum of polymer **PPy₁**

Figure 3.21: FTIR spectrum of polymer **PPy₃**
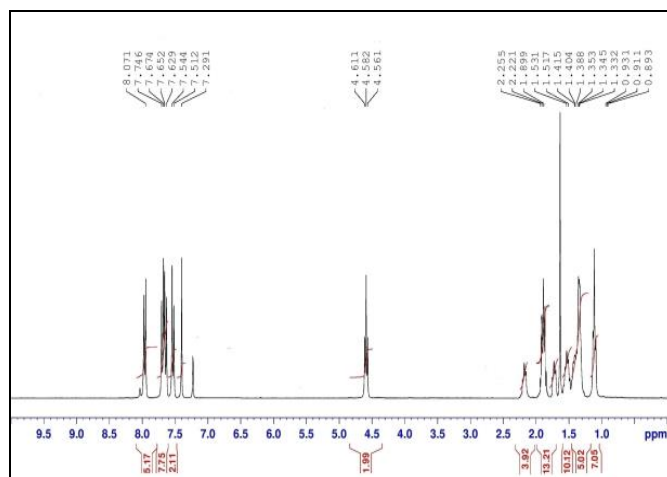
Figure 3.22: ^{1}H NMR spectrum of polymer **PPy₃**

3.9 SYNTHESIS OF THIOPHENE-CYANOPYRIDINE BASED POLYMERS, TPy$_{1-3}$ (SERIES-4)

Synthetic pathways for the polymerization of monomer **17** with boronic acids *viz.* 1,4-phenylenebisboronic acid **4a**, 4,4′-biphenyldiboronic acid **4b** and 9,9-dihexylfluorene-2,7-diboronic acid **4c** to obtain required thiophene-cyanopyridine based polymers, **TPy$_{1-3}$** (**Series-4**) have been described in **Scheme 3.7**.
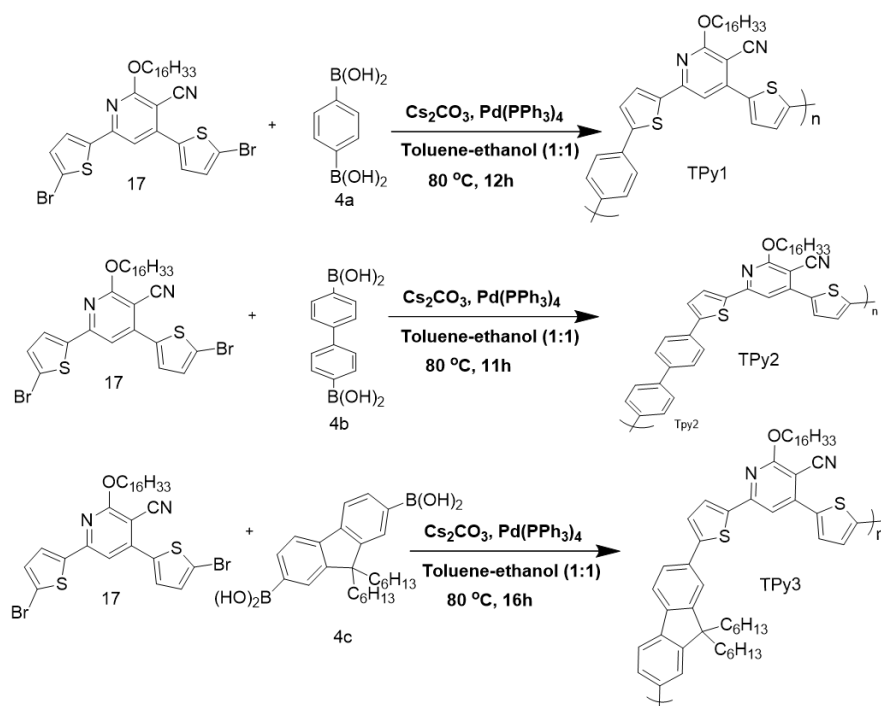
Scheme 3.7: Synthesis of polymers **TPy$_{1-3}$**

3.9.1 General method for the synthesis of polymers, TPy$_{1-3}$

A mixture of cyanopyridine based monomer **17,** (1 g, 1.5 mmol), Cs$_2$CO$_3$ (3.4 g, 10.5 mmol), and Pd(PPh$_3$)$_4$ (0.84 g, 0.75 mmol) in 20 mL of dried 1:1 mixture toluene and ethanol mixture was taken in a 100 mL two neck round bottom flask. To above mixture, 1.5 mmol of respective boronic acid, *viz.* 1,4-phenylenebisboronic acid **4a** (for *TPy$_1$*), 4,4′-biphenyldiboronic acid **4b** (for *TPy$_2$*) or 9,9-dihexylfluorene-2,7-diboronic acid **4c** (for *TPy$_3$*) was added and refluxed under argon atmosphere. The reaction mixture was cooled to room temperature and excess solvent was removed under reduced pressure. The obtained reaction mass was further dissolved in CH$_2$Cl$_2$ and filtered using the Celite bed to remove catalytic traces. The obtained filtrate was

thoroughly washed with distilled water to remove traces of solvent and base. Then the solvent in the organic layer was removed under vacuum. Further, to remove the lower weight oligomer fractions, the resultant crude product was subjected to Soxhlet extraction using the solvents methanol, acetone and hexane sequentially. Finally, the crude product was dissolved in limited amount of chloroform, followed by re-precipitation using methanol to get the pure polymer.

TPy₁: Fluorescent yellowish color solid, Yield 65%. FTIR (cm⁻¹): 2221 (C≡N), 2918 (C-H). ¹H NMR (300 MHz, CDCl₃, δ ppm): 0.89-1.88 (m, 31H), 4.55-4.61 (b, 2H), 7.39-7.70 (m, 9H). $\overline{M}_w$: 33.2 kDa, PDI: 1.23. Elemental Anal. Calcd (%) for **TPy₁**: C, 74.46; H, 7.89; N, 4.57; Found: C, 74.44; H, 7.88; N, 4.55.

TPy₂: Pale yellow color solid, Yield 68%. FTIR (cm⁻¹): 2218 (C≡N), 2918 (C-H). ¹H NMR (300 MHz, CDCl₃, δ ppm): 0.89-1.88 (m, 31H), 4.56-4.61 (b, 2H), 7.39-7.71 (m, 13H). $\overline{M}_w$: 44.2 kDa, PDI: 1.24. Elemental Anal. Calcd (%) for **TPy₂**: C, 76.70; H, 7.61; N, 4.07; Found: C, 76.69; H, 7.60; N, 4.06.

TPy₃: Whitish yellow powder, Yield 69%. FTIR (cm⁻¹): 2212 (C≡N), 2918 (C-H). ¹H NMR (300 MHz, CDCl₃, δ ppm): 0.89-1.95 (m, 43H), 4.48-4.62 (b, 6H), 7.52-8.05 (m, 11H). $\overline{M}_w$: 52.8 kDa, PDI: 1.21. Elemental Anal. Calcd (%) for **TPy₃**: C, 78.75; H, 8.81; N, 3.22; Found: C, 78.74; H, 8.80; N, 3.21.

3.9.2   Results and Discussion

The targeted new polymers **TPy₁₋₃** were obtained in good yield following renowned Suzuki coupling polymerization reaction, under anhydrous condition. Their chemical structures were well established using FTIR, ¹H NMR spectral and elemental analyses. Further, ¹H NMR spectrum of all the polymers showed peaks at δ 0.8-1.9, 4.5 and 7.2-8.04, ppm indicating the presence of alkyl chain, -OCH₂ proton and the aromatic protons, respectively. Finally, all the polymers **TPy₁₋₃** were subjected to GPC analysis for determining $\overline{M}_w$ and polydispersity indices of **TPy₁₋₃**. The GPC results revealed that, their $\overline{M}_w$ are 33264, 44227 and 52863 g/mol, respectively and the polydispersity indices are 1.23, 1.24 and 1.21, respectively. **Figures 3.23** and **3.24** display FTIR spectra of polymers **TPy₁** and **TPy₃**, respectively, while **Figure 3.25** shows ¹H NMR spectra of polymer **TPy₃**.

Figure 3.23: FTIR spectrum of polymer **TPy₁**
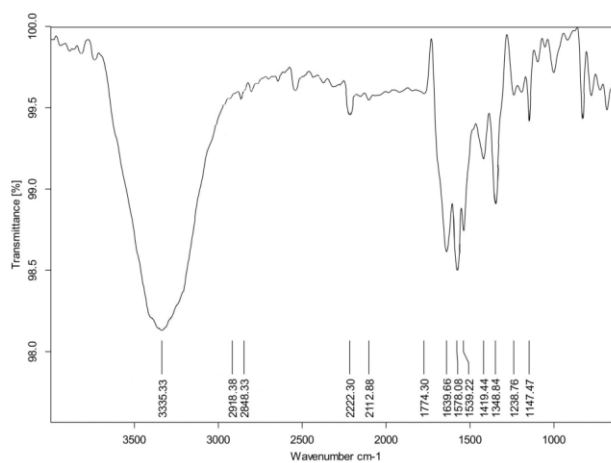
Figure 3.24: FTIR spectrum of polymer **TPy₃**
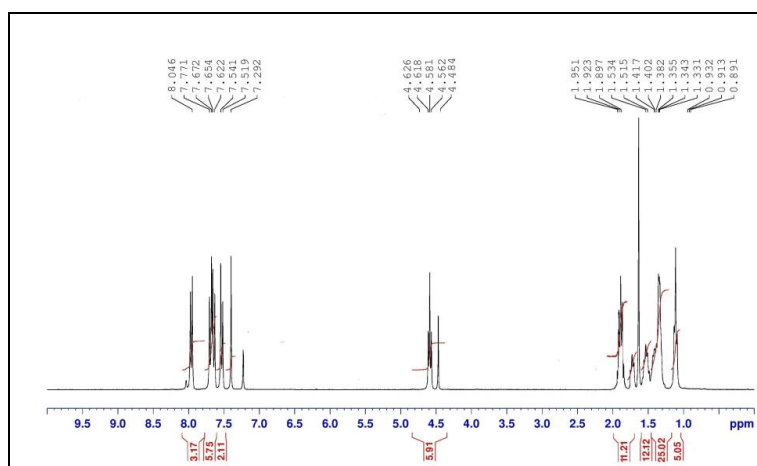
Figure 3.25: ¹H NMR spectrum of polymer **TPy₃**

3.10 SYNTHESIS OF CYANOPYRIDINE BASED POLYMERS CARRYING THIADIAZOLE UNIT, TDPy₁₋₄ (SERIES-5)

Synthetic strategy for the condensation of monomer **4** with comonomer 2,1,3-benzothiadiazole-4,7-bis(boronic acid pinacol ester) **5a** (for **TDPy₁ and TDPy₂**) and naphtho[1,2-c:5,6-c′bis[1,2,5]thiadiazole-5,10-diboronic acid bis(pinacol) ester **5b** (for **TDPy₃ and TDPy₄**) to get required cyanopyridine based polymers carrying thiadiazole unit, **TDPy₁₋₄** (**Series-5**) has been described in **Scheme 3.8**.
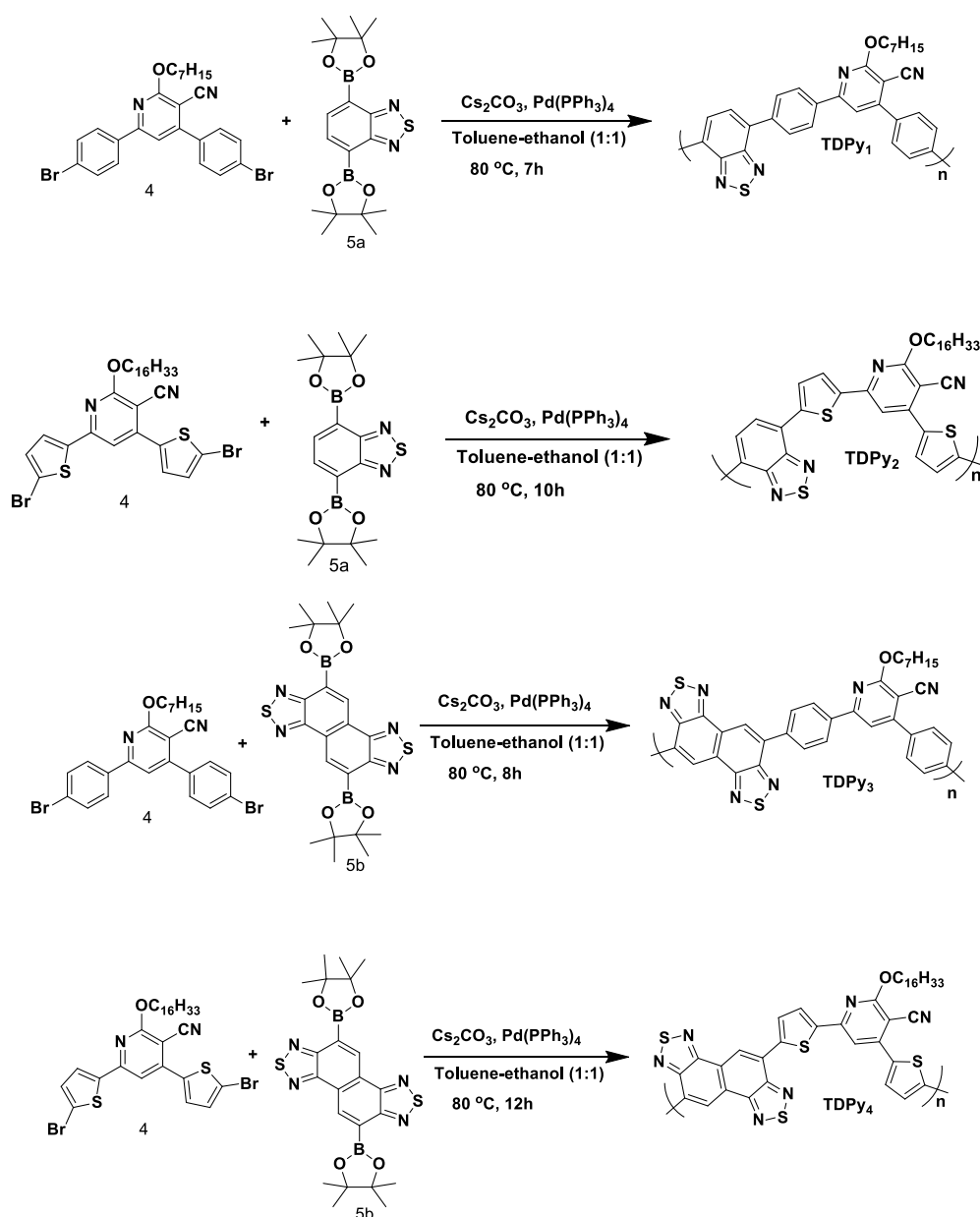
Scheme 3.8: Synthesis of polymers **TDPy₁₋₄**

3.10.1 General method for the synthesis of polymers, TDPy₁₋₄

A solution of cyanopyridine derivative (monomer **4** or **17**, 1.5 mmol), Cs_2CO_3 (3.4 g, 10.5 mmol), and $Pd(PPh_3)_4$ (0.84 g, 0.75 mmol) in 20 mL of dried 1:1 mixture of toluene and ethanol was taken in a 100 mL two neck round bottom flask. To this mixture, 1.5 mmol of respective boronic acid, *viz.* 2,1,3-benzothiadiazole-4,7-bis(boronic acid pinacol ester, **5a** (for **TDPy₁** and **TDPy₂**) and naphtho[1,2-c:5,6-c′bis[1,2,5]thiadiazole-5,10-diboronic acid bis(pinacol) ester, **5b** (for **TDPy₃** and **TDPy₄**) was added and refluxed under inert atmosphere. The excess solvent was removed under reduced pressure. The obtained reaction mass was further treated with excess of CH_2Cl_2 and filtered using the Celite bed to remove catalytic traces. The obtained filtrate was thoroughly washed with distilled water to remove traces of solvent and base. Then, the solvent in the organic layer was removed under the vacuum. Further, to remove the lower weight oligomer fractions, the resultant crude product was subjected to Soxhlet extraction using the solvents methanol, acetone and hexane sequentially. Finally, the crude product was dissolved in a minimum amount of $CHCl_3$, followed by re-precipitation using methanol to get the pure polymer.

TDPy₁: Yellow solid, Yield 61%. FTIR (cm⁻¹): 2222 (C≡N), 2918 (C-H). NMR (300 MHz, $CDCl_3$, δ ppm): 1.19-1.87 (m, 13H), 4.54-4.59 (b, 2H), 7.56-8.29 (m, 11H). $\overline{M}_w$: 22.92 kDa, PDI: 1.78. Elemental Anal. Calcd (%) for **TDPy₁**: C, 73.78; H, 5.59; N, 11.10; Found: C, 73.85; H, 5.69; N, 11.14.

TDPy₂: Pale yellow powder, Yield 69%. FTIR (cm⁻¹): 2224 (-C≡N), 2913 (-C-H). NMR (300 MHz, $CDCl_3$, δ ppm): 0.90-1.85 (m, 31H), 4.45-4.62 (b, 2H), 7.31-7.81 (m, 7H). $\overline{M}_w$: 32.17 kDa, PDI: 1.84. Elemental Anal. Calcd (%) for **TDPy₂**: C, 67.25; H, 6.58; N, 8.71; Found: C, 67.29; H, 6.55; N, 8.73.

TDPy₃: Whitish yellow solid, Yield 72%. FTIR (cm⁻¹): 2222 (C≡N), 2918 (C-H). ¹H NMR (300 MHz, $CDCl_3$, δ ppm): 0.89-1.89 (m, 13H), 4.46-4.51 (b, 2H), 7.40-7.71 (m, 11H). $\overline{M}_w$: 33.83 kDa, PDI: 1.97. Elemental Anal. Calcd (%) for **TDPy₃**: C, 68.60; H, 4.61; N, 13.71; Found: C, 68.61; H, 4.57; N, 13.69.

TDPy₄: Pale yellow powder, Yield 69%. FTIR (cm⁻¹): 2222 (C≡N), 2918 (C-H). ¹H NMR (300 MHz, $CDCl_3$, δ ppm): 0.89-1.88 (m, 31H), 4.56-4.61 (b, 2H), 7.28-7.71

(m, 7H). $\overline{M}_w$: 32.76 kDa, PDI: 1.74. Elemental Anal. Calcd (%) for **TDPy4**: C, 63.97; H, 5.64; N, 11.19; Found: C, C, 63.99; H, 5.61; N, 11.23.

3.10.2 Results and Discussion

The target polymers **TDPy1-4** were obtained in good yield directly by Suzuki coupling polymerization reaction. Their chemical structures were well-established using FTIR, ^{1}H NMR spectral and elemental analyses. Further, all the polymers in their ^{1}H NMR spectra exhibited peaks at δ 0.8-1.88, 4.5-4.6 and 7.2-7.70 ppm indicating the presence of alkyl chain, -OCH$_2$ proton and the aromatic protons, respectively. Finally, the new polymers **TDPy1-4** were subjected to GPC analysis for determining $\overline{M}_w$ and polydispersity index. Their $\overline{M}_w$ values were found to be 22,916, 32,166, 33,830 and 32,756 g/mol, respectively and the polydispersity index values were found to be 1.78, 1.84, 1.97 and 1.74, respectively. **Figures 3.26** and **3.28** display FTIR spectra of polymers **TDPy1** and **TDPy3**, respectively, while **Figures 3.27 and 3.29** show ^{1}H NMR spectra of polymers **TDPy1** and **TDPy3**, respectively.
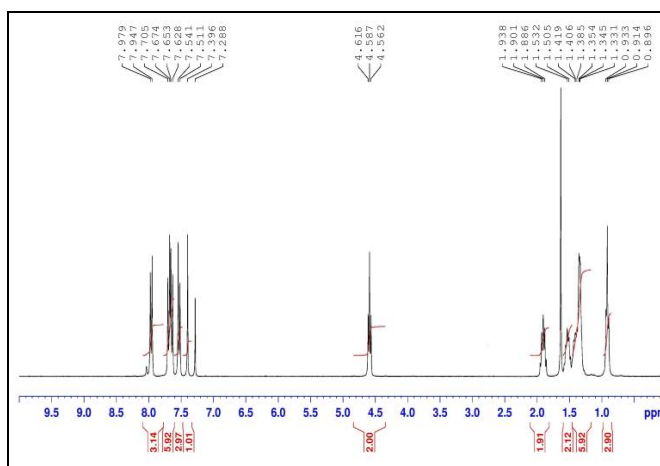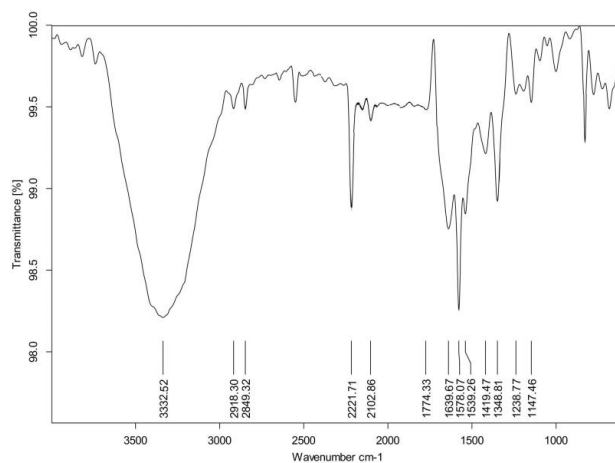

Figure 3.26: FTIR spectrum of polymer **TDPy1**
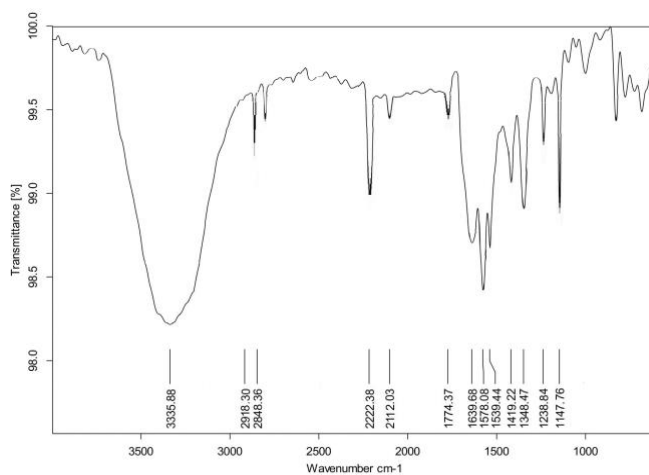
Figure 3.27: ^{1}H NMR spectrum of polymer **TDPy₁**

Figure 3.28: FTIR spectrum of polymer **TDPy₃**

Figure 3.29: ^{1}H NMR spectrum of polymer **TDPy₃**

3.11 SYNTHESIS OF HETEROAROMATIC BASED POLYMERS CARRYING IMINE LINKAGE, Py$_{1-4}$ (SERIES-6)

Synthetic approach used for the preparation of newly designed heteroaromatic based polymers carrying imine linkage, **Py$_{1-4}$ (SERIES-6)** from cyanopyridine based monomers and phenylenediamines has been described in **Scheme 3.9**.
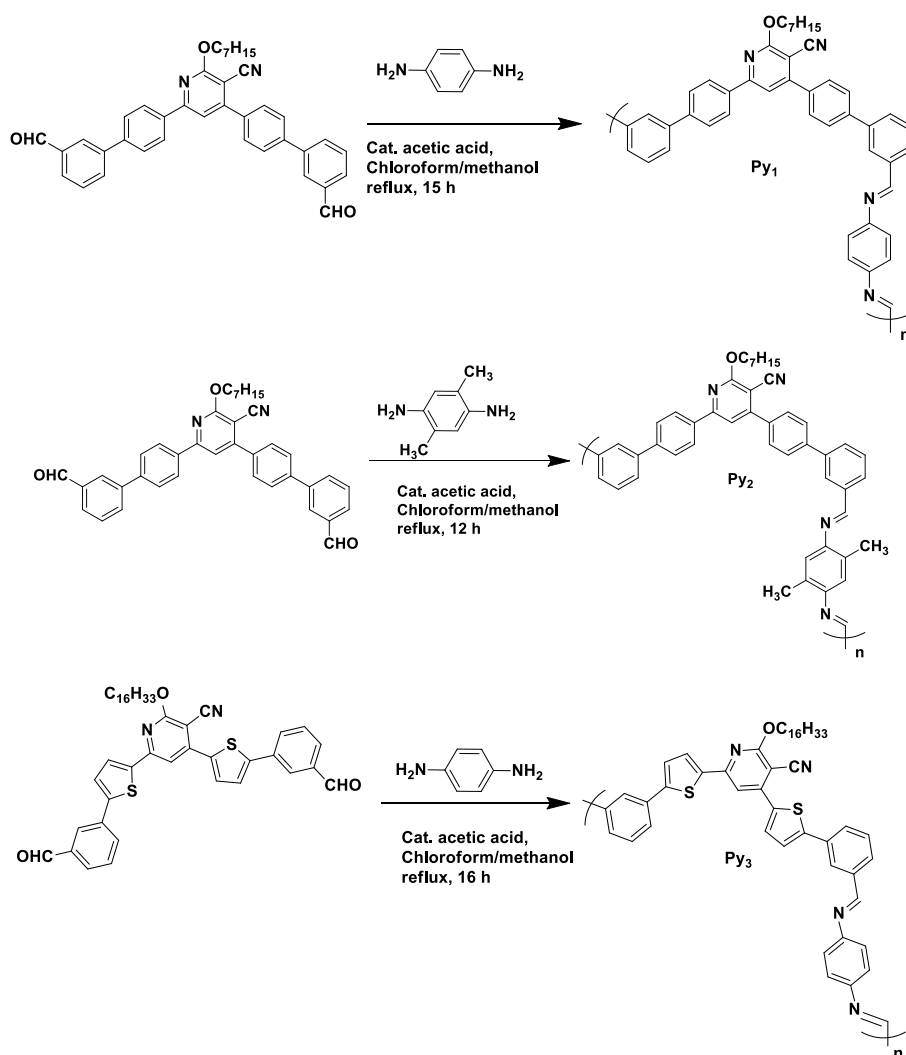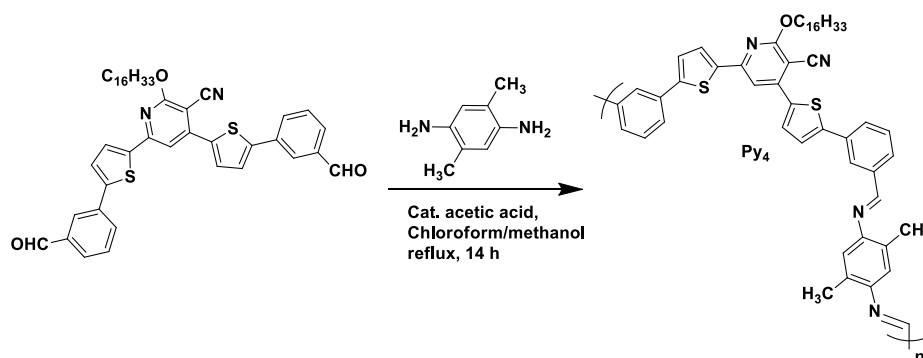
Scheme 3.9: Synthesis of polymers **Py1-4**

3.11.1 General method for the synthesis of polymers Py1-4

To a stirred solution of un/substituted phenylenediamine (0.70 mmol) in 2:1 of chloroform/methanol mixture, cyanopyridine based monomer **7** or **18** (0.60 mmol) was added drop-wise with constant stirring under nitrogen atmosphere. Catalytic amount (4 drops) of glacial acetic acid was added to the reaction mass under vigorous stirring. The reaction mixture was refluxed for 12 h. After completion of the reaction (monitored by TLC), solvent was removed using rotary evaporator at reduced pressure. Thus, obtained residue was quenched to 100 mL of cold water and stirred for 20 mins. The solid product was filtered, washed with acetone, and finally purified by re-precipitation method using chloroform and methanol mixture.

Py1: Yellow colour solid, Yield 62%. FTIR: 2221 cm^{-1} (C≡N), 2918 cm^{-1} (C-H). ^{1}H NMR (300 MHz, CDCl$_3$, δ ppm): 0.85-1.54 (m, 11H), 1.88-1.99 (m, 2H), 4.57-4.61 (b, 2H), 7.22-7.98 (m, 23H). $\overline{M}_w$: 11.4 kDa, PDI: 2.13. Elemental Anal. Calcd (%) for polymer **Py1**: C, 82.91; H, 6.51; N, 8.23 Found: C, 82.95; H, 6.48; N, 8.24.

Py2: Pale yellow colour solid, Yield 67%. FTIR: 2217 cm^{-1} (C≡N), 2917 cm^{-1} (C-H). ^{1}H NMR (300 MHz, CDCl$_3$, δ ppm): 0.89-1.53 (m, 13H), 1.88-1.93 (m, 6H), 4.57-4.61 (b, 2H), 7.40-8.27 (m, 21H). $\overline{M}_w$: 10.9 kDa, PDI: 2.04. Elemental Anal. Calcd (%) for polymer **Py2**: C, 82.96; H, 6.67; N, 8.06; Found: C, 82.99; H, 6.66; N, 8.09.

Py3: Pale yellow colour solid, Yield 74%. FTIR: 2222 cm^{-1} (C≡N), 2918 cm^{-1} (C-H). ^{1}H NMR (300 MHz, CDCl$_3$, δ ppm): 0.85-1.99 (m, 31H), 4.56-4.61 (b, 2H), 7.40-8.08 (m, 19H). $\overline{M}_w$: 9.5 kDa, PDI: 2.09. Elemental Anal. Calcd (%) for polymer **Py3**: C, 76.10; H, 6.64; N, 7.10; Found: C, 76.07; H, 6.63; N, 7.13.

Py₄: Pale yellow colour powder, Yield 65%. FTIR: 2217 cm⁻¹ (C≡N), 2910 cm⁻¹ (C-H). ¹H NMR (300 MHz, CDCl₃, δ ppm): 0.90-1.54 (m, 31H), 1.88-2.23 (m, 6H), 4.57-4.61 (b, 2H), 7.40-8.28 (m, 17H). $\overline{M}_w$: 11.78 kDa, PDI: 2.01. Elemental Anal. Calcd (%) for polymer **Py₄**: C, 76.55; H, 7.38; N, 6.61; Found: C, 76.59; H, 7.36; N, 6.59.

3.11.2 Results and Discussion

The final polymers **Py₁₋₄** were obtained in good yield by condensing the dialdehyde derivatives with phenylene diamines in presence of trace of acid catalyst. Their chemical structures were well-established using FTIR, ¹H NMR spectral and elemental analyses. In FTIR spectrum of monomer **7**, the carbonyl stretching of aldehyde group was observed at 1692 cm⁻¹, but in FTIR spectra of polymers this peak disappeared and a new aromatic C=N stretching was observed at 1640 cm⁻¹. Further, in ¹H NMR spectra of all the polymers the aldehydic peak remained absent, which confirms the formation of imine linkage in all the polymers. Finally, GPC analysis was carried out to all the polymers, **Py₁₋₄** to determine their $\overline{M}_w$ and polydispersity index. According to the analysis, their $\overline{M}_w$ were found to be 11,425, 10,898, 9,526 and 11,778 g/mol, respectively and the polydispersity were shown to be 2.13, 2.04, 2.09 and 2.01, respectively. **Figures 3.30** and **3.32** display FTIR spectra of polymers **Py₁** and **Py₃**, respectively, while **Figures 3.31** and **3.33** show ¹H NMR spectra of polymers **Py₁** and **Py₃**, respectively.
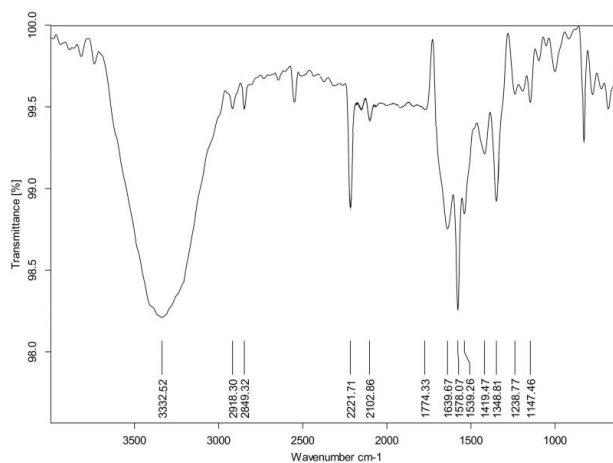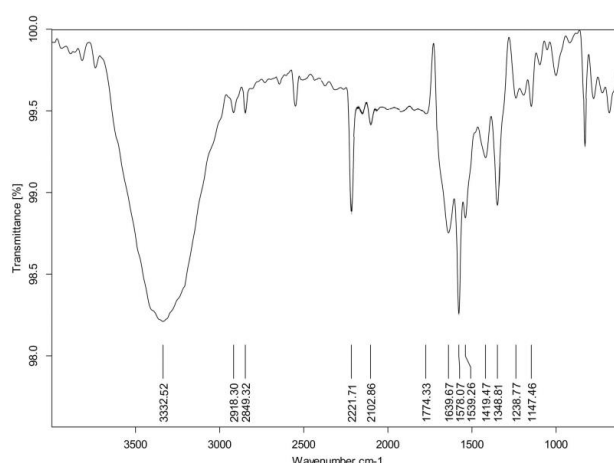
Figure 3.30: FTIR spectrum of polymer **Py₁**
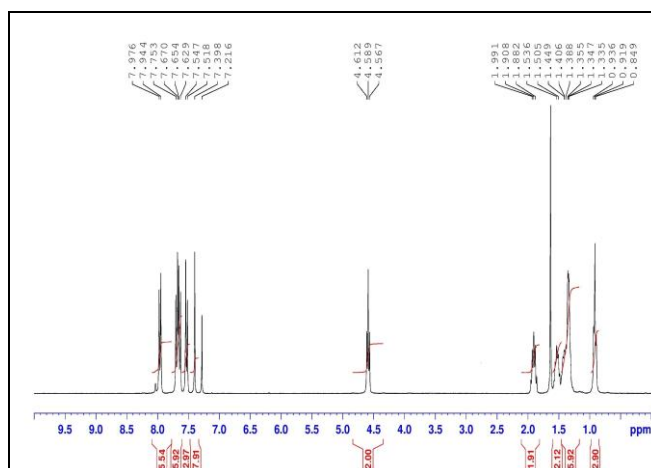
Figure 3.31: ^{1}H NMR spectrum of polymer **Py₁**
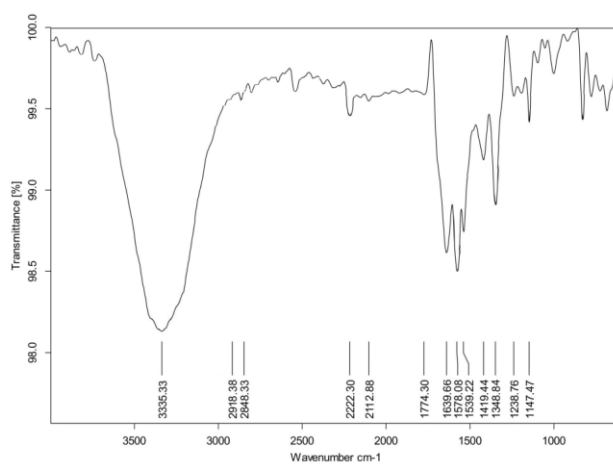
Figure 3.32: FTIR spectrum of polymer **Py₃**
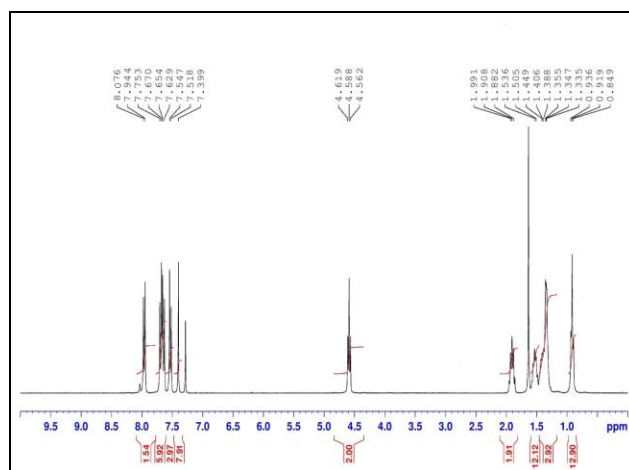
Figure 3.33: ^{1}H NMR spectrum of polymer **Py₃**

3.12 CONCLUSIONS

In conclusion, six new series of polymers, *viz.* **VPPy$_{1-3}$** (**Series-1**), **VTPy$_{1-3}$** (**Series-2**), **PPy$_{1-3}$** (**Series-3**), **TPy$_{1-3}$** (**Series-4**), **TDPy$_{1-4}$** (**Series-5**), and **Py$_{1-4}$** (**Series-6**) were successfully synthesized from their respective monomers, through multistep reactions. Synthetic methods for the preparations of unknown intermediates, monomers and polymers were developed. The reactions conditions with regard to selection of solvent, temperature, time, and catalyst were optimized. Their purification methods were established. Chemical structures of all the new intermediates, monomers and polymers were evidenced by FTIR, ^{1}H NMR, and elemental analyses. The molecular weight of the polymers was determined, and they lie in the range of 7,500-57,000 g/mol. All the polymers show good film forming ability due to high molecular weight. They are readily soluble in common organic solvents. Upcoming chapter, *i.e.* **Chapter 4** includes in-depth thermal, electrochemical, optical and theoretical studies of these newly synthesized polymers.

PHOTOPHYSICAL, ELECTROCHEMICAL, THEORETICAL AND THERMAL STUDIES

Abstract

This chapter covers a detailed investigation of photophysical, electrochemical, thermal properties of newly synthesized π-conjugative polymers. It also includes their computational studies involving HOMO-LUMO calculations. Further, the correlations between their structure and properties have been discussed.

4.1 PHOTOPHYSICAL INVESTIGATION

Linear optical studies of any material involve the interaction of electromagnetic radiation with it. Among many methods, the UV absorption and fluorescence emission spectral techniques are the most important tools to explain the chemistry and physics of the materials. It is well-established that, investigation of interaction between polymeric materials and light is essential for the determination of various optical and optoelectronic properties as well as their applications in the field of optoelectronics. Measurement of UV-vis absorption parameters of a polymer is the fundamental spectroscopic method, which gives useful information regarding its structure and characterization. This technique can be used to determine the extent of polymerization as well as the completion of polymerization reaction.

4.1.1 UV-visible absorption and fluorescence emission spectroscopic studies of polymers

Generally, the observed electronic transitions in absorption spectroscopy of conjugated polymers are attributed to electronic excitation from π to π^* states while transitions in emission spectroscopy is due relaxation from π^* to π states. Upon electronic excitation of the polymer by photons, a number of photo-physical processes take place, *viz.* fluorescence, phosphorescence, or radiation-less decay, which results in acquisition of some interesting photonic properties.

Fluorescence is an optical phenomenon that explains the behavior of a material under the irradiation of photon. In principle, when a photon is incident on a conjugated polymer backbone, if its energy matches with the band gap energy of

polymer, that photon can be absorbed under the formation of an electron-hole pair (exciton) (**Figure 4.1**). After the absorption of the photon, polymer reaches to the excitation state (Frank-Condon principle), then the excited molecule relaxes to the lowest energy level to attain stability (Bassler et al. 2003 and Arkhipov et al. 2004). After a short span of time, when the formed exciton has diffused to a certain distance, it recombines and decays, either radiatively under the emission of a photon (in a process called fluorescence) or non-radiatively as heat. Emission processes in conjugated polymers are schematically represented in **Figure 4.1**.
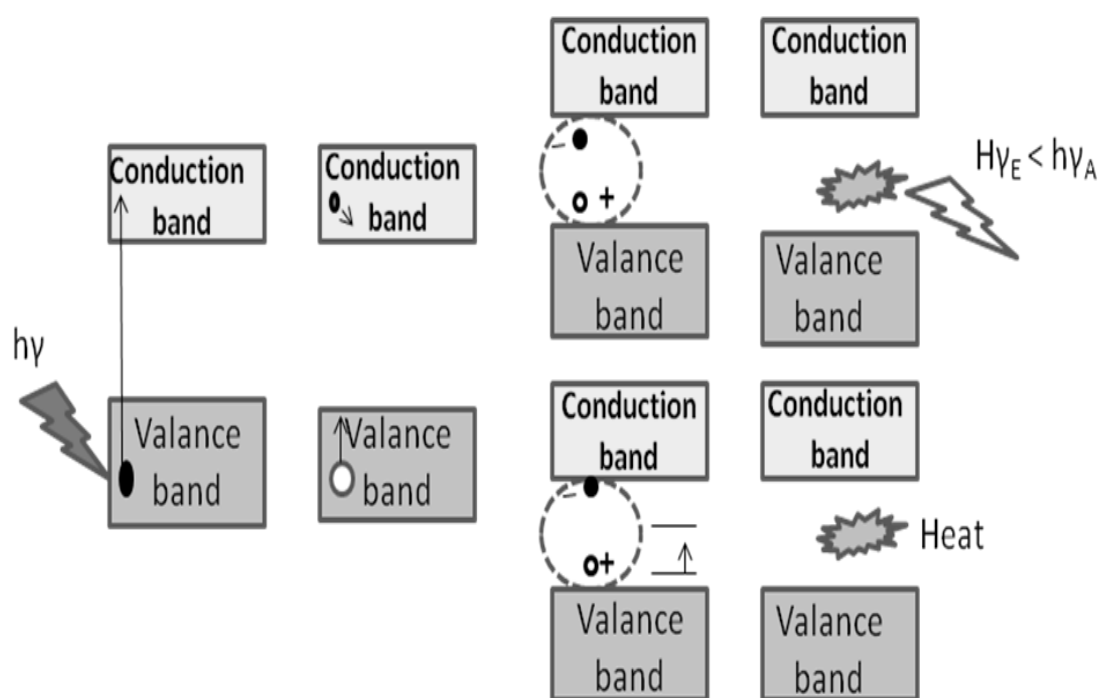
Figure 4.1: Fluorescence emission process in conjugating polymers

4.1.2 Instrumentation, materials and methods

The UV-visible spectra of polymers were measured using Perkin Elmer Lambda-750 UV-visible spectrophotometer and Ocean optics fiber optics spectrometers. The absorption of these polymers was recorded at lab temperature in dilute THF (analytical grade) solutions. Fluorescence emission spectra of polymers were recorded using Perkin Elmer LS55 fluorescence spectrophotometer. Studies were carried out in dilute THF solutions. The emission spectra were obtained by irradiative excitation at the wavelength of their absorption maxima. The fluorescence

quantum yields of the polymers were calculated against the standard, *viz.* quinine sulfate, by taking quantum yield of quinine sulfate in 0.05 M H_2SO_4 as 52 %.

4.1.3 Results and discussion

The UV-vis absorption and emission behavior of new six series of polymers, *viz.* **VPPy₁₋₃** (**Series-1**), **VTPy₁₋₃** (**Series-2**), **PPy₁₋₃** (**Series-3**), **TPy₁₋₃** (**Series-4**), **TDPy₁₋₄** (**Series-5**), and **Py₁₋₄** (**Series-6**) were evaluated using UV-Vis absorption and emission spectroscopy both in THF solution at concentration of 10^{-6}M and thin film states, in order to assess their optical band gap and its related parameters. Both UV-vis and PL spectra of the polymers are depicted in **Figures 4.2-4.7** and their analysis data, *viz.* λ_{max}, λ_{em}, E_g, HOMO-LUMO, Stoke shift, quantum yield and molar absorption coefficient (ε) are summarized in **Table 4.1**. Series-wise spectral results are discussed in the following section.

Polymers VPPy₁₋₃ (Series-1)

The UV-vis absorption and fluorescence emission spectra of all the polymers **VPPy₁₋₃** both in solution and film states are portrayed in **Figures 4.2a-d**.

It is seen that the absorption maxima obtained for solution of **VPPy₁₋₃** at 377, 364 and 368 nm, have been red shifted to 401, 390 and 395 nm in their film state, respectively. Evidently, the red shift of about 24, 26 and 27 nm for the polymers has confirmed the presence of inter-chain interactions and inter chain mobility of the excitons and excimers generated within the polymer molecules in solid state. Further, in case of **VPPy₁** and **VPPy₃**, the λ_{max} values are red-shifted due to presence of electron withdrawing cyano and bromo groups respectively, when compared to that of **VPPy₂**. Similar trend has been observed for the λ_{max} obtained for the polymers measured in film state also. These results clearly indicated that, all the polymers exhibit identical electronic properties both in solution and solid states. Furthermore, the optical band gaps of these polymers were calculated from the onset absorption maximum λ_{max} of the thin film using the formula, *i.e.* $E_g = 1240/\lambda_{max}$ where λ_{max} being the absorption onset wavelength of the polymers. Accordingly, their optical band gaps were found to be 2.55, 2.63 and 2.61 eV, respectively. Such polymers are highly preferred in LED applications. The observed high values may be due to extended

conjugation and structural combinations of different hole and electron transporting moieties in the polymer chain. Finally, molar extinction coefficients (ε) of polymers were determined according to Lambert-Beer law. The molar extinction coefficients were calculated to be 17,621, 16,128 and 15,964 $M^{-1}cm^{-1}$ for polymers **VPPy$_{1-3}$**, respectively.

Fluorescence emission spectra of **VPPy$_{1-3}$**, generated by irradiative excitation at their respective wavelengths of the absorption maxima are given in **Figure 4.2 (c)** (at concentration of 10^{-6} M in THF), and **Figure 4.2 (d)** (at film state) and their corresponding data are summarized in **Table 4.1**. As seen from the spectra, the polymers **VPPy$_{1-3}$** displayed characteristic intense emission bands λ_{em} at 439, 418, and 421 nm, in solution state and fluorescent bands at 467, 450 and 457 nm in film state, respectively. The observed bathochromic shift in emission maxima of film form is mainly attributed to π to π^* stacking of polymer chains. Thus, the photophysical study clearly revealed that, the new polymers are intense blue light emitters both in solution and film states, when irradiated with UV light.

Further, Stoke shifts of **VPPy$_{1-3}$** were calculated using their corresponding λ_{max} and λ_{em} values, measured in their dilute THF solutions at concentration 10^{-6} M and their values are summarized in **Table 4.1**. The calculated values were found to be 3746, 3549 and 3421 cm^{-1} for **VPPy$_{1-3}$**, respectively. The observed highest value in case of **VPPy$_1$** is ascribed to the presence of strong electron withdrawing cyanovinylene linkage in the polymer chain. Furthermore, the fluorescence quantum yield (Φ_f) of polymer solution was calculated by comparing with standard reference quinine sulphate (dissolved in 0.05 M sulfuric acid, having fluorescence quantum yield of 52%). The fluorescence quantum yields of **VPPy$_{1-3}$** were found to be 27.90, 35.10 and 34.70%, respectively. All the polymers exhibited good fluorescence quantum yields in the range of 27-35% when compared to some of the previously reported cyanopyridine based conjugated polymers. Conclusively, these blue light emitting polymers possessing good fluorescence quantum yield are potential candidates for PLED applications as emitters.
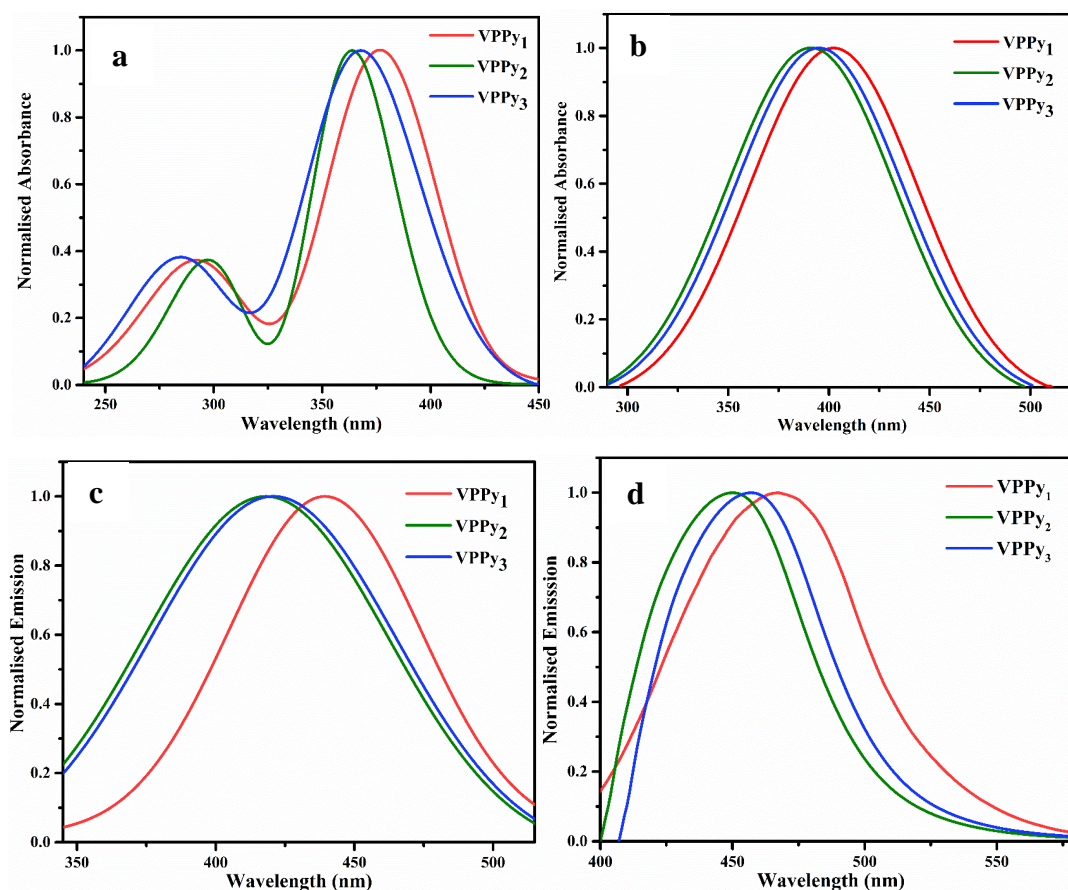
Figure 4.2: (**a**) UV-vis absorption spectra of polymers **VPPy₁₋₃** in solution state; (**b**) UV-vis absorption spectra of polymers **VPPy₁₋₃** in film state (**c**) Fluorescence emission spectra of polymers **VPPy₁**, **VPPy₂** and **VPPy₃** in solution (THF); (**d**) Fluorescence emission spectra of polymers **VPPy₁**, **VPPy₂** and **VPPy₃** in film state

Polymers VTPy₁₋₃ (Series-2)

Figures 4.3a-d show the UV-vis absorption and fluorescence emission spectra of polymers **VTPy₁₋₃** in solution as well as film state.

It has been noticed that, the absorption maxima of **VTPy₁₋₃** appeared at 360, 353 and 355 nm in solution state; these values have been red shifted to 397, 377 and 390 nm in their film state, respectively. Obviously, the observed red shift values of about 37, 24 and 35 nm for the polymers indicated the presence of inter-chain interactions and inter chain mobility of the excitons and excimers produced in solid state. Further, in case of **VTPy₁** and **VTPy₃**, the values of λ_{max} are red-shifted due to presence of electron pulling cyano and bromo groups respectively, when compared to that of **VTPy₂**. In film state also, similar trend has been observed. From the results it is clear that, all the polymers exhibit identical electronic properties both in solution

and solid states. The optical band gaps of these polymers were calculated from the onset absorption maximum λ_{max} of the thin film and were found to be 2.55, 2.64 and 2.58 eV, respectively. So, these polymers are most suitable for LED applications. Because of extended conjugation and structural combinations of different hole and electron transporting moieties in the polymer chain, these materials exhibit good semiconducting property. Further, the molar extinction coefficients were found to be 12232, 14193 and 16212 M^{-1}cm^{-1} for **VTPy$_{1-3}$,** respectively.

Figure 4.3c shows fluorescence emission spectra of **VTPy$_{1-3}$** by irradiative excitation at their respective wavelengths of the absorption maxima at solution state (at concentration of 10^{-6}M in THF), while **Figure 4.3d** indicates emission spectra in film state. The corresponding optical data are summarized in **Table 4.1**. In their spectra, the polymers display characteristic intense emission bands λ_{em} at 465, 418, and 442 nm, in solution state and fluorescent bands at 482, 432 and 457 nm in film state, respectively. The observed bathochromic shift in film form is mainly ascribed to π–π* stacking of polymer chains. Thus, the new polymers were shown to be good blue light emitters both in solution and film states.

Further, Stoke shifts of **VTPy$_{1-3}$** were determined using their λ_{max} and λ_{em} values, measured in their dilute THF solutions at concentration 10^{-6}M and their values are tabulated in **Table 4.1**. The calculated values were found to be 6272, 4405 and 5545 cm^{-1} for polymers **VTPy$_{1-3}$** respectively. The observed highest value in case of **VTPy$_1$** is mainly due to the presence of strong electron withdrawing cyanovinylene linkage in the polymer chain. Furthermore, the fluorescence quantum yield (Φ_f) of polymer in solution state was calculated by comparing with standard reference quinine sulphate (dissolved in 0.05 M sulfuric acid, having fluorescence quantum yield of 52%). The fluorescence quantum yields of **VTPy$_{1-3}$** were found to be 21.38, 36.07 and 44.65, respectively. These polymers exhibited good fluorescence quantum yield in the range of 21-45% which are comparable to some of the cyanopyridine based conjugated polymers reported in the literature. Thus, these blue light emitting polymers with good fluorescence quantum yield are suitable materials for PLED applications as emitters.
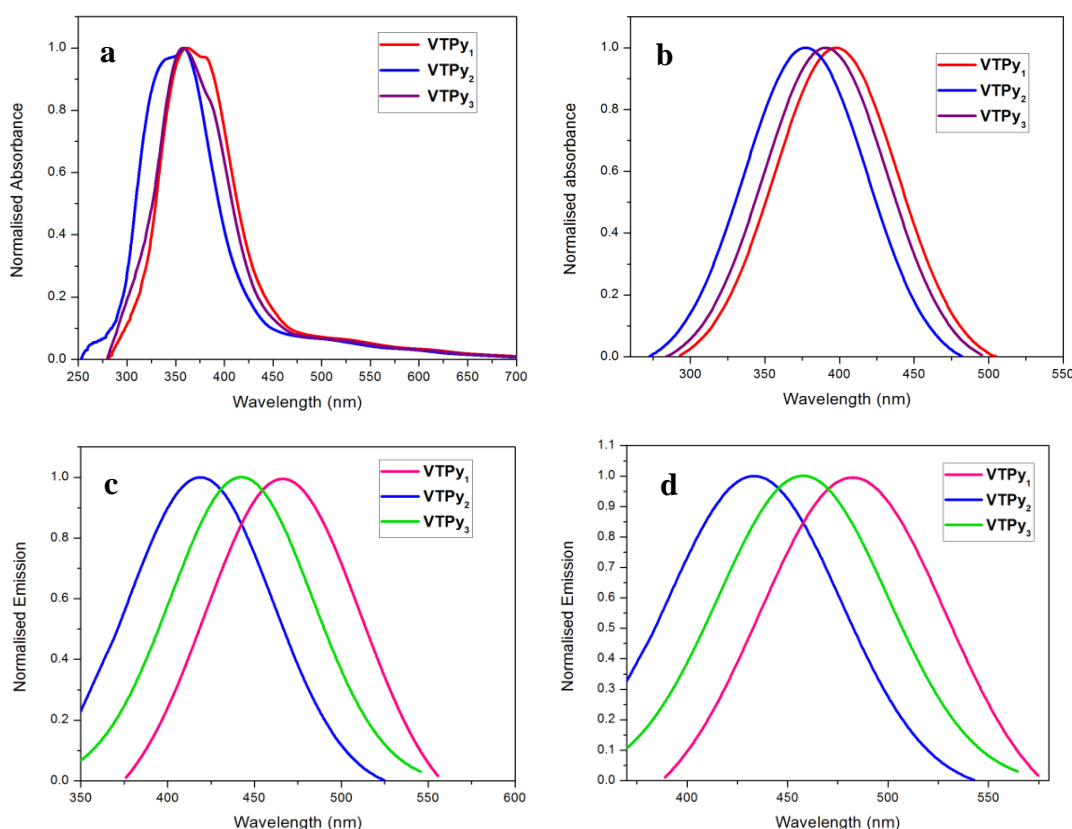
Figure 4.3: (a) UV-vis absorption spectra of polymers **VTPy₁₋₃** in solution state; **(b)** UV-vis absorption spectra of polymers **VTPy₁₋₃** in film state **(c)** Fluorescence emission spectra of polymers **VTPy₁**, **VTPy₂** and **VTPy₃** in solution (THF); **(d)** Fluorescence emission spectra of polymers **VTPy₁**, **VTPy₂** and **VTPy₃** in film state

Polymers PPy₁₋₃ (Series-3)

The UV-vis, absorption spectra of polymers **PPy₁₋₃**, recorded in THF (10^{-6} M conc) solution and thin coated solid film, respectively are portrayed in **Figures 4.4a-b** and their pertaining spectral data are summarized in **Table 4.1**. Their absorption maxima λ_{max} obtained in solution state were found to be 344, 354 and 371 nm, while a slight red shifted absorption of 365, 371 and 380 nm were observed in thin film state, respectively. However, the observed red shift of about 21 nm (**PPy₁**), 17 nm (**PPy₂**) and 9 nm (**PPy₃**) in the absorption spectra confirmed the effect of inter-chain interaction and inter-chain mobility of the excitons and excimers generated with in solid film state. Thus, the polymers **PPy₁₋₃**, displayed similar electronic behaviors both in solution as well in thin film states. Further, their optical band gaps were calculated

from the onset absorption edge λ^b_{onset} of UV-Vis. spectra obtained from thin film state and accordingly, they were found to be in the decreasing order of **PPy₁** (2.63 eV) > **PPy₂** (2.58 eV) > **PPy₃** (2.53 eV). Such polymers with wide energy band gap are highly preferred in blue light PLED application. Finally, their molar extinction coefficients **(ε)** were found to be 12,648 $M^{-1}cm^{-1}$ **(PPy₁)**, 14,942 $M^{-1}cm^{-1}$ **(PPy₂)** and 15,325 $M^{-1}cm^{-1}$**(PPy₃)**.

      Figures 4.4c-d showcase the PL emission spectra of **PPy₁₋₃** recorded at their respective excitation wavelengths in THF (10^{-6} M concentration) solution and thin coated polymer film state, respectively, and their resultant spectral data are summarized in **Table 4.1**. From the **Figures 4.4c-d**, it is clear that, the polymers displayed intense emission bands λ_{em} in THF solution at 384, 392, and 403 nm, while, in the thin film, their λ_{em} values were slightly shifted to 412, 429 and 442 nm, respectively. This can be accredited to the π–π* stacking of polymer chains in thin films. Further, the Stoke shifts of **PPy₁₋₃** were evaluated from the difference between the absorption maxima (λ_{max}) and emission maxima (λ_{em}) values obtained in solution state. The calculated Stoke shifts are 1820, 2200 and 2170 cm^{-1} for **PPy₁₋₃**, respectively. Further, polymer solution fluorescence quantum yields (Φ_f) were determined using quinine sulphate as a standard reference (degassed in 0.05 M sulfuric acid, with Φ_f of 52%). The Φ_f values for **PPy₁₋₃**, were found to be 39.45, 45.17 and 49.27%, respectively. The obtained results were comparable to the previously reported conjugated polymers based on cyanopyridine scaffold. Overall, these blue light emitting polymers, **PPy₁₋₃**, possess fairly good Φ_f values and therefore, they can be employed as potential emitters for PLED device application.
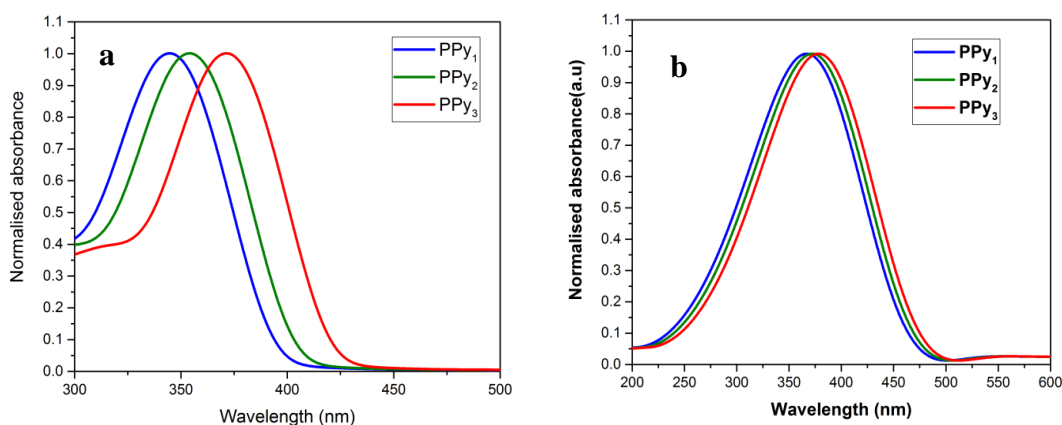
Figure 4.4: (a) UV-vis absorption spectra of polymers **PPy₁₋₃** in solution state; **(b)** UV-vis absorption spectra of polymers **PPy₁₋₃** in film state **(c)** Fluorescence emission spectra of polymers **PPy₁**, **PPy₂** and **PPy₃** in solution (THF); **(d)** Fluorescence emission spectra of polymers **PPy₁**, **PPy₂** and **PPy₃** in film state

Polymers TPy₁₋₃ (Series-4)

The absorption spectra of polymers **TP₁₋₃** recorded in THF (10^{-6} M concentration) solution and thin coated solid film, respectively are displayed in **Figures 4.5a-b** and their corresponding spectral data are tabulated in **Table 4.1**. The λ_{max} values obtained in solution state were found to be 333, 357 and 367 nm, while slight red shifted values of 356, 382 and 402 nm were observed in thin film state, respectively. The observed red shift of about 23 nm (for **TPy₁**), 25 nm (for **TPy₂**) and 35 nm (for **TPy₃**) in their spectra indicated the influence of inter-chain interaction and inter-chain mobility of the excitons and excimers generated within the polymer in solid film state. Further, the obtained results revealed that, the polymers **TPy₁₋₃**, displayed similar electronic behaviors in solution as well in thin film states. Furthermore, their optical band gaps, as calculated from the onset absorption edge λ_{onset}^{b} of the UV-vis. spectra (**Figure 4.5b**), were found to be in the decreasing order of **TPy₁** (2.80 eV) > **TPy₂** (2.70 eV) > **TPy₃** (2.59 eV). Such polymers are potential candidates for PLED applications, as blue emitters. Also, their molar extinction coefficients **(ε)** were calculated to be 14492 (**TPy₁**), 15258 (**TPy₂**) and 18866 M⁻¹cm⁻¹(**TPy₃**), respectively.

Figures 4.5c-d, showcase the PL emission spectra of **TPy₁₋₃** recorded at their respective excitation wavelengths in THF (10^{-6} M conc.) solution and thin coated

polymer film state, respectively, and their resultant spectral data are tabulated in **Table 4.1**. From the **Figures 4.5c-d**, it is clear that, the polymers exhibited intense emission bands in THF solution at 378, 405, and 419 nm, while in the thin film, these values were slightly shifted to 418, 432 and 441 nm, respectively. The reason may be due to the π to π* stacking of polymer chains in thin films. Further, the calculated Stoke shifts were found to be 3575, 3320 and 3380 cm^{-1} for **TPy$_{1-3}$**, respectively. Further, polymer solution fluorescence quantum yields (Φ$_f$), as determined against quinine sulphate as standard reference (degassed in 0.05 M sulfuric acid, with Φ$_f$ of 52%), were found to be 35.47, 39.12 and 48.32%, respectively, which are comparable to the previously reported conjugated polymers based on cyanopyridine scaffold. Overall, these blue light emitting polymers, **TPy$_{1-3}$**, possess fairly good Φ$_f$ values and therefore, they can be employed as potential emitter for PLED device applications.

Figure 4.5: (a) UV-vis absorption spectra of polymers **TPy$_{1-3}$** in solution state; **(b)** UV-vis absorption spectra of polymers **TPy$_{1-3}$** in film state **(c)** Fluorescence emission spectra of polymers **TPy$_1$**, **TPy$_2$** and **TPy$_3$** in solution (THF); **(d)** Fluorescence emission spectra of polymers **TPy$_1$**, **TPy$_2$** and **TPy$_3$** in film state
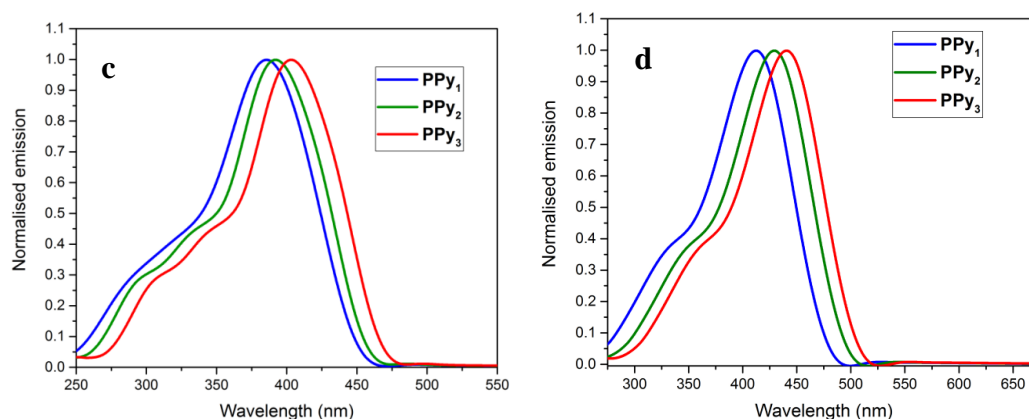
Polymers TDPy$_{1-4}$ (Series-5)

Figures 4.6a-b show the absorption spectra of polymers **TDP$_{1-4}$**, recorded in THF (10^{-6} M conc) solution and thin coated solid film, respectively and their pertaining spectral data are summarized in **Table 4.1**. The absorption maxima λ_{max} obtained in solution state were found to be 371, 377, 384 and 390 nm, where as a slight red shifted absorption of 392, 399, 422 and 428 nm were observed in thin film state, respectively. Here, the observed red shift of about 21nm (in case of **TDPy$_1$**), 22 nm (in case of **TDPy$_2$**) and 38 nm (in case of **TDPy$_3$**), 38 nm (in case of **TDPy$_4$**) in their spectra established the influence of inter-chain interaction and inter-chain mobility of the excitons and excimers generated within the polymers. Also, these results indicated, that the polymers showed similar electronic behaviors both in solution as well in thin film states. Further, their optical band gaps were determined using the onset absorption edge λ_{onset}^{b} of the spectrum obtained from thin film (**Figure 4.6b**). They were found to be in the decreasing order of **TDPy$_1$** (2.27 eV) > **TDPy$_2$** (2.23 eV) > **TDPy$_3$** (2.16 eV) > (2.14 eV). So, these polymers with proper band gap are potential materials in blue light PLED applications. Finally, their molar extinction coefficients **(ε)** were calculated to be 16789 (for **TDPy$_1$**), 17725 (for **TDPy$_2$**) and 17235 (for **TDPy$_3$**), 18723 M^{-1}cm^{-1} (for **TDPy$_4$**) respectively.

Figures 4.6c-d, showcase the PL emission spectra of **TDPy$_{1-4}$** recorded at their respective excitation wavelengths in THF (10^{-6} M concentration) solution and thin coated polymer film state, respectively, and their resultant spectral data are given in **Table 4.1**. From the spectra it is clear that, the polymers displayed intense emission bands λ_{em} in THF solution at 493, 506, 515 and 526 nm, while, in the thin film state, λ_{em} were slightly shifted to 512, 527, 530 and 542 nm, respectively, which can be accredited to the π–π^* stacking of polymer chains in thin films. Further, the calculated Stoke shifts of the polymers are 6670, 6762, 6624 and 6630 cm^{-1} for **TDPy$_{1-4}$**, respectively. Furthermore, Φ_f values, as determined against reference quinine sulphate, were found to be 32.42, 34.89, 33.72 and 35.57% for **TDPy$_{1-4}$**, respectively. These results are comparable to the previously reported conjugated polymers derived from cyanopyridine system. Overall, these blue light emitting polymers, **TDPy$_{1-4}$**,

possess fairly good Φ_f values and therefore, they can be employed as potential emitter for PLED device applications.
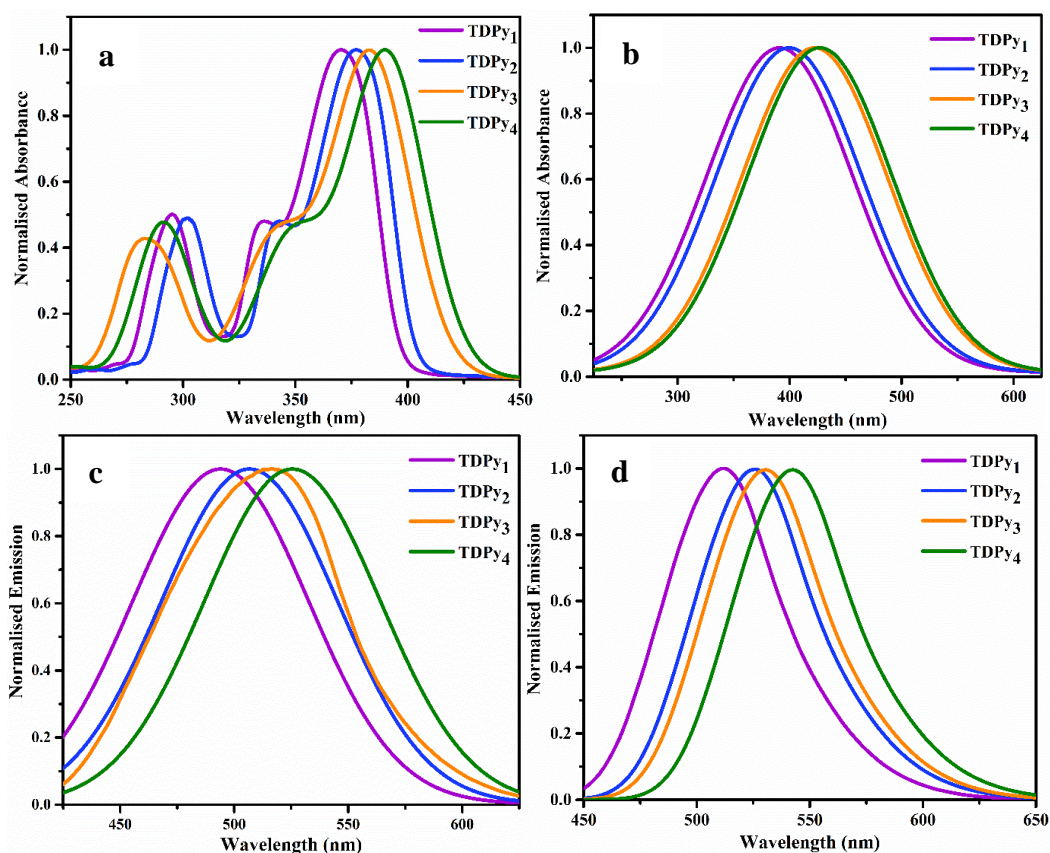
Figure 4.6: (a) UV-vis absorption spectra of polymers **TDPy₁₋₄** in solution state; **(b)** UV-vis absorption spectra of polymers **TDPy₁₋₄** in film state **(c)** Fluorescence emission spectra of polymers **TDPy₁**, **TDPy₂** and **TDPy₃** in solution (THF); **(d)** Fluorescence emission spectra of polymers **TDPy₁**, **TDPy₂** and **TDPy₃** in film state

Polymers Py₁₋₄ (Series-6)

The UV-vis spectra of polymers **Py₁₋₄**, recorded in THF (10^{-6} M conc) solution and thin coated solid film, respectively are presented in **Figures 4.7a-b** and their corresponding data are tabulated in **Table 4.1**. As shown in the spectra, polymers **Py₁₋₄** in solution state exhibited λ_{max} at 340, 346, 358 and 364 nm, while in thin film state, they displayed λ_{max} at 368, 375, 385 and 392 nm, respectively. Here, the observed red shift of about 28 nm (for **Py₁**), 29 nm (for **Py₂**) and 27 nm (for **Py₃**), 28 nm (for **Py₄**) in their spectra indicated the effect of inter-chain interaction and inter-chain mobility of the excitons and excimers generated within the sample. Also, the results supported

that, the polymers **Py₁₋₄**, show similar electronic behaviors both in solution and in thin film states. Their optical band gaps, as calculated using the values of λ_{onset}^{b} of UV-Vis. spectra in thin film state (**Figure 4.7b**), were found to be in the decreasing order of **Py₁** (2.68 eV) > **Py₂** (2.64 eV) > **Py₃** (2.56 eV), **Py₄** (2.54 eV). These polymers with moderate band gap are preferred in blue light PLED applications. Lastly, their molar extinction coefficients **(ε)** were determined to be 8948 (for **Py₁**), 9756 (for **Py₂**) and 9855 (for **Py₃**), 9955 M⁻¹cm⁻¹(for **Py₄**).

Figures 4.7c-d, showcase the PL emission spectra of **Py₁₋₄** recorded at their respective excitation wavelengths in THF (10⁻⁶ M conc.) solution and thin coated polymer film state, respectively, and their corresponding spectral data are given in **Table 4.1**. From the spectra it is clear that, the polymers exhibited intense emission bands in THF solution at 384, 392, 407 and 419 nm, while in the thin film state, their values slightly shifted to 430, 436, 454, and 461 nm, respectively. This difference can be ascribed to the π–π* stacking of polymer chains in thin films. Further, the calculated Stoke shifts are 3370, 3392, 3363 and 3606 cm⁻¹ for **Py₁₋₄**, respectively. Furthermore, the Φ_f values for **Py₁₋₄**, were determined to be 32.89, 31.37, 33.87 and 34.79%, respectively. Interestingly, the obtained results are comparable to the previously reported conjugated polymers based on cyanopyridine system. Overall, these blue light emitting polymers, **Py₁₋₄**, possess fairly good Φ_f values and therefore, they can be employed as potential emitter for PLED device applications.
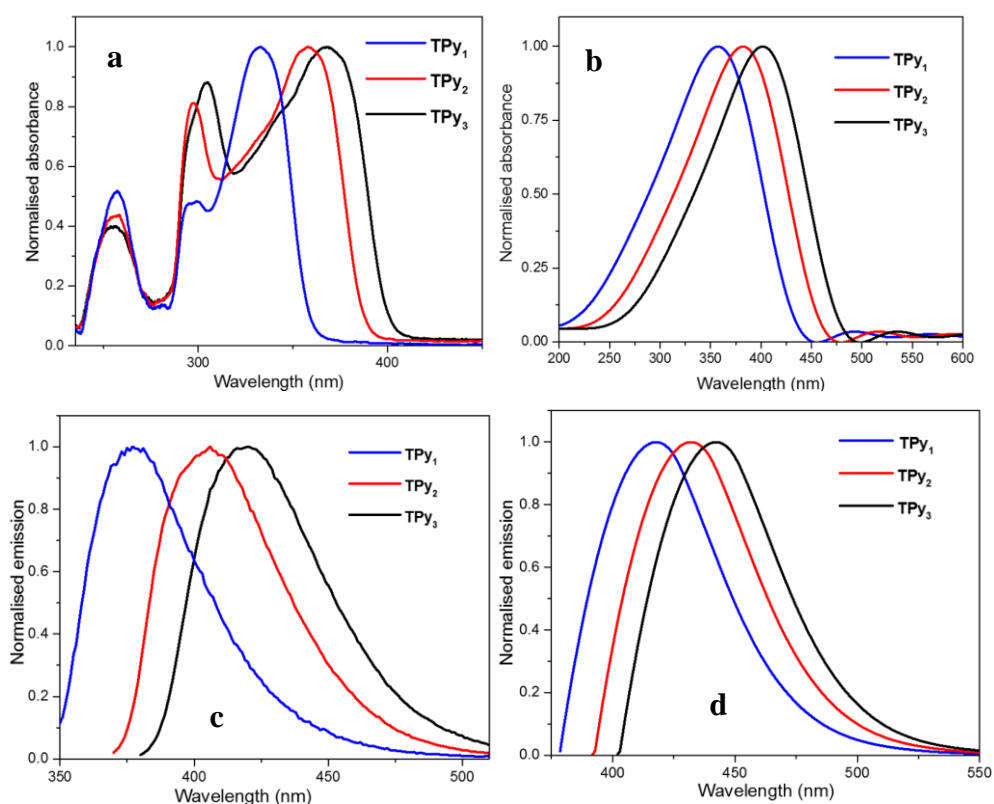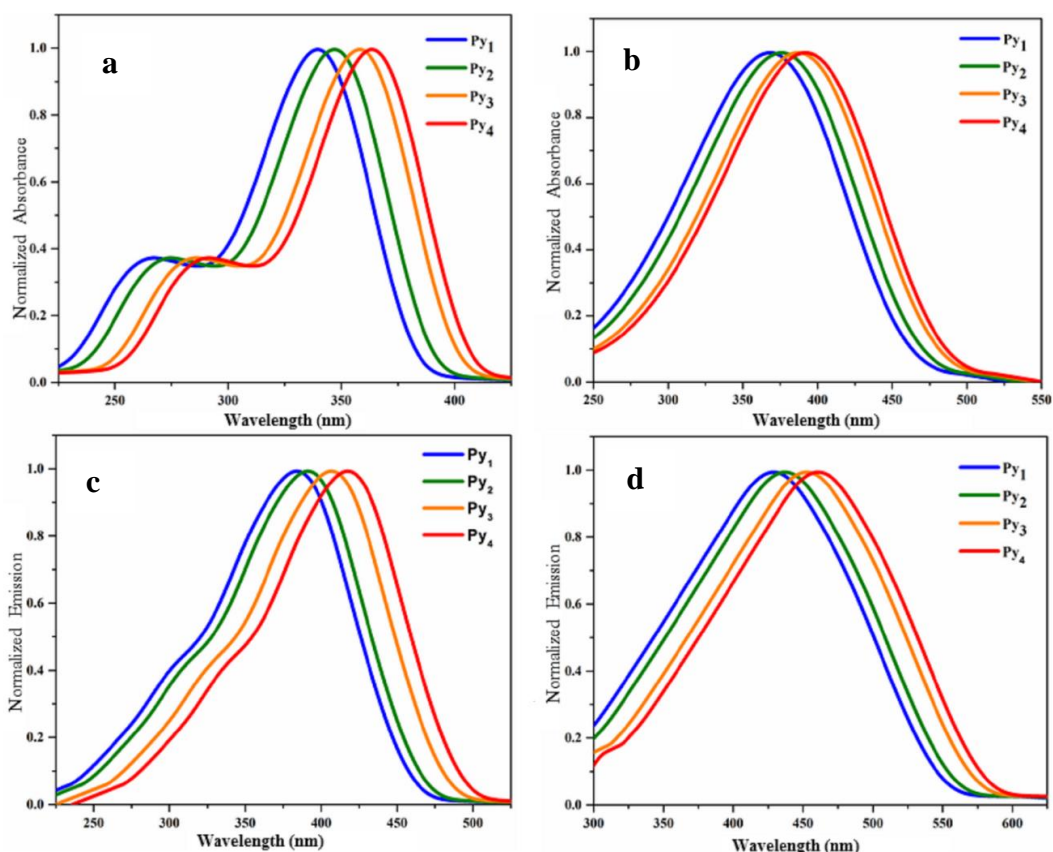
Figure 4.7: (a) UV-vis absorption spectra of polymers **Py₁₋₄** in solution state; **(b)** UV-vis absorption spectra of polymers **Py₁₋₄** in film state **(c)** Fluorescence emission spectra of polymers **Py₁**, **Py₂** and **Py₃** in solution (THF); **(d)** Fluorescence emission spectra of polymers **Py₁**, **Py₂** and **Py₃** in film state

4.2 INTRODUCTION TO ELECTROCHEMICAL STUDIES

Electrochemical studies of the conjugated polymers play an important role in understanding their basic electronic structures. Further it describes their redox properties, which are used in the determination of HOMO-LUMO energy levels, band gap and charge carrying properties. The electrochemical study needs a technique for preparing them in the convenient form of thin films on electrode (metal, glassy carbon, any semiconductor) surfaces in their future applications. Generally, cyclic voltammetry (CV) is employed for electrochemical studies.

4.2.1 CYCLIC VOLTAMMETRY

Cyclic voltammetry (CV) was introduced by Hickling for electrochemical studies of materials in the year late 50's (Hickling 1942). Further, Janietz et al. (1997) used this technique for measuring ionization potentials of conjugated polymers

and also their bandgaps. Cyclic voltammetric set-up constitutes an electrochemical cell working in a three-electrode configuration and a potentiostat. These three electrodes (working, counter, and reference) are connected to a potentiostat, whose function is to supply a current, which is regulated in the particular voltage range (–2.5 to +2.5 V). The electrodes are immersed in an electrolyte, which provides the ionic conductivity. Generally glassy carbon button electrode is used as working electrode; on which a polymer film is coated. In the case of *p*-doping, which corresponds to oxidation of the polymer, electrons are transferred from polymer to metal and the reverse for *n*-doping, which corresponds to a reduction. The resulting transfer of charges during the doping process gives rise to the current flowing through the working electrode. The corresponding potential of the working electrode indicates the absolute potential (versus the reference electrode) at which the conjugated polymer is doped. Importantly, the separation between the potentials of the *p*-type doping and the *n*-type doping processes indicates the value of electrochemical band gap. The onset potentials for *p*-doping and *n*-doping are calculated as the intersection of the baseline with the tangent of the current curve at the half maximum of the current curve. The electrochemical reactions on electrode surface are represented in **Figure 4.8**.
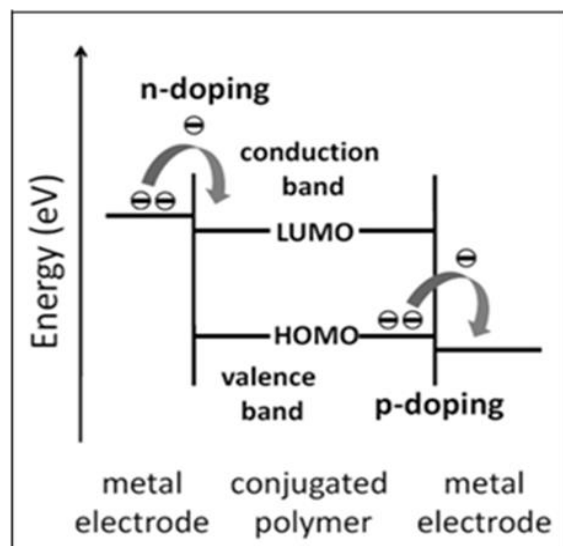
Figure 4.8: Electrochemical reactions on electrode surface

4.2.2 Experimental protocols for electrochemical studies

      The electrochemical studies were carried out using AUTOLAB PGSTAT 30 electrochemical analyzer. Cyclic voltammograms were recorded using a three-

electrode cell system, with a glassy carbon button as working electrode, a platinum (Pt) wire as counter electrode and an Ag/AgCl electrode as the reference electrode.

In the CV experiments, polymer to be analyzed was coated on a glassy carbon button electrode by evaporating their $CHCl_3$ or DMF solutions. The CV was conducted in 0.1 M tetrabutylammoniumperchlorate (TBAPC) solution in dry acetonitrile at a scan rate 25 mV/s. As the set-up is sensitive to the presence of air in the cell, the entire cell was flushed with nitrogen prior to running the experiments. The electrochemical reduction behavior of the polymers was studied in the potential range 0 to –2.5 V, whereas the oxidation cyclic voltammograms were recorded by sweeping the potential in the range 0 to +2.5 V. Experiments were conducted at laboratory temperature.

The onset oxidation and reduction potentials were used to estimate the highest occupied molecular orbital (HOMO) and the lowest unoccupied molecular orbital (LUMO) energy levels of the polymers. Their HOMO and LUMO energy levels are calculated from the following equations (**Equations 4.1** and **4.2**).

$$E_{HOMO} = - e\,(E_{oxd} + 4.80) \qquad (4.1)$$

$$E_{LUMO} = - e\,(E_{red} + 4.80) \qquad (4.2)$$

where E_{HOMO} and E_{LUMO} are the onset potentials versus standard calomel electrode (SCE) for the oxidation and reduction of the material referred, were used for the calculation. Further, their electrochemical bandgaps were determined by the difference between HOMO and LUMO energy levels.

$$E_g = E_{LUMO} - E_{HOMO} \qquad (4.3)$$

where E_g is electrochemical bandgap in eV.

The electrochemical experimental data were recorded for polymer coated on glassy carbon from chloroform solution (2 mg/mL) with Ag/AgCl as reference electrode and calibrated against Fc/Fc^+ redox couple for which ionization energy is taken to be 4.80 eV. The electrochemical characterization data of polymers are summarized in **Table 4.1.**

4.2.3 Results and discussion

From electrochemical data, important factors such as HOMO/LUMO energy levels, barrier potentials and bandgaps of polymers were calculated as their characterization parameters. Further, their series-wise discussion on structure-property relationship has been given in the following section.

Polymers VPPy$_{1-3}$ (Series-1)

. In cyclic voltammograms of all polymers, only reduction potential was observed and there was no oxidation potential witnessed as shown in **Figure 4.9.** Hence, LUMO of the polymers were calculated using $E_{LUMO} = -e\,[E_{red} + 4.8 - E_{FOC}]$. Here, the ionization potential for Fc/Fc$^+$ measured was 0.47 V vs. Ag/AgCl. Measured LUMO energy levels for **VPPy$_{1-3}$** were –2.63, –2.73 and –2.70 eV, respectively. Since oxidation potential was not observed for the polymers, HOMO was calculated from the optical band gap obtained from UV-vis spectra for polymer films. The HOMO for **VPPy$_{1-3}$** were –5.18, –5.36 and –5.31 eV, respectively.
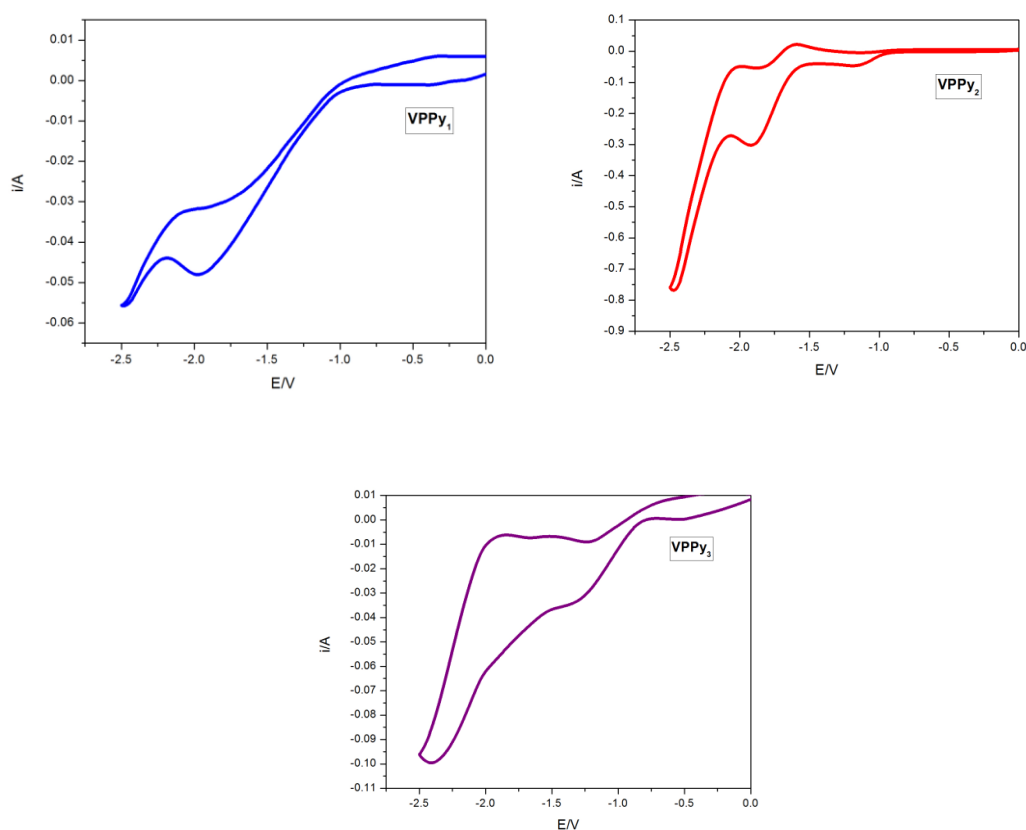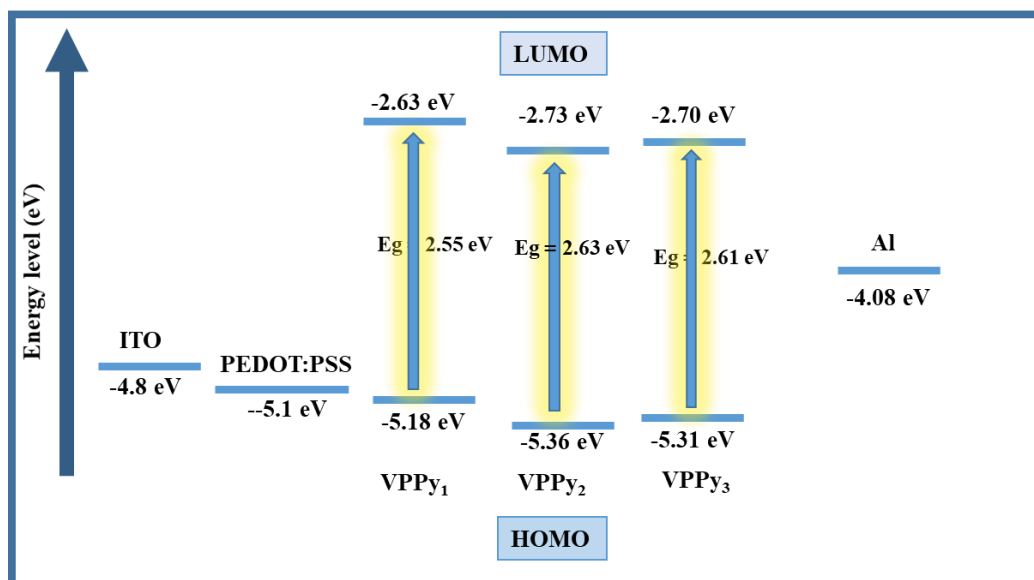
Figure 4.9: Cyclic voltammograms and energy level diagram
of polymers **VPPy₁₋₃**

Polymers VTPy₁₋₃ (Series-2)

   Figure 4.10 depicts CV traces of polymers, **VTPy₁₋₃**. From the results, it is clear that only reduction potentials were observed but not oxidation potentials. Similar observations were reported for some of the cyanopyridine based polymers. Using the reduction potential data, the required LUMO energy levels of the polymers were calculated following the equation, $E_{LUMO} = - e\,[E_{red} + 4.8 - E_{FOC}]$. Here, the measured ionization potential E_{FOC} for Fc/Fc⁺ was 0.47 V vs. Ag/AgCl electrode.   Accordingly, the calculated LUMO energy levels for **VTPy₁₋₃** were shown to be –2.65, –2.25 and –2.49 eV, respectively. From the results it is evident that **VTPy₂** showed the highest energy level among the three polymers, which is attributed to presence of unsubstituted vinylene group in polymer chain, while other two structures possess electron withdrawing CN/Br group attached to vinylene group causing little higher levels. Further, since their CV traces show no oxidation potentials, required HOMO energy levels of polymers were calculated from their optical band gaps, obtained from UV-Vis absorption spectra of polymer films. Thus, the calculated values for **VTPy₁₋₃** were found to be – 4.70, – 4.59 and – 4.7 eV, respectively.
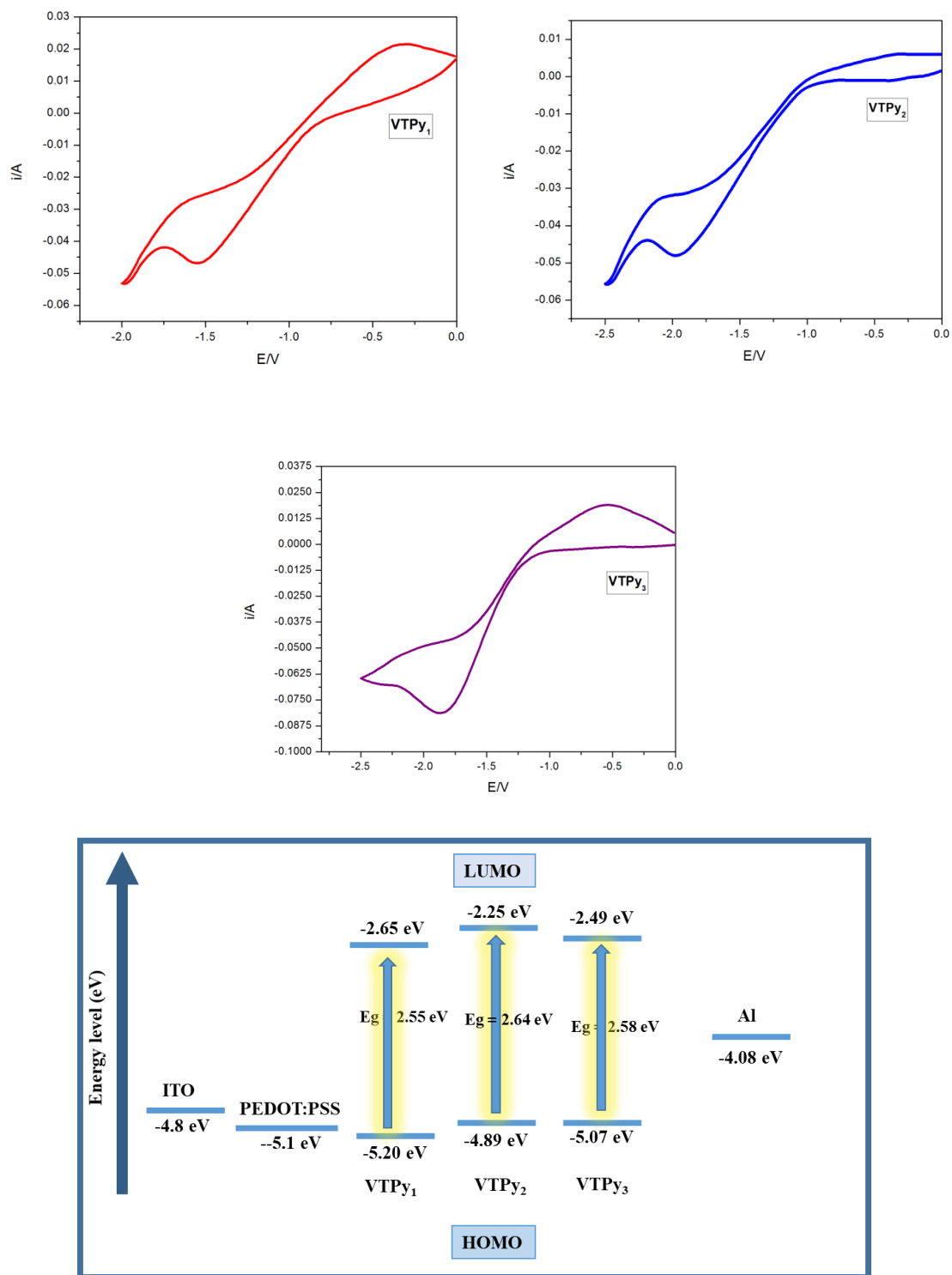
Figure 4.10: Cyclic voltammograms and energy level diagram of polymers **VTPy₁₋₃**

Polymers PPy₁₋₃ (Series-3)

The LUMO energy levels of the **PPy₁₋₃** were calculated by substituting the reduction potential value obtained from the CV traces into the equation: $E_{LUMO} = -e [E_{red} + 4.8 - E_{FOC}]$. Here, E_{FOC} refers to standard potential of Fc/Fc⁺ electrode. Hence, the LUMO energy levels for **PPy₁₋₃** and were estimated to be –2.53, –2.63 and –2.78 eV, respectively. However, the polymer **PPy₁**, displayed the highest LUMO energy level compared to both **PPy₂** and **PPy₃**, which can be ascribed to absence of strong electron donating scaffold in polymer chain. Since CV traces of **PPy₁₋₃** showed no oxidation potentials, the required HOMO levels were determined from their optical energy band gap. Thus, the HOMO energy levels for **PPy₁₋₃** were found to be –5.17, –5.21 and –5.31 eV, respectively. The calculated electrochemical parameters are depicted in **Table 4.1**. **Figure 4.11** shows cyclic voltammagrams of the polymers **PPy₁₋₃.**
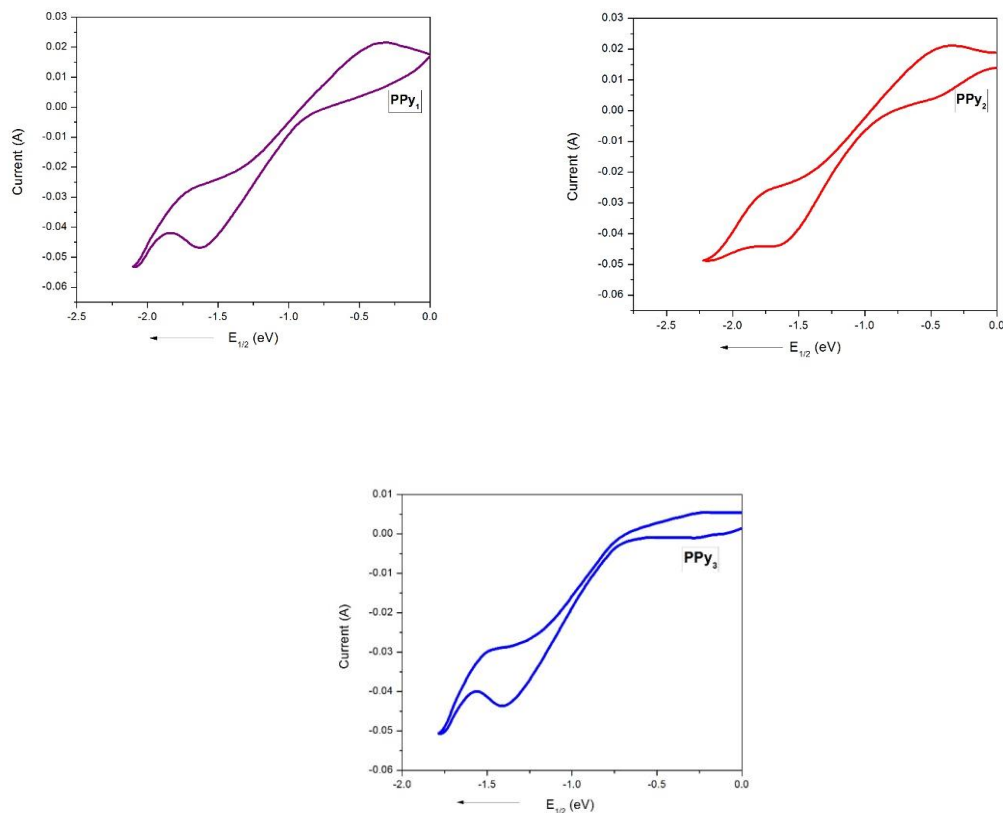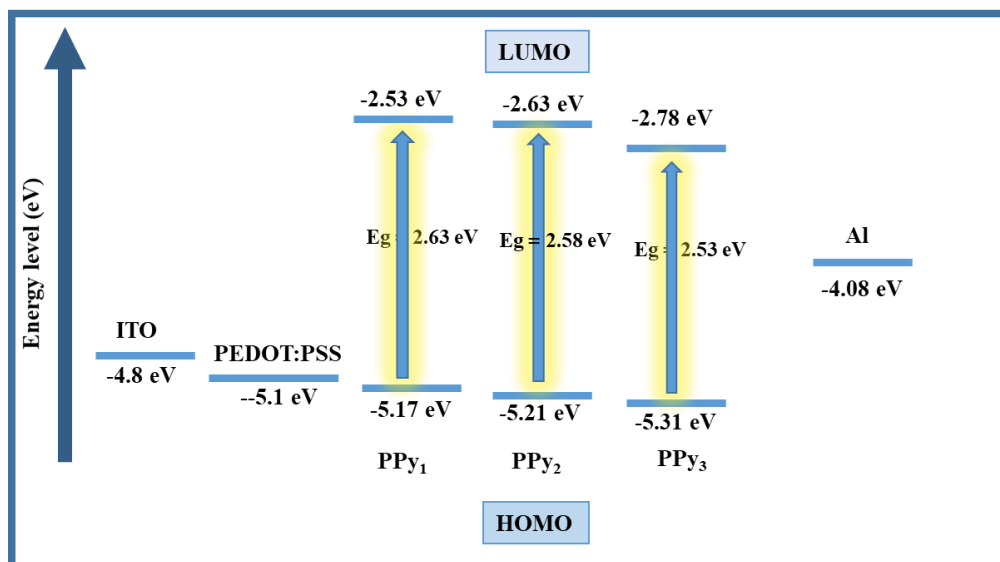
Figure 4.11: Cyclic voltammograms and energy level diagram of polymers **PPy₁₋₃** Polymers **TPy₁₋₃ (Series-4)**

The LUMO energy levels of the polymers **TPy₁₋₃** were calculated by substituting the obtained reduction potential values from the CV traces in the equation: $E_{LUMO} = -e[E_{red} + 4.8 - E_{FOC}]$. As mentioned earlier, E_{FOC} indicates standard potential of Fc/Fc⁺ electrode. Subsequently, their LUMO energies were estimated to be –2.00, –2.17 and –2.19 eV, respectively. Since CV traces of **TPy₁₋₃** showed no oxidation potentials, the required HOMO energy levels were determined from their optical energy band gaps. Thus, the HOMO energy levels for **TPy₁₋₃** were found to be –4.8, –4.87 and –4.78 eV, respectively. The calculated electrochemical datas are shown in **Table 4.1**. **Figure 4.12** displays the CV traces of the polymers **TPy₁₋₃**.
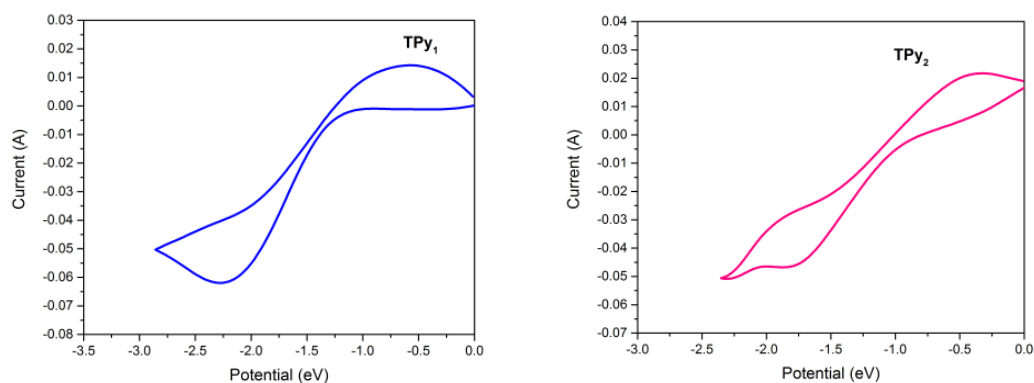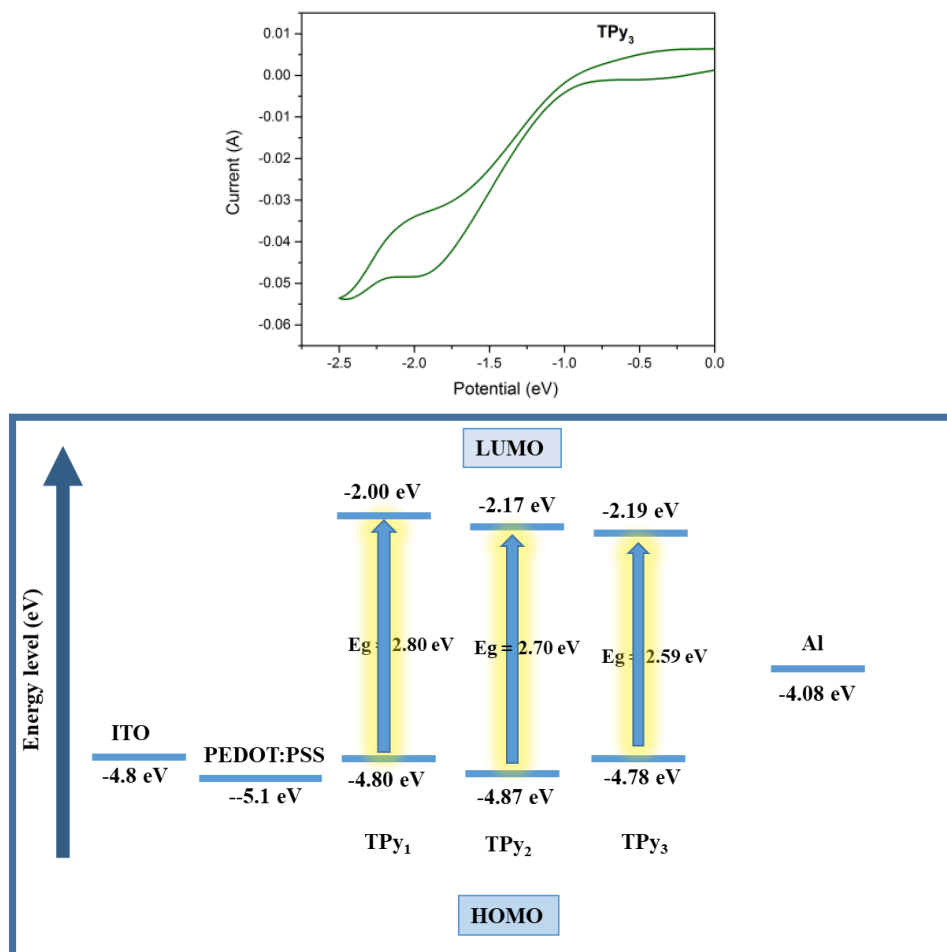
Figure 4.12: Cyclic voltammograms and energy level diagram of polymers **TPy₁₋₃**

Polymers TDPy₁₋₄ (Series-5)

The LUMO energy levels of the **TDPy₁₋₄** were calculated by using the formula: $E_{LUMO} = -e[E_{red} + 4.8 - E_{FOC}]$. Here, the E_{red} values were obtained directly from their CV curves. The experimentally obtained LUMO energy levels of **TDPy₁₋₄** are –2.96, –3.33, –3.35 and –3.46 eV, respectively. Since CV traces of the polymers showed no oxidation potentials, the required HOMO energy levels were determined from their optical energy bandgaps. Thus, the HOMO energy levels for **TDPy₁₋₄** were found to be –5.23, –5.56, –5.51 and –5.60 eV, respectively. The calculated HOMO-LUMO levels and bandgaps are shown in **Table 4.1**. **Figure 4.13** indicates the CV traces of the polymers **TPy₁₋₄**.
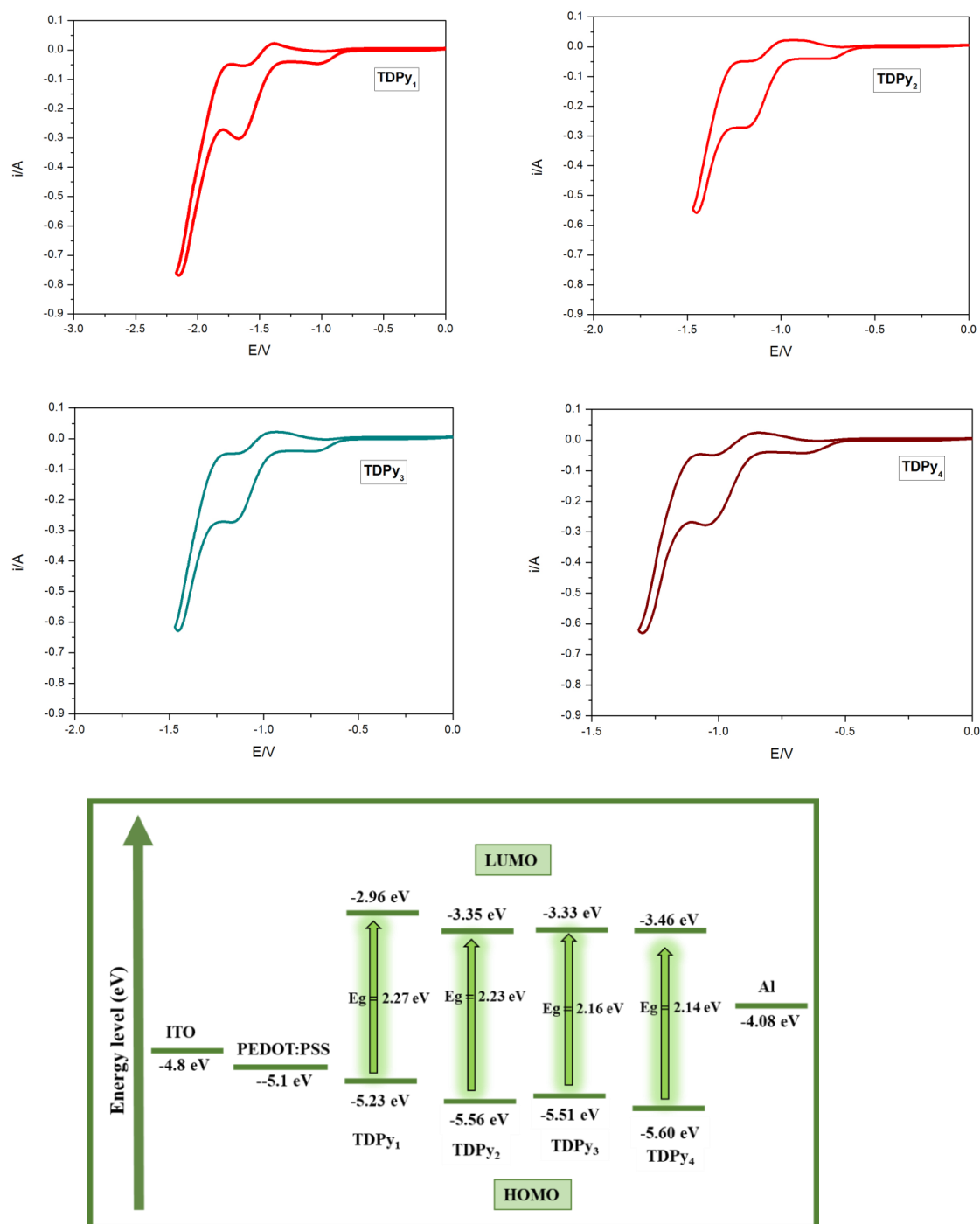
Figure 4.13: Cyclic voltammograms and energy level diagram of polymers **TDPy$_{1-4}$**

Polymers Py$_{1-4}$ (Series-6)

As explained earlier, the LUMO energy levels of the polymers **Py$_{1-4}$** were calculated with the help of equation: $E_{LUMO} = -e[E_{red} + 4.8 - E_{FOC}]$, using

experimentally obtained E_{red} values from the CV traces of the polymers (**Figure 4.14**). Accordingly, the LUMO energy levels for four polymers of the **Series-6** were estimated to be −3.25, −3.21, −3.36 and −3.29 eV, respectively. Since CV traces of **Py$_{1-4}$** showed no oxidation potentials, the required HOMO levels were determined from their optical energy band gap. Thus, the HOMO energy levels of **Py$_{1-4}$** were found to be −5.93, −5.85, −5.92 and −5.83 eV, respectively. All the electrochemical data of the polymers were summarized in **Table 4.1**.
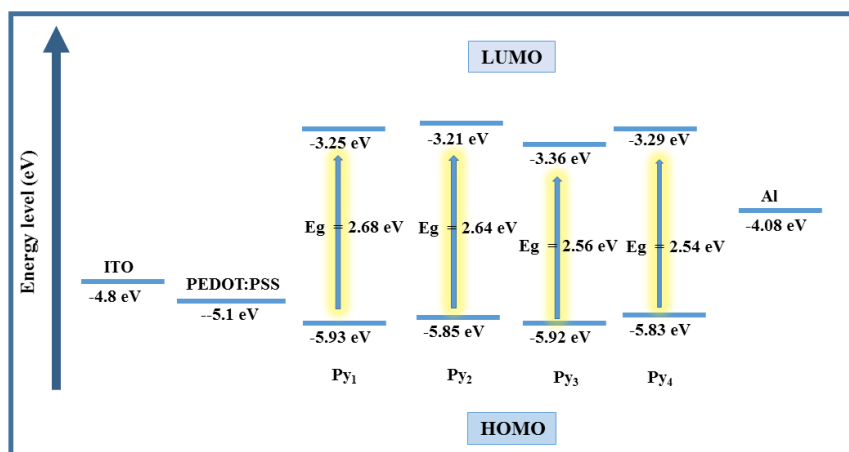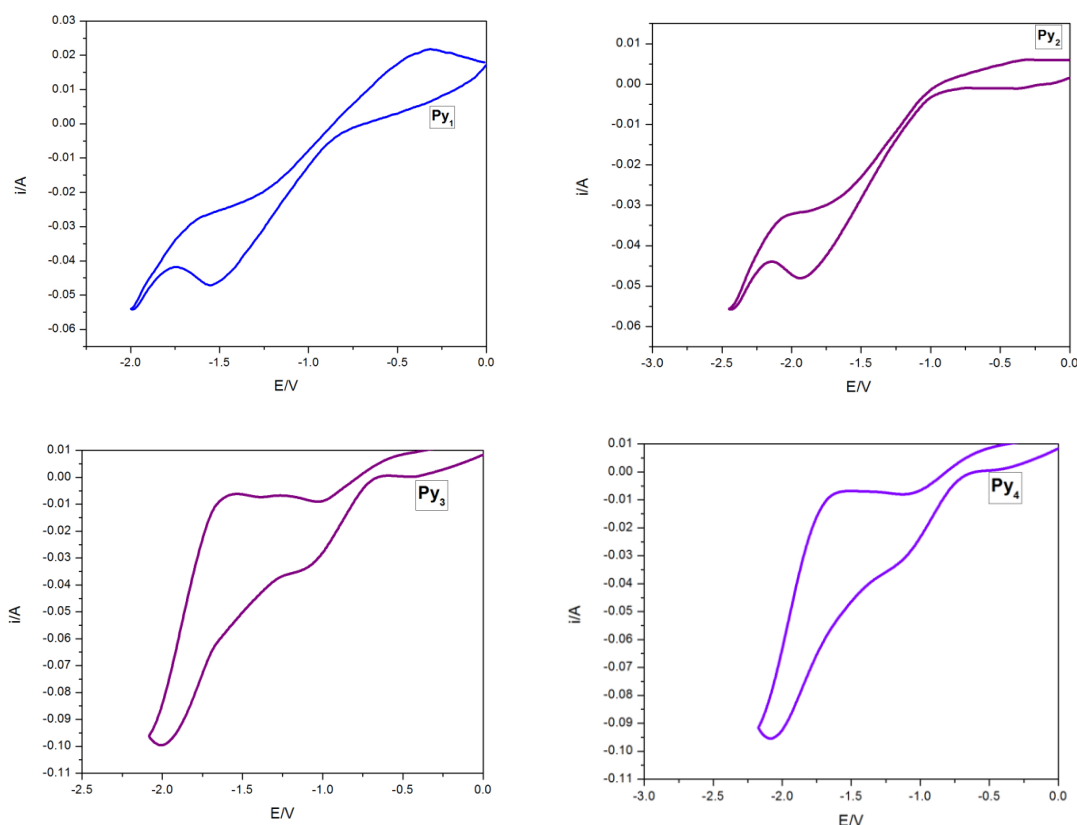
Figure 4.14: Cyclic voltammograms and energy level diagram of polymers **Py$_{1-4}$**

Table 4.1: Photophysical and electrochemical data of new polymers (**Series 1-6**)

Polymer	UV -Visible			Fluorescence		E_g^{opt}	LUMO (CV)	HOMO	Stoke Shift	Φ_f (%)	$\varepsilon(M^{-1}\ cm^{-1})$
	λ_{max}^a nm	λ_{max}^b nm	λ_{onset}^b nm	λ_{em}^a nm	λ_{em}^b nm	eV	eV	eV	cm^{-1}		at λ_{max}^a
VPPy$_1$	377	401	486	439	467	2.55	−2.63	−5.18	3746	27.90	17,621 (377 nm)
VPPy$_2$	364	390	471	418	450	2.63	−2.73	−5.36	3549	35.10	16,128 (364 nm)
VPPy$_3$	368	395	475	421	457	2.61	−2.70	−5.31	3421	34.70	15,964 (368 nm)
VTPy$_1$	360	397	486	465	482	2.55	−2.65	−5.20	6272	21.38	12,232 (360 nm)
VTPy$_2$	353	377	469	418	432	2.64	−2.25	−4.89	4405	36.07	14,193 (353 nm)
VTPy$_3$	355	390	481	442	457	2.58	−2.49	−5.07	5545	44.65	16,214 (355 nm)
PPy$_1$	344	365	470	384	412	2.63	−2.53	−5.17	3028	39.45	12,648 (344 nm)
PPy$_2$	354	371	481	392	429	2.58	−2.63	−5.21	2738	45.17	14,942 (354 nm)
PPy$_3$	371	380	491	403	442	2.53	−2.78	−5.31	2140	49.27	15,325 (371 nm)
TPy$_1$	333	356	434	378	418	2.80	−2.00	−4.80	3575	35.47	14,492 (333 nm)
TPy$_2$	357	382	459	405	431	2.70	−2.17	−4.87	3320	39.12	15,258 (357 nm)
TPy$_3$	367	402	478	419	441	2.59	−2.19	−4.78	3382	48.32	18,866 (367 nm)
TDPy$_1$	371	392	546	493	512	2.27	−2.96	−5.23	6670	32.42	16,869 (371 nm)
TDPy$_2$	377	399	555	506	527	2.23	−3.33	−5.56	6762	34.89	17,716 (377 nm)
TDPy$_3$	384	422	574	515	530	2.16	−3.35	−5.51	6624	33.72	17,018 (384 nm)
TDPy$_4$	390	428	580	526	542	2.14	−3.46	−5.60	6630	35.57	18,845 (390 nm)
Py$_1$	340	368	463	384	430	2.68	−3.25	−5.93	3370	32.89	8,948 (340 nm)
Py$_2$	346	375	470	392	436	2.64	−3.21	−5.85	3392	31.37	9,756 (346 nm)
Py$_3$	358	385	484	407	454	2.56	−3.36	−5.92	3363	33.87	9,855 (358 nm)
Py$_4$	364	392	488	419	461	2.54	−3.29	−5.83	3606	34.79	9,955 (364 nm)

[a] Solution state, [b] Film state, Φ_f Fluorescence quantum yield of polymer in solution.

ε Molar absorption coefficient at respective absorption wavelength in solution,

CV   Cyclic voltammetry

4.3 THERMAL ANLYSIS OF POLYMERS

In principle, thermogravimetric analysis (TGA) measures the mass of a sample as a function of temperature. TGA techniques are quite useful to detect changes in the mass of a sample (gain or loss) or to evaluate step-wise changes in mass (usually as a percentage of the initial sample mass) with temperature. Also, the thermograms indicate the temperatures that characterize a step in the mass loss or mass gain. Further, thermal analysis data is applicable to study the thermal stability of materials and permits to draw conclusions about their structural constituent.

Polymers VPPy$_{1-3}$ (Series-1)

The thermal studies of the polymers were carried out by thermogravimetric analysis (TGA), using a 10 °C min^{-1} temperature ramp starting from 50 to 550 ºC in a nitrogen atmosphere. The acquired thermograms indicate that, all the polymers of the **Series-1** exhibit a high degree of thermal stability up to 300 ºC mainly due to presence of rigid heterocyclic ring system in the main chain. Further, the observed 15-20% weight loss after 300 °C may be attributed to the degradation of the alkoxy side chains in the polymers. The gradual weight loss above 350 °C may be ascribed to the slow degradation of the main polymer chain, which led to the final residue. Similar observations have been reported in the literature for some of the cyanopyridine based polymers. The degradation temperatures of the polymers **VPPy$_{1-3}$** were found to be 308, 301 and 303 °C, respectively. **Figure 4.15** illustrates the thermogravimetric traces of polymers **VPPy$_{1-3}$**.
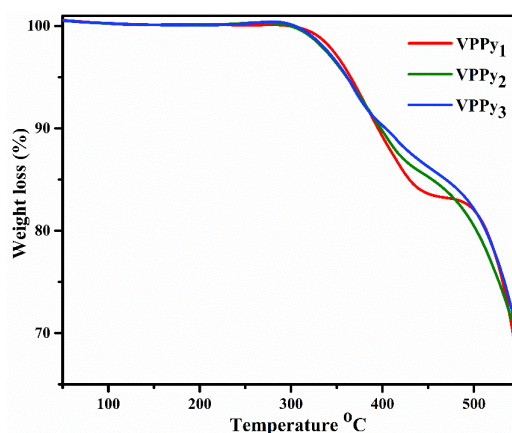
Figure 4.15: Thermogravimetric traces of **VPPy$_{1-3}$**

Polymers VTPy$_{1-3}$ (Series-2)

Polymers **VTPy$_{1-3}$** (**Series-2**) were subjected to thermogravimetric analysis (TGA), using a 10 °C min^{-1} temperature ramp starting from 50 to 550 °C in a nitrogen atmosphere. **Figure 4.16** shows the obtained thermograms of the polymers. From the results, it is clear that, all the polymers of the series show good thermal stability up to 300 °C because of the presence of rigid heterocyclic rings, *viz.* cyanopyridine and thiophene in the main chain. Further, the observed ≈ 20% weight loss after 320 °C may be attributed to the degradation of the $C_{16}H_{33}O$

side chains in the polymers. The gradual weight loss above 350 ºC may be due to the slow degradation of the polymer backbone to give final residue. The observed results are in agreement with that of reported cyanopyridine based polymers. The decomposition temperatures of polymers **VTPy₁₋₃** were found to be 325, 309 and 305 ºC, respectively.
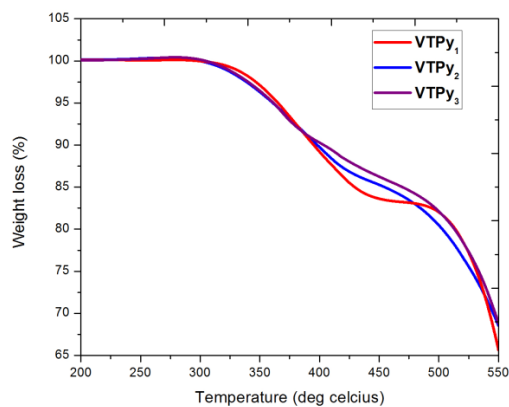
Figure 4.16 Thermogravimetric traces of **VTPy₁₋₃**

Polymers PPy₁₋₃ (Series-3)

Thermograms obtained for TGA analysis of polymers **PPy₁₋₃** (**Series-3**), carried out in a nitrogen atmosphere by temperature ramp of 10 ºC min⁻¹ ranging from 50 to 650 ºC, are displayed in **Figure 4.17**. It is seen from the results, the thermal degradation temperatures of **PPy₁, PPy₂** and **PPy₃**, were found to be 334, 349 and 317 ºC, respectively. Interestingly, all the polymers demonstrated a high degree of thermal stability, which can be attributed to the existence of rigid aromatic heterocyclic ring systems in the polymer main chain. Further, at 300 ºC, about 10-15% of weight loss was observed mainly due to the degradation of the heptoxyl alkyl side chain on the cyanopyridine scaffold. Finally, a gradual loss in weight was noticed over 350 ºC, which can be attributed to the further degradation of the macromolecular chain, which results in residue formation. Similar results were observed for cyanopyridne based conjugative polymers reported earlier.
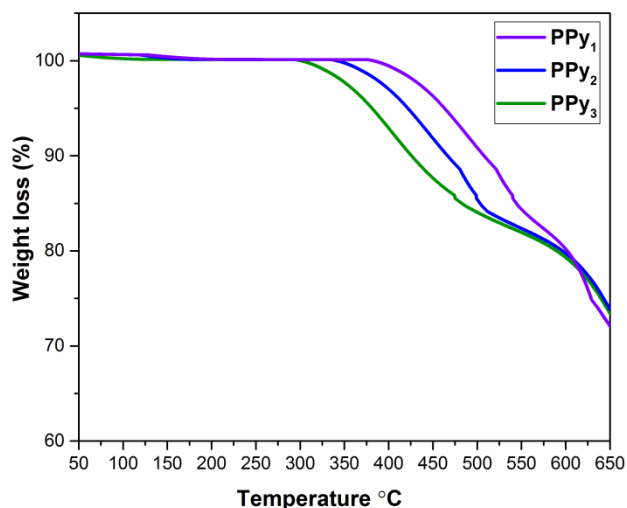
Figure 4.17 Thermogravimetric traces of **PPy₁₋₃**

Polymers TPy₁₋₃ (Series-4)

In order to access the thermal stability of the synthesized polymers **TPy₁₋₃**, the TGA investigation were carried out in a nitrogen atmosphere by temperature ramp of 10 ^{o}C min^{-1} ranging from 50 to 600 ^{o}C. Their thermograms are depicted in **Figure 4.18**. As seen from the traces, the thermal degradation temperatures of **TPy₁**, **TPy₂** and **TPy₃** are 349, 368 and 328 ^{o}C, respectively. Remarkably, all the polymers **TPy₁₋₃**, demonstrated very high degree of thermal stability, which can be attributed to the presence of rigid cyanopyridine, thiophene and phenylene ring systems in the polymer main chain. Further, at 300 ^{o}C, about 20-25% of weight loss was observed mainly due to the degradation of the hexadecoxyl side chain on the cyanopyridine scaffold. Finally, a gradual loss in weight was observed over 350 ^{o}C, which can be ascribed to the further degradation of the macromolecular chain, which resulted in residue formation.
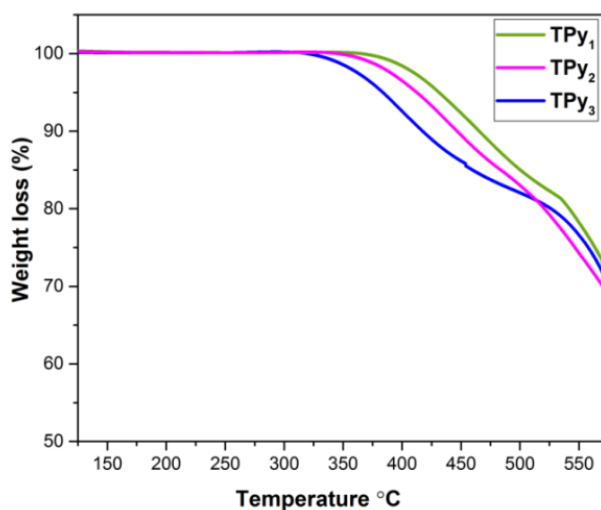
Figure 4.18: Thermogravimetric traces of **TPy$_{1-3}$**

Polymers TDPy$_{1-4}$ (Series-5)

In order to study the thermal behavior of the synthesized polymers **TDPy$_{1-4}$**, their TGA investigations were carried out in a nitrogen atmosphere by temperature ramp of 10 ^{o}C min^{-1} ranging from 50 to 600 ^{o}C. Their thermograms are shown in **Figure 4.19**. According to the results, the thermal degradation temperatures of **TDPy$_1$**, **TDPy$_2$**, **TDPy$_3$** and **TDPy$_4$** are 305, 357, 349 and 388 ^{o}C, respectively. Similar to earlier series, all the polymers **TPy$_{1-4}$**, demonstrated a good thermal stability. This can be attributed to the presence of rigid thiadiazole, cyanopyridine and phenylene ring systems in the polymer main chain. Further, at 300 ^{o}C, about 20-25% of weight loss was noticed. This is mainly due to the degradation of the hexadecoxyl side chain on the cyanopyridine ring. Finally, a gradual loss in weight was observed over 350 ^{o}C, which can be attributed to the further degradation of the macromolecular chain, to form residue.
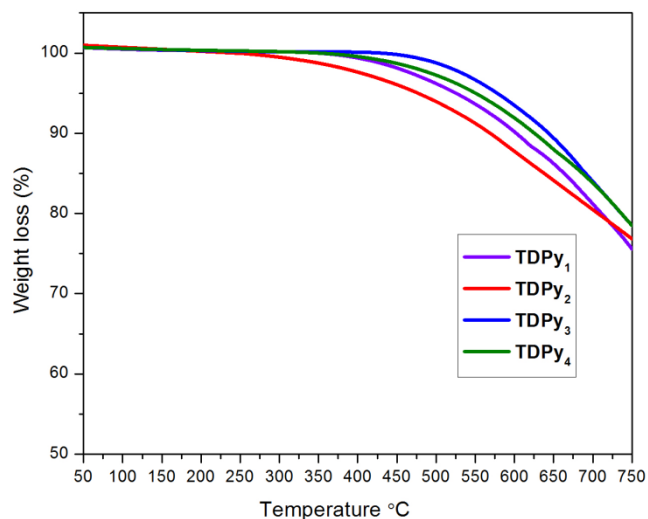
Figure 4.19: Thermogravimetric traces of **TDPy1-4**

Polymers Py1-4 (Series-6)

Polymers **Py1-4** of **Series-6** were subjected to TGA studies in order to assess their thermal stability. Experiments were carried out in a nitrogen atmosphere by temperature ramp of 10 ^{o}C min^{-1} ranging from 50 to 600 ^{o}C. **Figure 4.20** shows experimentally obtained thermograms. As observed from the results, **Py1**, **Py2**, **Py3** and **Py4** possess decomposition temperatures of 326, 339 and 343, 345 ^{o}C, respectively. Here also, all the polymers **Py1-4**, demonstrated a high degree of thermal stability, which can be attributed to the presence of rigid cyanopyridine rings linked through imine linkage in the polymer chain. Similar to earlier series, at around 300 ^{o}C, about 20-25% of weight loss was observed mainly due to the degradation of the alkoxy side chain on the cyanopyridine scaffold. Finally, a regular loss in weight was observed over 350 ^{o}C. This can be attributed to the further degradation of the macromolecular chain to various side products.
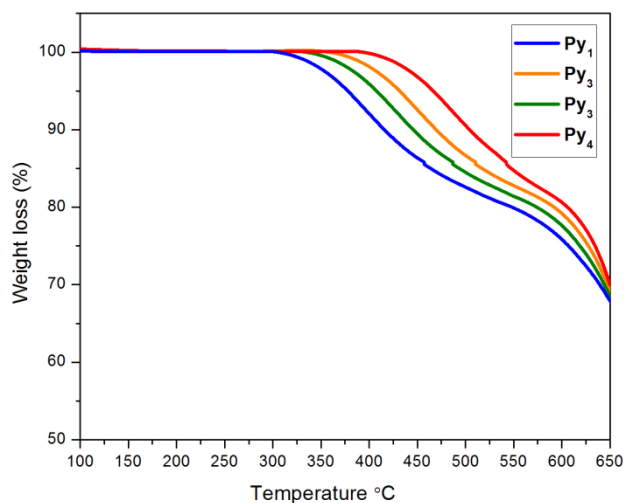
Figure 4.20: Thermogravimetric traces of **Py$_{1-4}$**

4.4 INTRODUCTION TO COMPUTATION STUDY

One of the main goals in the field of electrically conducting polymers is to develop a complete understanding of the relationship between the chemical structure of the polymer and its electronic as well as conduction properties. The desired electronic properties could be induced by specific synthesis following molecular design. The conduction properties of an undoped polymer, in terms of the band theory of solids, are known to be related to its electronic properties, such as the ionization potential (IP), electronic affinity (EA), and band gap (E$_g$). The key factor that, determines the intrinsic properties of the conjugated polymers is their band structures, particularly the positions of the conduction and valence bands and the energy gap between them. Therefore, the π-electrons in conducting polymers play a major role in determining their electrical conductivity and band structure. The energy between the valence and conduction band of a polymer is related to the lowest energy of its monomer units and to the bandwidth resulting from the overlap between the monomer orbitals. A band gap is defined as the difference between the highest occupied molecular orbital (HOMO) and the lowest unoccupied molecular orbital (LUMO) energy levels in the polymer as represented in **Equation 4.3.** Thus, electrical conductivity is directly related to the HOMO and LUMO energy of the molecule.

$$E_g = E_{LUMO} - E_{HOMO} \quad (eV) \tag{4.3}$$

Computational modeling can provide factors that affect various opto-electronic properties such as light absorption, emission, chain conformations, electronic structures *etc*. In literature, many quantum-mechanical simulations have been focused on the donor-acceptor concept in conjugated polymer systems to study the structural fine-tuning with regard to energy level modulation. For future judicious design of conjugated donor-acceptor configured polymer systems, computational modelling is quite useful tool.

DFT calculations with hybrid functional are considered to be one of the reliable computational approaches and are generally used in the field of optoelectronics in order to gain deeper insight into the molecular geometry and electron distribution in the polymer as well as its optical behavior in the excited state. To estimate the electron density distribution of the frontier orbitals of the polymer, DFT calculations were performed at the B3LYP/TZVP level using Turbomole 7.2V software. Only one repeating unit of each polymer was subjected to the computational calculation, with alkyl chains replaced by CH_3 groups hypothetically in order to minimize the computational complexity without compromising the quantitative picture. The geometries were first optimized with semi empirical AM1/COSMO basis using MOPAC in Tmolex. The results of computational studies of series-wise polymers have been discussed in the following section.

Polymers VPPy$_{1-3}$ (Series-1)

The optimized geometries as well as electronic distribution in HOMO and LUMO levels of repeating unit of polymers are portrayed in **Figure 4.21** The calculated HOMO levels of **VPPy$_1$**, **VPPy$_2$** and **VPPy$_3$** were found to be –6.13, –5.37 and –5.47 eV, whereas their LUMO levels were obtained to be –2.44, –2.04 and –2.14 eV, respectively. Their band gaps were shown to be 3.69, 3.33 and 3.33 eV, respectively. All these data are summarized in **Table 4.2**. The present predicted HOMO/LUMO values of the polymers moderately differ from their experimentally obtained values, which may be due to various effects such as conformational order in bulk state, effect of solvent and electrolyte that were not taken into account. From the data, it is clear that the electron density in HOMO levels of **VPPy$_2$** and **VPPy$_3$** were found to be higher on donor part indicating that the HOMO energy level is affected by

both the electron donor units in the polymer chain. However, the electron density of their LUMO levels is almost localized on the electron withdrawing cyanopyridine unit. Interestingly, in case of **VPPy₁** electron density of HOMO is localized on cyanopyridine ring while that of LUMO is confined on cyanovinyelene linkage, demonstrating that electron withdrawing ability of cyanovinylene moiety dominates over that of cyanopyridine ring.

Polymer	Optimized Geometry	HOMO	LUMO
VPPy₁			
VPPy₂			
VPPy₃			
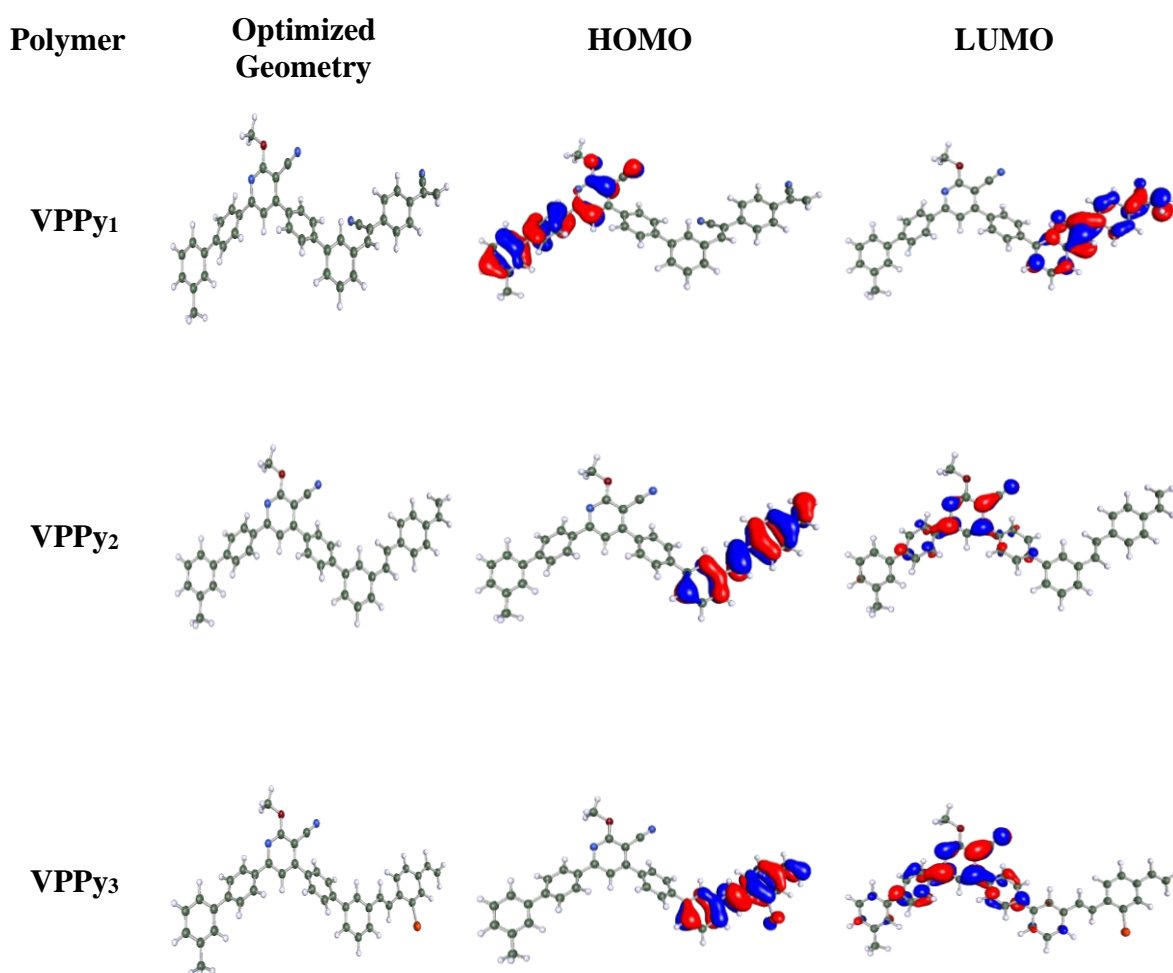
Figure 4.21: Optimized geometries and simulated FMO energy levels of **VPPy₁₋₃**

Polymers VTPy₁₋₃ (Series-2)

     Figure 4.22 illustrates the optimized geometries as well as electronic distribution in HOMO and LUMO levels of repeating unit of polymers **VTPy₁₋₃** (**Series-2**). Here, the obtained HOMO levels of **VTPy₁, VTPy₂** and **VTPy₃** are −5.94,

–5.56 and –5.76 eV, while their LUMO levels are –2.64, –2.42 and –2.45 eV, respectively. Their band gaps were calculated to be 3.29, 3.13 and 3.31 eV, respectively. **Table 4.2** summarizes all the simulated data. These predicted HOMO/LUMO values differ from their experimentally obtained values. This may be due to various parameters like conformational order in bulk state, effect of solvent and electrolyte *etc*.

Polymer	Optimized Geometry	HOMO	LUMO
VTPy₁			
VTPy₂			
VTPy₃			
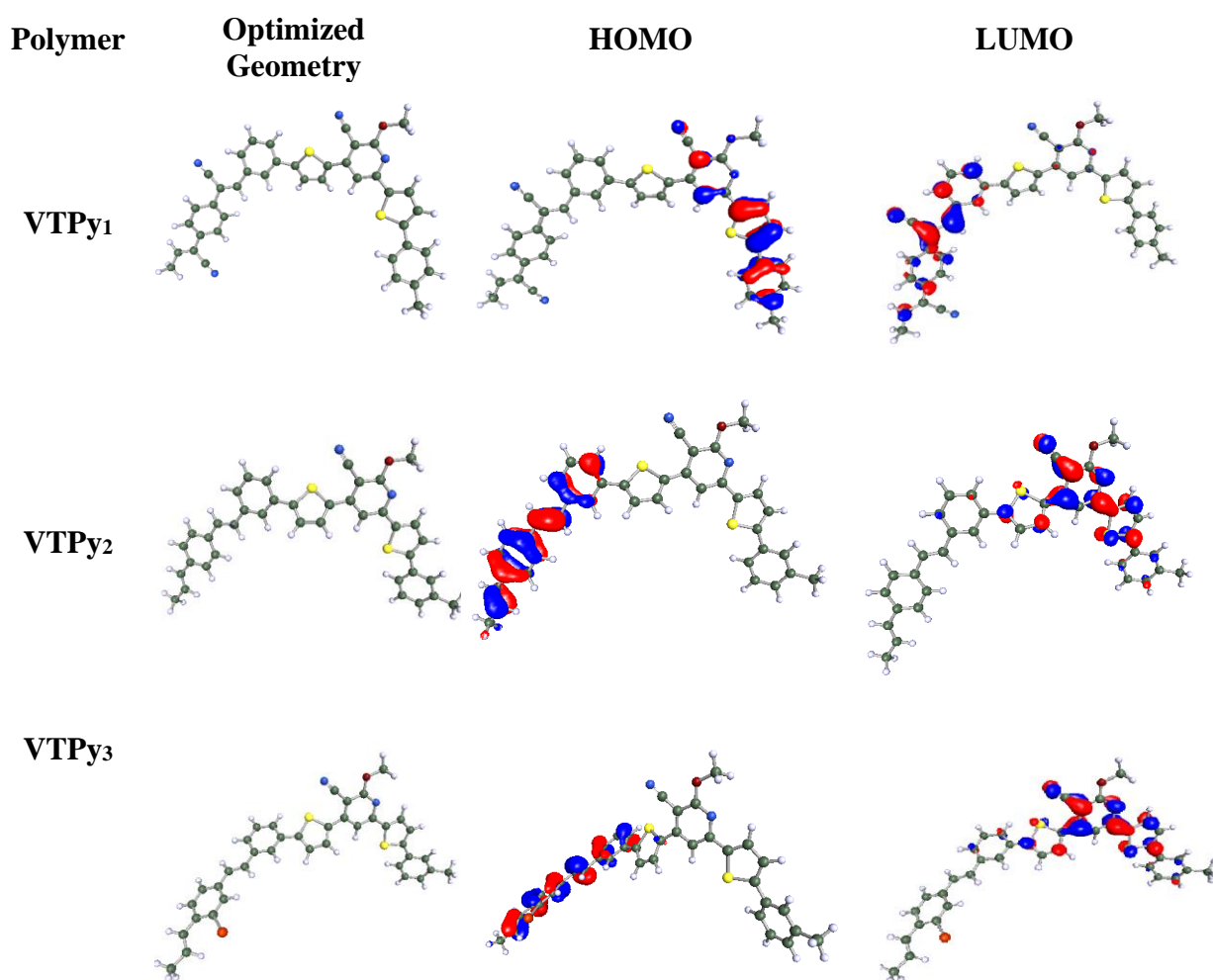
Figure 4.22: Optimized geometries and simulated FMO energy levels of **VTPy₁₋₃**

Evidently, the electron density in HOMO levels of VTPy2 and VTPy3 is found to be higher on donor part showing that the HOMO energy level is affected by both the electron donor units in the polymer chain. On the other hand, the electron density of their LUMO levels is almost localized on the electron pulling cyanopyridine unit. In case of VTPy1 electron density of HOMO is localized on

cyanopyridine ring while that of LUMO is confined on cyanovinyelene unit, demonstrating that electron withdrawing ability of cyanovinylene moiety dominates over that of cyanopyridine scaffold.

Polymers PPy$_{1-3}$ (Series-3)

  Figure 4.23 shows the optimized molecular geometries of the repeated units of the **PPy$_{1-3}$**, along with electronic distributions in their FMO energy levels. The simulated HOMO levels of **PPy$_1$**, **PPy$_2$** and **PPy$_3$** were found to be -5.80, -5.73 and -5.66 eV, whereas their LUMO levels were obtained to be -1.85, -1.97 and -2.12 eV, respectively. Their bandgaps were calculated to be 3.95, 3.76 and 3.54 eV, respectively. **Table 4.2** summarizes all these data. The observed difference in predicted FMO energy values from experimentally determined values may be ascribed to the fact that, while performing the simulations, the various realistic phenomena such as effect of solvent, electrolyte and conformational order in bulk state were not being taken into account. It is quite evident that, in HOMO energy levels of **PPy$_{1-3}$**, the electron density is mainly concentrated on donor part. Whereas, in LUMO levels, the electron density is mostly localized on the electron deficient cyanopyridine scaffold.

Polymer	Optimized Geometry	HOMO	LUMO
PPy₁			
PPy₂			
PPy₃			
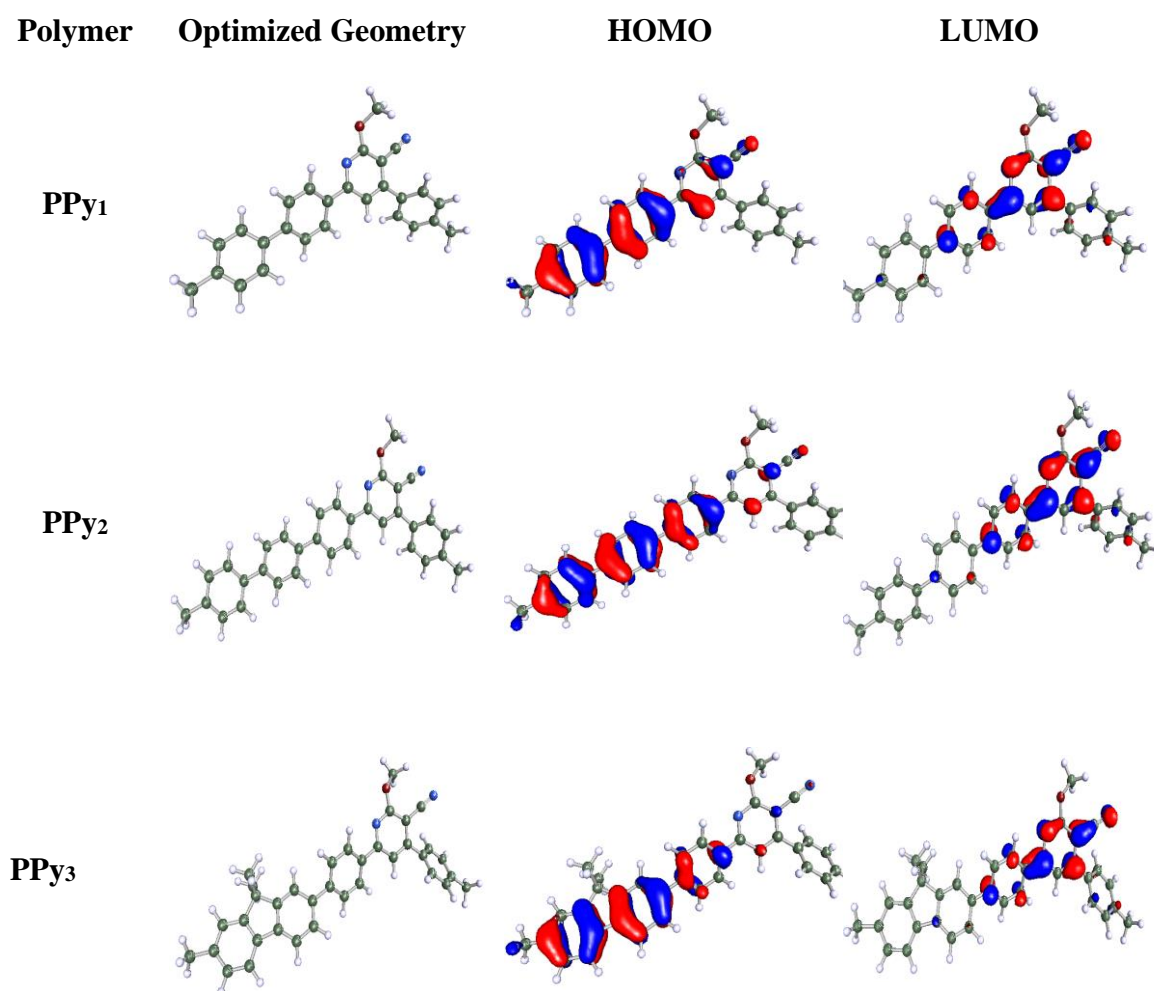
Figure 4.23: Optimized geometries and simulated FMO energy levels of **PPy₁₋₃**

Polymers TPy₁₋₃ (Series-4)

Polymers **TPy₁₋₃ (Series-4)** were subjected to computational studies in order to optimize molecular geometries of the repeated units of the polymers **TPy₁₋₃** and to find out electron distribution in their FMO energy levels. The corresponding results are displayed in **Figure 4.24** and the data are tabulated in **Table 4.2**. The HOMO energy levels of **TPy₁**, **TPy₂** and **TPy₃** were found to be –5.94, –5.56 and –5.76 eV, whereas their LUMO levels were obtained to be –2.64, –2.42 and –2.45 eV, respectively. Their calculated band gaps are 3.30, 3.14 and 3.31 eV, respectively. Here also, the predicted values differ from experimental values because of the reasons explained in the earlier series. It is observed that, in HOMO energy levels of **TPy₁₋₃**,

the electron density is largely concentrated on donor part, while in LUMO levels, the electron density is highly localized on the electron deficient cyanopyridine scaffold.

Polymer	Optimized Geometry	HOMO	LUMO
TPy₁			
TPy₂			
TPy₃			
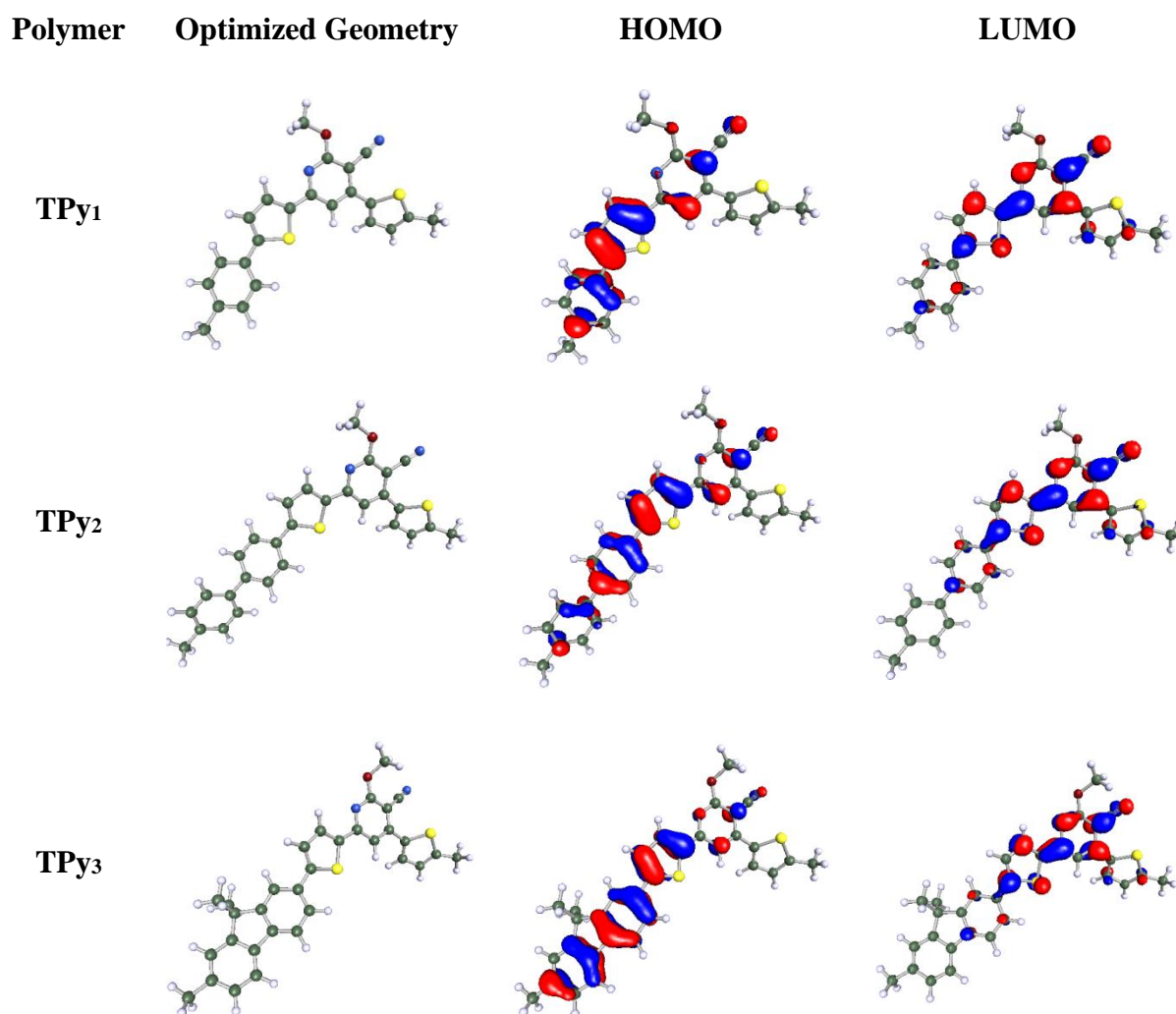
Figure 4.24: Optimized geometries and simulated FMO levels of **TPy₁₋₃**

Polymers TDPy₁₋₄ (Series-5)

Optimized geometries as well as electron distribution in FMO energy levels of polymers **TDPy₁₋₄** (**Series-5**) were simulated with the help of computational studies. The predicted results are shown in **Figure 4.25** and the corresponding data are summarized in **Table 4.2**. The HOMO energy levels of **TDPy₁**, **TDPy₂** and **TDPy₃**, **TDPy₄** were found to be −6.12, −5.86 and −6.13, −5.88 eV, whereas their LUMO levels were obtained to be −2.66, −2.92 and −3.09, −3.19 eV, respectively. Their band

gaps were shown to be 3.46, 2.94 and 3.04, 2.69 eV, respectively. Similar to the results of earlier series, the predicted FMO energy values are slightly different from experimental data. It is clearly seen that, in HOMO energy levels of **TDPy1-4**, the electron density is mainly concentrated on donor part, while in LUMO levels, the electron density is mostly localized on the electron deficient cyanopyridine scaffold.

Polymer	**Optimized Geometry**	**HOMO**	**LUMO**
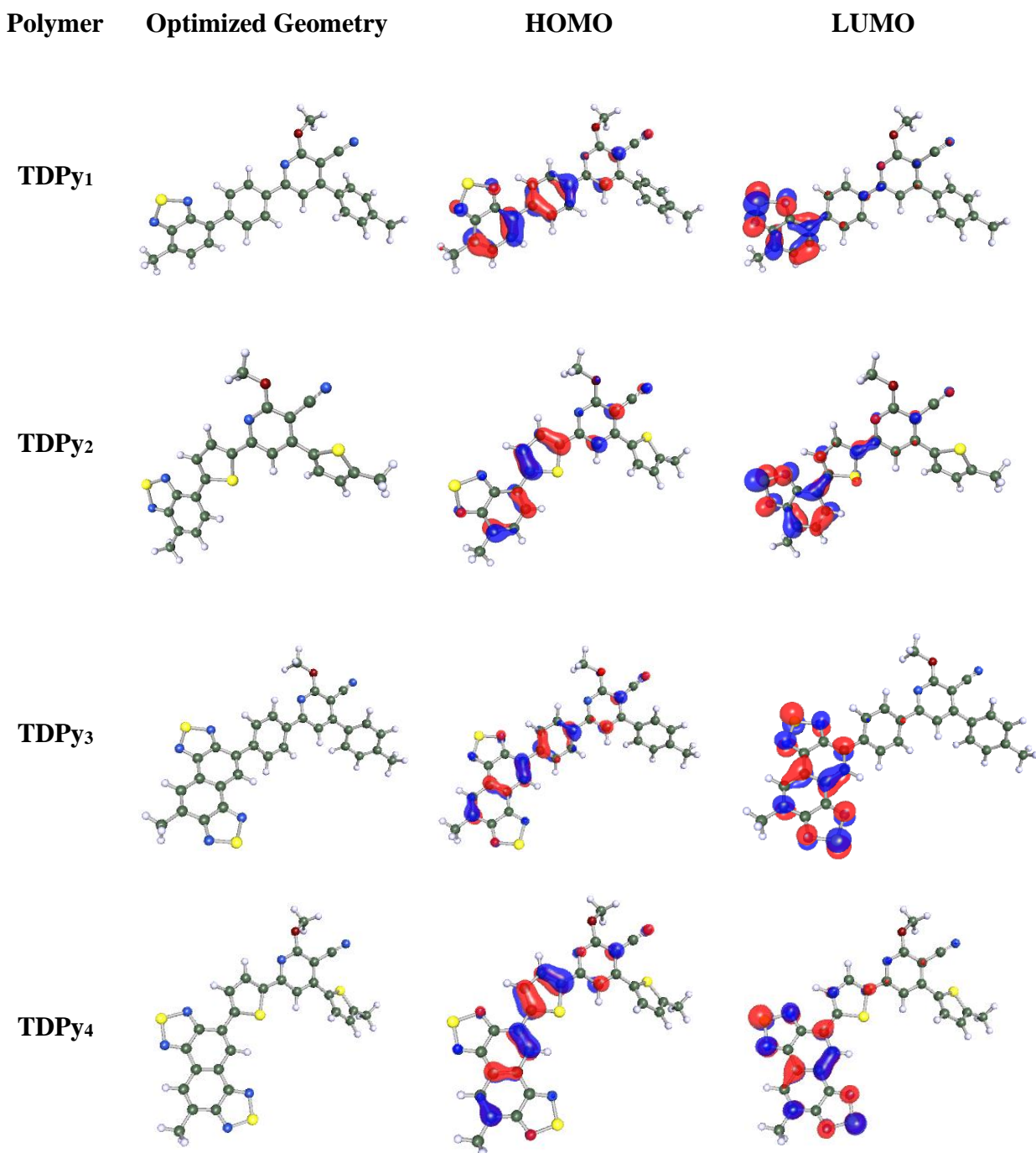
Figure 4.25: Optimized geometries and simulated FMO levels of **TDPy1-4**

Polymers Py$_{1-4}$ (Series-6)

The optimized molecular geometries of the repeated units of the **Py$_{1-4}$**, obtained from their computation studies are displayed in **Figure 4.26**, along with electron distributions in their HOMO-LUMO energy levels. Their corresponding data are summarized in **Table 4.2**. As seen from the results, the HOMO energy levels of **Py$_1$**, **Py$_2$** and **Py$_3$**, **Py$_4$** are −5.83, −5.60, −5.87 and −5.65 eV, whereas their LUMO levels are −2.29, −2.28, −2.47 and −2.48 eV, respectively. Their band gaps were shown to be 3.54, 3.32 and 3.39, 3.17 eV, respectively. It has been observed that there is a small difference in theoretical and experimental FMO energy values of the polymers. The optimized molecular geometries of **Py$_{1-4}$** reveal that, in HOMO energy levels , the electron density is mainly concentrated on donor units, *viz.* phenylene and thiophene scaffolds. Whereas, in LUMO levels, the electron density is mostly localized on the electron deficient cyanopyridine scaffold.

Polymer	Optimized Geometry	HOMO	LUMO
Py₁			
Py₂			
Py₃			
Py₄			
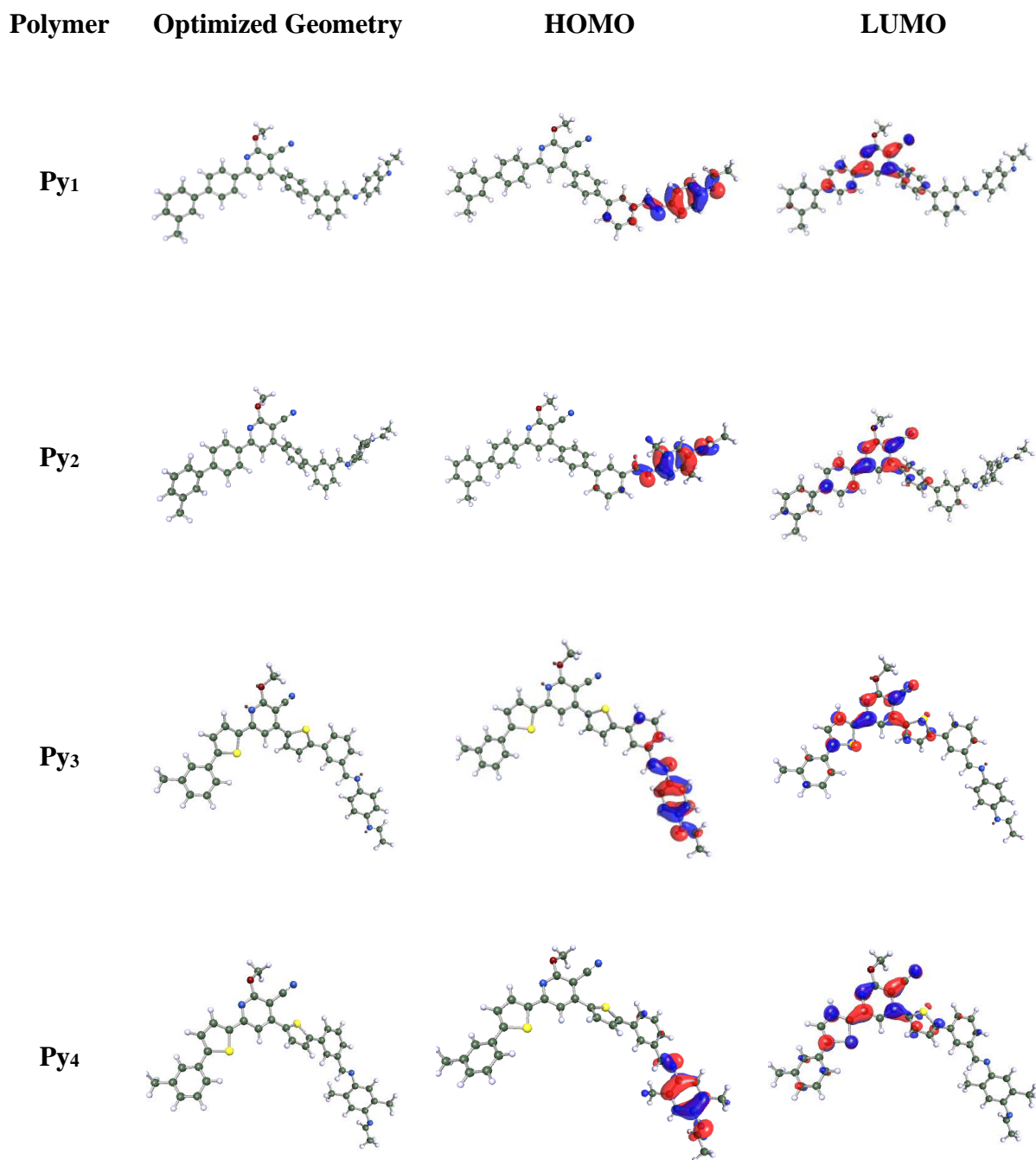
Figure 4.26: Optimized geometries and simulated FMO levels of **Py₁-₄**

Table 4.2: Theoretically determined FMO energy levels of new polymers

Polymer	HOMO (DFT) eV	LUMO (DFT) eV	E_g^{DFT} eV
VPPy₁	−6.13	−2.44	3.69
VPPy₂	−5.37	−2.04	3.33
VPPy₃	−5.47	−2.14	3.33
VTPy₁	−5.94	−2.64	3.29
VTPy₂	−5.56	−2.42	3.13
VTPy₃	−5.76	−2.45	3.31
PPy₁	−5.80	−1.85	3.95
PPy₂	−5.73	−1.97	3.76
PPy₃	−5.66	−2.12	3.54
TPy₁	−5.94	−2.64	3.30
TPy₂	−5.56	−2.42	3.14
TPy₃	−5.76	−2.45	3.31
TDPy₁	−6.12	−2.66	3.46
TDPy₂	−5.86	−2.92	2.94
TDPy₃	−6.13	−3.09	3.04
TDPy₄	−5.88	−3.19	2.69
Py₁	−5.83	−2.29	3.54
Py₂	−5.60	−2.28	3.32
Py₃	−5.87	−2.47	3.39
Py₄	−5.65	−2.48	3.17

4.5 CONCLUSIONS

All the six new series of polymers, *viz.* **VPPy₁₋₃** (**Series-1**), **VTPy₁₋₃** (**Series-2**), **PPy₁₋₃** (**Series-3**), **TPy₁₋₃** (**Series-4**), **TDPy₁₋₄** (**Series-5**), and **Py₁₋₄** (**Series-6**) were subjected to photophysical, electrochemical, thermal and theoretical studies. The results of photophysical studies revealed that, conductive polymers in solution state exhibit λ_{max}, λ_{em}, E_g, HOMO level, Stoke shift, quantum yield and molar extinction coefficient in the range of 340 to 390 nm, 380 to 580 nm, 2.14 to 2.80 eV, −4.70 to −5.30 eV, 2700 to 6700 cm⁻¹, 21 to 49 %, and 9000 to 18,000 M⁻¹cm⁻¹, respectively,

while in film state they show λ_{max}, and λ_{em} in the order of 370 to 420 and 430 to 540 nm, respectively. Further, their LUMO levels were calculated to be in the range of −1.90 to −2.90 eV, by using E_{red} values obtained from their electrochemical studies. Furthermore, their theoretical studies revealed that, their HOMO, LUMO and E_g values are in the order of −5.32 to −6.13 eV, −1.90 to −3.2 eV and 2.69 to 3.95 eV, respectively. Also, their optimized geometries indicated that, in HOMO energy levels the electron density is highly localized on donor units, while in LUMO energy levels electron density is concentrated on electron deficient units. Their thermal study confirmed that, polymer **TDPy4** of the **Series-5** possesses very good thermal stability, *i.e.* stable up to 388 °C. In the present study, all the designed polymers showed the band gap in the order of 2.69 to 3.95 eV because of the donor-acceptor concept involved in conjugative chain. Conclusively, the study revealed that the bandgap of the polymer can be tuned by changing the donor/acceptor strength as well as conjugation path length through structural variations. Most of the polymers showed desirable photophysical, electrochemical and thermal properties, they are potential candidates for PLED applications.

ELECTROLUMINESCENCE STUDIES

Abstract

This chapter comprises a brief introduction to electroluminescence devices and fabrication studies of PLED's using newly synthesized conjugative polymers as emissive materials. It also includes a concise discussion on the results of device studies.

5.1 INTRODUCTION TO ELECTROLUMINESCENCE IN POLYMERS

The first discovery of EL in organic materials was in the early 1950s by A. Bernanose and his group (1955). They applied high-voltage alternating current (AC) fields in air to organic materials such as acridine, either coated on or dissolved in a natural polymer, cellulose or cellophane thin films. In 1960, Pope and co-workers, at New York University described the essential energetic requirements, *i.e.* work functions for both hole and electron injecting electrode contacts. Such contacts are the basis of charge injection in all the present OLED devices. In fact, Pope et al. also first investigated direct current (DC) electroluminescence under vacuum on a pure single crystal of anthracene as well as on anthracene crystals doped with tetracene in 1963.

Electroluminescence using polymer films was first observed by R. Partridge (1983). These devices device comprised a film of poly(*N*-vinylcarbazole) placed between two charge injecting electrodes. According to literature, the first diode device was reported at Eastman Kodak by Ching W. Tang and Steven Van Slyke in 1987. This device employed a new two-layer structure with separate hole transporting and electron transporting layers so that recombination and light emission occurred in the mid of the organic coatings. This has resulted in a reduction in operating voltage and also, improvements in efficiency. This discovery led to the current era of OLED research and device production.

Research into PLED peaked in 1990 with Burroughes *et al.* at Cambridge reporting a high efficiency green light-emitting polymer based device using 100 nm thick films of poly(*p*-phenylene vinylene). As emitting materials, polymeric/organic substances enjoy many advantages over inorganic ones, such as good film-forming

properties, susceptible to structure modification, light weight, wider viewing angles, higher response time, low cost, so on (Akcelrud, 2003).

PLED's have attracted broad interests mainly due to their large potentials in serving next generation displays and illuminants. Now, they are the cutting edge of lighting and display technology. Today, most of the commercially available small-screen OLED displays are being fabricated by vacuum sublimation. However, this technique of fabrication is expensive and time consuming, and controlling uniformity and doping concentration over large areas is very difficult with this technique. Furthermore, during evaporation, vapors condensed on cooler walls can flake off, contaminating the system and substrate. Consequently, solution techniques like spin-coating, ink-jet printing, and screen printing have gained much interest since they do not require vacuum, consume less time, and allow deposit of thin layer over a large area at low cost. As these organic materials are capable of dissolving in different volatile solvents, the desired thickness of the deposits can easily be achieved by spraying the solution using modern techniques. Whatever may be the technique, during deposition, uniform thickness of each layer plays a crucial role for device fabrication in order to ensure good lifetime of the device.

It is important to note that, the complexity in arranging organic molecules and constructing PLED devices is still challenging. When compared to the small molecule counterparts, conductive polymers show high film-forming property that enables a uniform deposition *via* solution-based techniques, which are preferred in industrial applications. Many conjugative polymers have been extensively studied, and morphology controlled tuning the solubility and stability is intensely conducted to achieve improved device performance. Normally, to enhance the solubility, one solution lies in the synthesis of ladder-type conducting polymers, which leads to a higher solubility ascribed to a high degree of coplanarity. In addition, a full color display can be realized by controlling the molecular structure to regulate the HOMO-LUMO energy gap to realize desired luminous properties.

EL mechanism:

A typical PLED device is composed of a layer of electrically conductive organic material placed between two electrodes, the anode and cathode, all uniformly

deposited on an indium tin oxide (ITO) substrate. **Figure 5.1** illustrates a typical electroluminescent device and its mechanism. During operation, when a voltage is applied and a current of electrons flow through the EL device from cathode to anode, as electrons are injected into the lowest unoccupied molecular orbitals (LUMO) of the organic layer at the cathode and withdrawn from the the highest occupied molecular orbitals (HOMO) at the anode. The latter process may also be considered as the injection of holes into the HOMO. The generated electron and the hole recombine in the deposited emitting material, forming an exciton, a bound state of the electron and hole. The decay of this excited state causes a relaxation of the energy levels of the electron, accompanied by emission of radiation whose wavelength is in the visible region. The wavelength of this radiation depends on the band gap of the emitting material, or the energy difference between the HOMO and LUMO levels. EL efficiency, the most important property of EL device, may be expressed as a percentage, is the ratio of luminous/photo flux to power.
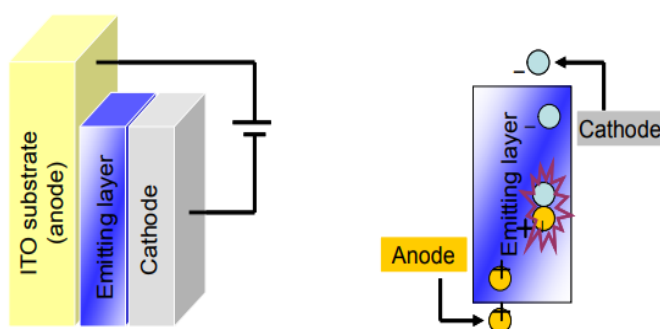
Figure 5.1: Organic EL device and mechanism of EL

The first PLED, reported as single-layer device with PPV inserted between two electrodes simply, emitted a yellow-green light，with EL efficiency of only 0.05%. In contrast to the easy fabrication process, the performance of this single-layer PLED was typically unsatisfactory due to the high carrier injection barrier, unbalanced carrier injection and recombination zone being close to electrode-emitting layer interfaces Burroughes et al. 1990.

To improve device performance, multilayer PLEDs consisting of a hole-transporting layer (HTL), an emitting layer and an electron-transporting layer (ETL), sandwiched between two electrodes, were designed. Nevertheless, fabrication of the

multilayer PLEDs is usually a difficult task, since the emitting layer might be re-dissolved during subsequent spin-coating of the electron injection/transport layer. To achieve PLEDs of high external quantum efficiency, two key parameters are important. Firstly, a high internal quantum efficiency including a high photoluminescence quantum efficiency of the emissive material, singlet formation *via* spin statics and a high fraction of recombination of electrons and holes in the emissive layer; and a high out-coupling efficiency such that a high fraction of photons escape the device.

The performance of PLED's strongly depends on materials, fabrication and the structure of the device. In the present study indium tin oxide (ITO) is used as anode, the new polymer as emitting layer and metal aluminum as cathode. Here, investigations are focused to fully understand and develop the method of fabrication of PLEDs using the available resources and to understand the effect of polymer structure on device parameters.

5.2 GENERAL PROCEDURE FOR DEVICE FABRICATION

In the present research, PLED devices were fabricated with a configuration of ITO/PEDOT:PSS/Polymer/Al in order to investigate the electroluminescent (EL) behavior of the newly synthesized polymers as emissive materials. The device fabrication follows sandwich type of structure with poly(3,4-ethylenedioxythiophene):poly(styrenesulphonate) (PEDOT: PSS) coated indium tin oxide (ITO) glass as the anode, the spin coated newly synthesized polymer as the emissive layer and aluminum as the cathode. While fabricating PLEDs of device configuration ITO/PEDOT: PSS/polymer/Al, first the indium tin oxide (ITO) coated glass substrates with a sheet resistance of 20 Ω/square and a thickness (ITO) of 120 nm were cleaned using deionized water, acetone, trichloroethylene and isopropyl alcohol sequentially for about 30 min each using an ultrasonic bath and dried in a vacuum oven. Then ITO surface was treated with oxygen plasma for about 10 minutes to increase its work function. Later, a hole injection layer of PEDOT: PSS was spin coated on the cleaned and patterned ITO substrate at 4000 rpm to achieve about 50-60 nm in thickness, and subsequently it was dried by baking at 120 ${}^{\circ}$C in vacuum for 50 min. Then, the emitting polymer layer was spin cast onto the PEDOT: PSS layer at a

speed of 2000 rpm from chlorobenzene solution (10 mg/mL) through a 0.45 µm teflon filter, followed by vacuum annealing at 150 °C for ~2 h in order to remove the organic fraction. Finally, the coated ITO was transferred to a deposition chamber, where a layer of Al electrode was vacuum deposited on the polymer layer with about 200 nm in thickness by thermal evaporation method at a pressure of 1×10^{-6} Torr. Four pixels, each of active area of 4×4 mm^2 were defined per substrate and used to assess the reproducibility of the device performance. The complete fabricated devices were finally annealed at 100 °C in vacuum for 5 min before being characterized. All the characterizations of the light-emitting diode devices were carried out at room temperature under ambient conditions without protective encapsulation. Horiba Fluromax-4 spectrophotometer was used for the experiments. **Figure 5.2** shows the schematic diagram of the devices fabricated using newly synthesized conductive polymers belonging to six series.
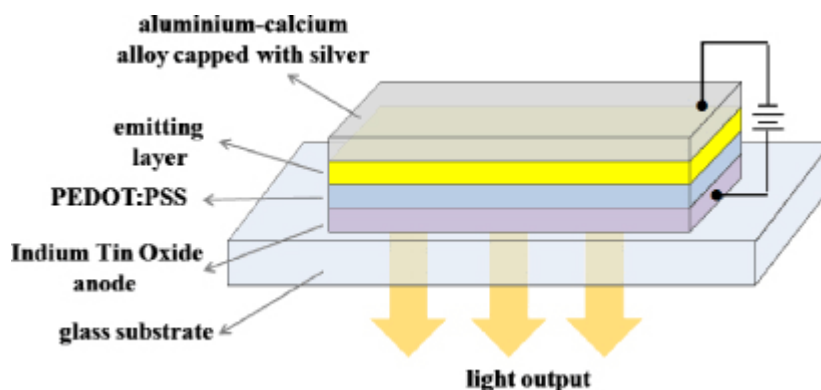
Figure 5.2: Schematic representation of the device fabrication

5.3 RESULTS AND DISCUSSION

Results of PLED devices, fabricated using the newly synthesized polymers are discussed in the following section.

Polymers VPPy$_{1-3}$ (Series-1)

The fabricated PLED devices with the configuration ITO/PEDOT:PSS/**VPPy$_{1-3}$**/Al using the polymers **VPPy$_{1-3}$** display characteristic electroluminescence spectra and J-V curves as shown **Figures 5.3** and **5.4** respectively. The procured J-V curves indicate that, the current density of the polymer increases exponentially with the increasing forward bias voltage, which is a typical diode characteristic. The PLED

devices show low threshold voltages of 5.45, 5.23 and 5.29 V for **VPPy₁**, **VPPy₂** and **VPPy₃**, respectively, which might be attributed to the lower energy barrier for electron injection from the aluminum electrode. This may be due to low lying LUMO level of the polymer. The obtained low threshold voltage values are comparable with some of the previously reported light-emitting polymers showing good EL performance. The EL emission maximum of polymers **VPPy₁**, **VPPy₂** and **VPPy₃** were found to be 488, 482 and 483 nm, respectively at driving voltage of 5V. Conclusively, the results reveal that, all the three polymers display light blue electroluminescence at low threshold voltage in the order of 5.23-5.45 V.
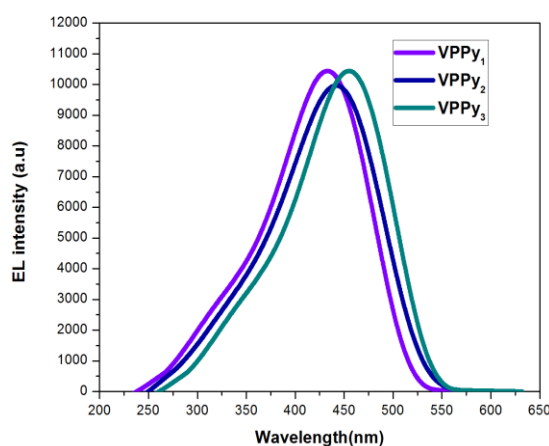
Figure 5.**3:** EL spectra of **VPPy₁**, **VPPy₂** and **VPPy₃** at driving voltage of 5 V
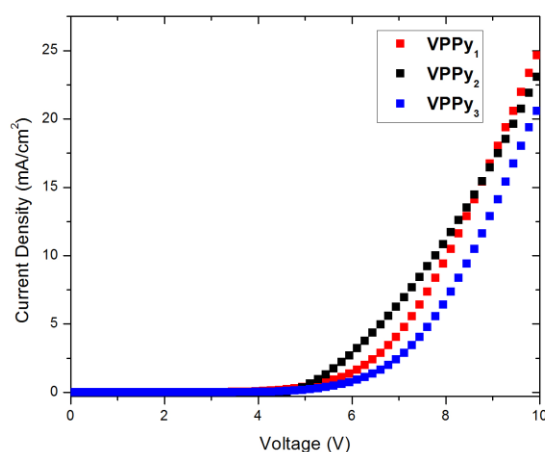
Figure 5.**4:** Current-voltage characteristics of ITO/PEDOT: PSS/**VPPy₁₋₃**/Al devices

Polymers VTPy₁₋₃ (Series-2)

Results generated from PLED devices, fabricated with a configuration of ITO/PEDOT:PSS/**VTPy₁₋₃**/Al using the polymers **VTPy₁₋₃**, are summarized in **Figures 5.5** and **5.6**. The observed EL emission maximum of **VTPy₁**, **VTPy₂** and **VTPy₃ (Figure 5.5)** were found to be 476, 469 and 471 nm, respectively at 5 V (driving voltage). The current density-voltage characteristics of the devices (**Figure 5.6**) indicate that, the current density increases exponentially with the increasing forward bias voltage, similar to polymers of previous series. Further, the devices show low threshold voltage of 3.5, 3.75 and 3.9 V for **VTPy₁**, **VTPy₂** and **VTPy₃**, respectively. This can be attributed to the lower energy barrier for electron injection from the aluminum electrode, because of low lying LUMO level of the polymer. These results are comparable to that of some of the previously reported light-emitting similar polymers. The EL emission maxima of polymers **VTPy₁**, **VTPy₂** and **VTPy₃** were found to be 476, 4689 and 471 nm, respectively at driving voltage of 5 V. Thus, the results clearly indicate that, all the polymers display bright blue electroluminescence at low threshold voltage of 3.5-3.9 V.
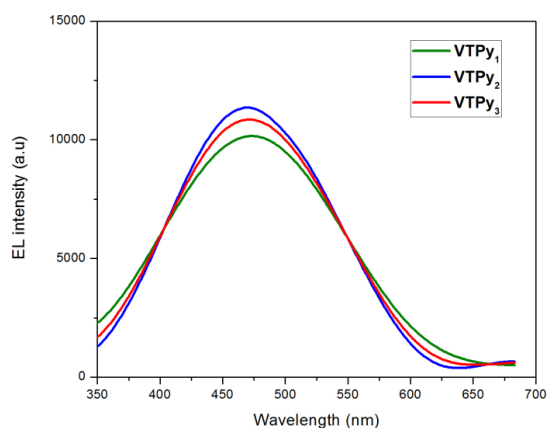
Figure 5.5: EL spectra of **VTPy₁**, **VTPy₂** and **VTPy₃** at driving voltage of 5 V
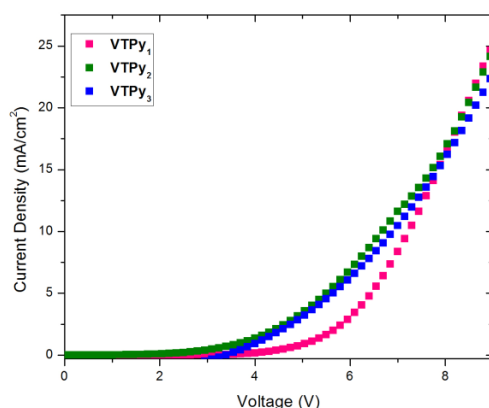
Figure 5.**6:** Current-voltage characteristics of ITO/PEDOT: PSS/**VTPy₁₋₃**/Al devices

Polymers PPy₁₋₃ (Series-3)

Figures 5.7 and **5.8** show EL emission spectra and *J-V* (current-voltage) characteristic curves of the new ITO/PEDOT:PSS/**PPy₁₋₃**/Al configured PLED devices employing polymers **PPy₁₋₃**, respectively. Interestingly, a steady rise in the current density with the increasing forward bias voltage indicating distinctive diode characteristic, has been observed. Further, the new devices display low threshold voltage of 3.40, 4.58 and 5.20 V for **PPy₁**, **PPy₂** and **PPy₃**, respectively. This may be due to their low LUMO energy levels that reduces the energy barrier of electron injection from the cathode. Further, their EL emission maxima were found to be 425 nm (**PPy₁**), 438 nm (**PPy₂**), and 452 nm (**PPy₃**) at driving voltage of 12 V. From the results it is quite evident that, the new polymers display blue and dark blue electroluminescence with lower threshold voltages of 3.40-5.20 V. Thus, these cyanopyridine based conjugative polymers have displayed better performance than previously reported similar type of polymers.
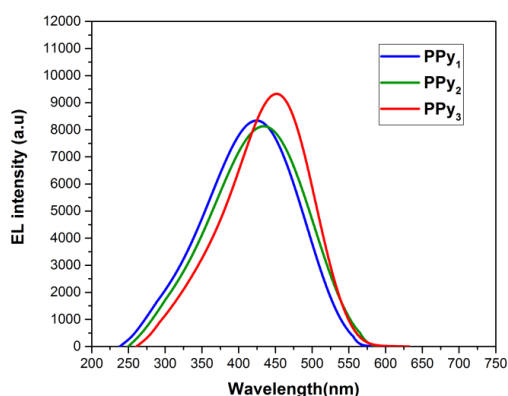
Figure 5.7: EL spectra of **PPy₁₋₃** at driving voltage of 12V
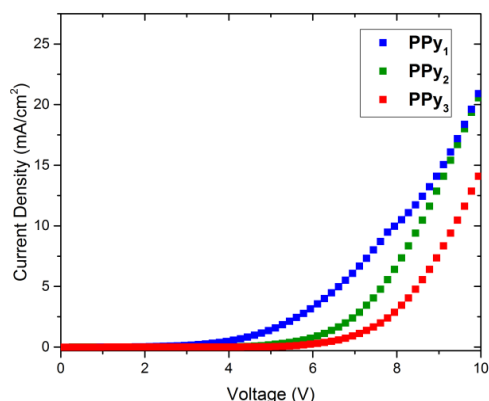
Figure 5.8: Current-voltage characteristics of ITO/PEDOT: PSS/**PPy₁₋₃**/Al devices

Polymers TPy₁₋₃ (Series-4)

Figures 5.9 and **5.10,** showcase the EL emission spectra and *J-V* (current-voltage) characteristic curves of the PLED devices, employing the polymers **TPy₁₋₃,** respectively. Here also, a steady rise in the current density with the increasing forward bias voltage has been notices indicating distinctive diode characteristic. Further, the polymers display low threshold voltage of 4.20, 4.55 and 4.80 V respectively. This can be explained on the basis of their low LUMO energy level that reduces the energy barrier of electron injection from the cathode. It has been observed that, their EL emission maxima are 476 nm (**TPy₁**), 469 nm (**TPy₂**), and 471 nm (**TPy₃**) at driving voltage of 12 V. Convincingly, the polymers **TPy₁₋₃** display blue and dark blue electroluminescence with a lower threshold voltage of 4.20-4.80 V.
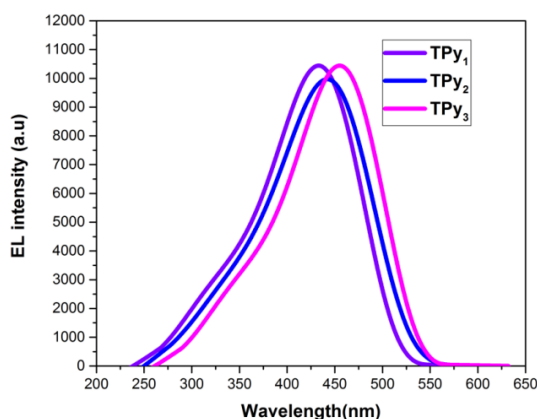
Figure 5.9: EL spectra of of polymers **TPy₁** at driving voltage of 12V
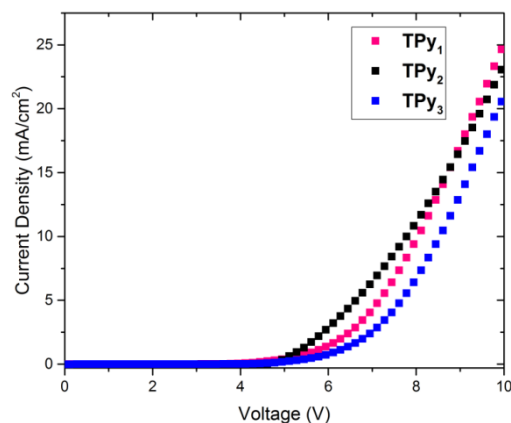
Figure 5.10: Current-voltage characteristics of ITO/PEDOT: PSS/**TPy₁₋₃** /Al devices
Polymers TDPy₁₋₄ (**Series-5**)

The obtained EL emission spectra and J-V-curves of the newly fabricated devices with configuration ITO/PEDOT:PSS/**TDPy₁₋₄**/Al have been summarized in **Figures 5.11** and **5.12**, respectively. As seen from the graph, there is a steady rise in the current density with the gradual increasing forward bias voltage showing distinctive diode characteristic. Also, it was observed low threshold voltages of 5.22, 5.71, 4.11 and 3.12 V for **TDPy₁**, **TDPy₂** ,**TDPy₃** and **TDPy₄**, respectively, which may be due to their low LUMO energy level that reduces the energy barrier of electron injection from the cathode. Further, their observed EL emission maxima are 522 nm (**TDPy₁**), 508 nm (**TDPy₂**), 507 nm (**TDPy₃)** and 496 nm **(TDPy₄)** at driving voltage of 12 V. From the results it is quite evident that, the polymers of the series display a strong green electroluminescence with a lower threshold voltage of 4.20-4.80 V.
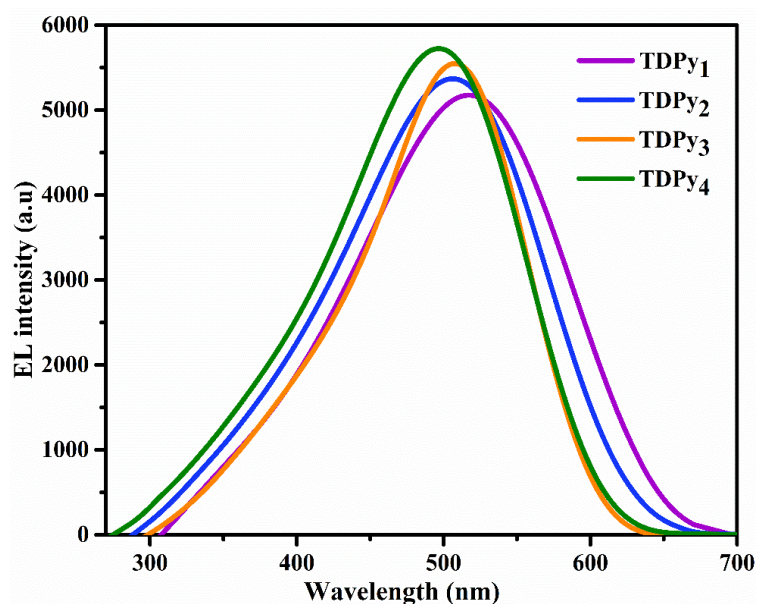
Figure 5.11: EL spectra of **TDPy₁₋₄** at driving voltage of 12V
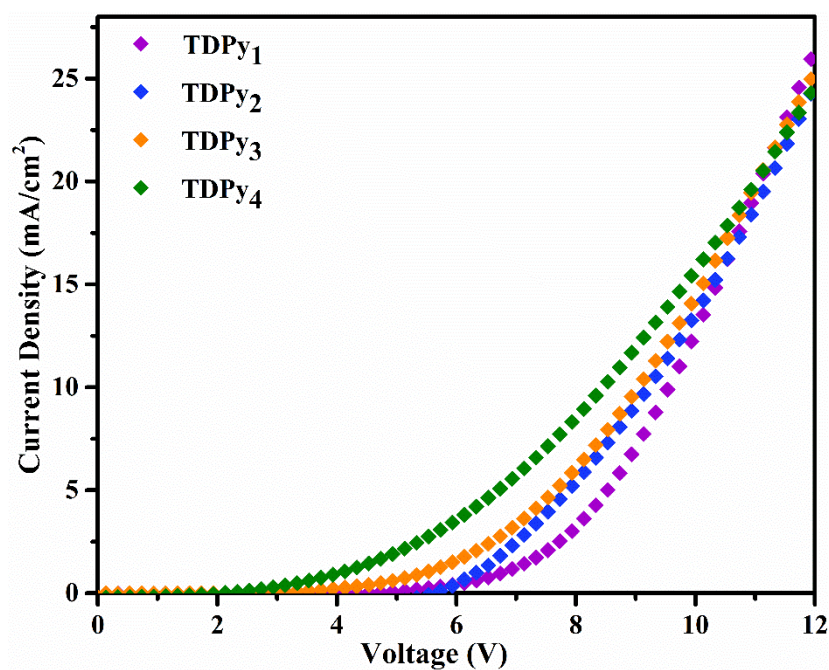
Figure 5.12: Current-voltage plots for ITO/PEDOT: PSS/**TDPy₁₋₃** /Al devices

Polymers Py₁₋₄ (Series-6)

Figure 5.13 shows the EL emission spectra, while **Figure 5.14** showcases the J-V (current-voltage) characteristic curves of the new PLED devices with configuration ITO/PEDOT:PSS/**Py₁₋₄**/Al. As observed in the previous series of

polymers, a steady rise in the current density with the increasing forward bias voltage, was noticed. Of course, this is characteristic of distinctive diode. Further, their threshold voltages were found to be 5.06, 5.57, 5.77 and 4.04 V, respectively. This observed low value might be attributed to their low LUMO energy levels. As indicated from the graphs, their EL emission maxima are 477 nm (**Py$_1$**), 471 nm (**Py$_2$**), 475 nm (**Py$_3$**) and 466 nm (**Py$_4$**) at driving voltage of 12 V. Thus, the new polymers **Py$_{1-4}$** displayed good blue electroluminescence with a lower threshold voltage of 4.04-5.77 eV. Device parameters of the newly synthesized polymers belonging to all the six series are summarized in **Table 5.1** for comparison.
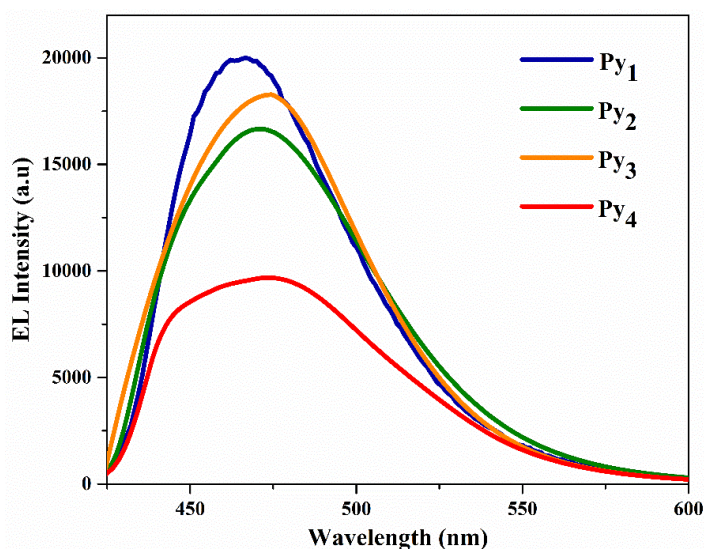
Figure 5.13: EL spectra of **Py$_{1-4}$** at driving voltage of 12V
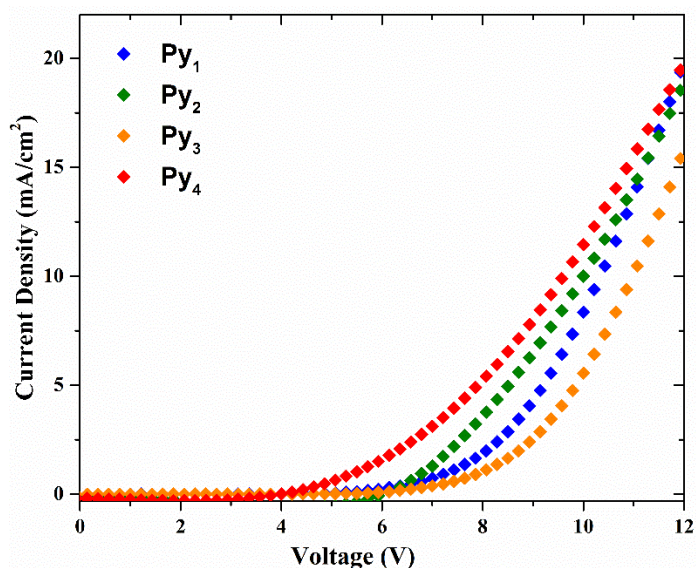
Figure 5.14: Current-voltage characteristics of ITO/PEDOT: PSS/**Py1-4** /Al devices

Table 5.1: Results of PLED devices using new polymers as emitters

Polymer	Threshold voltage (V)	EL emission maximum (nm)	Color
VPPy₁	5.45	488	Light Blue
VPPy₂	5.23	482	Light Blue
VPPy₃	5.29	483	Light Blue
VTPy₁	3.50	476	Blue
VTPy₂	3.75	469	Blue
VTPy₃	3.90	471	Blue
PPy₁	3.40	425	Blue
PPy₂	4.58	438	Blue
PPy₃	**5.20**	**452**	**Dark Blue**
TPy₁	4.20	476	Blue
TPy₂	4.55	469	Blue
TPy₃	**4.80**	**471**	**Dark Blue**
TDPy₁	5.22	522	Green
TDPy₂	5.71	508	Green
TDPy₃	4.11	507	Green
TDPy₄	3.12	496	Green
Py₁	5.06	477	Blue
Py₂	5.57	471	Blue
Py₃	5.77	475	Blue
Py₄	4.04	466	Blue

5.4 CONCLUSIONS

All the polymers of the **Series 1-6** showed a steady rise in the current density with the increasing forward bias voltage indicating distinctive diode characteristic. Further, the PLED devices fabricated using new polymers displayed low threshold voltage in the range of 3.12-5.77 eV. The observed lower values might be due to low LUMO energy levels of polymers. Furthermore, their EL emission maxima were found to be in the range of 425-527 nm with color ranging from blue to green, at driving voltage of 12 V. Conclusively, these newly designed polymers based on certain assumptions were found to be good emitters for the application in PLEDs. As these polymers possess good solubility in common organic solvents, there were no difficulties to get thin films during fabrication process. Since they have comparatively higher molecular weights, stable and uniform thin films could be obtained in the devices.

<div style="text-align: center;">**SUMMARY AND CONCLUSIONS**</div>

Abstract:

This chapter contains summary of the entire work carried out and important conclusions drawn from it. It also includes a brief account on the scope for future work.

6.1 SUMMARY

Conjugated polymers based on heteroaromatics are of prime importance in the last few decades due to their remarkable optical and electrochemical properties. These polymers were shown to possess many optoelectronic applications, which include mainly electroluminescent devices, photovoltaic cells and field effect transistors. Such polymers are prospective candidates for optoelectronic devices because of their many obvious advantages such as mechanical flexibility, impact resistance, optical transparency, thermal as well as photochemical stability, film forming ability, ease of fabrication, ability to form radical cations and hence possession of high charge carrier mobility. In this research field, the major challenge until now has been to obtain highly efficient and spectral stable light-emitting polymers which are very limited in literature. A major problem in PLEDs is unbalanced charge injection and transport due to intrinsic nature of emitting polymers involved. Moreover, in most of the luminescent conjugated polymers, hole injection and transport are more feasible than the electron injection and transport due to their high LUMO energy level, which leads to the imbalance in the rate of electron and hole injection, resulting in lowering of device efficiency. Several approaches have been attempted to improve the charge injection/transport of light emitting polymers. One such attractive strategy involves incorporation of both electron donating and electron accepting moieties in the rigid polymer backbone. Although several Donor-Acceptor type of conjugated polymers were reported in the literature, still there are ample of scopes to explore new Donor-Acceptor type polymers with desired optical and electroluminescence properties.

Based on the literature survey, it has been aimed at design and synthesis new series of D-A type conjugated polymers with possible applications in PLED. Accordingly, six new series of D-A type conjugated polymers carrying substituted

phenylene, thiophene, phenylenevinylene, biphenyl, fluorene and imine, as electron donors and cyanopyridine, cyanovinylene, thiadiazole scaffolds as electron acceptor moieties, have been designed. They are as follows:

(i) Phenylene-cyanopyridine based polymers carrying vinylene linkage, **VPPy$_{1-3}$ (Series-1)**

(ii) Thiophene-cyanopyridine based polymers carrying vinylene linkage, **VTPy$_{1-3}$ (Series-2)**

(iii) Phenylene-cyanopyridine based polymers, **PPy$_{1-3}$** (**Series-3**)

(iv) Thiophene-cyanopyridine based polymers, **TPy$_{1-3}$** (**Series-4**)

(v) Thiadiazole-cyanopyridine based polymers, **TDPy$_{1-4}$ (Series-5)**

(vi) Cyanopyridine based polymers carrying imine linkage, **Py$_{1-4}$ (Series-6)**

All the polymers, monomers and their intermediates were characterized using NMR, FTIR spectroscopic and elemental analyses. Their weight average molecular mass ($\overline{M}_w$) along with polydispersity index (PDI) were determined from Gel permeation chromatography (GPC) technique. Their thermal stability was investigated by the thermo gravimetric analysis (TGA). Further, their photophysical properties in both solution as well as solid film were studied by employing UV-Vis. absorption as well PL emission spectroscopy. In addition, their HOMO-LUMO energy levels were determined using both spectral as well as cyclic voltammetric (CV) method. Further, DFT (density functional theory) studies were performed on the newly synthesized polymers, by considering the repeating units (monomers) at B3LYP/TZVP level using using the software Turbomole 7.2. Finally, light emitting nature of newly synthesized polymers was determined by fabricating PLED devices. The device was fabricated with the configuration, ITO/PEDOT: PSS/Polymer/Al, where the polymer functions as a light emissive layer in their respective device. In addition, the polymer structure and its effect on the various properties have been well explained.

6.2 CONCLUSIONS

On the basis of the experimental results, following important conclusions have been drawn.

- Based on literature survey, twenty new D-A type conjugated polymers have been successfully designed.

- New synthetic methods have been developed to achieve higher yield; the reaction parameters have been optimized and purification techniques were established.

- The newly synthesized cyanopyridine based conjugated polymers possess good optical and electrochemical properties. As these polymers showed the band gaps ranging from 2.14 to 2.80 eV, they are potential candidates for PLED applications.

- Their theoretical studies clearly revealed that, these polymers possess band gaps in the range 2.69 to 3.95 eV; the observed values were slightly higher than the corresponding optical band gaps.

- The polymers showed good film forming ability in the devices, as they have high molecular weight with solubility in common organic solvents.

- All the polymers exhibit high degree of thermal stability, typically the polymer **TDPy₄** showed highest onset decomposition temperature of 388 ºC. Therefore, these polymers would lead to stable PLED devices when used as emitters.

- The quantum yields of the new polymers were found to be in the range 21.38 to 49.27 %. Amongst them, **PPy₃** and **TPy₃** containing fluorene scaffold exhibited the maximum quantum yield of 49.27 and 48.32%, respectively. So, these polymers are expected to show good electroluminescence behavior.

- Finally, the PLED devices, fabricated using these newly synthesized polymers as blue/green emitters displayed moderate to good performance at threshold voltages of 3.12-5.77 V. Amongst them, **PPy₃** and **TPy₃** showed intense emission maxima in the region of 450-470 nm (dark blue) at threshold voltage of about 5 V.

To sum up, by appropriately optimizing the molecular structures of conductive polymers, it is possible to further ameliorate the performance of the PLED devices. Thus, following appropriate design strategies, new conjugative polymers can be designed so as to fine tune the required optical, electrochemical and thermal properties of them, for specific applications.

6.3 SCOPE FOR FUTURE WORK

The most efficient polymers **PPy₃** and **TPy₃** can be subjected to further in-depth PLED device studies to evaluate all the device parameters. Moreover, the low band gap polymers **TDPy₁₋₄** possessing good charge carrying property may find their applications in designing heterojunction solar cells. The active polymers can also be studied for evaluation of NLO properties, keeping in view of their applications in optical switching and optical limiters. Some of the new intermediates and monomers can be used for investigation of medicinal properties.

REFERENCES

Akcelrud, L. (2003). "Electroluminescent polymers." *Prog. Polym. Sci*. 28, 875-962.

Akoudad, S. and Roncali, J. (1998). "Electro-generated poly(thiophenes) with extremely narrow band-gap and high stability under *n*-doping cycling." *Chem. Commun.,* 2081-2082.

Alessandro, A., Silvia, B., Antonio, F. and Giorgio, A.P. (1997). "Facile, regioselective synthesis of highly solvatochromic thiophene-spaced *N*-Alkyl pyridinium dicyano methanides for second-harmonic generation." *J. Org. Chem.,* 62(17), 5755-5765.

Andersson, M.R., Thomas, O., Mammo, W., Svensson, M., Theander, M. and Inganäs, O. (1999). "Substituted poly(thiophene)s designed for optoelectronic devices and conductors." *J. Mater. Chem.* 9, 1933-1940.

Arkhipov, V.I., Emelianova, E.V., and Bassler, H. (2004). "Quenching of excitons in doped disordered organic semiconductors." *Phys. Rev. B.,* 70(20), 205205-205212.

Babudri, F., Cardone, A., Farinola, G.M., Naso, F., Cassano, T., Chiavarone, C. and Tommasi, R. (2003). "Synthesis and optical properties of a copolymer of tetrafluoro- and dialkoxy-Substituted poly(*p*-phenylenevinylene) with a high percentage of fluorinated units." macromolecular chemistry and physics." *Macromol. Chem. Phys.,* 204(13), 1621-1627.

Baek, M.J., Fei, G., Lee, S.H., Zong, K. and Lee, Y.S. (2009). "Poly(2,5-dihexyloxyphenylene vinylene-*alt*-2,2-dibutylpropylenedioxythiophene): Synthesis and characterization for photovoltaic applications." *Synth. Met*., 159(13), 1261-1266.

Baibarac, M., Lira-Cantu, M., Oro´ Sol, J., Baltog I., Casan-Pastor, N. and Gomez-Romero, P. (2007). "Poly(*N*-vinylcarbazole) and carbon nanotubes based composites and their application to rechargeable lithium batteries." *Compos. Sci. Technol.,* 67(11-12), 2556-2563.

Bässler, H., Arkhipov, V.I., Emelianova, E.V., Gerhard, A., Hayer, A., Im, C. and Rissler, J. (2003). "Excitons in π-conjugated polymers." *Synth. Met.,* 135-136(4), 377-382.

Batista, R.M.F., Costa, S.P.G., Belsley, M. and Raposo, M.M. (2007). "Synthesis and second-order nonlinear optical properties of new chromophores containing benzimidazole, thiophene, and pyrrole heterocycles." *Tetrahedron*, 63(39), 9842-9849.

Becker, M.W., Sapochak, L.S., Ghosen, R., Xu, C., Dalton, L.R., Shi, Y., Steier, Y.H. and Jen, A.K.Y. (1994). "Large and stable nonlinear optical effects observed for a polyimide covalently incorporating a nonlinear optical chromophore." *Chem. Mater.*, 1994, 6(2), 104-106.

Bernanose A. (1955). "Electroluminescence in organic compounds". *J. Phys.* (*52*), 509-514.

Bernier, S., Garreau, S., Béra-Abérem, M., Gravel, C. and Leclerc, M. (2002). "A versatile approach to affinity chromic polythiophenes." *J. Am. Chem. Soc.* 124(42), 12463-12468.

Bhuiyan,. M.D.H., Teshome, T., Gainsford, G.J., Ashraf, M., Clays, K., Asselberghs, I. and Kay, A.J. (2010). "Synthesis, characterization, linear and non-linear optical (NLO) properties of some Schiff's bases." *Opt. Mat.*, 32(6), 669-672.

Bradley, D.D.C. (1993). "Conjugated polymer electroluminescence." *Synth. Met.,* 54(1-3), 401-415.

Bredas, J.L. (1985). 1985. "Relationship between band gap and bond length alteration in organic conjugated polymer." *J. Chem. Phys.,* 82, 3808-3812.

Bredas, J.L., Themans, B., Andre, J.M., Chance, R. and Silbey, R. (1984). "The role of mobile organic radicals and ions (Solitons, polarons and bipolarons) in the transport properties of doped conjugated polymers." *Synth. Met*., 9(2), 265-274.

Bundgaard, E. and Krebs, F.C. (2007). "Large-area photovoltaics based on low band gap copolymers of thiophene and benzothiadiazole or benzo-bis(thiadiazole)." *Sol. Energy Mater. Sol. Cells.,* 91(11) 1019-1025.

Burroughes, J. H., Bradley, D. D. C., Brown, A. R., Marks, R. N., Mackay, K., Friend, R. H., Burns, P. L., and Holmes, A. B. (1990). "Light-emitting diodes based on conjugated polymers." *Nature,* 347(6293), 539-541.

Carella, A., Castaldo, A., Centore, R., Fort, A. and Sirigu, A. (2002). "Synthesis and second order nonlinear optical properties of new chromophores containing 1,3,4-oxadiazole and thiophene rings." *J. Chem. Perkin.Trans.2.,* 1791-1795.

Cassano, T., Tommasi, R., Babudri, F., Cardone, A., Farinola, G.M. and Naso, F. (2002). "High third-order nonlinear optical susceptibility in new fluorinated poly(*p*-phenylenevinylene) copolymers measured with the Z-scan technique." *Opt. Lett.,* 27(24), 2176-2178.

Chan, H.S.O and Ng, S.C. (1998) "Synthesis, characterization and applications of thiophene based functional polymers." *Prog. Polym. Sci.,* 23(7), 1167-1231.

Chen, H., Huang, H., Tian, Z., Shen, P., Zhao, B. and Tan, S. (2010). "Synthesis and photovoltaic performances of 2,5-dioctyloxy-1,4-phenylenevinylene and terthiophene copolymers with di(p-tolyl)phenylamine and oxadiazole side groups." *Eur. Polym. J.,* 46(4), 673-680.

Chen, T., Jen, A.K.Y. and Cai, Y. (1995). "Facile approach to nonlinear optical side-chain aromatic polyimides with large second-order nonlinearity and thermal stability." *J. Am. Chem. Soc.,* 117(27), 7295-7296.

Chen, Y., Liao, C. and Wu, T. (2002) "Synthesis and characterization of luminescent copolyethers with alternate stilbene derivatives and aromatic 1,3,4-oxadiazoles." *Polymer*, 43, 4545–4555.

Chi, S.H., Hales, J.M., Fuentes-Hernandez, C., Tseng, S.Y., Cho, J.Y., Odom, S.A., Zhang, Q.S., Barlow, Schrock, R.R., Marder, S.R., Kippelen, B. and Perry, J.W. (2008). "Thick optical-quality films of substituted poly-acetylenes with large, ultrafast third-order nonlinearities and application to image correlation." *Adv. Mater.,* 20(17), 3199-3203.

Cho, B.R., Kim, Y.H., Son, K.W., Khalil, C., Kim, Y.H. and Jeon, S. (2002). "Synthesis and nonlinear optical properties of 1,3,5-tricyano-2,4,6-tris [2-(thiophen-2-yl)vinyl] benzene derivatives." *Bull. Korean Chem. Soc.,* 23(9), 1253-1256.

Choon, S.N., Lu, H.F., Chan, H.S.O., Fujii, A., Laga, T. and Yoshino, T. (2001). "Novel efficient blue fluorescent polymers comprising alternating phenylene pyridine

repeat units: Their syntheses, characterization, and optical properties." *Macromolecules*, 34(20), 6895-6903.

Chung, I.S. and Kim, S.Y. (1997). "Synthesis and characterization of wholly aromatic polyamides containing pendent amino and cyano groups." *Polym. Bull.,* 38(6), 635-642.

Colladet, K., Fourier, S., Cleij, T.J., Lutsen, L., Gelan, J., Vanderzande, D., Nguyen, L.H., Neugebauer, H., Sariciftci, S., Aguirre, A., Janssen, G. and Goovaerts, E. (2007). "Low band gap donor-acceptor conjugated polymers toward organic solar cells applications." *Macromolecules*, 40(1), 65-72.

Danel, A., He, Z., Harry, G., Milburna, W. and Tomasik, P. (1999). "Electroluminescence from novel pyrazole-based polymer systems." *J. Mater. Chem.*, 9, 339-342.

de Leeuw, D.M., Simenon, M.M.J., Brown, A.R. and Einerhand, R.E.F. (1997). "Stability of n-type doped conducting polymers and consequences for polymeric microelectronic devices". *Synth. Met.* 87, 53-59.

Diaz, A.F., Kanazawa, K. and Gardini, G.P. (1979). "Electrochemical polymerization of pyrrole." *J. Chem. Soc., Chem. Commun.,* 632-635.

Dyer, A.L., Craig, M.R., Babiarz, J.E., Kiyak, K. and Reynolds, J.R. (2010). "Orange and red to transmissive electrochromic polymers based on electron-rich dioxythiophenes." *Macromolecules,* 43(10), 4460-4467.

Elsenbaumer, R.L., Jen, A.K.Y. and Oboody, R. (1986). "Processible and environmentally stable conducting polymers." *Synth. Met.*, 15(2-3), 169-174.

Emilie, M.G., Kim, Y.G., Jeremiah, K.M., Jones, A.G., McCarley, T.D., Vishal S., Yang, Y. and Reynolds, J.R. (2006). "Optimization of Narrow Band-Gap Propylenedioxythiophene: Cyanovinylene Copolymers for Optoelectronic Applications". *Macromolecules 39*, 9132-9142.

Epstein, A.J., Blatchford, J.W., Wang, Z.H., Jessen, S.W., Gebler, D.D., Lin, L.B., Gustsfson, T.L., Wang, H.L., Park, Y.W., Swager, T.M. and MacDiarmid, A.G.

(1996). "Poly(*p*-pyridine)- and poly(*p*-pyridyl vinylene)-based polymers: Their photo physics and application to SCALE devices." *Synth. Met.,* 78(3), 253-261.

Franz, E., Frank, W. and Felix, S. (1995). "Synthesis and solvatochromic properties of donor-acceptor-substituted oligothiophenes." *J. Org. Chem.*, 60(7), 2082-2091.

Galand, E.M., Kim, Y.G., Mwaura, J.K., Jones, A.G., McCarley, T.D., Shrotriya,V., Yang, Y. and Reynolds, J.R. (2006). "Optimization of narrow band-gap propylenedioxythiophene: cyanovinylene copolymers for optoelectronic applications." *Macromolecules*, 39(26), 9132-9142.

Grazulevicius, J.V., Strohriegl, P., Pielichowski, J. and Pielichowski, K. (2003). "Carbazole-containing polymers: synthesis, properties and applications." *Prog. Polym. Sci.,* 28(9), 1297-353.

Grigoras, M. and Antonoaia, N.C. (2005). "Synthesis of isoelectronic polyazomethine and poly(arylene vinylene) by a palladium-catalyzed Suzuki coupling method." Polym. Int.*, 54(12), 1641-1646.*

Günes, S., Neugebauer, H. and Sariciftci, S. N. (2007). "Conjugated polymer-based organic solar cells." *Chem. Rev.*, 107, 1324-1338.

Hao, J., Han, M.J., Guo, K., Zhao, Y., Qiu L., Shen, Y. and Meng, X. (2008). "A novel NLO: Synthesis azothiophene-based chromophore, characterization, thermal stability and optical nonlinearity." *Mater. Lett.,* 62(6-7), 973-976.

He, M., Zhou, Y., Dai, J., Liu, R., Cui, Y. and Zhang, T. (2009). "Synthesis and nonlinear optical properties of soluble fluorinated polyimides containing hetarylazo chromophores with large hyperpolarizability." *Polymer*, 50(16), 3924-3931.

Heeger, A.J. (2000). "Semiconducting and metallic polymers: The fourth generation of polymeric materials." *Nobel lecture,* December 8.

Hegde, P.K., Adhikari, A.V., Manjunatha, M.G., Poornesh, P. and Umesh, G. (2009). "Third-order nonlinear optical susceptibilities of new copolymers containing alternate 3,4-dialkoxythiophene and (1,3,4-oxadiazolyl)pyridine moieties." *Opt. Mater.*, 31(6), 1000-1006.

Hemavathi, B., T.N. Ahipa, S. Pillai, R.K. Pai,(2015) "Cyanopyridine based conjugated polymer-synthesis and characterization"., *Polym. (United Kingdom).*, *(78)* 22-30.

Hongli, W., Zhen, L., Bin, H., Zuoquan, J., Yanke, L., Hui, W., Jingui, Q., Gui, Y. Yunqi, L. and Yinglin, S. (2006). "Synthesis, light-emitting and optical limiting properties of new donor-acceptor conjugated polymers derived from 3,5-dicyano-2,4,6-tristyrylpyridine." *React. Funct. Polym.*, 66(9), 993-1002.

Hu, J.L., Li, B., Meng, F.S., Ding, F., Qian, S.X. and Tian, H. (2004). "Two-photon absorption properties of hyperbranched conjugated polymers with triphenylamine as the core." *Polymer,* 45(21), 7143-7149.

Izumi, T., Kobashi, S., Takimiya, K., Aso, Y. and Otsubo, T. (2003). "Synthesis and spectroscopic properties of a series of -blocked long oligothiophenes up to the 96-mer: revaluation of effective conjugation length", *J. Am. Chem. Soc.,* 125, 5286-5287.

Janietz, S. and Wedel, A. (1997). "Electrochemical redox behavior and electroluminescence in the mixed energy-sufficient system thianthrene and 2-(4-biphenyl)-5-(4-*tert*-butylphenyl)-1,3,4-oxadiazole." *Adv. Mater.,* 9(5), 403-407.

Jen, K., Maxifield, M., Shacklette, L.W. and Elsenbaumer, R.L. (1987). "Highly-conducting, poly(2,5-thienylene vinylene)prepared *via* a soluble precursor polymer." *J. Chem. Soc., Chem. Commun.,* 309-311.

John, A,. Microyannidis, Ioakim, Spiliopoulos,(2004). "Synthesis and optical properties of novel blue light emitting poly (*p*-phenylene vinylene) derivatives with pendant oxadiazole or cyano groups." *J polym sci part A: Polym chem.*, (42) 1768-1778.

Jumin, H., Mei-Juan, H., Kunpeng, G., Yuxia, Z., Ling, Q., Yuquan, S. and Xiaoguang, M. (2008). "A novel NLO azothiophene-based chromophore: Synthesis, characterization, thermal stability and optical nonlinearity." *Mater. Lett.*, 62(6-7), 973- 975.

Jung, M. S., Lee, T.W., Hyeon-Lee, J., Sohn, B.H. and Jung, I. (2006). "Synthesis and characterizations of a polyimide containing a triphenylamine derivative as an interlayer in polymer light-emitting diode." *Polymer,* 47(8), 2670-2676.

Junjian, L., Shen, P., Zhao, B., Yao, B., Xie, Z., Liu, E. and Tan, S. (2008). "Two novel triphenylamine-substituted poly (p-phenylenevinylene) derivatives: synthesis, photo- and electroluminescent properties." *Eur. Polym., J.,* 44(7), 2348-2355.

Kallmann, H.; Pope, M. (1960). "Bulk conductivity in organic crystals". *Nature*, 186, 31-33.

Karthikeyan, B., Anija, M., Sandeep, S.C.S., Nadeer, M.T.M. and Philip, R. (2008) "Optical and nonlinear optical properties of copper nano-composite glasses annealed near the glass softening temperature." *Opt. Commun*., 281(10), 2933-2937.

Kim, D., Kim, S., Zyung, T., Kim, J., Cho, I. and Choi, S.K. (1996). "Synthesis of a new Class of processable electroluminescent poly(cyanoterephthalylidene) derivative with a tertiary amine linkage." *Macromolecules,* 29(10)*,* 3657-3660.

Kim, J. H. and Lee, H. (2003). "Efficient poly (*p*-phenylenevinylene) derivative with 1,2-diphenyl-2-cyanoethene for single layer light-emitting diodes." *Synth. Met.,* 139(2), 471-478.

Kim, J., Seo, Y., Lee, W., Hong, Y., Lee, S.K., Shinc, W.S., Moonc, S. and Kanga, I. (2011). "Synthesis and properties of phenothiazylene vinylene and bithiophene-based copolymers for organic thin film transistors." *Synth. Met.,* 161(1-2), 72-78.

Kim, J.H. (2008). "Synthesis and electro-optical properties of poly(*p*-phenylenevinylene) derivative with conjugated 1,3,4-oxadiazole pendant and its AC electroluminescence." *Synth. Met.,* 158(21-24), 1028-1036.

Kim, K., Hong, Y.R., Lee, S.W., Jin, J.I., Park, Y., Sohn, B.H., Kim, W.H and Park, J.K. (2001). "Synthesis and luminescence properties of poly(*p*-phenylenevinylene) derivatives carrying directly attached carbazole pendants." *J. Mater. Chem*., 11, 3023-3030.

Koeckelberghs, G., Sioncke, S., Verbiest, T., Persoons, A. and Samyn, C. (2003). "Synthesis and properties of chiral helical chromophore functionalized

polybinaphthalenes for second-order nonlinear optical application." *Polymer,* 44(14), 3785-3794.

Kohler, A., Wilson, J.S. and Friend, R.H. (2002). "Fluorescence and phosphorescence in organic materials." *Adv. Mater.,* 14(10), 701-707.

Kroon, R., Lenes, M., Hummelen, J.C., Blom, P.W.M. and de-Boer, B. (2008). "Small band gap polymers for organic solar cells (Polymer material development in the last 5 years)". *Polym. Rev.*, 48, 531-582.

Kurian, P.A., Vijayan,C., Sathiyamoorthy, K., Sandeep, S.C.S. and Philip, R. (2007). "Exitonic transitions and off-resonant optical limiting in CdS quantum dots stabilized in a synthetic glue metrics." *Nano. Res. Lett.* 2(11), 561-568.

Leng, W.N., Zhou, Y.M., Xu, Q.H. and Liu, J.Z. (2001). "Synthesis of nonlinear optical polyimides containing benzothiazoe moiety and their electro-optical and thermal properties." *Polymer,* 42(22), 9253-9259.

Levi, M.D., Fisyuk, A.S., Demadrille, R., Markevich, E., Gofer, Y., Aurbacha, D. and Pron, A. (2006). "Unusually high stability of a poly(alkyl quaterthiophene-alt-oxadiazole) conjugated copolymer in its *n* and *p*-doped states." *Chem. Commun*., 3299-3301.

Li, Y., Li, H., Xu, B., Li, Z., Chen, F., Feng, D., Zhang, J. and Tian, W. (2010). "Molecular structure-property engineering for photovoltaic applications: Fluorene-acceptor alternating conjugated copolymers with varied bridged moieties." *Polymer,* 51(8), 1786-1795.

Liang, Y., Feng, D., Guo, J., Szarko, J.M., Ray, C., Chen, L.X. and Yu, L. (2009) "Regioregular oligomer and polymer containing thieno[3,4-*b*]thiophene moiety for efficient organic solar cells." *Macromolecules*, 42(4), 1091-1098.

Ling, Q., Liaw, D., Zhu, C., Chan, D.S., Kang, E. and Neoh, K. (2008). "Polymer electronic memories: Materials, devices and mechanisms." *Prog. Polym. Sci*., 33(10), 917-978.

Liu, B., Yu, W.L., Lai, Y.H. and Huang, W. (2001). "Blue-light-emitting fluorene-based polymers with tunable electronic properties." *Chem. Mater.,* 13(16), 1984-1991.

Liu, G., Ling, Q.D., Kang, E.T., Neoh, K.G., Liaw, D.J. and Chang, F.C. (2007). "Bistable electrical switching and write-once read-many-times memory effect in a donor-acceptor containing polyfluorene derivative and its carbon nanotube composites." *J. App. Phy.*, 102(2), 024502-024510.

Lowe, J.P. and Kafafi, S.A. (1984). "Effects of chemical substitution on polymer band gaps: transferability of band-edge energies." *J. Am. Chem. Soc.*, 106(20), 5837-5841.

Manjunatha, M.G., Adhikari, A.V. and Hegde, P.K. (2009). "Design and synthesis of new donor-acceptor type conjugated copolymers derived from thiophenes." *Eur. Polym., J.*, 45(3), 763-771.

Manjunatha, M.G., Adhikari, A.V., Hegde, P.K., Suchand-sandeep, C.S. and Philip, R. (2009). "A new nonlinear optically active donor-acceptor type conjugated polymer: Synthesis and electrochemical and optical characterization." *J. Electron. Mater.,* 39(12), 2711-2719.

Michelle, S.L., Jiang, X., Sen, L., Petra, H., and Alex, K.Y.J. (2002). "Effect of cyano substituents on electron affinity and electron-transporting properties of conjugated polymers." *Macromolecules*, 35(9), 3532-3538.

Michinobu, T., Okoshi, K., Osako, H., Kumazawa, H. and Shigehara, H. (2008). "Band-gap tuning of carbazole-containing donor-acceptor type conjugated polymers by acceptor moieties and p-spacer groups." *Polymer,* 49(1), 192-199.

Mikroyannidis, J.A., Damouras, P.A., Maragos, V.G., Tsai, L.R. and Chen, Y. (2009). "Synthesis, photophysics and electroluminescence of new vinylene-copolymers with 2,4,6-triphenylpyridine kinked segments along the main chain." *Eur. Polym. J.*, 45(1), 284-294.

Miller, G.G., Ronald, L. and Elsenbaumer. (1986). "Highly conducting, soluble, and environmentally-stable poly (3-alkylthiophenes)." *J. Chem. Soc., Chem. Commun.*, 1346-1349.

Mircea, G. and Nicoleta, C.A. (2005) "Synthesis and characterization of some carbazole-based imine polymers ." *Eur. Polym. J.,* 41(5), 1079-1089.

Mori, T. and Kijima, M. (2009). "Synthesis and electroluminescence properties of carbazole-containing 2,6-naphthalene-based conjugated polymers." *Eur. Polym. J.,* 45(4), 1149-1157.

Myung-Jin, B., Lee, S.H., Zong, K. and Lee, Y. (2010). "Low band gap conjugated polymers consisting of alternating dodecylthieno[3,4-b]thiophene-2-carboxylate and one or two thiophene rings: Synthesis and photovoltaic property." *Synth. Met.,* 160(11-12), 1197-1203.

Nan, H., Yu, C., Jinrui, B., Jun, W., Werner, J.B. and Jinhui, Z. (2009). "Preparation and optical limiting properties of multi-walled carbon nanotubes with π-conjugated metal-free phthalocyanine moieties." *Phys. Chem. C.,* 113(30), 13029-13035.

Ojha, U.P., Krishnamoorthy and Anilkumar. (2003). "Synthesis and characterization of aromatic polyoxadiazoles containing 3,4-alkylenedioxythiophnes." *Synth. Met.,* 132(3), 279-283.

Okumoto, K. and Shirota, Y. (2001). "Development of high-performance blue-violet-emitting organic electroluminescent devices". *Appl. Phys. Lett.,* 79(9), 1231-1233.

Ong, B.S., Wu. Y., Liu, P. and Gardner, S. (2004). "High-performance semiconducting polythiophenes for organic thin-film transistors." *J. Am. Chem. Soc., 126*(11), 3378-3379.

Pai, C.L., Liu, C.L., Chen, W.C and Jenekhe, S.A. (2006). "Electronic structure and properties of alternating donor-acceptor conjugated copolymers: 3,4-Ethylenedioxythiophene (EDOT) copolymers and model compounds." *Polymer*, 47(2), 699-708.

Pal, B., Yen, W.Y., Yang, J.S. and Su, W.F. (2007). "Substituent effect on the optoelectronic properties of alternating fluorene-thiophene copolymers." *Macromolecules, 40(23), 8189-8194.*

Paoli, M.D. and Gazotti, W.A. (2002). "Electrochemistry, polymers and opto-electronic devices: A combination with a future." *J. Braz. Chem. Soc.,* 13(4), 410-424.

Partridge, R. H. (1983). "Electroluminescence from polyvinylcarbazole films: 1. Carbazole cations." *Polymer (Guildf).,* 24(6), 733-738.

Peng, Q., Lu, Z.Y., Huang, Y., Xie, M.G., Xiao, D., Han, S.H., Peng, J.B. and Cao, Y. (2004). "Novel efficient green electroluminescent conjugated polymers based on fluorene and triarylpyrazoline for light-emitting diodes." *J. Mater. Chem*., 14, 396-401.

Perzon, E., Wang, X., Admassie, S., Inganäs, O. and Andersson, M.R. (2006). "An alternating low bandgap polyfluorene for optoelectronic devices." *Polymer*, 47(12), 4261-4268.

Pina, J., Melo, J.S., Burrows, H.D, Bilge, A., Farrell, A., Forster, M. and Scherf, U. (2006). "Spectral and photophysical studies on cruciform oligothiophenes in solution and the solid state" *J. Phys. Chem., B.* 110(31), 15100-15106.

Politis, J.K., Somoza, F., Kampf, J.W. and Curtis, M.D. (1999). "A comparison of structures and optoelectronic properties of oxygen- and sulfur-containing heterocycles: conjugated nonylbisoxazole and nonylbithiazole oligomers." *Chem. Mater.,* 1999, 11(8), 2274-2284.

Qian, Y., Meng, K., Lu, C.G., Lin, B., Huan, W. and Cui, Y. (2009). "The synthesis photophysical properties and two-photon absorption of triphenylamine multipolar chromophores." *Dyes Pigm.,* 80(1), 174-180.

Qian, Y., Xiao, G., Wang, G., Sun, Y., Cui, Y. and Yuan, C. (2006). "Synthesis and third-order optical nonlinearity in two-dimensional A-π-D-π-A carbazole-cored chromophores." *Dyes Pigm.,* 71(2), 109-117.

Qin, A., Jim, C.K.W., Lu, W., Lam, J.W.Y., Häussler, M., Dong, Y., Sung, H.H.Y., Williams, I.D., Wong, K.L.G. and Tang, B.Z. "Click polymerization: Facile synthesis of functional poly(aroyltriazole)s by metal-free, region-selective 1,3-dipolar polycycloaddition." *Macromolecules,* 40(7), 2308-2317.

Qiu, F., Zhou Y., Liu, J. and Zhang, X. (2006). "Preparation, morphological and thermal stability of polyimide/silica hybrid material containing dye NBDPA." *Dyes Pigm.,* 71(1), 37-42.

Rao, V.P., Cai, Y.M. and Jen, A.K.Y. (1994). "Ketene dithioacetal as a π-electron donor in second-order nonlinear optical chromophores." *Chem. Soc., Chem. Commun.,* 1689-1690.

Rao, V.P., Jen, A.K.Y., Wong, K.Y and Drost, K.J. (1993). "Novel push-pull thiophenes for second order nonlinear optical applications." *Tetrahedron Lett.* 34(11), 1747-1750.

Rao, V.P., Jen, A.K.Y., Wong, K.Y. and Drost, K.J. (1993). "Dramatically enhanced second-order nonlinear optical susceptibilities in tricyanovinylthiophene derivatives." *J. Chem. Soc., Chem. Commun.,* 1118-1120.

Roncali, J., Garreau, R., Yassar, A., Marque, P., Garnier, F. and Lemaire, M. (1987). "Effects of steric factors on the electro-synthesis and properties of conducting poly(3-alkylthiophenes)." *J. Phys. Chem.,* 91(27), 6706-6714.

Rosa, M.F.B., Susana, P.G.C., Belsley and Manuela, M.R. (2007) "Synthesis and second-order nonlinear optical properties of new chromophores containing benzimidazole, thiophene, and pyrrole heterocycles." *Tetrahedron*, 63(39), 9842-9849.

Rosso, P.G.D., Almassio, M.F., Palomar, G.R. and Garay, R.O. (2011). "Nitroaromatic compounds sensing. Synthesis, photophysical characterization and fluorescence quenching of a new amorphous segmented conjugated polymer with diphenylfluorene chromophores." *Sen. Actuators, B*, 160(1), 524-532.

Saadeh, H., Gharavi, A., Yu, D. and Yu, L. (1997). "Polyimides with a diazo chromophore exhibiting high thermal stability and large electro-optic coefficients." *Macromolecules,* 1997, 30(18), 5403-5407.

Samoc, M., Samoc, A. and Davies, B.L. (1998) "Femto second Z-scan and degenerate four-wave mixing measurements of real and imaginary parts of the third-order nonlinearity of soluble conjugated polymers." *J. Opt. Soc. Am. B.,* 15(2) 817-825.

Samoc, M., Samoc, A. and Davies, B.L. (2000). "Two-photon and one-photon resonant third-order nonlinear optical properties of π-conjugated polymers." *Synth. Met.,* 109(1-3), 79-83.

Schroeder, B.C., Nielsen, C.B., Kim, Y.J., Smith, J., Huang, Z., Durrant, J., Watkins, S. E., Song, K., Anthopoulos, T.D. and McCulloch, I. (2011). "Benzotrithiophene co-polymers with cigh charge carrier mobilities in field-effect transistors." *Chem. Mater.,* 23(17), 4025-4031.

Seung, W.K., Jung, B.J., Ahn, T. and Shim, H.K. (2002). "Novel poly(*p* phenylenevinylene)s with an electron-withdrawing cyanophenyl group." *Macromolecules*, 35(16), 6217-6223.

Sheik-Bahae, M., Said, A.A. and Wei, T. (1990). "Sensitive measurement of optical nonlinearities using a single beam." *IEEE. J. Quantum. Electron.,* 26(4), 760-769.

Shin, W.S., Kim, S.C., Lee, S., Jeon, S., Kim, M., Naidu, B.V.K., Jin, S., Lee, J., Lee J.W. and Gal, Y. (2007). "Synthesis and photovoltaic properties of a low-band-gap polymer consisting of alternating thiophene and benzothiadiazole derivatives for bulk-heterojunction and dye-sensitized solar cells." *J. Polym. Sci. A., Polym. Chem.,* 45(8), 1394-1402.

Sim, J.H., Ueno, E., Natori, I., Ha, J. and Sato, H. (2008). "Oxidation polymerization of *N*-butyl-*N*,*N*-diphenylamine (BDPA) and *N*-4-butylphenyl-*N*,*N*-diphenylamine (BTPA). *Synth. Met.,* 158(8-9), 345-349.

Sivaramakrishnan, S., Muthukumar, V.S., Sivasankara, S., Venkataramanaiah, S.K., Reppert, J., Rao, A.M., Anija, M., Philip, R. and Kuthirummal, N. (2007). "Nonlinear optical scattering and absorption in bismuth nanorod suspensions." *Appl. Phys. Lett*., 91(9), 093104-093107.

Smela, E. (2003). "Conjugated polymer actuators for biomedical applications." *Adv. Mater.*, 15(6), 481-494.

Sonar, P., Zhang, Z., Grimsdale, A.C., Mullen, K., Surin M., Lazzaroni, R., Leclere, P., Tierney, S., Heeney, M. and Mc-Culloch, I. (2004). "4-Hexylbithieno[3,2-*b*:2c3c-]pyridine: An efficient electron-accepting unit in fluorene and indenofluorene copolymers for light-emitting devices." *Macromolecules,* 37(3)*,* 709-715.

Sonmez, G., Meng, H. and Wudl, F. (2003). "Very stable low band gap polymer for charge storage purposes and near-infrared applications." *Chem. Mater.*, 15(26), 4923-4929.

Spanggaard, H. and Krebs, F.C. (2004). "A brief history of the development of organic and polymeric photovoltaics." *Sol. Energy Mater. Sol. Cells*, 83(2-3), 125-146.

Strukelj, M., Papadimitrakopoulos, F., Miller, T.M. and Rotheberg, L.J. (1995). "Design and application of electron-transporting organic materials." *Science,* 267(5206), 1969-1972.

Tambe, S.M., Kittur, A.A., Inamdar, S.R., Mitchell, G.R. and Kariduraganavar, M.Y. (2009). "Synthesis and characterization of thermally stable second-order nonlinear optical side-chain polyimides containing thiazole and benzothiazole push-pull chromophores." *Opt. Mater.,* 31(6), 817-825.

Tameev, A.R., Heb, Z., Milburn, G.H.W., Daneld, A., Tomasikd, P. and Vannikova, A. V. (2004) "Drift mobility of electrons in pyrazoline-containing copolymers." *Russ. J. Electrochem.,* 40(3), 359-363.

Tang, C. W., and S. A. VanSlyke. (1987). "OLED_1987.pdf." *Appl. Phys. Lett.,32(15), 275-320*

Tarkka, R.M., Zhang, X. and Jenekhe, S.A. (1996). "Electrically Generated Intramolecular Proton Transfer: Electroluminescence and Stimulated Emission from Polymers." *J. Am. Chem. Soc.*, 118(39), 9438-9439.

Tourillon. (1986). Handbook of Conducting Polymers; T. A. Stotheim, Ed. Marcel Dekker: New York, 294.

Tsutsumi, N., Morishima, M. and Sakai, W. (1998). "Nonlinear optical (NLO) polymers. NLO polyimide with dipole moments aligned transverse to the imide linkage." *Macromolecules,* 31(22), 7764-7769.

Udayakumar, D. and Adhikari, A.V. (2006). "Synthesis and characterization of new light-emitting copolymers containing 3,4-dialkoxythiophenes." *Synth. Met.,* 156(18-20), 1168-1173.

References

Udayakumar, D., Kiran, A.J., Adhikari, A.V., Chandrasekharan, K., Umesh, G. and Shashikala, H.D. (2006). "Third-order nonlinear optical studies of newly synthesized polyoxadiazoles containing 3,4-dialkoxythiophenes." *Chem. Phys*., 331(1), 125-130.

Viehbeck, A., Goldberg, M.J. and Kovac, C.A. (1990). "Electrochemical properties of polyimides and related imide compounds." *J. Electrochem. Soc.* 137(5), 1460-1466.

Waltman, R.J., Bargon, J. and Diaz, A.F., (1983). "Electrochemical studies of some conducting polythiophene films." *J. Phys. Chem.* 87(8), 1459-1463.

Walton, D.J. (1990). "Electrically conducting polymers." *Mater.Des.,* 11(3), 142-152.

Wang, H., Li, Z., Huang, B., Jiang, Z., Liang, Y., Wang, H., Qin, J., Yu, G., Liu, Y. and Song, Y. (2006). "Synthesis, light-emitting and optical limiting properties of new donor-acceptor conjugated polymers derived from 3,5-dicyano-2,4,6-tristyrylpyridine." *React. Funct. Polym.,* 66(9), 993-1002.

Wang, K.L., Liaw, D.J., Liou, W.T and Chen, W.T. (2008). "A novel fluorescent poly(pyridine-imide) acid chemosensor." *Dyes Pigm.,* 78(2) 93-100.

Wang, K.L., Liaw, D.J., Liou, W.T and Huang, S.T. (2008). "High glass transition and thermal stability of new pyridine-containing polyimides: Effect of protonation on fluorescence." *Polymer,* 49(6), 1538-1546.

Wang, X., Li, Y.F., Ma, T., Zhang, S. and Gong. C. (2006). Synthesis and characterization of novel polyimides derived from 2,6-bis[4-(3,4-dicarboxyphenoxy)benzoyl]pyridine dianhydride and aromatic diamines." *Polymer,* 47, 3774-3783.

Wienk, M.M., Struijk, M.P. and Janssen, R.A.J. (2006). "Low band gap polymer bulk heterojunction solar cells." *Chem. Phys. Lett*., 422(4-6), 488-491.

Wu, C.W., Liu and Chen, C.L. (2006). "Synthesis and characterization of new fluorene-acceptor alternating and random copolymers for light-emitting applications." *Polymer,* 47(2), 527-530.

Wu, X., Liu, Y. and Zhu, D. (2001). "Synthesis and characterization of a new conjugated polymer containing cyano substituents for light-emitting diodes." *J. Mater. Chem*., 11, 1327-1331.

Xu, S., Yang, M. and Cao, S. (2005). "A fluorescent co-polyimide containing perylene, fluorene and oxadiazole units in the main chain." *React. Funct. Polym.,* 66(4), 471-478.

Xue, J., Uchida, S., Rand, B.P. and Forrest, S.R. (2004). "4.2 % efficient organic photovoltaic cells with low series resistances." *Appl. Phys. Lett*., 84(16), 3013-3015.

Yanamao, D., Lu, J., Xu, Q., Yan, F., Xia, X., Wang, L. and Hu, L. 2010. "Effects of substituents on the third-order nonlinear optical properties of poly(3-alkoxythiophene) derivatives." *Synth. Met.* 160(5-6), 409 - 412.

Yang, B., Li, G., Zhang, X., Shu, X., Wang, A., Zhu, X. and Zhu, J. (2011). "Hg^{2+} detection by aniline-based conjugated copolymers with high selectivity." *Polymer,* 52(12), 2537-2541.

Yin, S.G., Wedel, A., Janietz, S., Krueger, H., Sainova, D., Arlt, K., Kuechlr, F. and Fischer, B., (2003). Synthetic and electroluminescent properties of polymer containing phenothiazene and oxadiazole units." *Synth. Met.,* 137(1-3), 1145-1466.

Yoon, K.R., Byun, N.M. and Lee, H. (2007). "Synthesis and characterization of carbazole based nonlinear optical polymers possessing chromophores in the main or side chains." *Synth. Met.,* 157(16-17),   603-610.

Yu L.P. and Dalton L.R. (1989). "Synthesis and characterization of new electro-active polymers ." *Synth. Met*., 29(1), 463-470.

Yu, C.Y., Ko, B.T., Ting. C. and Chen, C.P. (2009). "Two-dimensional regioregular polythiophenes with conjugated side chains for use in organic solar cells." *Sol. Energy Mater. Sol. Cells,* 93(5), 613-620.

Yu, L., Bao, Z. and Cai, R. (1993). "Conjugated, liquid crystalline polymers."*Angew. Chem. Int. Ed.,* 32(9), 1345-1347.

Yu, W.L., Meng, H., Pei, J. and Haung, W. (1998). "Tuning redox behavior and emissive wavelength of conjugated polymers by *p-n* diblock structures." *J. Am. Chem. Soc.,* 120(45), 11808-11809.

Zhan, X., Liu, Y., Wu, X., Wang, S. and Zhu, D. (2002). "New series of blue-emitting and electron-transporting copolymers based on fluorene." *Macromolecules*, 35(7), 2529-2537.

Zhang, H., Li, Y., Jiang, Q., Xie, M., Peng, J. and Cao, Y. (2007). "Novel green-emitting polymer containing fluorene and 1-(2-benzothiazolyl)-3,5-diphenylpyrazoline." *J. Mater. Sci.,* 42(12), 4476-4479.

Zhang, S., He, C., Liu, Y., Zhan, V.X and Chen, J. (2009). "Synthesis of a soluble conjugated copolymer based on dialkyl-substituted dithienothiophene and its application in photovoltaic cells." *Polymer,* 50(15), 3595-3599.

Zhao, B., Liu, D., Peng, L., Li, H., Shen, P., Xiang, N., Liu, Y. and Tan, S. (2009). "Effect of oxadiazole side chains based on alternating fluorene-thiophene copolymers for photovoltaic cells." *Eur. Polym., J.* 45(7), 2079-2086.

Zhao, W., Cai, W., Xu, R., Yang, W., Gong, X., Wu, H. and Cao, Y. (2010). "Novel conjugated alternating copolymer based on 2,7-carbazole and 2,1,3-benzoselenadiazole." *Polymer,* 51(14), 3196 -3202.

Zoombelt, A.P., Mark, A.M., Fonrodona, M., Nicolas, Y., Wienk, M.M., Rene, A.J. and Janssen, R.A.J. (2009). "The influence of side chains on solubility and photovoltaic performance of dithiophene-thienopyrazine small band gap copolymers." *Polymer*, 50(19), 4564-4570.

Zou, Y., Peng, B., Liu, B., Li, Y., He, Y., Zhou, K. and Pan, C. (2009). "Conjugated copolymers of cyano substituted poly(*p*-phenylene vinylene) with phenylene ethynylene and thienylene vinylene moieties: Synthesis, optical, and electrochemical properties." *J. Appl. Polym. Sci.*, 115(3), 1480-1488.

LIST OF PUBLICATIONS

Papers published in international journals

1. Naveenchandra Pilicode, Nimith K. M, Madhukara Acharya, Praveen Naik, Satyanarayan M. N, Airody Vasudeva Adhikari * (2019), "New blue light emitting cyanopyridine based conjugated polymers: From molecular engineering to PLED applications", *Journal of Photochemistry and Photobiology A: Chemistry*, 2019, doi:10.1016/j.jphotochem. 2019.04.012.

2. Naveenchandra Pilicode, K. M. Nimith, M. N. Satyanarayan, Airody Vasudeva Adhikari, (2018), "New cyanopyridine based conjugative polymers as blue emitters: Synthesis, photophysical, theoretical and electroluminescence studies". *Journal of Photochemistry and Photobiology A*: Chemistry, 2018, doi:10.1016/j.jphotochem.2018.05.037.

3. Naveenchandra.P, Praveen Naik, Nimith K. M, Madhukara Acharya, Satyanarayan M. N, A.Vasudeva Adhikari, "New Cyanopyridine Based Conjugated Polymers Carrying Auxiliary Electron Donors: From Molecular Design to Blue Emissive PLEDs" *Dyes and pigments*: 2019, doi:10.1016/j.dyepig.2019.108046.

4. Naveenchandra.P, Praveen Naik , Madhukara Acharya, A.Vasudeva Adhikari, "Synthesis, characterization and electroluminescence studies of cyanopyridine-based π-conjugative polymers carrying benzo[c][1,2,5]thiadiazole and naphtho[1,2-c:5,6-c′]bis([1,2,5]thiadiazole) units" *New Journal of Chemistry*, 2020, doi: 10.1039/D0NJ02141E.

5. Naveenchandra.P, Praveen Naik, Nimith K. M, A.Vasudeva Adhikari, "Nicotinonitrile centered luminescent polymeric materials: Structural, optical, electrochemical, and theoretical investigations" *Polymer engineering and science*, 2020, doi: 10.1002/pen.25493.

6. Naveenchandra.P, Praveen Naik, Nimith K. M, Madhukara Acharya, Satyanarayan M. N, A.Vasudeva Adhikari, "New cyanopyridine-based π-conjugative poly(azomethine)s: Synthesis, characterization and electroluminescence studies" *Polymers for Advanced Technologies,* 2020, doi:10.1002/pat.5067

Papers presented in national / international conferences

1. Naveenchandra Pilicode, Airody Vasudeva Adhikari[*], "Cyanopyridine Based Conjugative Polymers Carrying Fluorene for PLED Applications", 37th National Conference of Indian Council of Chemists (ICC-2018), held at National Institute of Technology Karnataka, Surathkal, December 12-14, 2018, India.

2. Naveenchandra. P, Madhukar A, Airody Vasudeva Adhikari[*], "New cyanopyridne light emitting polymers for PLED applications", International Conference on Emerging Trends in Chemical Sciences (ICETCS-2017), MIT, Manipal, September 14-16, 2017, India

3. Pilicode Naveenchandra, Vasudeva Adhikari[*], "Cyanopyridine based conjugated polymers for opto-electronic applications", International Conference on Advanced Polymers for Science and Technology (APST-2016), VIT University, Vellore, October 24-26, 2016, India.

4. P. Naveenchandra, M. S. Sunitha, Airody Vasudeva Adhikari[*], "New thiophene based donor-acceptor type conjugated polymers for non-linear optics". A poster presentation at the International Conference on Direct Digital Manufacturing and Polymers (ICDDMAP 2015), Karnataka University, Dharwad, October 28-31, 2015, India.

* * * * * * * * *

Curriculum Vitae

Present address

Permanent Address

Naveenchandra P.
Research Scholar
Department of Chemistry
National Institute of Karnataka
Srinivasnagar, Mangalore
Karnataka, India-575025
Email: naveecha87@gmail.com
Phone: +918618009201

Naveenchandra P.
Shri Rama Nilaya 6-90A
Sixth Block Krishnapura
Mangalore Taluk
Dakshina Kannada District
Karnataka, India-575014
Email: naveecha87@gmail.com
Phone: +919844768576

Research Experience:

07/2013-present: **Research scholar**
Department of Chemistry
National Institute of Technology Karnataka, India
Research: Design and synthesis of cyanopyridine based conjugated polymers for optoelectronic applications

06/2010-present: **Assistant Manager in product development lab**
BASF Coatings solutions (http://www.basf.com)
BASF India Ltd.
Research Area: Development of acrylic basecoat technology for automotive exterior applications

Education:

07/2013-present: **Ph.D.** (Polymer Chemistry)
Department of Chemistry
Polymer Division
National Institute of Technology Karnataka, India
Title: Design and synthesis of cyanopyridine based conjugated polymers for optoelectronic applications
Supervisor: Prof. A. Vasudeva Adhikari

06/2008-05/2010:   **M.Sc.** (Chemistry)
Department of Chemistry
Mangalagangothri, Konaje
Mangalore University

06/2005-05/2008:   **B.Sc**. (Chemistry)
Govinda Dasa First Grade College, Surathkal Mangalore University

Honors:

- **2010**: Awarded III rank in **M. Sc.** (Chemistry) from Mangalore University.

Skills:

- Strong knowledge and research experience in small organic molecules, and conjugated polymer synthesis and their characterization.

- Experience in handling UV-Vis, Spectrofluorometer, Electrochemical workstation, FTIR and other instruments

- Familiar with the interpretation of UV-vis, Fluorescence, NMR, LCMS, FAB mass, and other techniques

- Good in designing new polymers and development of cost-effective synthetic methods

Research Interest

- Synthesis and characterization conjugated polymers for optoelectronic applications

- Synthesis and characterization of wide band gap materials for PLED applications.

- Design of new fluorescent polymeric materials

****